

REPORT

Elia Asset N.V.

Belgian Offshore Grid


Environmental Impact Assessment: Numerical
modelling of sediment transport


01 July 2013 - version 1.0

Colophon

International Marine & Dredging Consultants

Address: Coveliersstraat 15, 2600 Antwerp, Belgium

: + 32 3 270 92 95

: + 32 3 235 67 11

Email: info@imdc.be

Website: www.imdc.be

Document Identification

Title	Environmental Impact Assessment: Numerical modelling of sediment transport
Project	Belgian Offshore Grid
Client	Elia Asset N.V.
Tender	Tender N°4074323
Document ref	I/RA/11413/13.006/LWA
Document name	K:\PROJECTS\11\11413 - Belgian Offshore Grid - Marine Consulting\10-Rap\DO-1 Marine Consulting\RA13006_SedimentationAndErosionPatterns\RA13006_Sediment transport modelling_v1.0.docx

Revision

Version	Date	Description	Author	Checked	Approved
1.0	01/07/13	Final report	LWA 	PEM 	MSA 

Distribution List

34	Hard copy	Jeroen Mentens (ELIA)
1	Pdf	Jeroen Mentens (ELIA)

Table of Contents

1. INTRODUCTION	1
1.1 THE ASSIGNMENT	1
1.2 AIM OF THE STUDY	1
1.3 OVERVIEW OF THE STUDY	2
1.4 STRUCTURE OF THE REPORT	2
2. DESCRIPTION OF NUMERICAL MODEL	3
2.1 HYDRODYNAMIC FLOW MODEL	3
2.1.1 Numerical grid and bathymetry	3
2.1.2 Boundary conditions	6
2.1.3 Validation	9
2.2 WAVE MODEL	12
2.2.1 Introduction	12
2.2.2 Numerical grid and bathymetry	12
2.2.3 Boundary conditions	14
2.2.4 Validation	18
2.3 SEDIMENT TRANSPORT MODEL	24
2.3.1 Boundary conditions and median grain size	24
3. SIMULATION RESULTS	25
3.1 SCENARIOS	25
3.2 SCHEMATISATION ANALYSIS	28
3.2.1 Summer condition (Morfac=1, +/- 2 weeks)	28
3.2.2 Winter condition (1-year-returned storm, Morfac=1, +/- 2 weeks)	38
3.3 STORM IMPACTS	48
3.3.1 1-year-returned storm (Morfac=1, +/- 2 weeks)	49
3.3.2 5-year-returned storm (Morfac=1, +/- 2 weeks)	55
3.4 LONG-TERM MORPHOLOGY ANALYSIS	60
3.4.1 Comparison with natural condition (Morfac=125, +/- 25 years)	60
3.4.2 Morphological evolution (Morfac=125, +/- 25 years)	63
3.5 NEUTRALISED EFFECTS OF TIDAL FORCING	69
3.5.1 1-year-returned storm	69
3.5.2 5-year-returned storm	71
3.6 OTHER SEDIMENT TRANSPORT FORMULAE	73
3.6.1 Soulsby / Van Rijn	73
3.6.2 Bijker (1971)	79
4. CONCLUSIONS	84

5. REFERENCES	86
6. APPENDIX	87
6.1 1-YEAR-RETURNED STORM (MORFAC=1, +/- 2 WEEKS)	87
6.1.1 Current ellipse	87
6.1.2 Residual current	90
6.1.3 Sedimentation/Erosion	93
6.2 5-YEAR-RETURNED STORM (MORFAC=1, +/- 2 WEEKS)	96
6.2.1 Current ellipse	96
6.2.2 Residual current	97
6.2.3 Sedimentation/Erosion	98
6.3 COMPARISON WITH NATURAL CONDITION (MORFAC=125, +/- 25 YEARS)	99
6.3.1 SIP I (single inactive point at Location I)	99
6.3.2 DIPP I (double inactive points perpendicular to main flow direction at Location I)	102
6.3.3 SIP II (single inactive point at Location II)	105
6.3.4 TIPA II (triple inactive points aligned to main flow direction at Location II)	108
6.3.5 DIPP II (double inactive points perpendicular to main flow direction at Location II) ...	111
6.4 MORPHOLOGICAL EVOLUTION (MORFAC=125, +/- 25 YEARS)	114
6.4.1 SIP I (single inactive point at Location I)	114
6.4.2 DIPP I (double inactive points perpendicular to main flow direction at Location I)	117
6.4.3 SIP II (single inactive point at Location II)	120
6.4.4 TIPA II (triple inactive points aligned to main flow direction at Location II)	123
6.4.5 DIPP II (double inactive points perpendicular to main flow direction at Location II) ...	126

List of Tables

TABLE 2-1: VALUES OF AVERAGED TIDAL RANGE OF THE SELECTED REPRESENTATIVE TIDAL PERIOD AND ANNUAL MEAN TIDAL RANGE AT THREE STATIONS.	7
TABLE 3-1: OVERVIEW OF SCENARIOS.	27

List of Figures

FIGURE 2-1: LAYOUT OF THE MODEL GRIDS	3
FIGURE 2-2: THREE DOMAINS AFTER DOMAIN DECOMPOSITION	4
FIGURE 2-3: BATHYMETRY MAP OF THE FLOW MODEL DOMAIN	5
FIGURE 2-4: THREE-DIMENSIONAL BATHYMETRY MAP OF THE BOG DOMAIN	5
FIGURE 2-5: TIDAL GAUGES IN THE MODEL DOMAIN	6
FIGURE 2-6: TIDAL RANGES AT THREE STATIONS IN 2009	7

FIGURE 2-7: MOVING AVERAGED TIDAL RANGE FOR SPRING-NEAP TIDAL CYCLE AT THREE STATIONS.	8
FIGURE 2-8: TIDAL ELEVATION OBSERVED AT MOW0 STATION DURING THE REPRESENTATIVE PERIOD.	8
FIGURE 2-9: LOCATION OF OBSERVATION POINTS (INDICATED BY THE SIGN OF RED "x").	10
FIGURE 2-10: COMPARISON OF TIDAL ELEVATION AT WESTHINDER	10
FIGURE 2-11: COMPARISON OF VELOCITY AT SCHEUR WIELINGEN	11
FIGURE 2-12: COMPARISON OF VELOCITY AT LODEWIJKBANK	11
FIGURE 2-13: THE WAVE MODEL GRIDS (MAIN WAVE MODEL: WAVE GRID , NESTED WAVE MODEL: BOG DOMAIN) AND THE THREE DOMAINS OF THE FLOW MODEL.	13
FIGURE 2-14: BATHYMETRY MAP OF THE WAVE MODEL AND THREE WAVE MONITORING STATIONS.	13
FIGURE 2-15: SIGNIFICANT WAVE HEIGHT OBSERVED AT WESTHINDER FROM 01-JULY-1990 TO 01-JULY-2010	14
FIGURE 2-16: UPPER PANELS: PERFORMANCE OF THE STATISTICAL MODEL; LOWER PANEL: CORRELATION BETWEEN VARIABLE LEVEL AND RETURN PERIOD.	15
FIGURE 2-17: PEAKS OF THE SIGNIFICANT WAVE HEIGHT MONITORED AT WESTHINDER	16
FIGURE 2-18: WIND CONDITIONS COLLECTED AT WESTHINDER DURING THE SELECTED 1-YEAR-RETURNED STORM PERIOD.	17
FIGURE 2-19: WAVE CONDITIONS COLLECTED AT SANDETTIE LIGHTSHIP DURING THE SELECTED 1-YEAR-RETURNED STORM PERIOD.	17
FIGURE 2-20: WIND CONDITIONS COLLECTED AT WESTHINDER DURING THE SELECTED 5-YEAR-RETURNED STORM PERIOD.	18
FIGURE 2-21: WAVE CONDITIONS COLLECTED AT SANDETTIE LIGHTSHIP DURING THE SELECTED 5-YEAR-RETURNED STORM PERIOD.	18
FIGURE 2-22: ONE-ON-ONE RELATION BETWEEN THE SIGNIFICANT WAVE HEIGHT CALCULATED BY DELFT3D-WAVE AND MEASURED AT THE WESTHINDER BUOY LOCATION.	20
FIGURE 2-23: VALIDATION OF THE DELFT3D-WAVE MODEL WITH FIELD MEASUREMENTS OF THE DIRECTIONAL WAVE BUOY AT THE WESTHINDER BANK. COMPARISON OF THE TIME SERIES OF THE SIGNIFICANT WAVE HEIGHT H_{M0} , THE MEAN ZERO-CROSSING WAVE PERIOD T_{M02} AND WAVE DIRECTION.	21
FIGURE 2-24: ONE-ON-ONE RELATION BETWEEN THE SIGNIFICANT WAVE HEIGHT CALCULATED BY DELFT3D-WAVE AND MEASURED AT THE WESTHINDER BUOY LOCATION.	22
FIGURE 2-25: VALIDATION OF THE DELFT3D-WAVE MODEL WITH FIELD MEASUREMENTS OF THE DIRECTIONAL WAVE BUOY AT THE WESTHINDER BANK. COMPARISON OF THE TIME SERIES OF THE SIGNIFICANT WAVE HEIGHT H_{M0} , THE MEAN ZERO-CROSSING WAVE PERIOD T_{M02} AND WAVE DIRECTION.	23
FIGURE 3-1: SCHEMATISATION SIP (SINGLE INACTIVE POINT, AREA: CA. 180 M X 220 M) LEFT PANEL: LOCATION I, RIGHT PANEL: LOCATION II.	25
FIGURE 3-2: SCHEMATISATION TIPA (TRIPLE INACTIVE POINTS ALIGNED TO THE MAIN FLOW DIRECTION, AREA: CA. 3*180 M X 220 M) LEFT PANEL: LOCATION I, RIGHT PANEL: LOCATION II.	26
FIGURE 3-3: SCHEMATISATION DIPP (DOUBLE INACTIVE POINTS PERPENDICULAR TO THE MAIN FLOW DIRECTION, AREA: CA. 180 M X 2*220 M) LEFT PANEL: LOCATION I, RIGHT PANEL: LOCATION II.	26
FIGURE 3-4: MAP OF AVERAGED CURRENT ELLIPSE FOR SIP I (BLACK) AND NC (PURPLE) IN SUMMER CONDITION WITH BATHYMETRY AS BACKGROUND.	29

FIGURE 3-5: MAP OF AVERAGED CURRENT ELLIPSE FOR TIPA I (BLACK) AND NC (PURPLE) IN SUMMER CONDITION WITH BATHYMETRY AS BACKGROUND.....	29
FIGURE 3-6: MAP OF AVERAGED CURRENT ELLIPSE FOR DIPP I (BLACK) AND NC (PURPLE) IN SUMMER CONDITION WITH BATHYMETRY AS BACKGROUND.....	30
FIGURE 3-7: MAP OF AVERAGED CURRENT ELLIPSE FOR SIP II (BLACK) AND NC (PURPLE) IN SUMMER CONDITION WITH BATHYMETRY AS BACKGROUND.....	30
FIGURE 3-8: MAP OF AVERAGED CURRENT ELLIPSE FOR TIPA II (BLACK) AND NC (PURPLE) IN SUMMER CONDITION WITH BATHYMETRY AS BACKGROUND.....	31
FIGURE 3-9: MAP OF AVERAGED CURRENT ELLIPSE FOR DIPP II (BLACK) AND NC (PURPLE) IN SUMMER CONDITION WITH BATHYMETRY AS BACKGROUND.....	31
FIGURE 3-10: MAP OF RESIDUAL CURRENT FOR SIP I (BLACK) AND NC (PURPLE) IN SUMMER CONDITION WITH DIFFERENCE OF RESIDUAL VELOCITY MAGNITUDE AS BACKGROUND AND ISOBATH LINES OF -25 M NAP.	32
FIGURE 3-11: MAP OF RESIDUAL CURRENT FOR TIPA I (BLACK) AND NC (PURPLE) IN SUMMER CONDITION WITH DIFFERENCE OF RESIDUAL VELOCITY MAGNITUDE AS BACKGROUND AND ISOBATH LINES OF -25 M NAP.	32
FIGURE 3-12: MAP OF RESIDUAL CURRENT FOR DIPP I (BLACK) AND NC (PURPLE) IN SUMMER CONDITION WITH DIFFERENCE OF RESIDUAL VELOCITY MAGNITUDE AS BACKGROUND AND ISOBATH LINES OF -25 M NAP.	33
FIGURE 3-13: MAP OF RESIDUAL CURRENT FOR SIP II (BLACK) AND NC (PURPLE) IN SUMMER CONDITION WITH DIFFERENCE OF RESIDUAL VELOCITY MAGNITUDE AS BACKGROUND AND ISOBATH LINES OF -25 M NAP.	33
FIGURE 3-14: MAP OF RESIDUAL CURRENT FOR TIPA II (BLACK) AND NC (PURPLE) IN SUMMER CONDITION WITH DIFFERENCE OF RESIDUAL VELOCITY MAGNITUDE AS BACKGROUND AND ISOBATH LINES OF -25 M NAP.	34
FIGURE 3-15: MAP OF RESIDUAL CURRENT FOR DIPP II (BLACK) AND NC (PURPLE) IN SUMMER CONDITION WITH DIFFERENCE OF RESIDUAL VELOCITY MAGNITUDE AS BACKGROUND AND ISOBATH LINES OF -25 M NAP.	34
FIGURE 3-16: MAP OF RESIDUAL SEDIMENT TRANSPORT FOR SIP I (BLACK) AND NC (PURPLE) IN SUMMER CONDITION WITH DIFFERENCE OF SEDIMENTATION/EROSION AS BACKGROUND AND ISOBATH LINES OF -25 M NAP.	35
FIGURE 3-17: MAP OF RESIDUAL SEDIMENT TRANSPORT FOR TIPA I (BLACK) AND NC (PURPLE) IN SUMMER CONDITION WITH DIFFERENCE OF SEDIMENTATION/EROSION AS BACKGROUND AND ISOBATH LINES OF -25 M NAP.....	36
FIGURE 3-18: MAP OF RESIDUAL SEDIMENT TRANSPORT FOR DIPP I (BLACK) AND NC (PURPLE) IN SUMMER CONDITION WITH DIFFERENCE OF SEDIMENTATION/EROSION AS BACKGROUND AND ISOBATH LINES OF -25 M NAP.....	36
FIGURE 3-19: MAP OF RESIDUAL SEDIMENT TRANSPORT FOR SIP II (BLACK) AND NC (PURPLE) IN SUMMER CONDITION WITH DIFFERENCE OF SEDIMENTATION/EROSION AS BACKGROUND AND ISOBATH LINES OF -25 M NAP.	37
FIGURE 3-20: MAP OF RESIDUAL SEDIMENT TRANSPORT FOR TIPA II (BLACK) AND NC (PURPLE) IN SUMMER CONDITION WITH DIFFERENCE OF SEDIMENTATION/EROSION AS BACKGROUND AND ISOBATH LINES OF -25 M NAP.....	37
FIGURE 3-21: MAP OF RESIDUAL SEDIMENT TRANSPORT FOR DIPP II (BLACK) AND NC (PURPLE) IN SUMMER CONDITION WITH DIFFERENCE OF SEDIMENTATION/EROSION AS BACKGROUND AND ISOBATH LINES OF -25 M NAP.....	38
FIGURE 3-22: MAP OF AVERAGED CURRENT ELLIPSE FOR SIP I (BLACK) AND NC (PURPLE) IN WINTER CONDITION WITH BATHYMETRY AS BACKGROUND.	39

FIGURE 3-23: MAP OF AVERAGED CURRENT ELLIPSE FOR TIPA I (BLACK) AND NC (PURPLE) IN WINTER CONDITION WITH BATHYMETRY AS BACKGROUND.	39
FIGURE 3-24: MAP OF AVERAGED CURRENT ELLIPSE FOR DIPP I (BLACK) AND NC (PURPLE) IN WINTER CONDITION WITH BATHYMETRY AS BACKGROUND.	40
FIGURE 3-25: MAP OF AVERAGED CURRENT ELLIPSE FOR SIP II (BLACK) AND NC (PURPLE) IN WINTER CONDITION WITH BATHYMETRY AS BACKGROUND.	40
FIGURE 3-26: MAP OF AVERAGED CURRENT ELLIPSE FOR TIPA II (BLACK) AND NC (PURPLE) IN WINTER CONDITION WITH BATHYMETRY AS BACKGROUND.	41
FIGURE 3-27: MAP OF AVERAGED CURRENT ELLIPSE FOR DIPP II (BLACK) AND NC (PURPLE) IN WINTER CONDITION WITH BATHYMETRY AS BACKGROUND.	41
FIGURE 3-28: MAP OF RESIDUAL CURRENT FOR SIP I (BLACK) AND NC (PURPLE) IN SUMMER CONDITION WITH DIFFERENCE OF RESIDUAL VELOCITY MAGNITUDE AS BACKGROUND AND ISOBATH LINES OF -25 M NAP.	42
FIGURE 3-29: MAP OF RESIDUAL CURRENT FOR TIPA I (BLACK) AND NC (PURPLE) IN SUMMER CONDITION WITH DIFFERENCE OF RESIDUAL VELOCITY MAGNITUDE AS BACKGROUND AND ISOBATH LINES OF -25 M NAP.	42
FIGURE 3-30: MAP OF RESIDUAL CURRENT FOR DIPP I (BLACK) AND NC (PURPLE) IN SUMMER CONDITION WITH DIFFERENCE OF RESIDUAL VELOCITY MAGNITUDE AS BACKGROUND AND ISOBATH LINES OF -25 M NAP.	43
FIGURE 3-31: MAP OF RESIDUAL CURRENT FOR SIP II (BLACK) AND NC (PURPLE) IN SUMMER CONDITION WITH DIFFERENCE OF RESIDUAL VELOCITY MAGNITUDE AS BACKGROUND AND ISOBATH LINES OF -25 M NAP.	43
FIGURE 3-32: MAP OF RESIDUAL CURRENT FOR TIPA II (BLACK) AND NC (PURPLE) IN SUMMER CONDITION WITH DIFFERENCE OF RESIDUAL VELOCITY MAGNITUDE AS BACKGROUND AND ISOBATH LINES OF -25 M NAP.	44
FIGURE 3-33: MAP OF RESIDUAL CURRENT FOR DIPP II (BLACK) AND NC (PURPLE) IN SUMMER CONDITION WITH DIFFERENCE OF RESIDUAL VELOCITY MAGNITUDE AS BACKGROUND AND ISOBATH LINES OF -25 M NAP.	44
FIGURE 3-34: MAP OF RESIDUAL SEDIMENT TRANSPORT FOR SIP I (BLACK) AND NC (PURPLE) IN SUMMER CONDITION WITH DIFFERENCE OF SEDIMENTATION/EROSION AS BACKGROUND AND ISOBATH LINES OF -25 M NAP.	45
FIGURE 3-35: MAP OF RESIDUAL SEDIMENT TRANSPORT FOR TIPA I (BLACK) AND NC (PURPLE) IN SUMMER CONDITION WITH DIFFERENCE OF SEDIMENTATION/EROSION AS BACKGROUND AND ISOBATH LINES OF -25 M NAP.	46
FIGURE 3-36: MAP OF RESIDUAL SEDIMENT TRANSPORT FOR DIPP I (BLACK) AND NC (PURPLE) IN SUMMER CONDITION WITH DIFFERENCE OF SEDIMENTATION/EROSION AS BACKGROUND AND ISOBATH LINES OF -25 M NAP.	46
FIGURE 3-37: MAP OF RESIDUAL SEDIMENT TRANSPORT FOR SIP II (BLACK) AND NC (PURPLE) IN SUMMER CONDITION WITH DIFFERENCE OF SEDIMENTATION/EROSION AS BACKGROUND AND ISOBATH LINES OF -25 M NAP.	47
FIGURE 3-38: MAP OF RESIDUAL SEDIMENT TRANSPORT FOR TIPA II (BLACK) AND NC (PURPLE) IN SUMMER CONDITION WITH DIFFERENCE OF SEDIMENTATION/EROSION AS BACKGROUND AND ISOBATH LINES OF -25 M NAP.	47
FIGURE 3-39: MAP OF RESIDUAL SEDIMENT TRANSPORT FOR DIPP II (BLACK) AND NC (PURPLE) IN SUMMER CONDITION WITH DIFFERENCE OF SEDIMENTATION/EROSION AS BACKGROUND AND ISOBATH LINES OF -25 M NAP.	48
FIGURE 3-40: BATHYMETRY MAP WITH ISOBATH CONTOUR LINES OF -25 M NAP; RED CROSS POINT FOR INSPECTION OF TIME SERIES VARIABLES.	49

FIGURE 3-41: TIME SERIES OF MODELLED SIGNIFICANT WAVE HEIGHT AND TIDAL ELEVATION DURING THE REPRESENTATIVE SPRING-NEAP TIDAL CYCLE IN WINTER CONDITION (1-YEAR-RETURNED STORM) AT THE RED CROSS POINT.	50
FIGURE 3-42: MAP OF MAXIMAL SIGNIFICANT WAVE HEIGHT OVER THE REPRESENTATIVE SPRING-NEAP TIDAL CYCLE IN WINTER CONDITION (1-YEAR-RETURNED STORM) WITH ISOBATH LINES OF -25 M NAP.	50
FIGURE 3-43: MAP OF AVERAGED CURRENT ELLIPSE WITH NATURAL CONDITION FOR WINTER (BLACK) AND SUMMER (PURPLE) CONDITIONS WITH BATHYMETRY AS BACKGROUND.	51
FIGURE 3-44: MAP OF AVERAGED CURRENT ELLIPSE WITH TIPA I FOR WINTER (BLACK) AND SUMMER (PURPLE) CONDITIONS WITH BATHYMETRY AS BACKGROUND.	52
FIGURE 3-45: MAP OF RESIDUAL CURRENT WITH NATURAL CONDITION FOR WINTER (BLACK) AND SUMMER (PURPLE) CONDITIONS WITH DIFFERENCE OF RESIDUAL VELOCITY MAGNITUDE AS BACKGROUND AND ISOBATH LINES OF -25 M NAP.	52
FIGURE 3-46: MAP OF RESIDUAL CURRENT WITH TIPA I FOR WINTER (BLACK) AND SUMMER (PURPLE) CONDITIONS WITH DIFFERENCE OF RESIDUAL VELOCITY MAGNITUDE AS BACKGROUND AND ISOBATH LINES OF -25 M NAP.	53
FIGURE 3-47: MAP OF RESIDUAL SEDIMENT TRANSPORT WITH NATURAL CONDITION FOR WINTER (BLACK) AND SUMMER (PURPLE) CONDITIONS WITH DIFFERENCE OF SEDIMENTATION/EROSION AS BACKGROUND AND ISOBATH LINES OF -25 M NAP.	54
FIGURE 3-48: MAP OF RESIDUAL SEDIMENT TRANSPORT WITH TIPA I FOR WINTER (BLACK) AND SUMMER (PURPLE) CONDITIONS WITH DIFFERENCE OF SEDIMENTATION/EROSION AS BACKGROUND AND ISOBATH LINES OF -25 M NAP.	54
FIGURE 3-49: TIME SERIES OF MODELLED SIGNIFICANT WAVE HEIGHT AND TIDAL ELEVATION DURING THE REPRESENTATIVE SPRING-NEAP TIDAL CYCLE IN WINTER CONDITION AT THE RED CROSS POINT.	55
FIGURE 3-50: MAP OF MAXIMAL SIGNIFICANT WAVE HEIGHT OVER THE REPRESENTATIVE SPRING-NEAP TIDAL CYCLE IN WINTER CONDITION WITH ISOBATH LINES OF -25 M NAP.	56
FIGURE 3-51: MAP OF AVERAGED CURRENT ELLIPSE WITH NATURAL CONDITION FOR WINTER (BLACK) AND SUMMER (PURPLE) CONDITIONS WITH BATHYMETRY AS BACKGROUND.	57
FIGURE 3-52: MAP OF AVERAGED CURRENT ELLIPSE WITH TIPA I FOR WINTER (BLACK) AND SUMMER (PURPLE) CONDITIONS WITH BATHYMETRY AS BACKGROUND.	57
FIGURE 3-53: MAP OF RESIDUAL CURRENT WITH NATURAL CONDITION IN WINTER (BLACK) AND SUMMER (PURPLE) CONDITIONS WITH DIFFERENCE OF RESIDUAL VELOCITY MAGNITUDE AS BACKGROUND AND ISOBATH LINES OF -25 M NAP.	58
FIGURE 3-54: MAP OF RESIDUAL CURRENT WITH TIPA I IN WINTER (BLACK) AND SUMMER (PURPLE) CONDITIONS WITH DIFFERENCE OF RESIDUAL VELOCITY MAGNITUDE AS BACKGROUND AND ISOBATH LINES OF -25 M NAP.	58
FIGURE 3-55: MAP OF RESIDUAL SEDIMENT TRANSPORT WITH NATURAL CONDITION IN WINTER (BLACK) AND SUMMER (PURPLE) CONDITIONS WITH DIFFERENCE OF SEDIMENTATION/EROSION AS BACKGROUND AND ISOBATH LINES OF -25 M NAP.	59
FIGURE 3-56: MAP OF RESIDUAL SEDIMENT TRANSPORT WITH TIPA I IN WINTER (BLACK) AND SUMMER (PURPLE) CONDITIONS WITH DIFFERENCE OF SEDIMENTATION/EROSION AS BACKGROUND AND ISOBATH LINES OF -25 M NAP.	60
FIGURE 3-57: BATHYMETRIC CHANGE OF TIPA I COMPARED TO NATURAL CONDITION AFTER +/- 5 YEARS WITH MORPHOLOGICAL ACCELERATION (MORFAC=125).	61
FIGURE 3-58 :BATHYMETRIC CHANGE OF TIPA I COMPARED TO NATURAL CONDITION AFTER +/- 10 YEARS WITH MORPHOLOGICAL ACCELERATION (MORFAC=125).....	61
FIGURE 3-59: BATHYMETRIC CHANGE OF TIPA I COMPARED TO NATURAL CONDITION AFTER +/- 15 YEARS WITH MORPHOLOGICAL ACCELERATION (MORFAC=125).....	62

FIGURE 3-60: BATHYMETRIC CHANGE OF TIPA I COMPARED TO NATURAL CONDITION AFTER +/- 20 YEARS WITH MORPHOLOGICAL ACCELERATION (MORFAC=125).....	62
FIGURE 3-61: BATHYMETRIC CHANGE OF TIPA I COMPARED TO NATURAL CONDITION AFTER +/- 25 YEARS WITH MORPHOLOGICAL ACCELERATION (MORFAC=125).....	63
FIGURE 3-62: MAP OF SEDIMENTATION/EROSION WITH NATURAL CONDITION DURING THE FIRST 5 YEARS WITH MORPHOLOGICAL ACCELERATION (MORFAC=125).	64
FIGURE 3-63: MAP OF SEDIMENTATION/EROSION WITH NATURAL CONDITION DURING THE SECOND 5 YEARS WITH MORPHOLOGICAL ACCELERATION (MORFAC=125).....	65
FIGURE 3-64: MAP OF SEDIMENTATION/EROSION WITH NATURAL CONDITION DURING THE THIRD 5 YEARS WITH MORPHOLOGICAL ACCELERATION (MORFAC=125).	65
FIGURE 3-65: MAP OF SEDIMENTATION/EROSION WITH NATURAL CONDITION DURING THE FOURTH 5 YEARS WITH MORPHOLOGICAL ACCELERATION (MORFAC=125).....	66
FIGURE 3-66: MAP OF SEDIMENTATION/EROSION WITH NATURAL CONDITION DURING THE FIFTH 5 YEARS WITH MORPHOLOGICAL ACCELERATION (MORFAC=125).	66
FIGURE 3-67: MAP OF SEDIMENTATION/EROSION WITH TIPA I DURING THE FIRST 5 YEARS WITH MORPHOLOGICAL ACCELERATION (MORFAC=125).	67
FIGURE 3-68: MAP OF SEDIMENTATION/EROSION WITH TIPA I DURING THE SECOND 5 YEARS WITH MORPHOLOGICAL ACCELERATION (MORFAC=125).	67
FIGURE 3-69: MAP OF SEDIMENTATION/EROSION WITH TIPA I DURING THE THIRD 5 YEARS WITH MORPHOLOGICAL ACCELERATION (MORFAC=125).	68
FIGURE 3-70: MAP OF SEDIMENTATION/EROSION WITH TIPA I DURING THE FOURTH 5 YEARS WITH MORPHOLOGICAL ACCELERATION (MORFAC=125).	68
FIGURE 3-71: MAP OF SEDIMENTATION/EROSION WITH TIPA I DURING THE FIFTH 5 YEARS WITH MORPHOLOGICAL ACCELERATION (MORFAC=125).	69
FIGURE 3-72: MAP OF SEDIMENTATION/EROSION DIFFERENCE BETWEEN THE SCENARIO WITH 1-YEAR-RETURNED STORM FOLLOWED BY 1-YEAR TIDAL FORCING AND THE SCENARIO ONLY WITH 1-YEAR TIDAL FORCING FOR NATURAL CONDITION	70
FIGURE 3-73: MAP OF SEDIMENTATION/EROSION DIFFERENCE BETWEEN THE SCENARIO WITH 1-YEAR-RETURNED STORM FOLLOWED BY 1-YEAR TIDAL FORCING AND THE SCENARIO ONLY WITH 1-YEAR TIDAL FORCING FOR TIPA I.....	71
FIGURE 3-74: MAP OF SEDIMENTATION/EROSION DIFFERENCE BETWEEN THE SCENARIO WITH 5-YEAR-RETURNED STORM FOLLOWED BY 5-YEAR TIDAL FORCING AND THE SCENARIO ONLY WITH 5-YEAR TIDAL FORCING FOR NATURAL CONDITION.	72
FIGURE 3-75: MAP OF SEDIMENTATION/EROSION DIFFERENCE BETWEEN THE SCENARIO WITH 5-YEAR-RETURNED STORM FOLLOWED BY 5-YEAR TIDAL FORCING AND THE SCENARIO ONLY WITH 5-YEAR TIDAL FORCING FOR TIPA I.....	72
FIGURE 3-76: LEFT UPPER PANEL: SEDIMENTATION/EROSION CALCULATED BY VAN RIJN (2000) FOR NATURAL CONDITION OVER 1 YEAR ONLY WITH TIDAL FORCING; RIGHT UPPER PANEL: SEDIMENTATION/EROSION CALCULATED BY SOULSBY/VAN RIJN FOR NATURAL CONDITION OVER 1 YEAR ONLY WITH TIDAL FORCING; LEFT LOWER PANEL: DIFFERENCE BETWEEN SEDIMENTATIONS/EROSIONS CALCULATED BY VAN RIJN (2000) AND BY SOULSBY/VAN RIJN; RIGHT LOWER PANEL: REGRESSION ANALYSIS OF SEDIMENTATIONS/EROSIONS CALCULATED BY VAN RIJN (2000) AND BY SOULSBY/VAN RIJN.	74
FIGURE 3-77: LEFT UPPER PANEL: SEDIMENTATION/EROSION CALCULATED BY VAN RIJN (2000) FOR TIPA I OVER 1 YEAR ONLY WITH TIDAL FORCING; RIGHT UPPER PANEL: SEDIMENTATION/EROSION CALCULATED BY SOULSBY/VAN RIJN FOR TIPA I OVER 1 YEAR ONLY WITH TIDAL FORCING; LEFT LOWER PANEL: DIFFERENCE BETWEEN SEDIMENTATIONS/EROSIONS CALCULATED BY VAN RIJN (2000) AND BY SOULSBY/VAN RIJN;	

RIGHT LOWER PANEL: REGRESSION ANALYSIS OF SEDIMENTATIONS/EROSIONS CALCULATED BY VAN RIJN (2000) AND BY SOULSBY/VAN RIJN.....	75
FIGURE 3-78: LEFT UPPER PANEL: SEDIMENTATION/EROSION CALCULATED BY VAN RIJN (2000) FOR NATURAL CONDITION OVER 2 WEEKS WITH 1-YEAR-RETURNED STORM AND TIDAL FORCING; RIGHT UPPER PANEL: SEDIMENTATION/EROSION CALCULATED BY SOULSBY/VAN RIJN FOR NATURAL CONDITION OVER 2 WEEKS WITH 1-YEAR-RETURNED STORM AND TIDAL FORCING; LEFT LOWER PANEL: DIFFERENCE BETWEEN SEDIMENTATIONS/EROSIONS CALCULATED BY VAN RIJN (2000) AND BY SOULSBY/VAN RIJN; RIGHT LOWER PANEL: REGRESSION ANALYSIS OF SEDIMENTATIONS/EROSIONS CALCULATED BY VAN RIJN (2000) AND BY SOULSBY/VAN RIJN.....	76
FIGURE 3-79: LEFT UPPER PANEL: SEDIMENTATION/EROSION CALCULATED BY VAN RIJN (2000) FOR TIPA I OVER 2 WEEKS WITH 1-YEAR-RETURNED STORM AND TIDAL FORCING; RIGHT UPPER PANEL: SEDIMENTATION/EROSION CALCULATED BY SOULSBY/VAN RIJN FOR TIPA I OVER 2 WEEKS WITH 1-YEAR-RETURNED STORM AND TIDAL FORCING; LEFT LOWER PANEL: DIFFERENCE BETWEEN SEDIMENTATIONS/EROSIONS CALCULATED BY VAN RIJN (2000) AND BY SOULSBY/VAN RIJN; RIGHT LOWER PANEL: REGRESSION ANALYSIS OF SEDIMENTATIONS/EROSIONS CALCULATED BY VAN RIJN (2000) AND BY SOULSBY/VAN RIJN.....	77
FIGURE 3-80: MAP OF SEDIMENTATION/EROSION DIFFERENCE BETWEEN THE SCENARIO WITH 1-YEAR-RETURNED STORM FOLLOWED BY 1-YEAR TIDAL FORCING AND THE SCENARIO ONLY WITH 1-YEAR TIDAL FORCING FOR NATURAL CONDITION BASED ON THE SEDIMENT TRANSPORT FORMULA SOULSBY/VAN RIJN.....	78
FIGURE 3-81: MAP OF SEDIMENTATION/EROSION DIFFERENCE BETWEEN THE SCENARIO WITH 1-YEAR-RETURNED STORM FOLLOWED BY 1-YEAR TIDAL FORCING AND THE SCENARIO ONLY WITH 1-YEAR TIDAL FORCING FOR TIPA I BASED ON THE SEDIMENT TRANSPORT FORMULA SOULSBY/VAN RIJN.	78
FIGURE 3-82: LEFT UPPER PANEL: SEDIMENTATION/EROSION CALCULATED BY VAN RIJN (2000) FOR NATURAL CONDITION OVER 1 YEAR ONLY WITH TIDAL FORCING; RIGHT UPPER PANEL: SEDIMENTATION/EROSION CALCULATED BY BIJKER (1971) FOR NATURAL CONDITION OVER 1 YEAR ONLY WITH TIDAL FORCING; LEFT LOWER PANEL: DIFFERENCE BETWEEN SEDIMENTATIONS/EROSIONS CALCULATED BY VAN RIJN (2000) AND BY BIJKER (1971); RIGHT LOWER PANEL: REGRESSION ANALYSIS OF SEDIMENTATIONS/EROSIONS CALCULATED BY VAN RIJN (2000) AND BY BIJKER (1971).	79
FIGURE 3-83: LEFT UPPER PANEL: SEDIMENTATION/EROSION CALCULATED BY VAN RIJN (2000) FOR TIPA I OVER 1 YEAR ONLY WITH TIDAL FORCING; RIGHT UPPER PANEL: SEDIMENTATION/EROSION CALCULATED BY BIJKER (1971) FOR TIPA I OVER 1 YEAR ONLY WITH TIDAL FORCING; LEFT LOWER PANEL: DIFFERENCE BETWEEN SEDIMENTATIONS/EROSIONS CALCULATED BY VAN RIJN (2000) AND BY BIJKER (1971); RIGHT LOWER PANEL: REGRESSION ANALYSIS OF SEDIMENTATIONS/EROSIONS CALCULATED BY VAN RIJN (2000) AND BY BIJKER (1971).	80
FIGURE 3-84: LEFT UPPER PANEL: SEDIMENTATION/EROSION CALCULATED BY VAN RIJN (2000) FOR NATURAL CONDITION OVER 2 WEEKS WITH 1-YEAR-RETURNED STORM AND TIDAL FORCING; RIGHT UPPER PANEL: SEDIMENTATION/EROSION CALCULATED BY BIJKER (1971) FOR NATURAL CONDITION OVER 2 WEEKS WITH 1-YEAR-RETURNED STORM AND TIDAL FORCING; LEFT LOWER PANEL: DIFFERENCE BETWEEN SEDIMENTATIONS/EROSIONS CALCULATED BY VAN RIJN (2000) AND BY BIJKER (1971); RIGHT LOWER PANEL: REGRESSION ANALYSIS OF SEDIMENTATIONS/EROSIONS CALCULATED BY VAN RIJN (2000) AND BY BIJKER (1971).	81
FIGURE 3-85: LEFT UPPER PANEL: SEDIMENTATION/EROSION CALCULATED BY VAN RIJN (2000) FOR TIPA I OVER 2 WEEKS WITH 1-YEAR-RETURNED STORM AND TIDAL FORCING; RIGHT UPPER PANEL: SEDIMENTATION/EROSION CALCULATED BY BIJKER (1971) FOR TIPA I OVER 2 WEEKS WITH 1-YEAR-RETURNED STORM AND TIDAL FORCING; LEFT LOWER PANEL: DIFFERENCE BETWEEN SEDIMENTATIONS/EROSIONS CALCULATED BY VAN RIJN (2000) AND BY BIJKER (1971); RIGHT LOWER PANEL: REGRESSION ANALYSIS OF SEDIMENTATIONS/EROSIONS CALCULATED BY VAN RIJN (2000) AND BY BIJKER (1971).	82

FIGURE 3-86: MAP OF SEDIMENTATION/EROSION DIFFERENCE BETWEEN THE SCENARIO WITH 1-YEAR-RETURNED STORM FOLLOWED BY 1-YEAR TIDAL FORCING AND THE SCENARIO ONLY WITH 1-YEAR TIDAL FORCING FOR TIPA I BASED ON THE SEDIMENT TRANSPORT FORMULA BIJKER (1971).....	83
FIGURE 3-87: MAP OF SEDIMENTATION/EROSION DIFFERENCE BETWEEN THE SCENARIO WITH 1-YEAR-RETURNED STORM FOLLOWED BY 1-YEAR TIDAL FORCING AND THE SCENARIO ONLY WITH 1-YEAR TIDAL FORCING FOR TIPA I BASED ON THE SEDIMENT TRANSPORT FORMULA BIJKER (1971).....	83
FIGURE 6-1: MAP OF AVERAGED CURRENT ELLIPSE WITH SIP I FOR WINTER (BLACK) AND SUMMER (PURPLE) CONDITIONS WITH BATHYMETRY AS BACKGROUND.	87
FIGURE 6-2: MAP OF AVERAGED CURRENT ELLIPSE WITH TIPA I FOR WINTER (BLACK) AND SUMMER (PURPLE) CONDITIONS WITH BATHYMETRY AS BACKGROUND.	88
FIGURE 6-3: MAP OF AVERAGED CURRENT ELLIPSE WITH SIP II FOR WINTER (BLACK) AND SUMMER (PURPLE) CONDITIONS WITH BATHYMETRY AS BACKGROUND.	88
FIGURE 6-4: MAP OF AVERAGED CURRENT ELLIPSE WITH TIPA II FOR WINTER (BLACK) AND SUMMER (PURPLE) CONDITIONS WITH BATHYMETRY AS BACKGROUND.	89
FIGURE 6-5: MAP OF AVERAGED CURRENT ELLIPSE WITH DIPP II FOR WINTER (BLACK) AND SUMMER (PURPLE) CONDITIONS WITH BATHYMETRY AS BACKGROUND.	89
FIGURE 6-6 OF RESIDUAL CURRENT WITH SIP I FOR WINTER (BLACK) AND SUMMER (PURPLE) CONDITIONS WITH DIFFERENCE OF RESIDUAL VELOCITY MAGNITUDE AS BACKGROUND AND ISOBATH LINES OF -25 M NAP.	90
FIGURE 6-7 OF RESIDUAL CURRENT WITH DIPP I FOR WINTER (BLACK) AND SUMMER (PURPLE) CONDITIONS WITH DIFFERENCE OF RESIDUAL VELOCITY MAGNITUDE AS BACKGROUND AND ISOBATH LINES OF -25 M NAP.	90
FIGURE 6-8 OF RESIDUAL CURRENT WITH SIP II FOR WINTER (BLACK) AND SUMMER (PURPLE) CONDITIONS WITH DIFFERENCE OF RESIDUAL VELOCITY MAGNITUDE AS BACKGROUND AND ISOBATH LINES OF -25 M NAP.	91
FIGURE 6-9 OF RESIDUAL CURRENT WITH TIPA II FOR WINTER (BLACK) AND SUMMER (PURPLE) CONDITIONS WITH DIFFERENCE OF RESIDUAL VELOCITY MAGNITUDE AS BACKGROUND AND ISOBATH LINES OF -25 M NAP.	91
FIGURE 6-10 OF RESIDUAL CURRENT WITH DIPP II FOR WINTER (BLACK) AND SUMMER (PURPLE) CONDITIONS WITH DIFFERENCE OF RESIDUAL VELOCITY MAGNITUDE AS BACKGROUND AND ISOBATH LINES OF -25 M NAP.	92
FIGURE 6-11: MAP OF RESIDUAL SEDIMENT TRANSPORT WITH SIP I FOR WINTER (BLACK) AND SUMMER (PURPLE) CONDITIONS WITH DIFFERENCE OF SEDIMENTATION/EROSION AS BACKGROUND AND ISOBATH LINES OF -25 M NAP.	93
FIGURE 6-12: MAP OF RESIDUAL SEDIMENT TRANSPORT WITH DIPP I FOR WINTER (BLACK) AND SUMMER (PURPLE) CONDITIONS WITH DIFFERENCE OF SEDIMENTATION/EROSION AS BACKGROUND AND ISOBATH LINES OF -25 M NAP.	94
FIGURE 6-13: MAP OF RESIDUAL SEDIMENT TRANSPORT WITH SIP II FOR WINTER (BLACK) AND SUMMER (PURPLE) CONDITIONS WITH DIFFERENCE OF SEDIMENTATION/EROSION AS BACKGROUND AND ISOBATH LINES OF -25 M NAP.	94
FIGURE 6-14: MAP OF RESIDUAL SEDIMENT TRANSPORT WITH TIPA II FOR WINTER (BLACK) AND SUMMER (PURPLE) CONDITIONS WITH DIFFERENCE OF SEDIMENTATION/EROSION AS BACKGROUND AND ISOBATH LINES OF -25 M NAP.	95
FIGURE 6-15: MAP OF RESIDUAL SEDIMENT TRANSPORT WITH DIPP II FOR WINTER (BLACK) AND SUMMER (PURPLE) CONDITIONS WITH DIFFERENCE OF SEDIMENTATION/EROSION AS BACKGROUND AND ISOBATH LINES OF -25 M NAP.	95

FIGURE 6-16: MAP OF AVERAGED CURRENT ELLIPSE WITH TIPA II FOR WINTER (BLACK) AND SUMMER (PURPLE) CONDITIONS WITH BATHYMETRY AS BACKGROUND.	96
FIGURE 6-17: MAP OF RESIDUAL CURRENT WITH TIPA II IN WINTER (BLACK) AND SUMMER (PURPLE) CONDITIONS WITH DIFFERENCE OF RESIDUAL VELOCITY MAGNITUDE AS BACKGROUND AND ISOBATH LINES OF -25 M NAP.	97
FIGURE 6-18: MAP OF RESIDUAL SEDIMENT TRANSPORT WITH TIPA II IN WINTER (BLACK) AND SUMMER (PURPLE) CONDITIONS WITH DIFFERENCE OF SEDIMENTATION/EROSION AS BACKGROUND AND ISOBATH LINES OF -25 M NAP.	98
FIGURE 6-19: BATHYMETRIC CHANGE OF SIP I COMPARED TO NATURAL CONDITION AFTER +/- 5 YEARS WITH MORPHOLOGICAL ACCELERATION (MORFAC=125).	99
FIGURE 6-20: BATHYMETRIC CHANGE OF SIP I COMPARED TO NATURAL CONDITION AFTER +/- 10 YEARS WITH MORPHOLOGICAL ACCELERATION (MORFAC=125).	100
FIGURE 6-21: BATHYMETRIC CHANGE OF SIP I COMPARED TO NATURAL CONDITION AFTER +/- 15 YEARS WITH MORPHOLOGICAL ACCELERATION (MORFAC=125).	100
FIGURE 6-22: BATHYMETRIC CHANGE OF SIP I COMPARED TO NATURAL CONDITION AFTER +/- 20 YEARS WITH MORPHOLOGICAL ACCELERATION (MORFAC=125).	101
FIGURE 6-23: BATHYMETRIC CHANGE OF SIP I COMPARED TO NATURAL CONDITION AFTER +/- 25 YEARS WITH MORPHOLOGICAL ACCELERATION (MORFAC=125).	101
FIGURE 6-24: BATHYMETRIC CHANGE OF DIPP I COMPARED TO NATURAL CONDITION AFTER +/- 5 YEARS WITH MORPHOLOGICAL ACCELERATION (MORFAC=125).	102
FIGURE 6-25: BATHYMETRIC CHANGE OF DIPP I COMPARED TO NATURAL CONDITION AFTER +/- 10 YEARS WITH MORPHOLOGICAL ACCELERATION (MORFAC=125).	103
FIGURE 6-26: BATHYMETRIC CHANGE OF DIPP I COMPARED TO NATURAL CONDITION AFTER +/- 15 YEARS WITH MORPHOLOGICAL ACCELERATION (MORFAC=125).	103
FIGURE 6-27: BATHYMETRIC CHANGE OF DIPP I COMPARED TO NATURAL CONDITION AFTER +/- 20 YEARS WITH MORPHOLOGICAL ACCELERATION (MORFAC=125).	104
FIGURE 6-28: BATHYMETRIC CHANGE OF DIPP I COMPARED TO NATURAL CONDITION AFTER +/- 25 YEARS WITH MORPHOLOGICAL ACCELERATION (MORFAC=125).	104
FIGURE 6-29: BATHYMETRIC CHANGE OF SIP II COMPARED TO NATURAL CONDITION AFTER +/- 5 YEARS WITH MORPHOLOGICAL ACCELERATION (MORFAC=125).	105
FIGURE 6-30: BATHYMETRIC CHANGE OF SIP II COMPARED TO NATURAL CONDITION AFTER +/- 10 YEARS WITH MORPHOLOGICAL ACCELERATION (MORFAC=125).	105
FIGURE 6-31: BATHYMETRIC CHANGE OF SIP II COMPARED TO NATURAL CONDITION AFTER +/- 15 YEARS WITH MORPHOLOGICAL ACCELERATION (MORFAC=125).	106
FIGURE 6-32: BATHYMETRIC CHANGE OF SIP II COMPARED TO NATURAL CONDITION AFTER +/- 20 YEARS WITH MORPHOLOGICAL ACCELERATION (MORFAC=125).	106
FIGURE 6-33: BATHYMETRIC CHANGE OF SIP II COMPARED TO NATURAL CONDITION AFTER +/- 25 YEARS WITH MORPHOLOGICAL ACCELERATION (MORFAC=125).	107
FIGURE 6-34: BATHYMETRIC CHANGE OF TIPA II COMPARED TO NATURAL CONDITION AFTER +/- 5 YEARS WITH MORPHOLOGICAL ACCELERATION (MORFAC=125).	108
FIGURE 6-35: BATHYMETRIC CHANGE OF TIPA II COMPARED TO NATURAL CONDITION AFTER +/- 10 YEARS WITH MORPHOLOGICAL ACCELERATION (MORFAC=125).	109
FIGURE 6-36: BATHYMETRIC CHANGE OF TIPA II COMPARED TO NATURAL CONDITION AFTER +/- 15 YEARS WITH MORPHOLOGICAL ACCELERATION (MORFAC=125).	109
FIGURE 6-37: BATHYMETRIC CHANGE OF TIPA II COMPARED TO NATURAL CONDITION AFTER +/- 20 YEARS WITH MORPHOLOGICAL ACCELERATION (MORFAC=125).	110

FIGURE 6-38: BATHYMETRIC CHANGE OF TIPA II COMPARED TO NATURAL CONDITION AFTER +/- 25 YEARS WITH MORPHOLOGICAL ACCELERATION (MORFAC=125).....	110
FIGURE 6-39: BATHYMETRIC CHANGE OF DIPP II COMPARED TO NATURAL CONDITION AFTER +/- 5 YEARS WITH MORPHOLOGICAL ACCELERATION (MORFAC=125).....	111
FIGURE 6-40: BATHYMETRIC CHANGE OF DIPP II COMPARED TO NATURAL CONDITION AFTER +/- 10 YEARS WITH MORPHOLOGICAL ACCELERATION (MORFAC=125).....	112
FIGURE 6-41: BATHYMETRIC CHANGE OF DIPP II COMPARED TO NATURAL CONDITION AFTER +/- 15 YEARS WITH MORPHOLOGICAL ACCELERATION (MORFAC=125).....	112
FIGURE 6-42: BATHYMETRIC CHANGE OF DIPP II COMPARED TO NATURAL CONDITION AFTER +/- 20 YEARS WITH MORPHOLOGICAL ACCELERATION (MORFAC=125).....	113
FIGURE 6-43: BATHYMETRIC CHANGE OF DIPP II COMPARED TO NATURAL CONDITION AFTER +/- 25 YEARS WITH MORPHOLOGICAL ACCELERATION (MORFAC=125).....	113
FIGURE 6-44: MAP OF SEDIMENTATION/EROSION WITH SIP I DURING THE FIRST 5 YEARS WITH MORPHOLOGICAL ACCELERATION (MORFAC=125).	114
FIGURE 6-45: MAP OF SEDIMENTATION/EROSION WITH SIP I DURING THE SECOND 5 YEARS WITH MORPHOLOGICAL ACCELERATION (MORFAC=125).	115
FIGURE 6-46: MAP OF SEDIMENTATION/EROSION WITH SIP I DURING THE THIRD 5 YEARS WITH MORPHOLOGICAL ACCELERATION (MORFAC=125).	115
FIGURE 6-47: MAP OF SEDIMENTATION/EROSION WITH SIP I DURING THE FOURTH 5 YEARS WITH MORPHOLOGICAL ACCELERATION (MORFAC=125).	116
FIGURE 6-48: MAP OF SEDIMENTATION/EROSION WITH SIP I DURING THE FIFTH 5 YEARS WITH MORPHOLOGICAL ACCELERATION (MORFAC=125).	116
FIGURE 6-49: MAP OF SEDIMENTATION/EROSION WITH DIPP I DURING THE FIRST 5 YEARS WITH MORPHOLOGICAL ACCELERATION (MORFAC=125).	117
FIGURE 6-50: MAP OF SEDIMENTATION/EROSION WITH DIPP I DURING THE SECOND 5 YEARS WITH MORPHOLOGICAL ACCELERATION (MORFAC=125).	118
FIGURE 6-51: MAP OF SEDIMENTATION/EROSION WITH DIPP I DURING THE THIRD 5 YEARS WITH MORPHOLOGICAL ACCELERATION (MORFAC=125).	118
FIGURE 6-52: MAP OF SEDIMENTATION/EROSION WITH DIPP I DURING THE FOURTH 5 YEARS WITH MORPHOLOGICAL ACCELERATION (MORFAC=125).	119
FIGURE 6-53: MAP OF SEDIMENTATION/EROSION WITH DIPP I DURING THE FIFTH 5 YEARS WITH MORPHOLOGICAL ACCELERATION (MORFAC=125).	119
FIGURE 6-54: MAP OF SEDIMENTATION/EROSION WITH SIP II DURING THE FIRST 5 YEARS WITH MORPHOLOGICAL ACCELERATION (MORFAC=125).	120
FIGURE 6-55: MAP OF SEDIMENTATION/EROSION WITH SIP II DURING THE SECOND 5 YEARS WITH MORPHOLOGICAL ACCELERATION (MORFAC=125).	120
FIGURE 6-56: MAP OF SEDIMENTATION/EROSION WITH SIP II DURING THE THIRD 5 YEARS WITH MORPHOLOGICAL ACCELERATION (MORFAC=125).	121
FIGURE 6-57: MAP OF SEDIMENTATION/EROSION WITH SIP II DURING THE FOURTH 5 YEARS WITH MORPHOLOGICAL ACCELERATION (MORFAC=125).	121
FIGURE 6-58: MAP OF SEDIMENTATION/EROSION WITH SIP II DURING THE FIFTH 5 YEARS WITH MORPHOLOGICAL ACCELERATION (MORFAC=125).	122
FIGURE 6-59: MAP OF SEDIMENTATION/EROSION WITH TIPA II DURING THE FIRST 5 YEARS WITH MORPHOLOGICAL ACCELERATION (MORFAC=125).	123
FIGURE 6-60: MAP OF SEDIMENTATION/EROSION WITH TIPA II DURING THE SECOND 5 YEARS WITH MORPHOLOGICAL ACCELERATION (MORFAC=125).	124

FIGURE 6-61: MAP OF SEDIMENTATION/EROSION WITH TIPA II DURING THE THIRD 5 YEARS WITH MORPHOLOGICAL ACCELERATION (MORFAC=125).	124
FIGURE 6-62: MAP OF SEDIMENTATION/EROSION WITH TIPA II DURING THE FOURTH 5 YEARS WITH MORPHOLOGICAL ACCELERATION (MORFAC=125).	125
FIGURE 6-63: MAP OF SEDIMENTATION/EROSION WITH TIPA II DURING THE FIFTH 5 YEARS WITH MORPHOLOGICAL ACCELERATION (MORFAC=125).	125
FIGURE 6-64: MAP OF SEDIMENTATION/EROSION WITH DIPP II DURING THE FIRST 5 YEARS WITH MORPHOLOGICAL ACCELERATION (MORFAC=125).	126
FIGURE 6-65: MAP OF SEDIMENTATION/EROSION WITH DIPP II DURING THE SECOND 5 YEARS WITH MORPHOLOGICAL ACCELERATION (MORFAC=125).	127
FIGURE 6-66: MAP OF SEDIMENTATION/EROSION WITH DIPP II DURING THE THIRD 5 YEARS WITH MORPHOLOGICAL ACCELERATION (MORFAC=125).	127
FIGURE 6-67: MAP OF SEDIMENTATION/EROSION WITH DIPP II DURING THE FOURTH 5 YEARS WITH MORPHOLOGICAL ACCELERATION (MORFAC=125).	128
FIGURE 6-68: MAP OF SEDIMENTATION/EROSION WITH DIPP II DURING THE FIFTH 5 YEARS WITH MORPHOLOGICAL ACCELERATION (MORFAC=125).	128

1. INTRODUCTION

1.1 THE ASSIGNMENT

The development of the Belgian Offshore Grid (BOG) aims to optimise the transport of future offshore electricity production to land. Elia Asset N.V. is responsible of that development and awarded International Marine and Dredging Consultants NV and its partner Tractebel Engineering the contract for Marine Consulting services. This order was issued based on the European Tender N°4074323 and the contract notice N° 2012/S 33-053758.

1.2 AIM OF THE STUDY

The overall aim of the Marine Consulting services is related to the following tasks:

- General coordination; project management and project planning;
- Feasibility study of the platform locations and submarine cable routings;
- Preparation of the input to the design basis;
- Preparation of and support to the seabed survey and sampling campaign;
- Follow-up of the seabed survey and laboratory tests;
- Identification of existing and any proposed third party crossings necessary to facilitate the laying of the submarine and land cables;
- Conceptual design of all required third party crossings (offshore and onshore), including the deliverance of all the relevant 'Letters of no Objection' for the crossings, necessary for permits and consents, management and preparation of all third party crossing agreements;
- Conceptual design of the land-fall solutions and the definition onshore cable routing;
- The preparation of all necessary permits and consents required to be submitted to the concerned Belgian Authorities, including all on-shore permits;
- Produce and deliver the Environmental Impact Assessment (EIA) for the marine aspects of the project;
- Formulation of an offshore foundation and submarine cable route maintenance programme;
- HS&E support conform to the Belgian and Flemish legislation;
- Ensure the coordination for safety and health.

1.3 OVERVIEW OF THE STUDY

The present study is part of the Environmental Impact Assessment (EIA). The description of the initial reference situation and the possible natural evolution of the subsurface is an important element of the EIA. In order to assess the autonomic evolution of the seafloor a numerical model had to be set up that simulates the tidal currents, wave action and sediment transport in and around the island location. The impact of the island with relation to these phenomena is also examined. In addition, the dredging and disposal methods for the construction of the artificial island will likely cause turbidity and sediment dispersion. In order to assess this impact of the dredging activities on the background turbidity and suspended sediment levels, a dredging plume model study is performed. A numerical model is applied that simulates the tidal currents and sediment transport in the project area.

The sediment transport modelling study and plume dispersion study are part of the EIA. Both reports are put integrally as attachment at the back of the EIA, the main results are presented in chapter 5.1 'Soil and Water' of the EIA.

The overview of these reports is listed below:

- Environmental Impact Assessment: I/RA/11413/12.266/CPA (IMDC, 2013a);
- Numerical Modelling of Sediment Transport: I/RA/11413/13.006/LWA (IMDC, 2013b);
- Numerical Modelling of Dredging Plume Dispersion: I/RA/11413/13.167/LWA (IMDC, 2013c).

The present study describes the numerical modelling of the sediment transport.

1.4 STRUCTURE OF THE REPORT

Chapter 2 describes the numerical flow, wave and sediment transport model. Chapter 3 gives an overview of the different scenarios that are examined and describes the applied schematisation. Results of storm impacts, long-term morphology analysis and application of other sediment transport formulae are presented separately. Conclusions are summarized in Chapter 4.

2. DESCRIPTION OF NUMERICAL MODEL

2.1 HYDRODYNAMIC FLOW MODEL

2.1.1 Numerical grid and bathymetry

The model is called “SBR model” (Sea – Belgian Offshore Grid – River) and it is nested into a larger mother model called “KaZNO model” (Figure 2-1). The computational grid size of the KaZNO model is 2.600 m × 7.000 m to 100 m × 140 m, and that of SBR model is 1.800 m × 2.700 m to 20 m × 30 m.

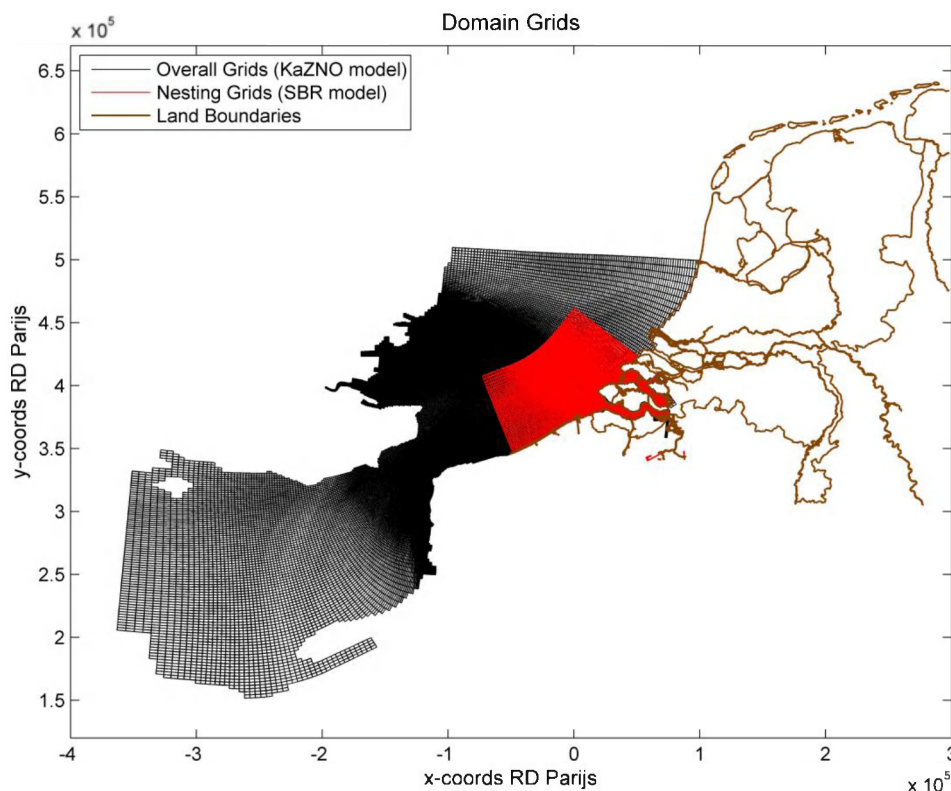


Figure 2-1: Layout of the model grids.

In order to obtain more detailed information in project zone which is called “Belgian Offshore Grid (BOG)”, a domain decomposition technique is employed to specifically refine this zone. The two alternatives Alpha AI1 and Alpha AI2 are indicated by the magenta crosses in Figure 2-2. In addition, domain decomposition is applied to the river domain but without any refinement, in order to reduce the computational time for the whole model domain. In BOG domain, the grid size reaches 235 m × 340 m to 110 m × 180 m.

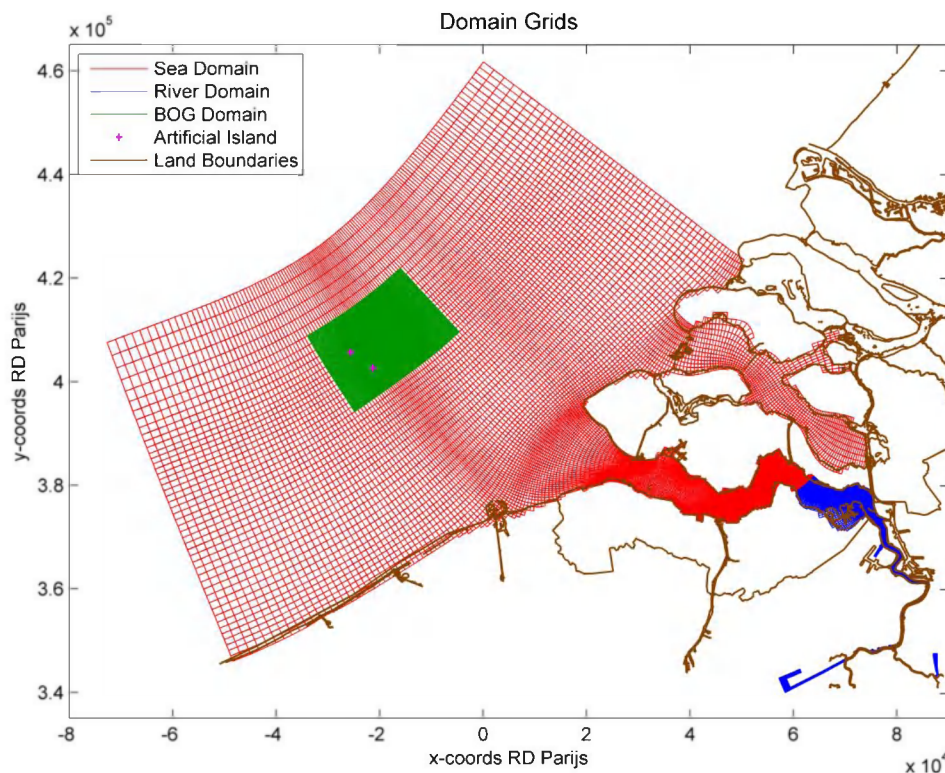


Figure 2-2: Three domains after domain decomposition.

The bathymetry map (Figure 2-3 and Figure 2-4) shows that the artificial island Alpha AI1 is situated at the Lodewijkbank with water depths around -20 to -30 m LAT¹. The artificial island Alpha AI2 is situated at the Blighbank with water depths around -15 to -22 m LAT.

¹ The model bathymetry is available in m NAP. For this reason, this vertical level is also used in the report and not only the project vertical reference level LAT. NAP = TAW + 2,333. At the project site, NAP = LAT + 2,08.

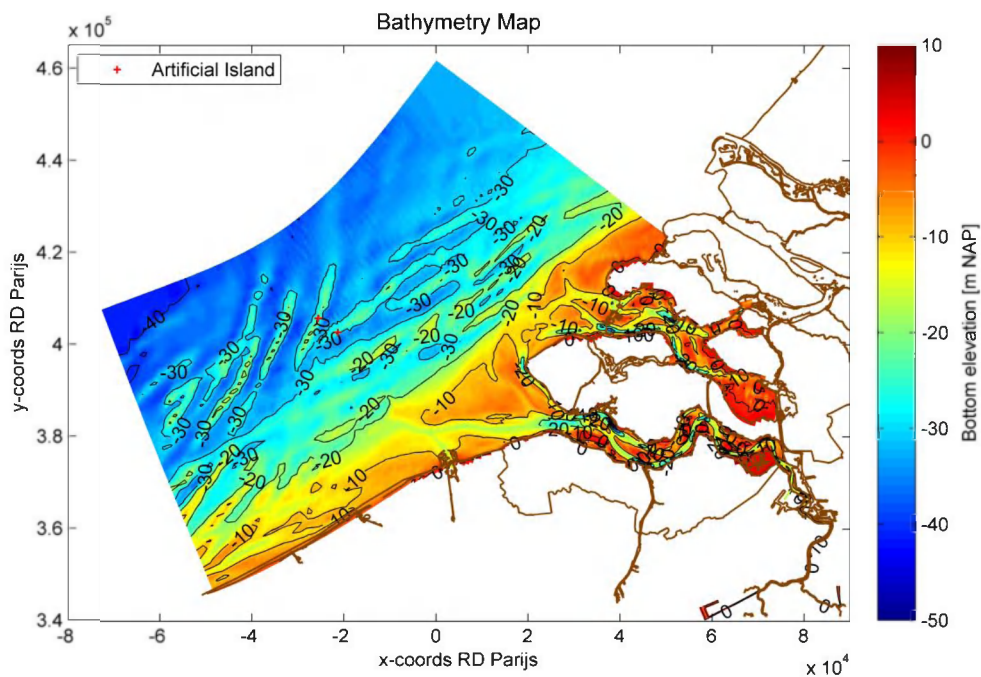


Figure 2-3: Bathymetry map of the flow model domain.

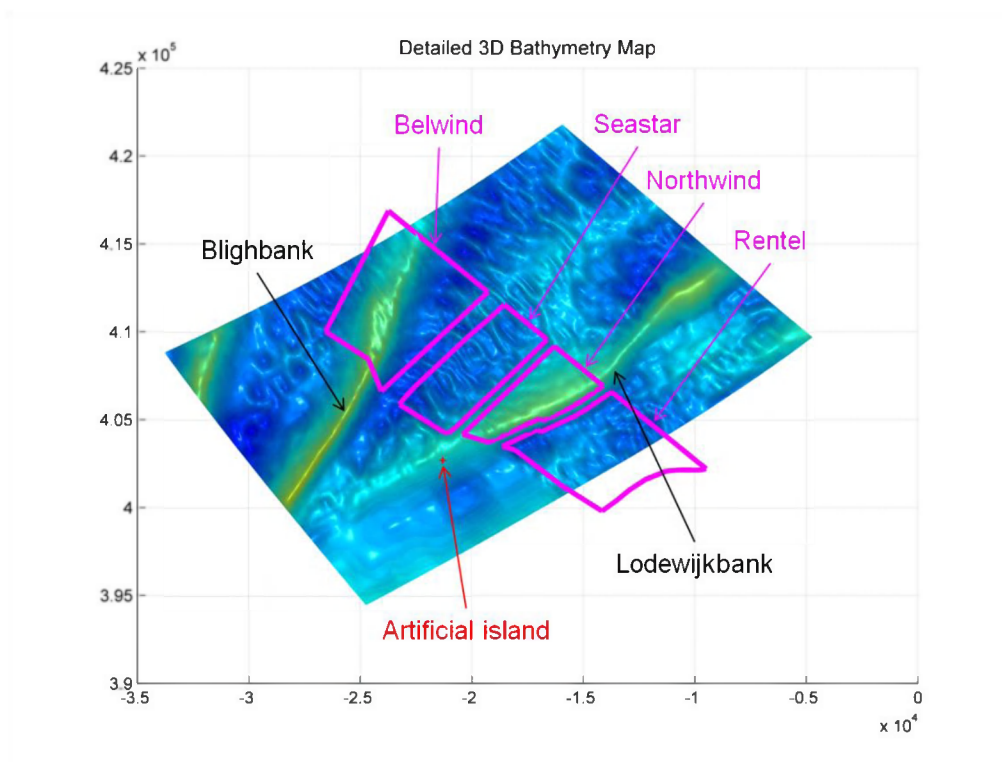


Figure 2-4: Three-dimensional bathymetry map of the BOG domain.

2.1.2 Boundary conditions

The SBR model is supplied by boundary conditions from the KaZNO model. In order to get a mean tidal forcing in this domain, one year of data of tidal ranges at three stations were statistically analysed and then a representative spring-neap tidal period was selected.

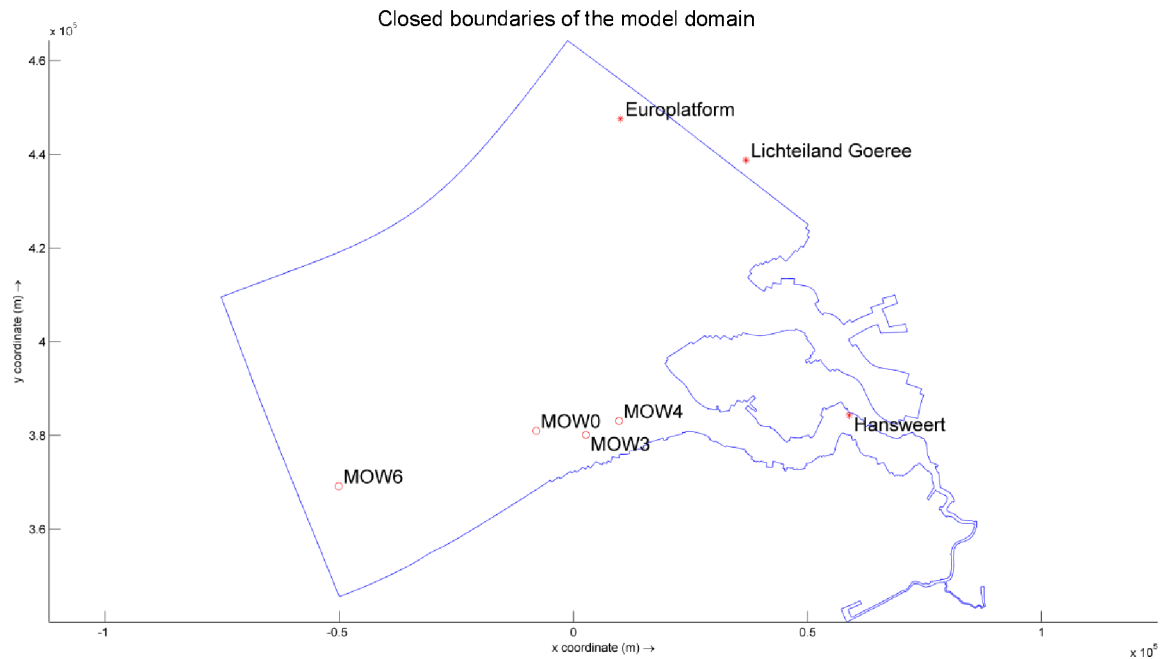


Figure 2-5: Tidal gauges in the model domain.

In fact, there are much more tidal gauges than what is shown in Figure 2-5. However, a complete set of tidal elevations for one year can only be found at the three stations, shown as stars in the figure.

Figure 2-6 shows the variation of tidal ranges at three observation stations during the whole year of 2009. The tidal range at Hansweert is much higher than those at the other stations, due to the tidal wave transformation in the estuary.

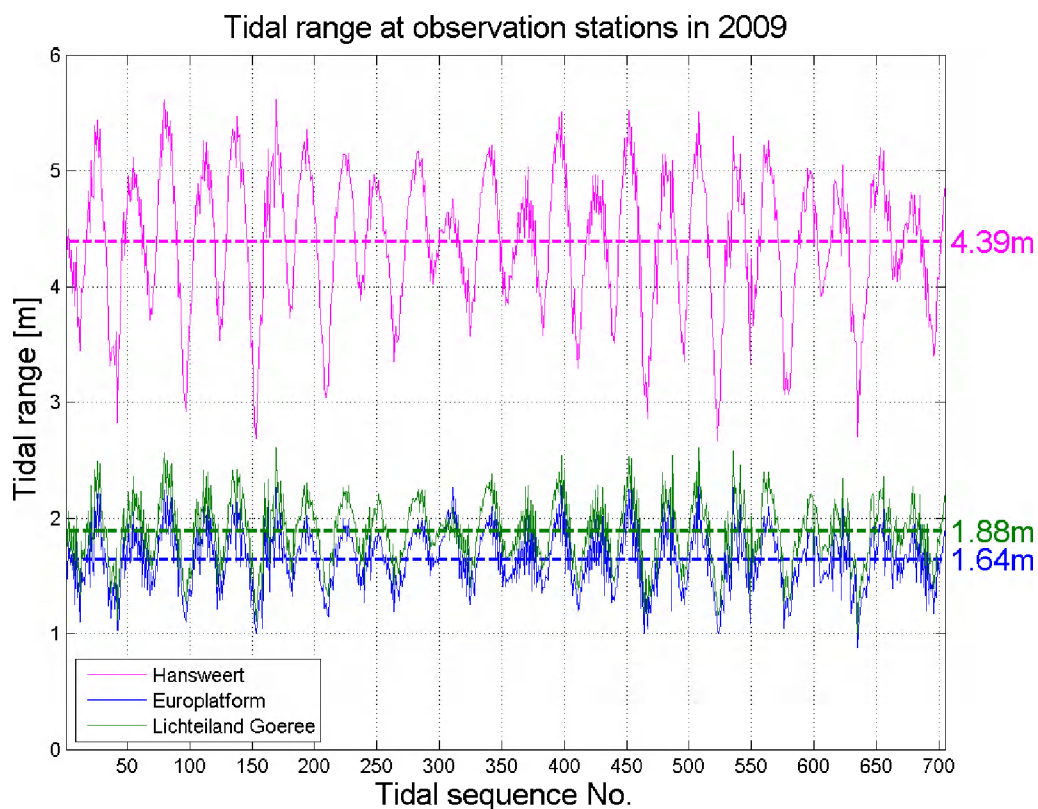


Figure 2-6: Tidal ranges at three stations in 2009.

Figure 2-7 shows that the three stations have an almost identical variation pattern in terms of the moving averaged tidal range for a spring-neap tidal cycle. The 394th spring-neap tidal cycle marked by the black dash line in the figure was selected as the representative tidal period to represent the mean tidal forcing of a whole year in this domain. Table 2-1 shows that the tidal ranges of the selected representative tidal period at the different three stations are all fairly close to their annual mean tidal ranges.

Table 2-1: Values of averaged tidal range of the selected representative tidal period and annual mean tidal range at three stations.

Location	averaged tidal range of the 394th spring-neap tidal cycle	annual mean tidal range
Europlatform	164,4 cm	164,3 cm
Lichteiland Goeree	188,6 cm	188,4 cm
Hansweert	441,8 cm	439,1 cm

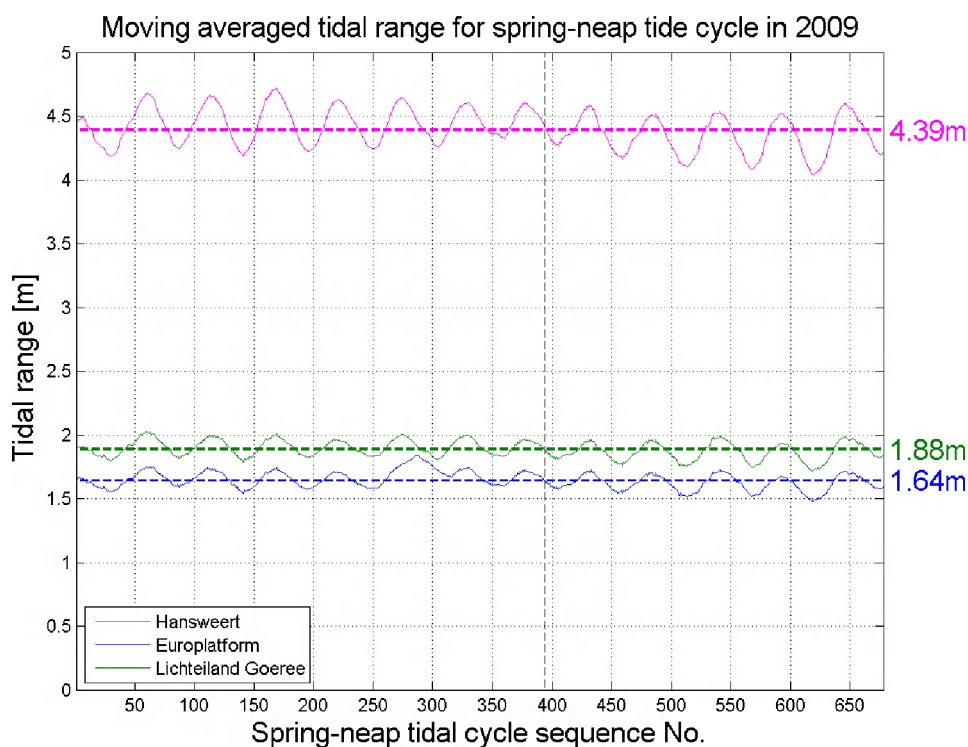


Figure 2-7: Moving averaged tidal range for spring-neap tidal cycle at three stations.

The annual representative spring-neap tidal cycle period is from 23-Jul-2009 14:00:00 to 07-Aug-2009 01:40:00, in total 20860 minutes (14 × 24 hours 50 minutes). The figure below shows the variation of the tidal elevation observed at the nearby tidal record station MOW0 during the representative spring-neap tidal period.

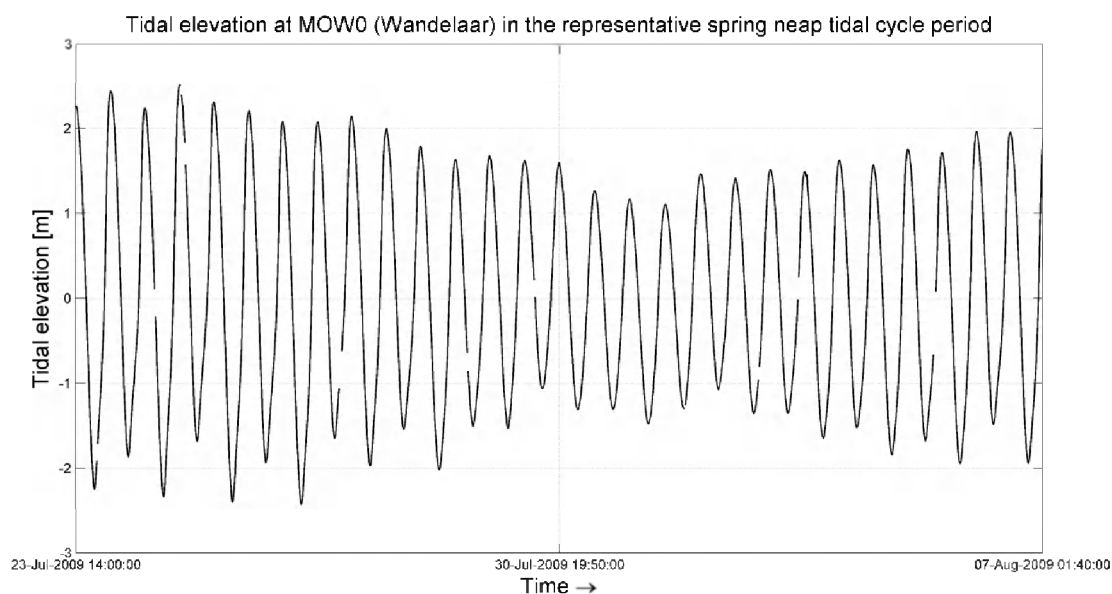


Figure 2-8: Tidal elevation observed at MOW0 station during the representative period.

2.1.3 Validation

The model validation period is from 12 April 2010 to 19 April 2010. Three measuring points are used for the model validation (Figure 2-9).

Firstly, a comparison of tidal elevation was carried out at Westhinder (Figure 2-10). There is a good agreement between the observation and modelling result, although the modelling result gives a maximum overestimation of around 10% in terms of the tidal range. More calibration of the mother model KaZNO is expected to reduce this overestimation.

The observed current velocity data at Scheur Wielingen in Figure 2-11 is actually sampled at -7.5 m below the water surface, and is not a depth averaged velocity. Due to the scarcity of available data, the observation point is also used to investigate the performance of the model in a qualitative point of view. From the figure, it can be seen that the model gives a satisfactory result compared to the observed data. The variation pattern of tidal current magnitude is captured by the model successfully, and the direction of current velocity is reproduced by the model quite well.

The velocity data at Lodewijkbank is collected in the Northwind (former Eldepasco) project area near to the project zone, 0.5 m above the bottom (at -26,23 m NAP) (Figure 2-9). At this point, the modelling result is shown to deviate from the observed data. However, the variation characteristics of the tidal current are effectively reproduced by the model. The magnitude of the current velocity is overestimated approximately 25% by the model, and the bias and RMSE are 0,079 m/s and 0,16 m/s respectively. On one side, this overestimation could be ascribed to the overestimation of the tidal range, which has been demonstrated in Figure 2-10. On the other side, the sampling point is located at the top of the sandbank, where the topography is highly variable (e.g. small dunes, ripples) and the hydrodynamics is locally complex. To resolve such high variability in sea bottom would of course result in a more detailed and refined numerical modelling scheme and associated increasing cost of computation time. In addition, the bathymetry input in the model is different from that found in the measurement (24,85 m vs. 26,73 m), which is also able to influence accuracy of the modelling.

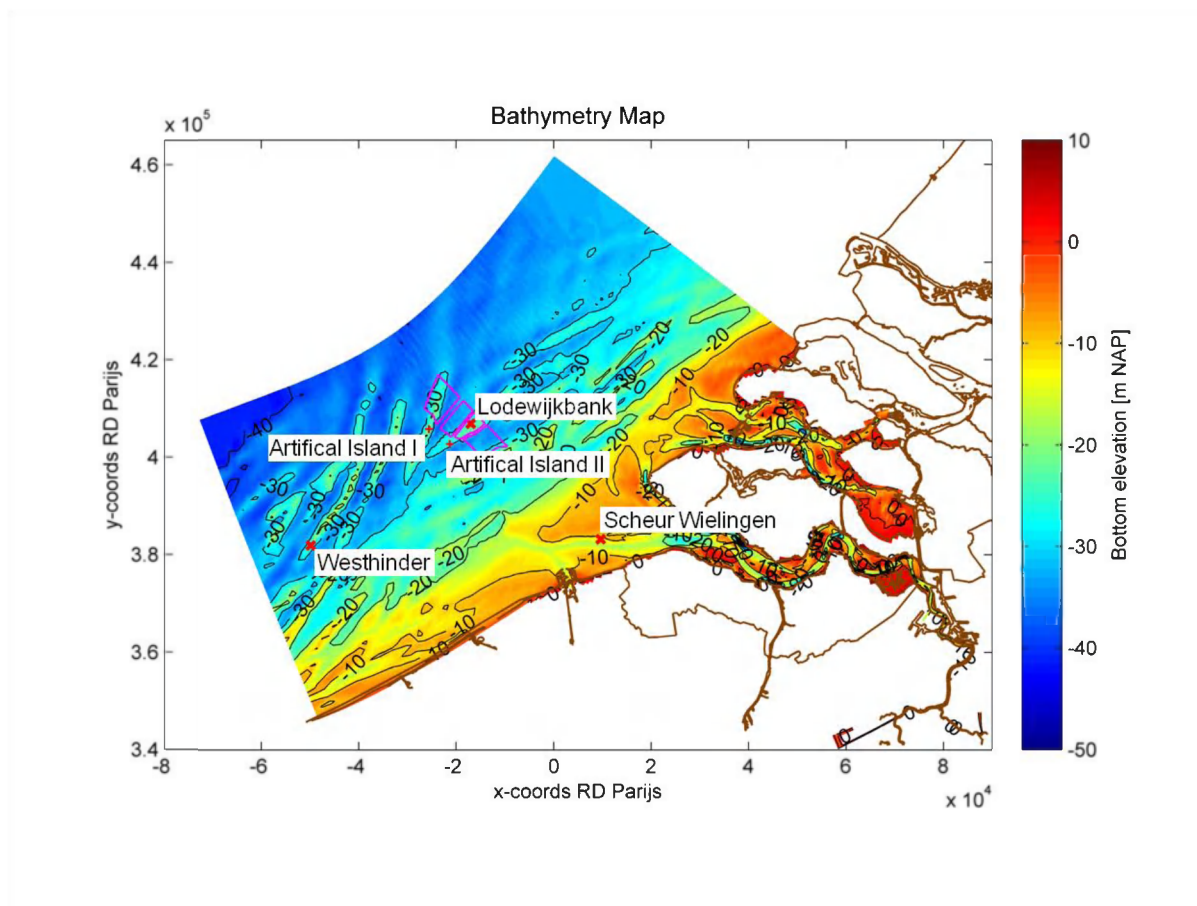


Figure 2-9: Location of observation points (indicated by the sign of red "x").

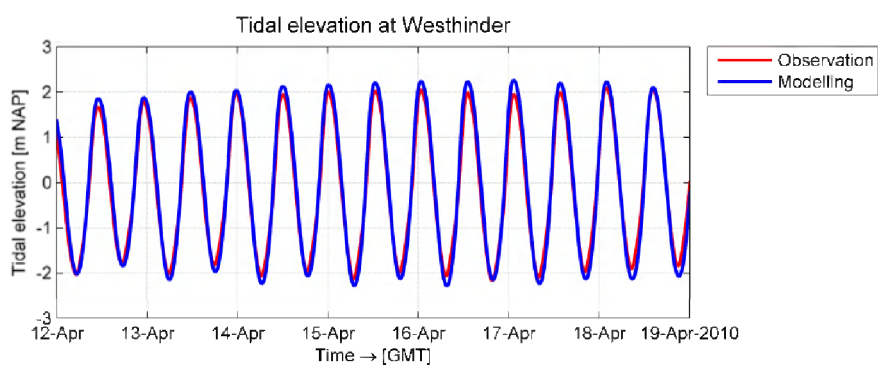


Figure 2-10: Comparison of tidal elevation at Westhinder.

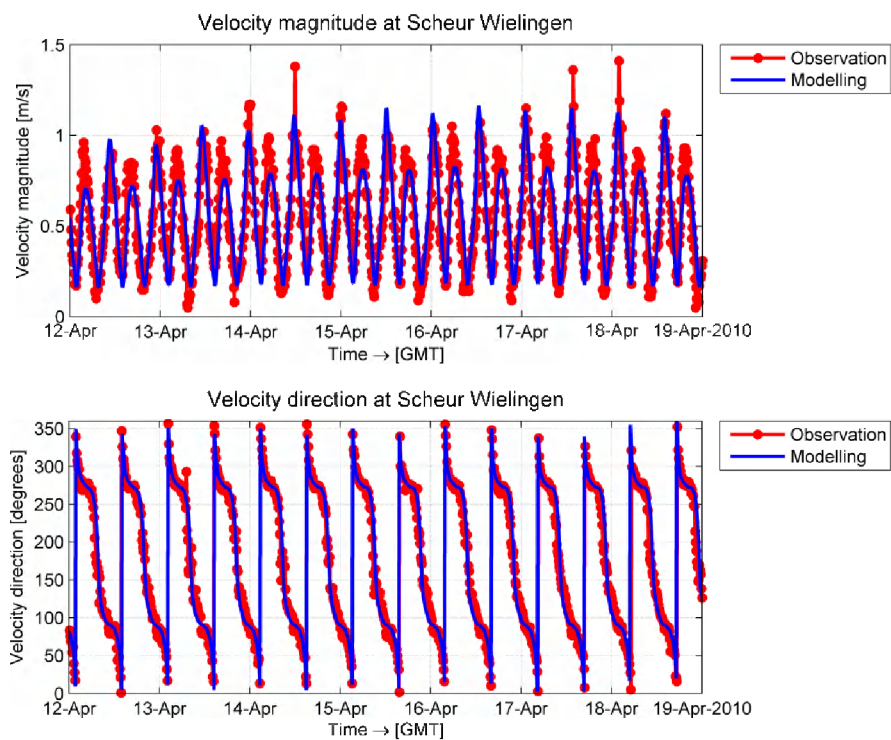


Figure 2-11: Comparison of velocity at Scheur Wielingen.

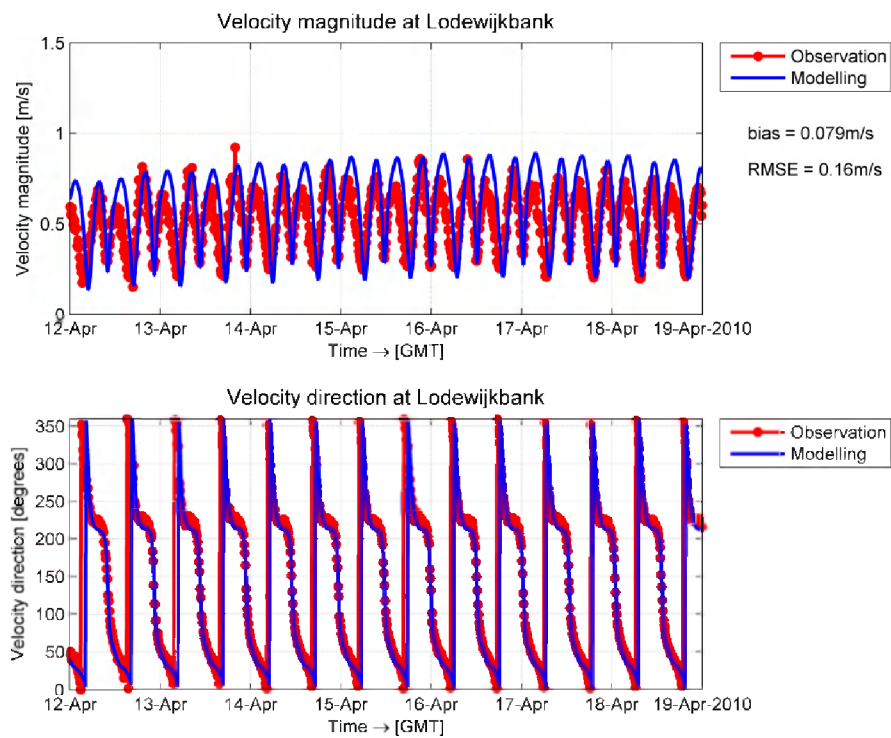


Figure 2-12: Comparison of velocity at Lodewijkbank.

2.2 WAVE MODEL

2.2.1 Introduction

In order to investigate the stability of the sandy subsurface under storm conditions, a wave model covering the sea domain of the flow model was developed using the wave module of Delft3D (Delft3D-WAVE). This is actually the same as the stand alone wave model SWAN (SWAN Cycle III version 40.72ABCDE) but integrated within Delft3D with a comprehensive user interface and allows coupling with the FLOW module.

SWAN (acronym for Simulating WAVes Nearshore), which is developed at the Delft University of Technology, is a third generation spectral wave model for obtaining realistic estimates of wave parameters in coastal areas, lakes and estuaries from given wind, bottom and current conditions. The model is based on the wave action balance with sources and sinks.

The following wave propagation processes are represented in SWAN (only the processes relevant to this case are given):

- Refraction due to spatial variations in bottom;
- Shoaling due to spatial variations in bottom;

The following wave generation and dissipation processes are represented in SWAN:

- Generation by wind;
- Dissipation by whitecapping;
- Dissipation by bottom friction;
- Wave-wave interactions (quadruplets and triads).

2.2.2 Numerical grid and bathymetry

The main wave model has a space-uniform resolution with a grid size of 1.000 m × 1.000 m (cf. Figure 2-13). To obtain a higher resolution for the alternative locations of the artificial island, a wave model with a grid size of approximately 230 m x 230 m is nested within the main wave model (cf. green grid in Figure 2-13, this is the same grid as the FLOW detailed grid BOG Domain). In Figure 2-14, showing the bathymetry map of the wave model, the wave monitoring stations “Sandettie Light (ship)” and “Europlatform” are indicated, from which sampled wave data were used to provide the boundary conditions for the wave model. Whereas sampled wave data from the other monitoring station “Westhinder” were used for the validation of the wave model. Also, the wind data at Westhinder was used to provide the wind boundary conditions of the wave model.

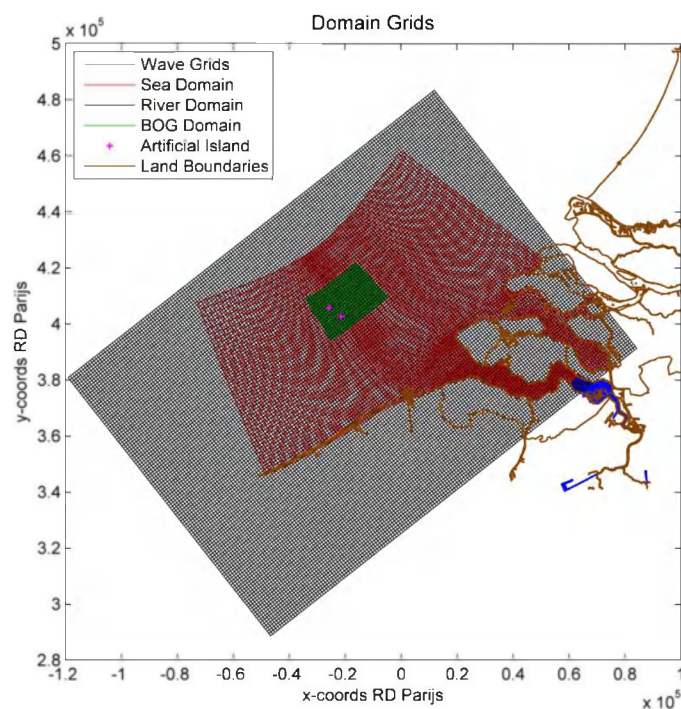


Figure 2-13: The wave model grids (main wave model: Wave Grid, nested wave model: BOG Domain) and the three domains of the flow model.

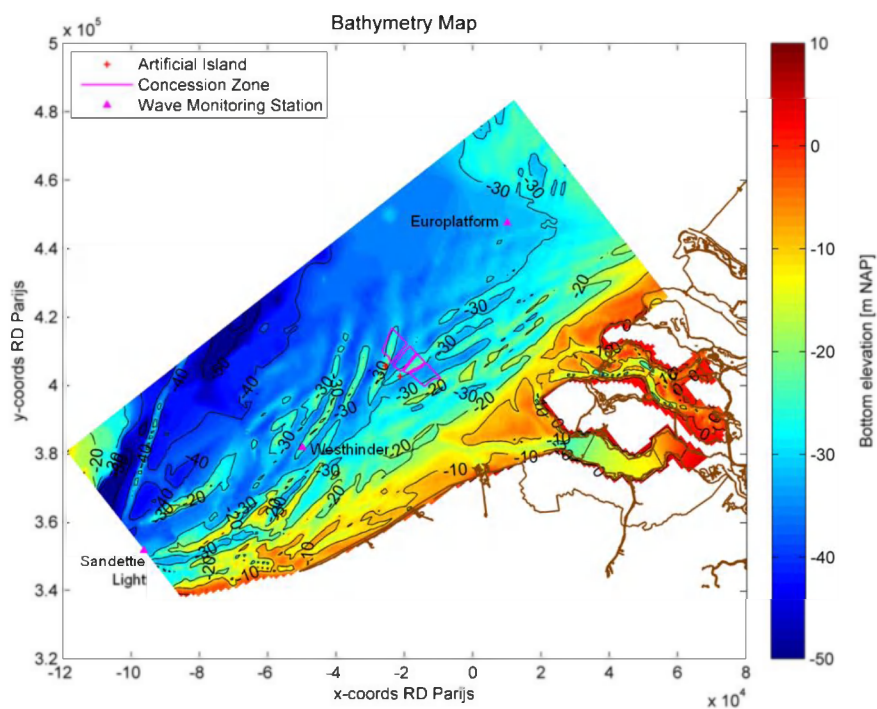


Figure 2-14: Bathymetry map of the wave model and three wave monitoring stations.

2.2.3 Boundary conditions

In order to determine the wave conditions for a 1- and 5-year-return storm, a wave dataset of 20 years collected at Westhinder was investigated. Taking 1-year-return storm for example, the significant wave height was used as an input variable to an extreme value analysis (EVA) tool developed at IMDC. Peaks of the significant wave height were firstly picked out by the tool and shown by red diamonds in Figure 2-15.

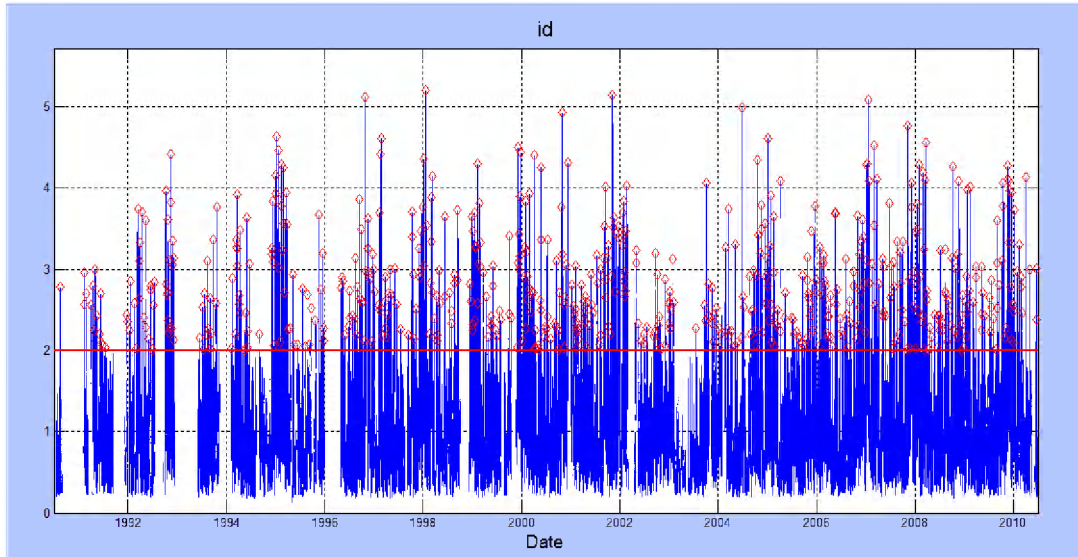


Figure 2-15: Significant wave height observed at Westhinder from 01-July-1990 to 01-July-2010.

Based on the peaks of the significant wave height, a correlation between the significant wave height and the return period was found by the EVA tool (Figure 2-16). The significant wave height in a one-year return storm is about 4.353 m. The two upper panels in this figure demonstrate the performance of the statistical model, from which a quite good agreement between real and modelled values can be observed.

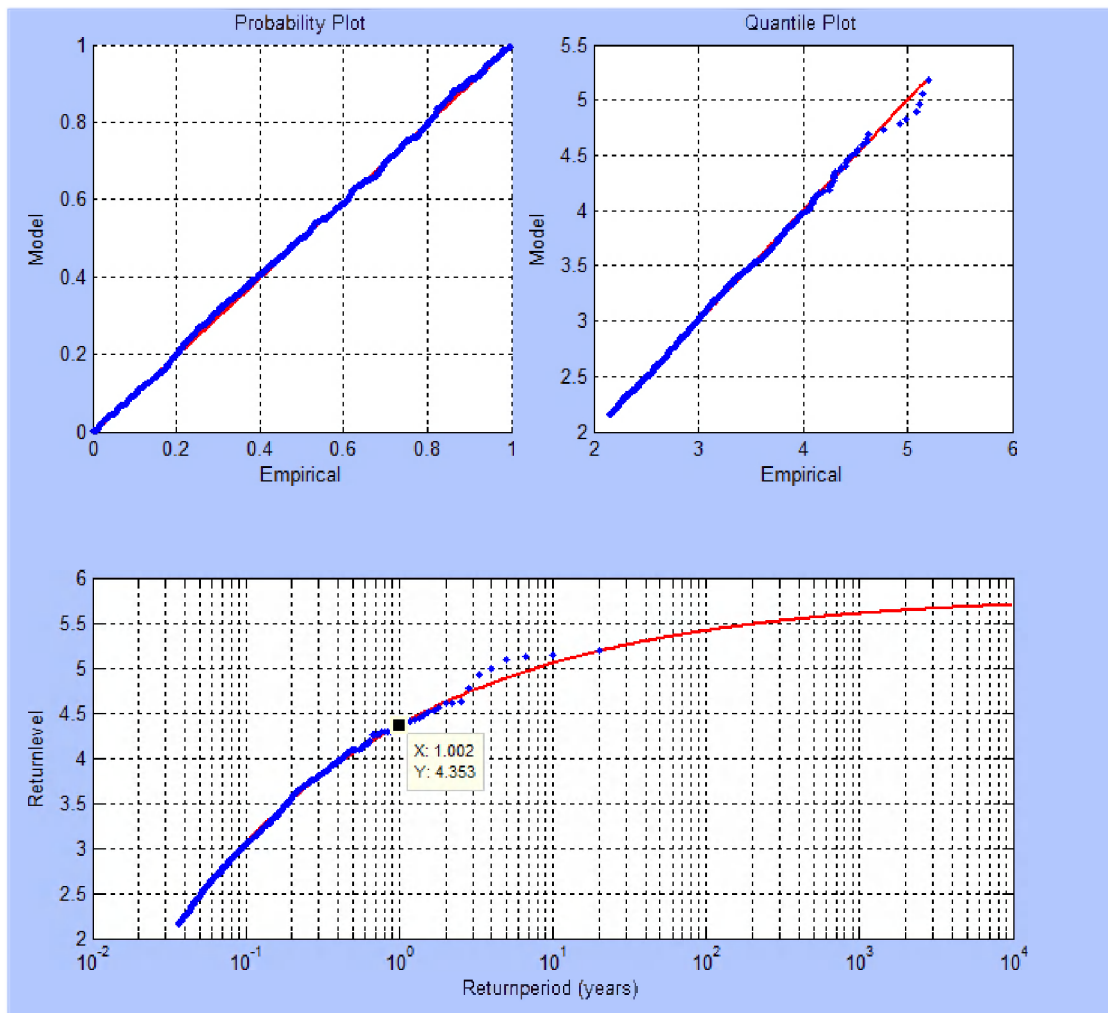
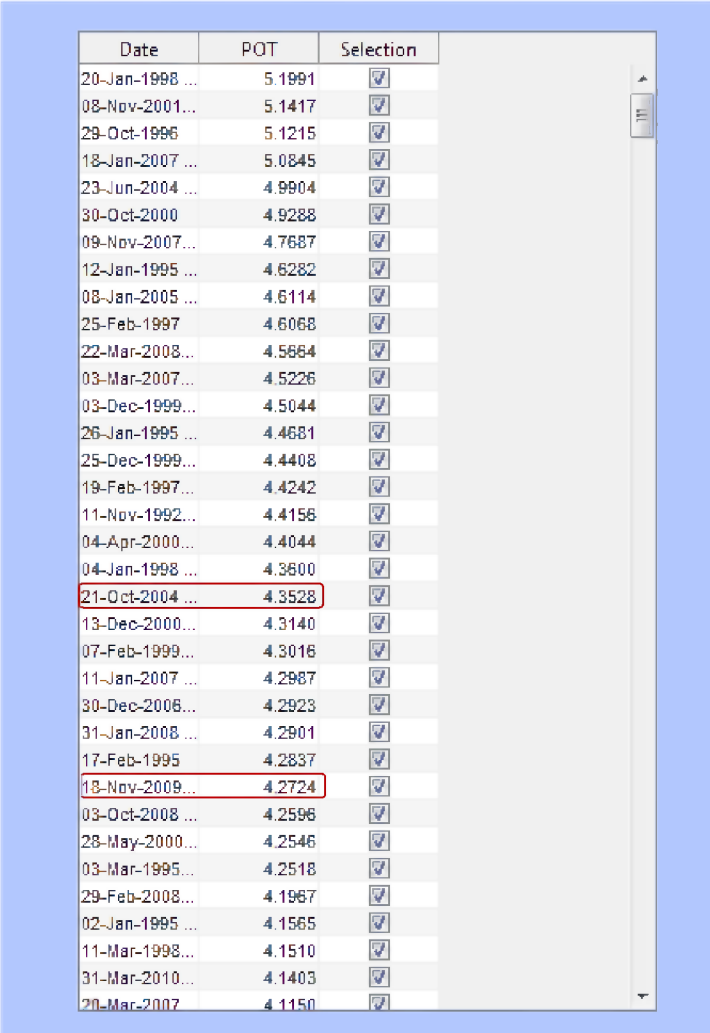


Figure 2-16: Upper panels: performance of the statistical model; lower panel: correlation between variable level and return period.

In Figure 2-17, the peaks of significant wave height are listed in a descending order. The 1-year-returned storm with significant wave height of 4,35 m occurs on 21-Oct-2004. But the sampled wave dataset at Sandettie Lightship is only available after 2005. The significant wave height (4,30 m) of the storm occurring on 11-Jan-2007 is quite close to that (4,35 m) of 1-year-returned storm. However a much larger storm with significant wave height of 5,09 m subsequently took place on 18-Jan-2007. If the wave peak (4,30 m) would be adapted to the lowest water at spring tide, the large storm with significant wave height of 5,09 m would be also included in the simulation period, as a result of which the significant wave height of the 1-year-returned storm becomes 5,09 m instead of 4,30 m during the simulation period. Another storm with a similar significant wave height of 4,27 m, which occurred on 18-Nov-2009 and was produced by a wind from west southwest (the predominant wind direction in the project area), is selected as the 1-year-returned storm. The same procedures were carried out and the 5-year-returned storm is selected (relevant figures are not shown here again). For both storms, the wind conditions collected at Westhinder during these storm periods were used as wind input for the wave model.



Date	POT	Selection
20-Jan-1998 ...	5.1991	<input checked="" type="checkbox"/>
08-Nov-2001...	5.1417	<input checked="" type="checkbox"/>
29-Oct-1996	5.1215	<input checked="" type="checkbox"/>
18-Jan-2007 ...	5.0845	<input checked="" type="checkbox"/>
23-Jun-2004 ...	4.9904	<input checked="" type="checkbox"/>
30-Oct-2000	4.9288	<input checked="" type="checkbox"/>
09-Nov-2007...	4.7687	<input checked="" type="checkbox"/>
12-Jan-1995 ...	4.6282	<input checked="" type="checkbox"/>
08-Jan-2005 ...	4.6114	<input checked="" type="checkbox"/>
25-Feb-1997	4.6068	<input checked="" type="checkbox"/>
22-Mar-2008...	4.5664	<input checked="" type="checkbox"/>
03-Mar-2007...	4.5226	<input checked="" type="checkbox"/>
03-Dec-1999...	4.5044	<input checked="" type="checkbox"/>
26-Jan-1995 ...	4.4681	<input checked="" type="checkbox"/>
25-Dec-1999...	4.4408	<input checked="" type="checkbox"/>
19-Feb-1997...	4.4242	<input checked="" type="checkbox"/>
11-Nov-1992...	4.4156	<input checked="" type="checkbox"/>
04-Apr-2000...	4.4044	<input checked="" type="checkbox"/>
04-Jan-1998 ...	4.3600	<input checked="" type="checkbox"/>
21-Oct-2004 ...	4.3528	<input checked="" type="checkbox"/>
13-Dec-2000...	4.3140	<input checked="" type="checkbox"/>
07-Feb-1999...	4.3016	<input checked="" type="checkbox"/>
11-Jan-2007 ...	4.2987	<input checked="" type="checkbox"/>
30-Dec-2006...	4.2923	<input checked="" type="checkbox"/>
31-Jan-2008 ...	4.2901	<input checked="" type="checkbox"/>
17-Feb-1995	4.2837	<input checked="" type="checkbox"/>
18-Nov-2009...	4.2724	<input checked="" type="checkbox"/>
03-Oct-2008 ...	4.2596	<input checked="" type="checkbox"/>
28-May-2000...	4.2546	<input checked="" type="checkbox"/>
03-Mar-1995...	4.2518	<input checked="" type="checkbox"/>
29-Feb-2008...	4.1967	<input checked="" type="checkbox"/>
02-Jan-1995 ...	4.1565	<input checked="" type="checkbox"/>
11-Mar-1998...	4.1510	<input checked="" type="checkbox"/>
31-Mar-2010...	4.1403	<input checked="" type="checkbox"/>
20-Mar-2007	4.1150	<input checked="" type="checkbox"/>

Figure 2-17: Peaks of the significant wave height monitored at Westhinder.

The selected 1- and 5-year-returned storm periods are simulated by consecutive stationary SWAN runs with an interval of 1 hour. Figure 2-18 and Figure 2-19 respectively display the wind input and wave boundary conditions, with an interval of 1 hour, applied to the wave model during the selected 1-year-returned storm period. The wind input and wave boundary conditions during the selected 5-year-returned storm period are equally displayed in Figure 2-20 and Figure 2-21. During the selected 1-year-returned storm period the predominant wind and wave direction was SW – WSW while during the selected 5-year-returned storm period the predominant wind and wave direction was NW-NNW.

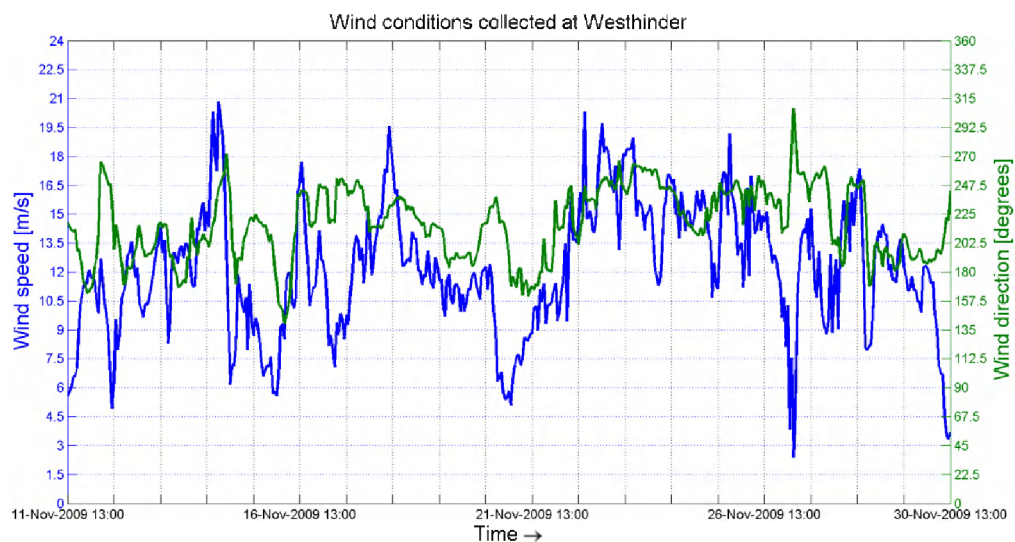


Figure 2-18: Wind conditions collected at Westhinder during the selected 1-year-returned storm period.

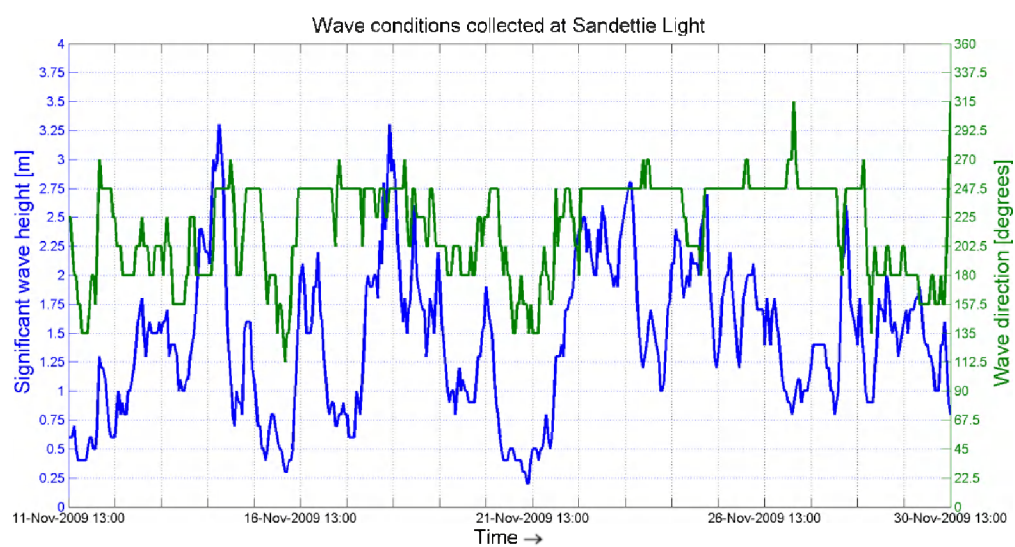


Figure 2-19: Wave conditions collected at Sandettie Lightship during the selected 1-year-returned storm period.

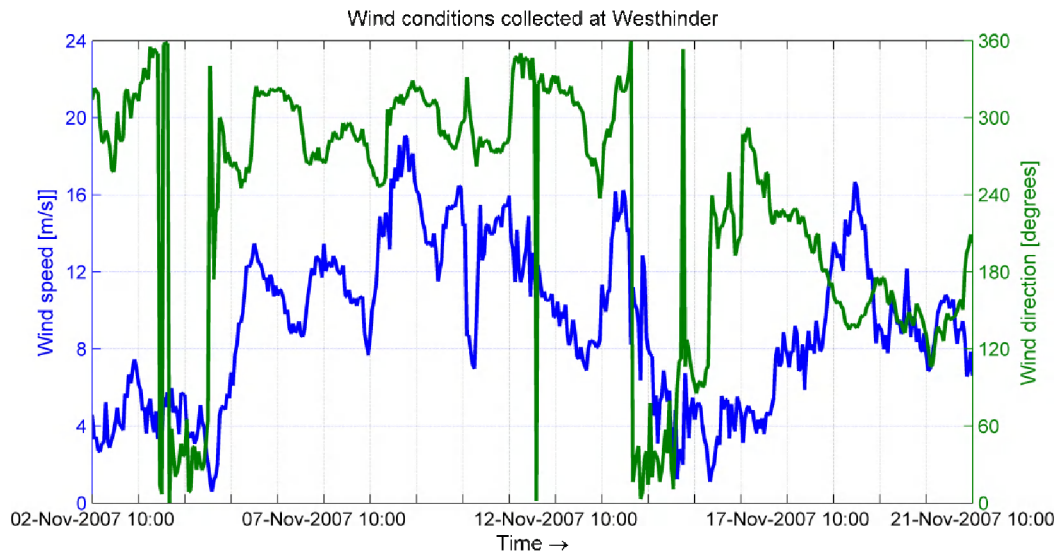


Figure 2-20: Wind conditions collected at Westhinder during the selected 5-year-returned storm period.

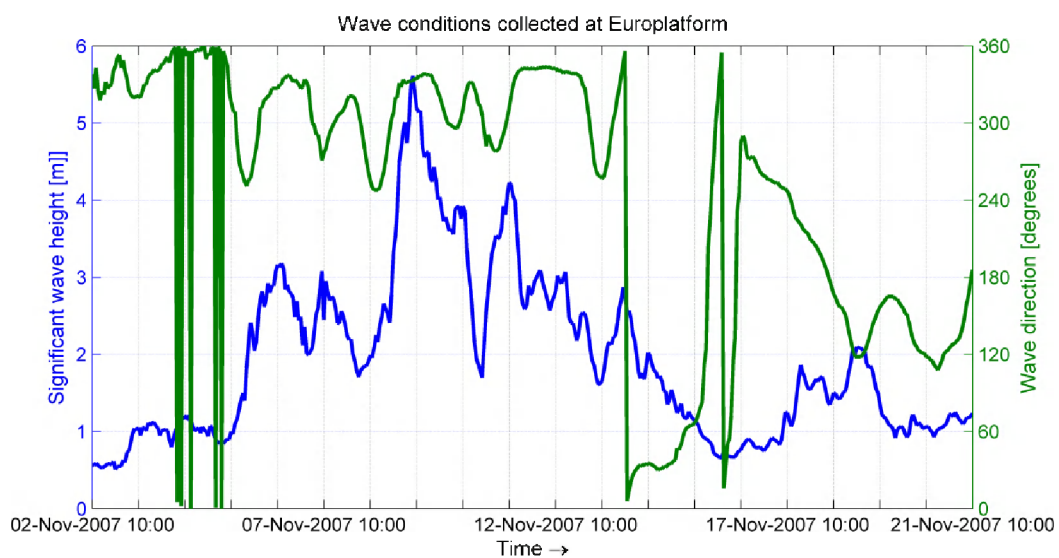


Figure 2-21: Wave conditions collected at Sandettie Lightship during the selected 5-year-returned storm period.

2.2.4 Validation

To validate the Delft3D-WAVE model, a comparison is made between the wave model results and the field measurements of the directional wave buoy at Westhinder. The validation is done by means of:

- A scatter diagram and a regression analysis of the significant wave height (cf. Figure 2-22 and Figure 2-24);

- A time series plot of the significant wave height H_{m0} , the mean zero-crossing wave period T_{m02} and the wave direction (cf. Figure 2-23 and Figure 2-25).

A quite good agreement is found between the modelled wave heights and the measured wave heights (cf. Figure 2-22 and Figure 2-24), certainly considering the fact that the Westhinder buoy is located in the main wave model with a coarse grid (1.000 m x 1.000 m). The spread of points around the regression line (red line in graph) is mainly due to the stationary mode of the simulations. In other words, the time it takes for a wave to travel from the Sandettie Lightship or Europlatform point to the Westhinder point and also variations in wind speed, direction and water level between time steps is not taken into account by the stationary simulations.

This good agreement is more apparent when comparing the time series (cf. Figure 2-23 and Figure 2-25). The mean zero-crossing wave period T_{m02} and the wave direction time series also show quite good agreement. Due to a difference in calculation of the wave period T_{m02} in SWAN and in the buoy measurements (IMDC, 2009), a correction was applied to the T_{m02} values calculated by SWAN to account for this difference. This has no effect on the wave periods within the model.

Due to this good agreement between simulation and measurement, no further calibration was deemed necessary.

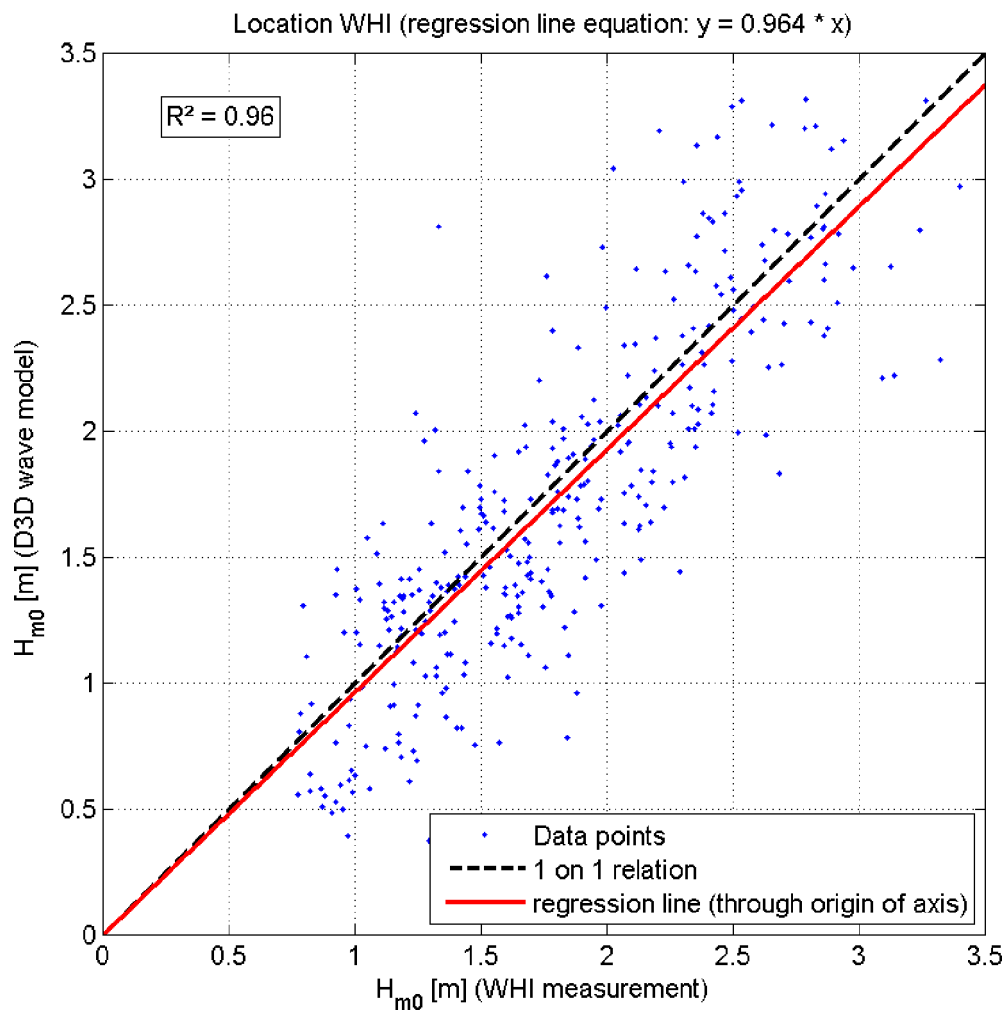


Figure 2-22: One-on-one relation between the significant wave height calculated by Delft3D-WAVE and measured at the Westhinder buoy location.

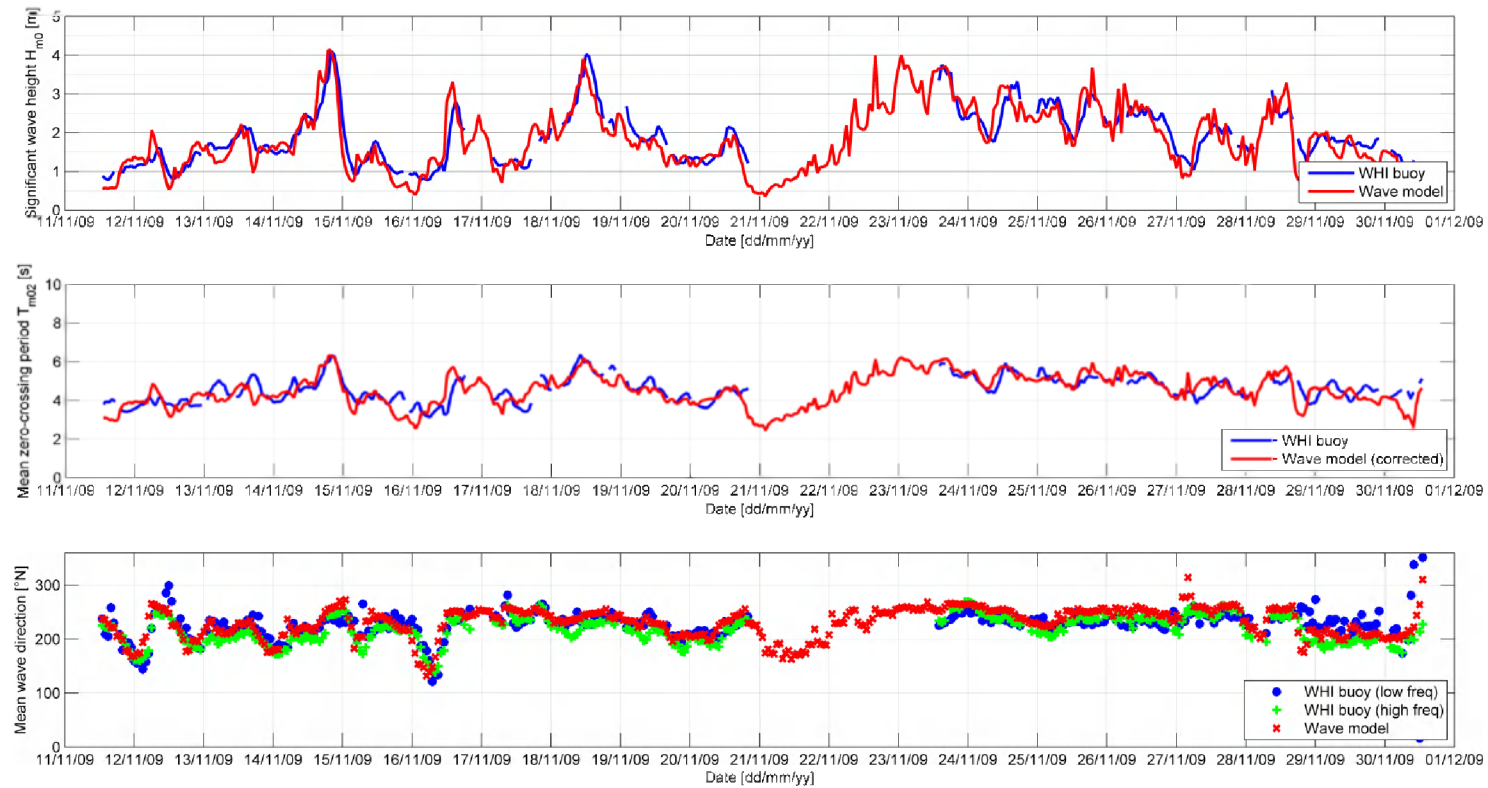


Figure 2-23: Validation of the Delft3D-WAVE model with field measurements of the directional wave buoy at the Westhinder bank. Comparison of the time series of the significant wave height H_{m0} , the mean zero-crossing wave period T_{m02} and wave direction.

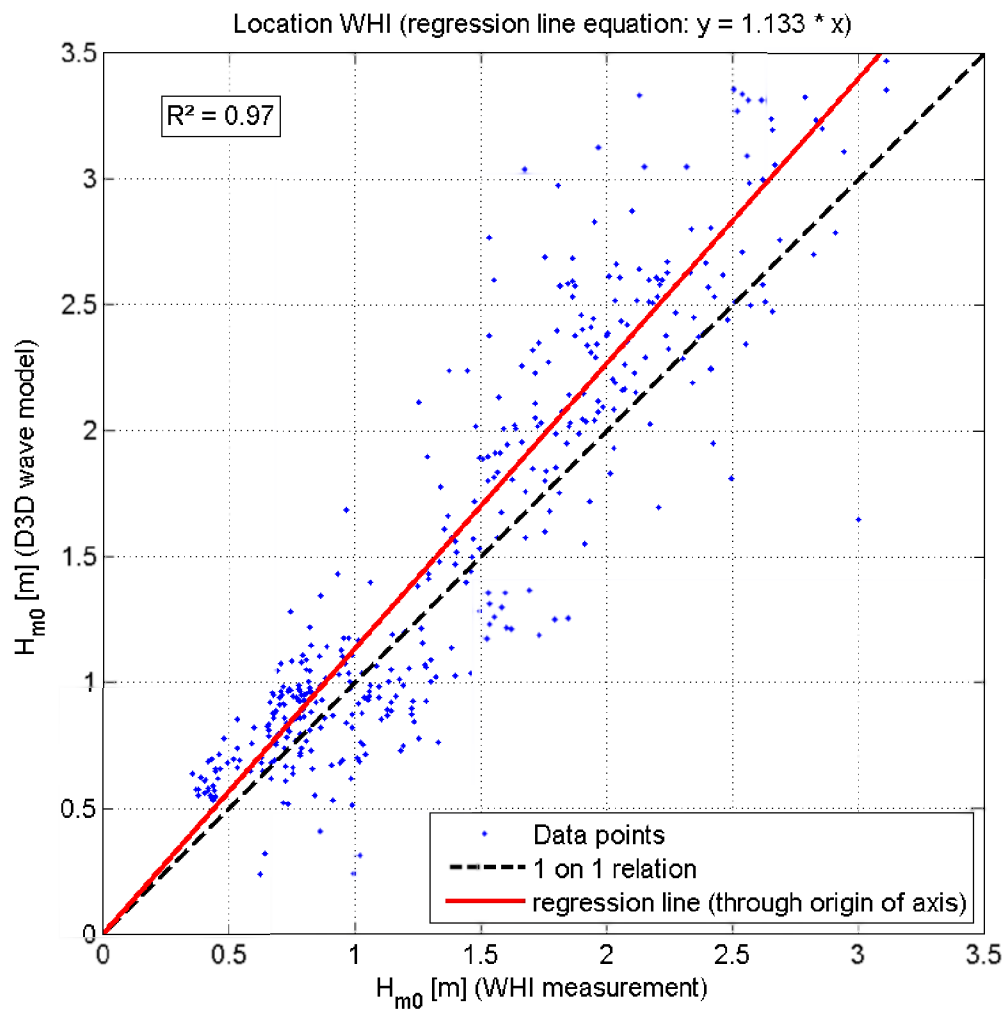


Figure 2-24: One-on-one relation between the significant wave height calculated by Delft3D-WAVE and measured at the Westhinder buoy location.

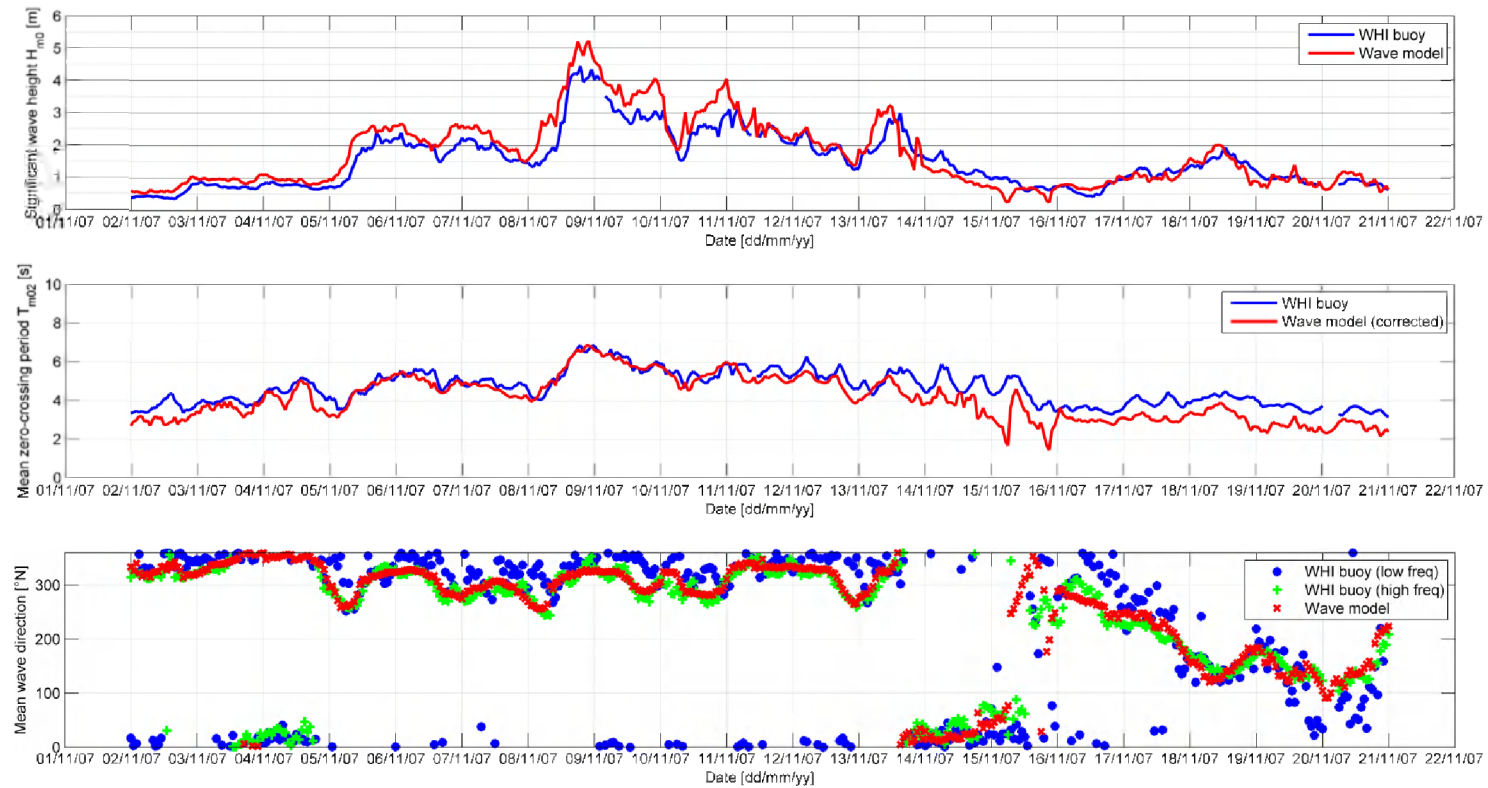


Figure 2-25: Validation of the Delft3D-WAVE model with field measurements of the directional wave buoy at the Westhinder bank. Comparison of the time series of the significant wave height H_{m0} , the mean zero-crossing wave period T_{m02} and wave direction.

2.3 SEDIMENT TRANSPORT MODEL

For the sediment transport, the Van Rijn TRANSPOR2000 approach is employed in the model (Van Rijn, 2003). The bed load transport and suspended transport are distinguished based on the reference height, below which the movement of sediment is treated as bed load transport whereas above the movement of sediment is treated as suspended transport. More detailed information about the approach can be found in the Delft3D-FLOW User Manual.

2.3.1 Boundary conditions and median grain size

In this model, the boundary condition for the sediment is specified by “equilibrium” concentrations. The equilibrium concentration is a function of the local current velocity. By this specification, the sediment concentrations are equal to those just inside the model domain, near-perfectly adapted sediment flux flows into the domain with little sedimentation or erosion near the model boundaries (Delft3D-FLOW User Manual).

According to the grain size distribution map (see IMDC, 2013a), the sediments in the project zone range between 200 and 500 μm . The sand from 300 to 350 μm is shown to cover most of the project zone. With the model updating of the grain size distribution is not feasible. Therefore a uniform grain size has to be selected. The model has been run respectively with grain sizes of 200, 350 and 500 μm for the selected representative spring-neap tidal cycle. The three scenarios with different grain sizes demonstrate almost the same direction of residual sediment transport (results are not shown here). 200 μm logically shows the highest residual sediment transport, maximally triple as much as 500 μm , while 350 μm only displays slightly larger residual sediment transport than 500 μm . Due to the largest coverage rate of sand from 300 to 350 μm in the project zone, a space-uniform grain size of 350 μm is adopted in the model.

3. SIMULATION RESULTS

3.1 SCENARIOS

The artificial island is schematised by three ways in the model: single inactive point (Figure 3-1), triple inactive points aligned to the main flow direction (Figure 3-2) and double inactive points perpendicular to the main flow direction (Figure 3-3). The different inactive points can be used to investigate impacts of the size of the artificial island on the ambient environment, in particular an extreme case that the artificial island is positioned perpendicularly to the main flow direction, is investigated by the double inactive points perpendicular to the main flow direction. The reference case is natural condition which does not have any artificial island. The sediment transport is investigated during two conditions. In the summer condition, only tidal forcing is considered for the formerly selected representative spring-neap tidal period. While in the winter condition, the tidal and wave forcings are coupled together in model. In addition, a technique of morphology acceleration is applied with the morphological scale factor (Morfac) to investigate the long-term morphological change driven by tides. The neutralisation of tidal forcing for impacts of 1-year-returned and 5-year-returned storms is investigated in the natural condition and the case with triple inactive points aligned to the main flow direction for Location I of the artificial island. Other two sediment transport formulae Bijker (1971) and Soulsby/Van Rijn (Delft3D-FLOW User Manual, 2011) are additionally used to be compared with the default transport formula Van Rijn (2000) within four scenarios. All scenarios performed in this study have been listed in Table 3-1.

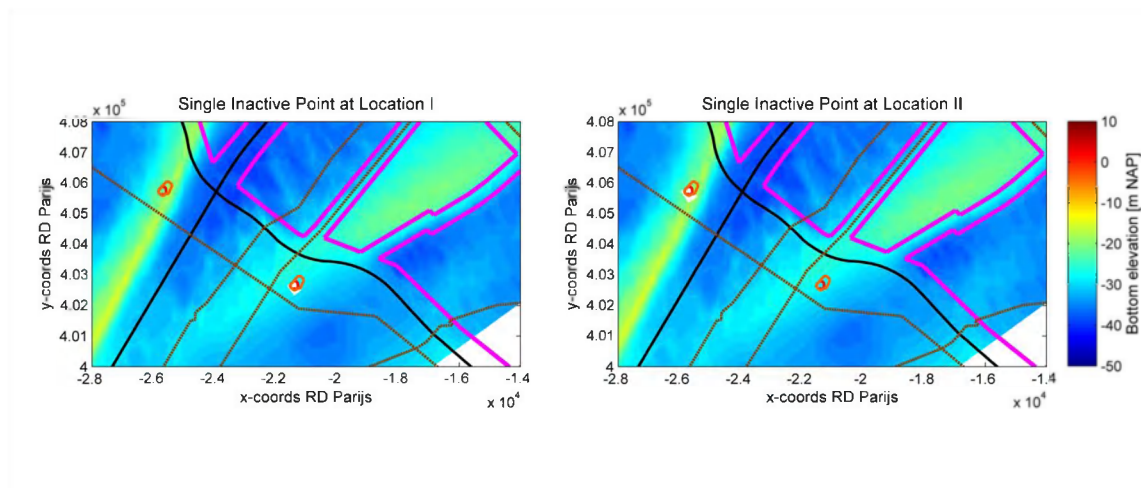


*Figure 3-1: Schematisation SIP (Single Inactive Point, area: ca. 180 m X 220 m)
left panel: Location I, right panel: Location II.*

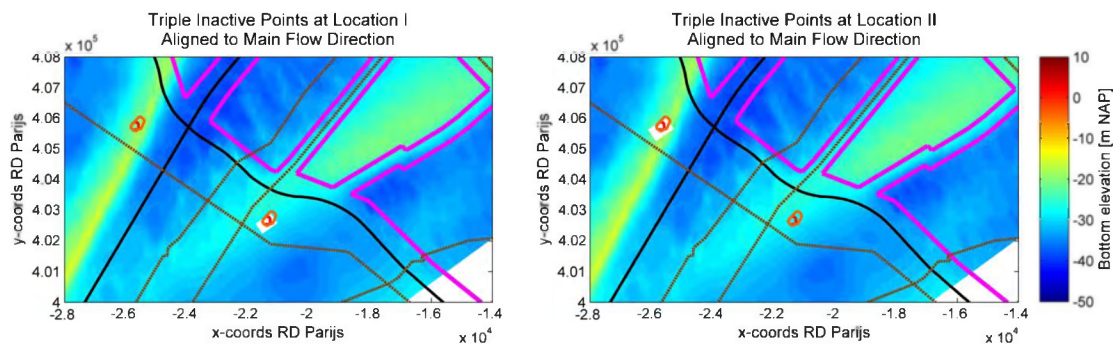


Figure 3-2: Schematisation TIPA (Triple Inactive Points Aligned to the main flow direction, area: ca. 3*180 m X 220 m)
left panel: Location I, right panel: Location II.

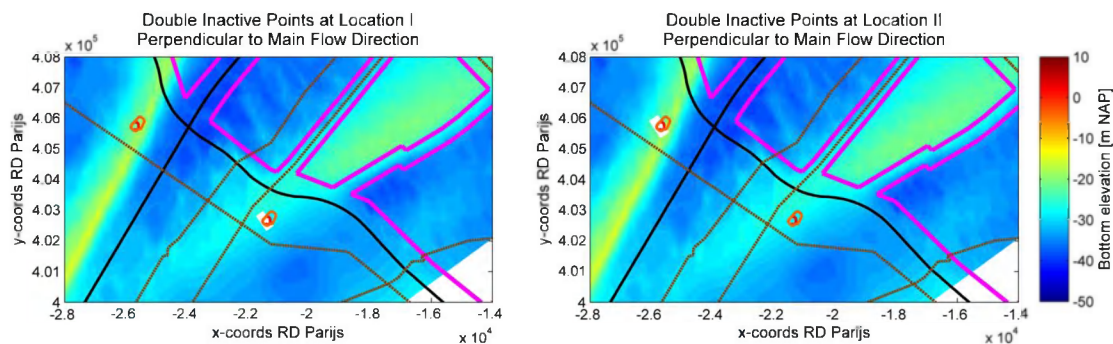


Figure 3-3: Schematisation DIPP (Double Inactive Points Perpendicular to the main flow direction, area: ca. 180 m X 2*220 m)
left panel: Location I, right panel: Location II.

Table 3-1: Overview of scenarios.

Model Set-up Island Case	summer condition, 14X24h50min, Morfac=1 (+/- 2 weeks)	winter condition, 1-year-returned storm, 14X24h50min, Morfac=1 (+/- 2 weeks)	winter condition, 5-year-returned storm, 14X24h50min, Morfac=1 (+/- 2 weeks)	summer condition, 5X14X24h50min, Morfac=125 (+/- 25 years)	summer condition, 14X24h50min, Morfac=25 (+/- 1 year)	winter condition, 1-year-returned storm, 14X24h50min, Morfac=1, followed by summer condition, 14X24h50min, Morfac=25, (+/- 1 year)	winter condition, 5-year-returned storm, 14X24h50min, Morfac=1, followed by summer condition, 14X24h50min, Morfac=125 (+/- 5 years)
NC	x	x	x	x	x*	x*	x
SIP I	x	x		x			
TIPA I	x	x	x	x	x*	x*	x
DIPP I	x	x		x			
SIP II	x	x		x			
TIPA II	x	x	x	x			
DIPP II	x	x		x			

NC: Natural Condition (without any artificial island);

SIP I: Single Inactive Point at Location I;

TIPA I: Triple Inactive Points Aligned to main flow direction at Location I;

DIPP I: Double Inactive Points Perpendicular to main flow direction at Location II;

SIP II: Single Inactive Point at Location I;

TIPA II: Triple Inactive Points Aligned to main flow direction at Location I;

DIPP II: Double Inactive Points Perpendicular to main flow direction at Location II;

summer condition: only tidal driven;

winter condition: tide + wave;

*: Other two sediment transport formulae Bijker (1971) and Soulsby/Van Rijn.

3.2 SCHEMATISATION ANALYSIS

The artificial island is schematised by SIP (single inactive point), TIPA (triple inactive points aligned to main flow direction) and DIPP (double inactive points perpendicular to main flow direction) at the two alternative locations. The schematisation analysis is performed by comparison with the natural condition in the summer and winter conditions. The comparison of averaged current ellipse, residual current and sedimentation/erosion is performed to analyse the impact of each schematisation compared to the natural condition based on scenarios with a simulation period around 2 weeks and without morphological acceleration.

3.2.1 Summer condition (Morfac=1, +/- 2 weeks)

In all figures shown thereafter, the magenta lines delineate the windmill concession zones, brown ones denote the submarine cables, and black ones mark pipelines.

3.2.1.1 Hydrodynamics

The hydrodynamics includes averaged current ellipse and residual current. Figure 3-4 ~ Figure 3-9 listed the comparison of the averaged current ellipse between each schematisation and natural condition at the two alternative locations. It could be found that the impacts of these schematisations are quite minor and only limited to the area adjacent to the artificial island.

The difference of residual current magnitude is calculated by results of the schematisation minus those of the natural condition. From Figure 3-10 to Figure 3-15 it could be also observed that the impacts of the schematisations on the residual current are mainly limited to the area near to the artificial island and distributed along the main flow direction from SW to NE. The size of artificial island is shown to influence the area affected by the schematisation significantly, and the orientation of the artificial island to the main flow direction is also shown to play an important role on the affected area.

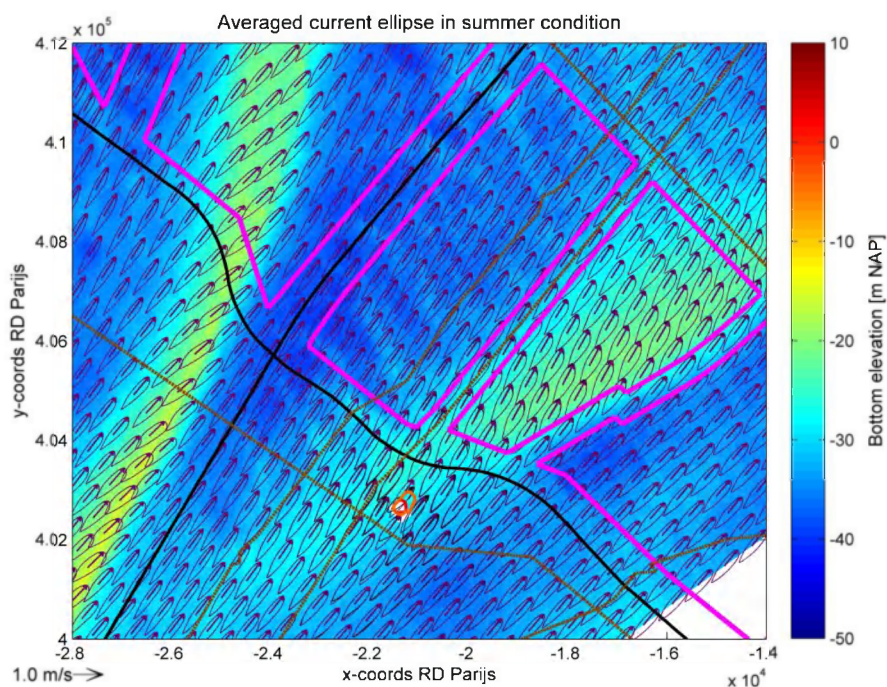


Figure 3-4: Map of averaged current ellipse for SIP I (black) and NC (purple) in summer condition with bathymetry as background.

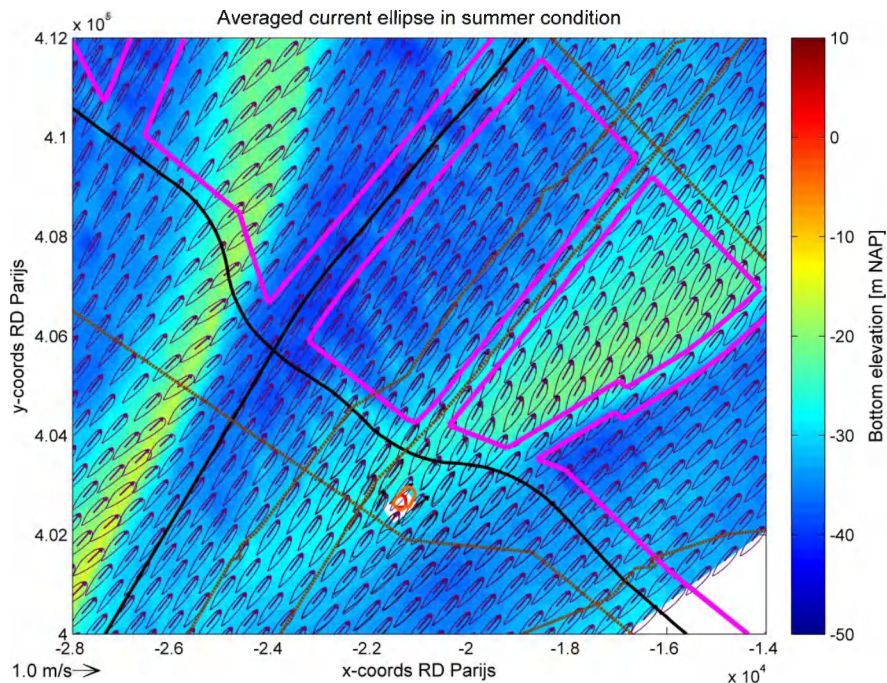


Figure 3-5: Map of averaged current ellipse for TIPA I (black) and NC (purple) in summer condition with bathymetry as background.

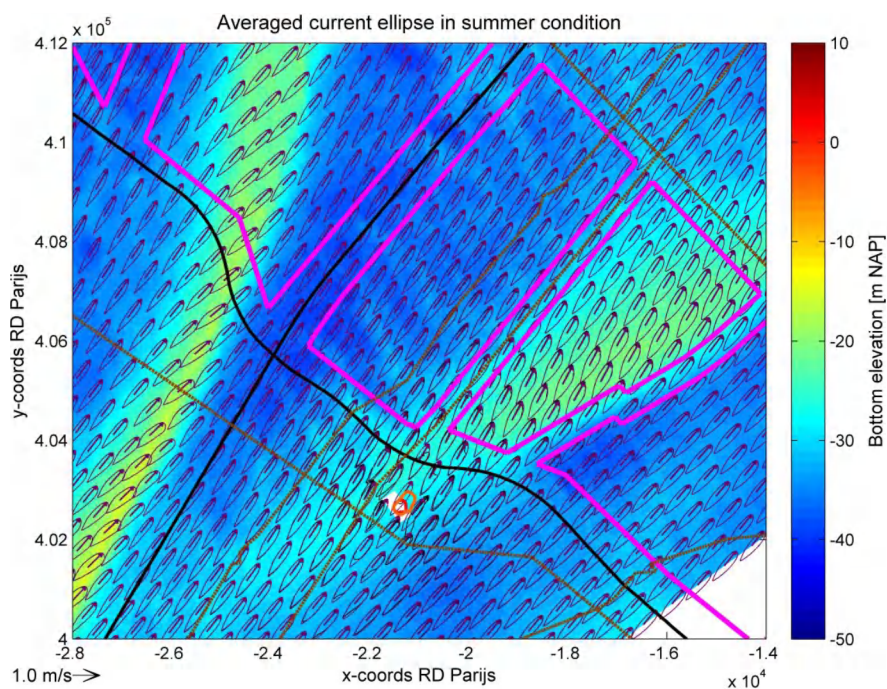


Figure 3-6: Map of averaged current ellipse for DIPP I (black) and NC (purple) in summer condition with bathymetry as background.

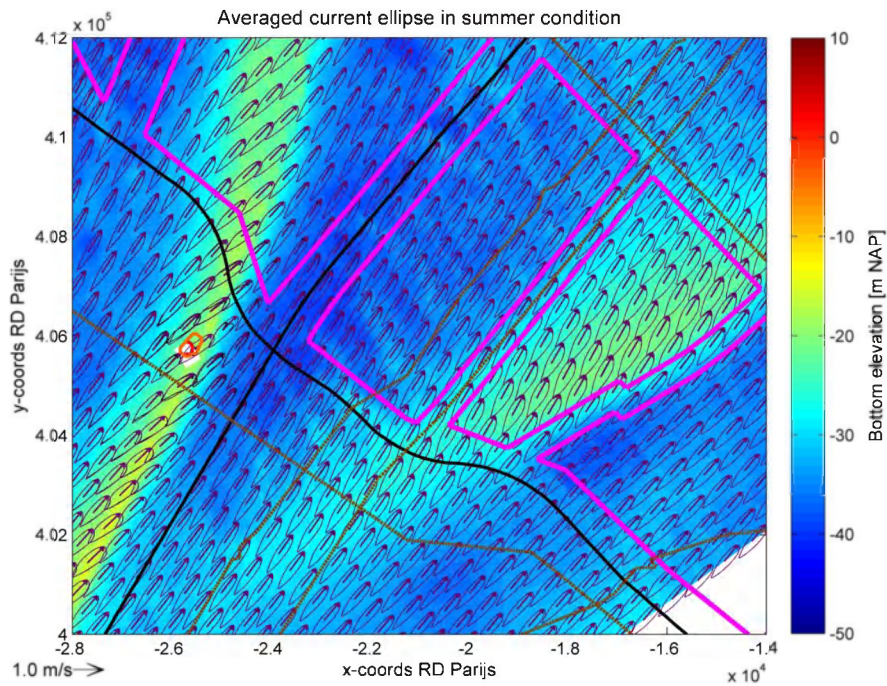


Figure 3-7: Map of averaged current ellipse for SIP II (black) and NC (purple) in summer condition with bathymetry as background.

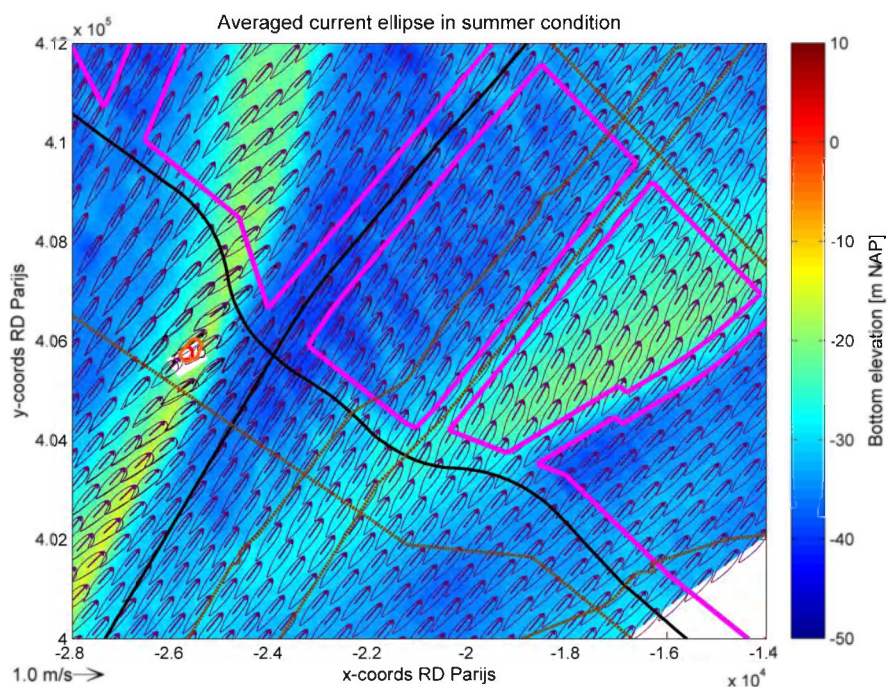


Figure 3-8: Map of averaged current ellipse for TIPA II (black) and NC (purple) in summer condition with bathymetry as background.

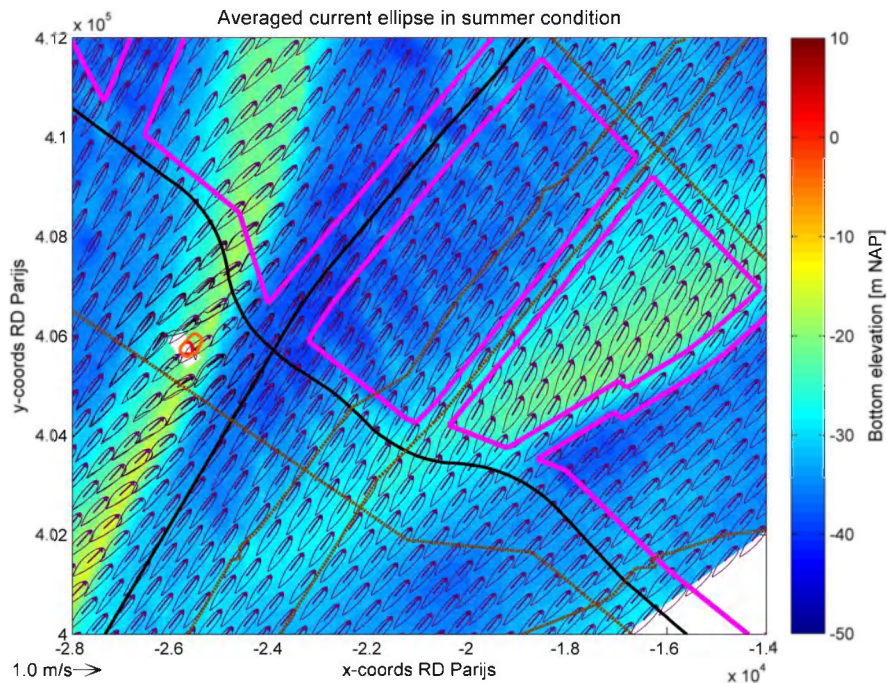


Figure 3-9: Map of averaged current ellipse for DIPP II (black) and NC (purple) in summer condition with bathymetry as background.

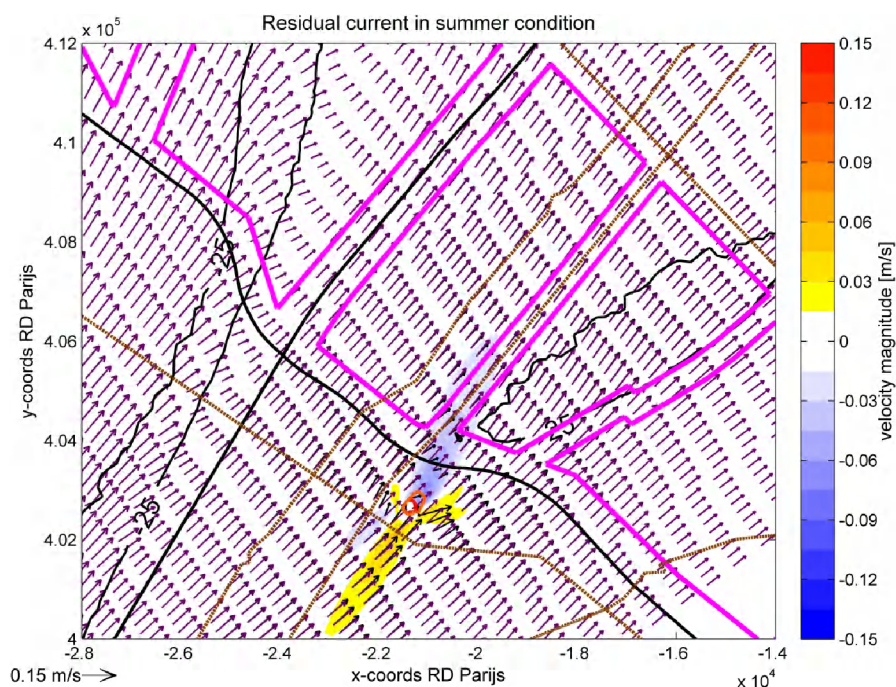


Figure 3-10: Map of residual current for SIP I (black) and NC (purple) in summer condition with difference of residual velocity magnitude as background and isobath lines of -25 m NAP.

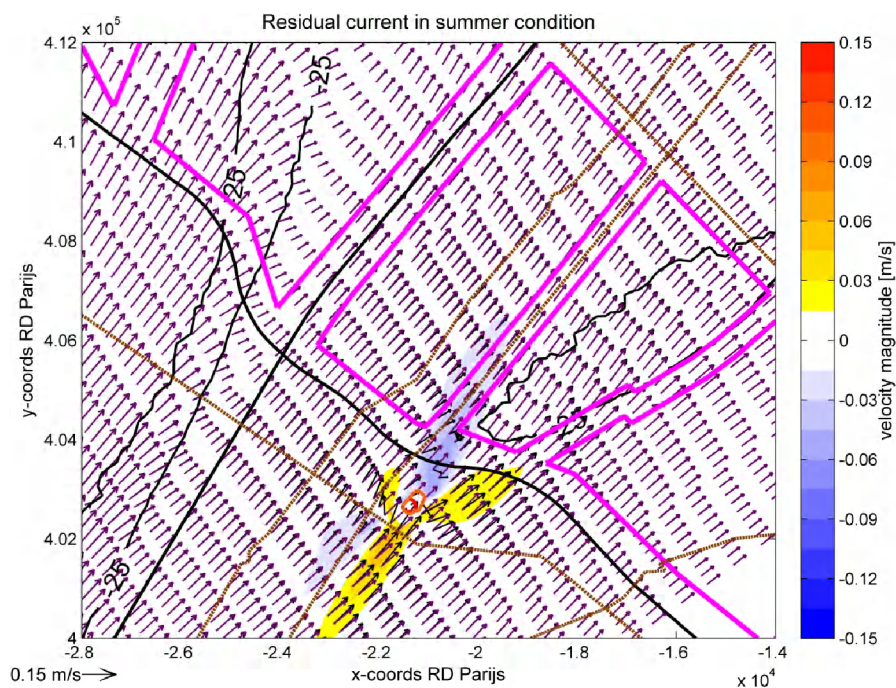


Figure 3-11: Map of residual current for TIPA I (black) and NC (purple) in summer condition with difference of residual velocity magnitude as background and isobath lines of -25 m NAP.

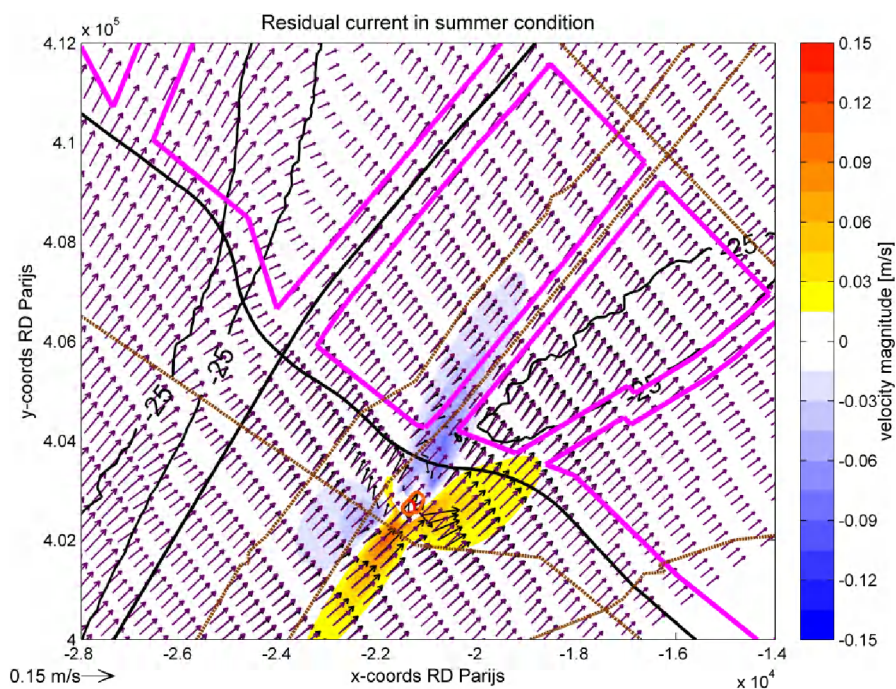


Figure 3-12: Map of residual current for DIPP I (black) and NC (purple) in summer condition with difference of residual velocity magnitude as background and isobath lines of -25 m NAP.

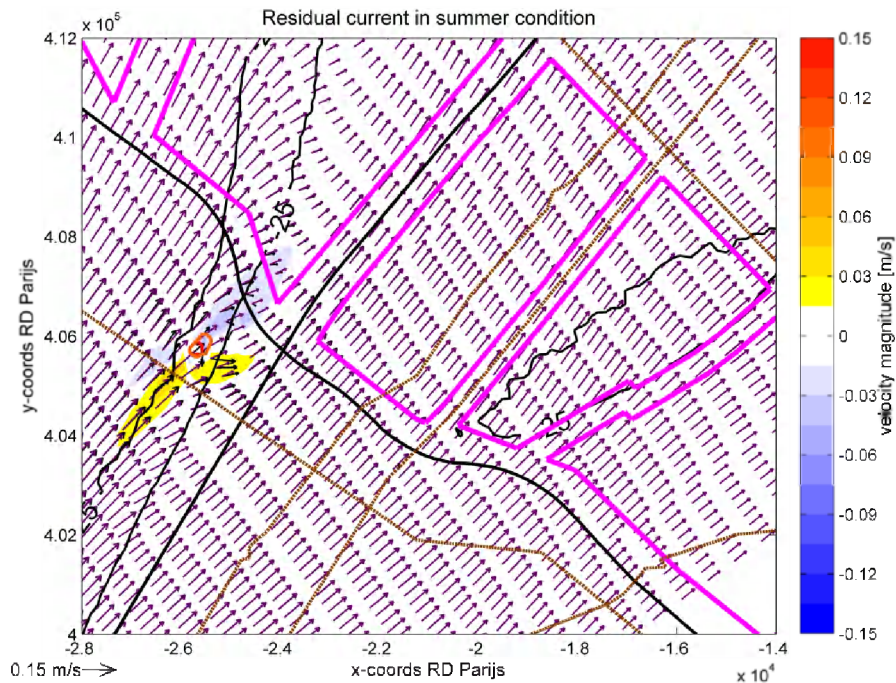


Figure 3-13: Map of residual current for SIP II (black) and NC (purple) in summer condition with difference of residual velocity magnitude as background and isobath lines of -25 m NAP.

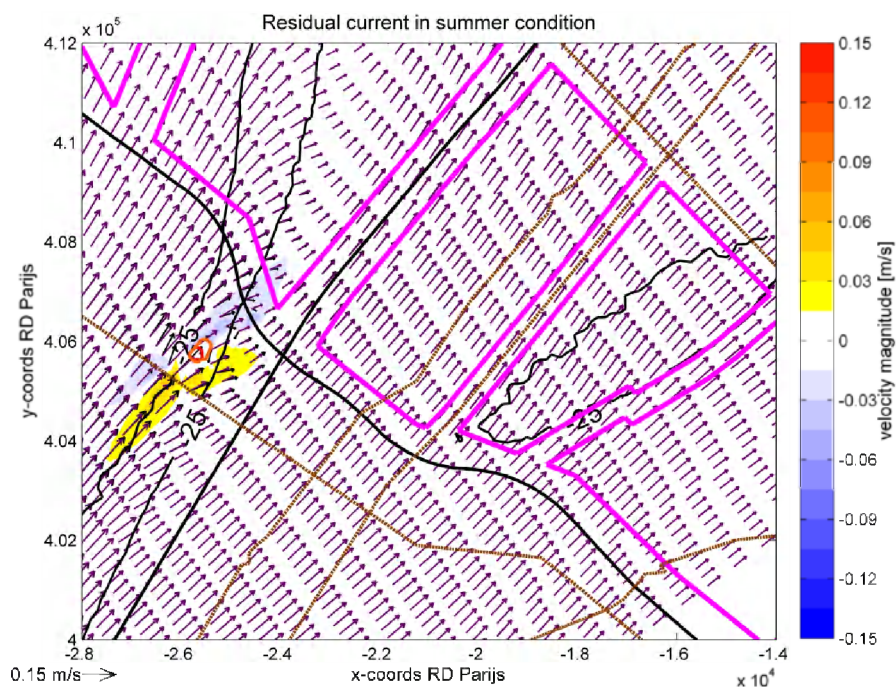


Figure 3-14: Map of residual current for TIPA II (black) and NC (purple) in summer condition with difference of residual velocity magnitude as background and isobath lines of -25 m NAP.

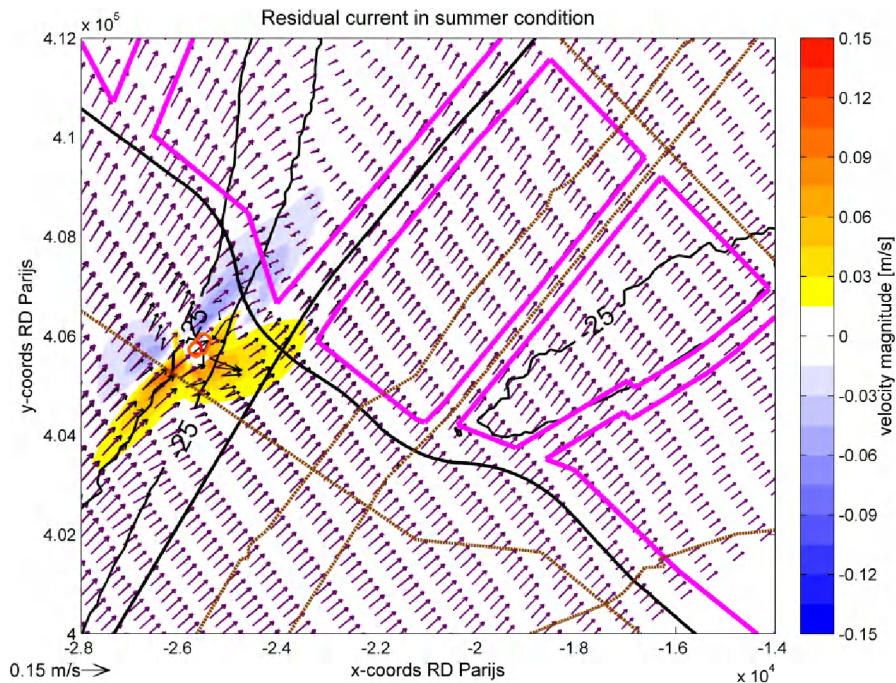


Figure 3-15: Map of residual current for DIPPII (black) and NC (purple) in summer condition with difference of residual velocity magnitude as background and isobath lines of -25 m NAP.

3.2.1.2 Sedimentation / Erosion

The residual sediment transport forms sedimentation/erosion. The difference of sedimentation/erosion is essentially caused by difference of residual sediment transport. From Figure 3-16 to Figure 3-21 it could be found that the impacts of the schematisations on the natural condition are still very small for both alternative locations of the artificial island. The size of artificial island and orientation of artificial island to the main flow direction demonstrate evident roles on the area affected by the artificial island. In addition, compared to the natural condition some erosion seems be produced at the submarine cable by TIPA I, TIPA II and DIPP II (Figure 3-17, Figure 3-20 and Figure 3-21).

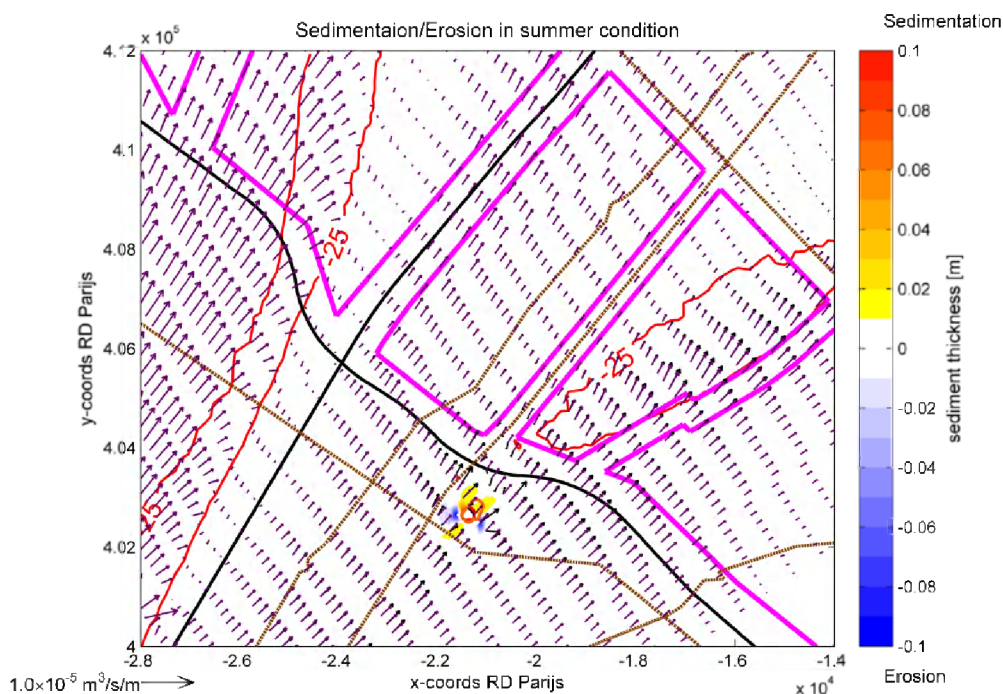


Figure 3-16: Map of residual sediment transport for SIP I (black) and NC (purple) in summer condition with difference of sedimentation/erosion as background and isobath lines of -25 m NAP.

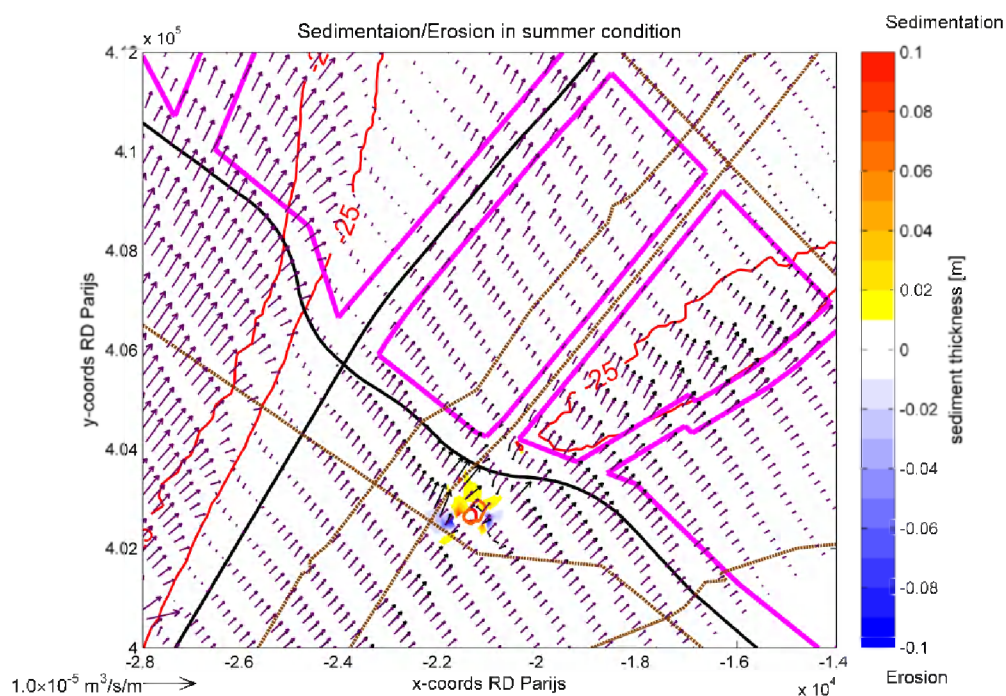


Figure 3-17: Map of residual sediment transport for TIPA I (black) and NC (purple) in summer condition with difference of sedimentation/erosion as background and isobath lines of -25 m NAP.

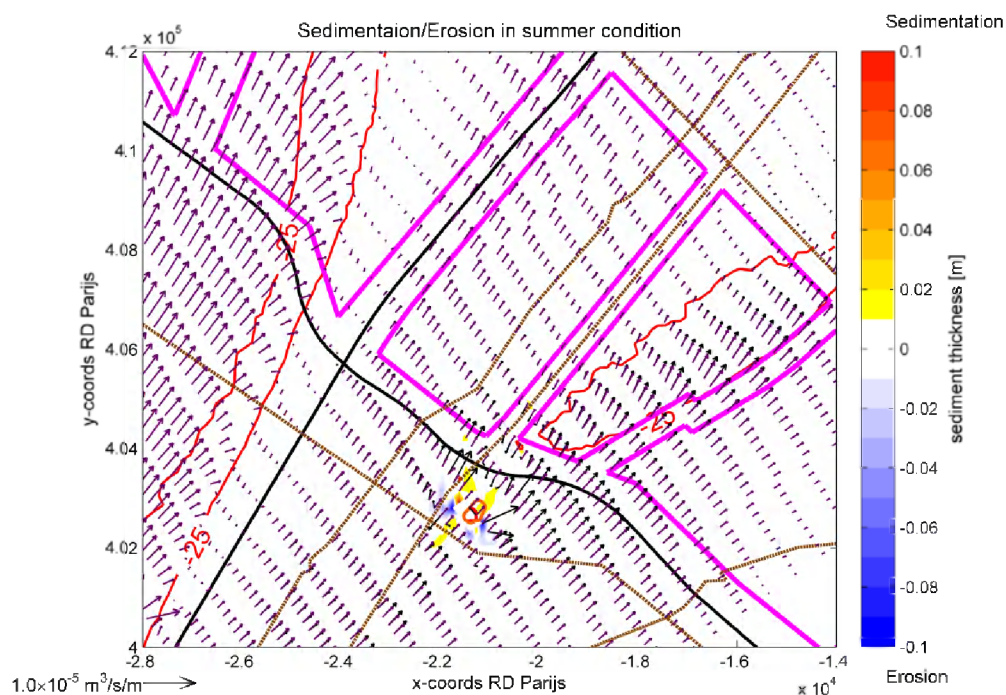


Figure 3-18: Map of residual sediment transport for DIPP I (black) and NC (purple) in summer condition with difference of sedimentation/erosion as background and isobath lines of -25 m NAP.

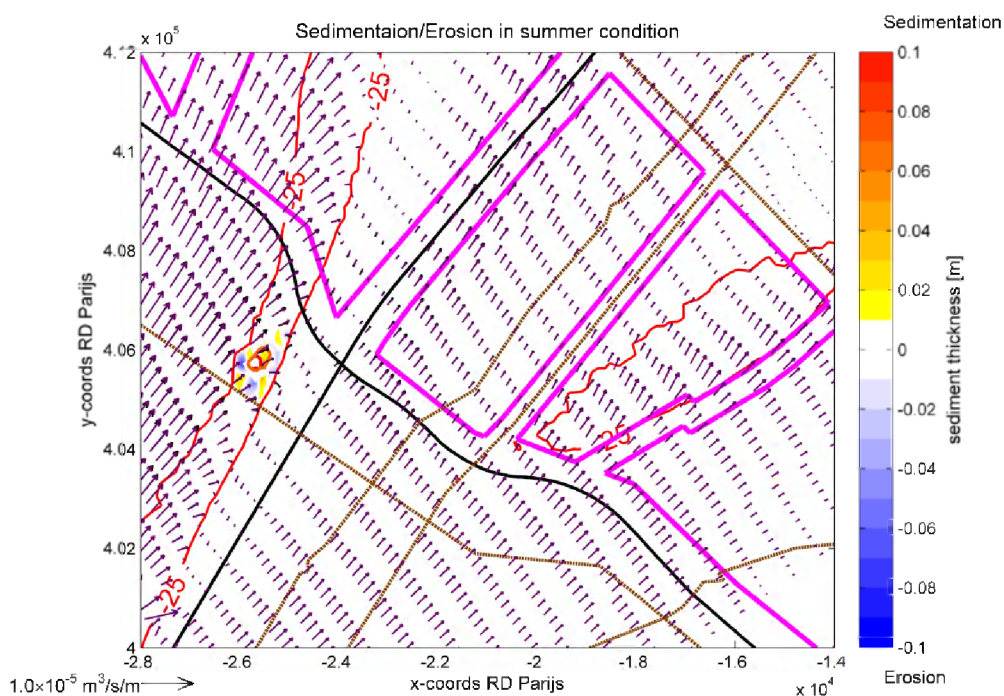


Figure 3-19: Map of residual sediment transport for SIP II (black) and NC (purple) in summer condition with difference of sedimentation/erosion as background and isobath lines of -25 m NAP.

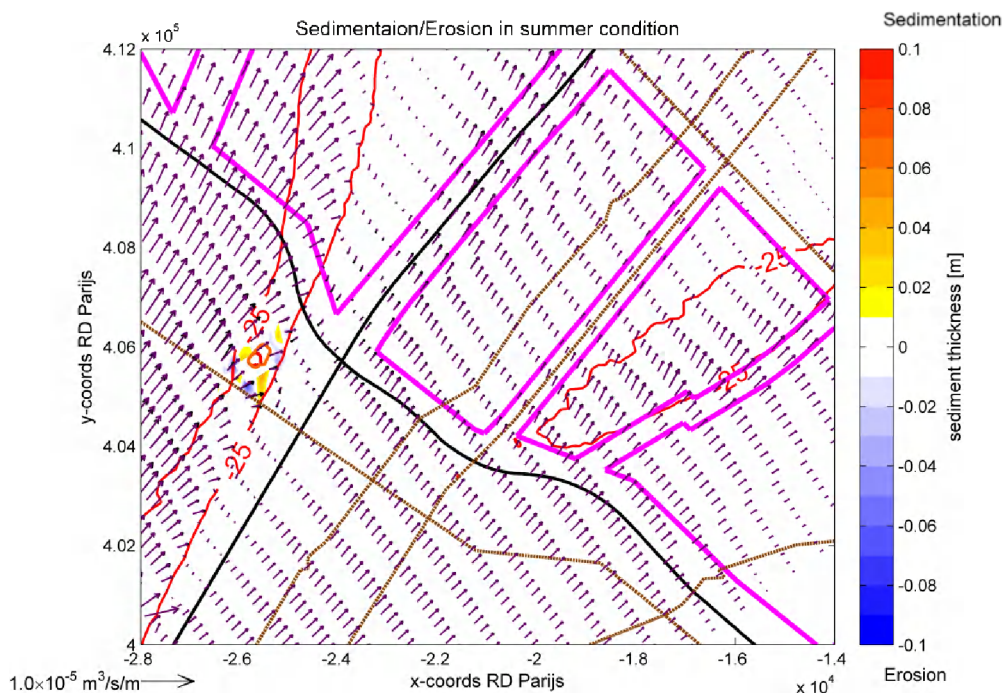


Figure 3-20: Map of residual sediment transport for TIPA II (black) and NC (purple) in summer condition with difference of sedimentation/erosion as background and isobath lines of -25 m NAP.

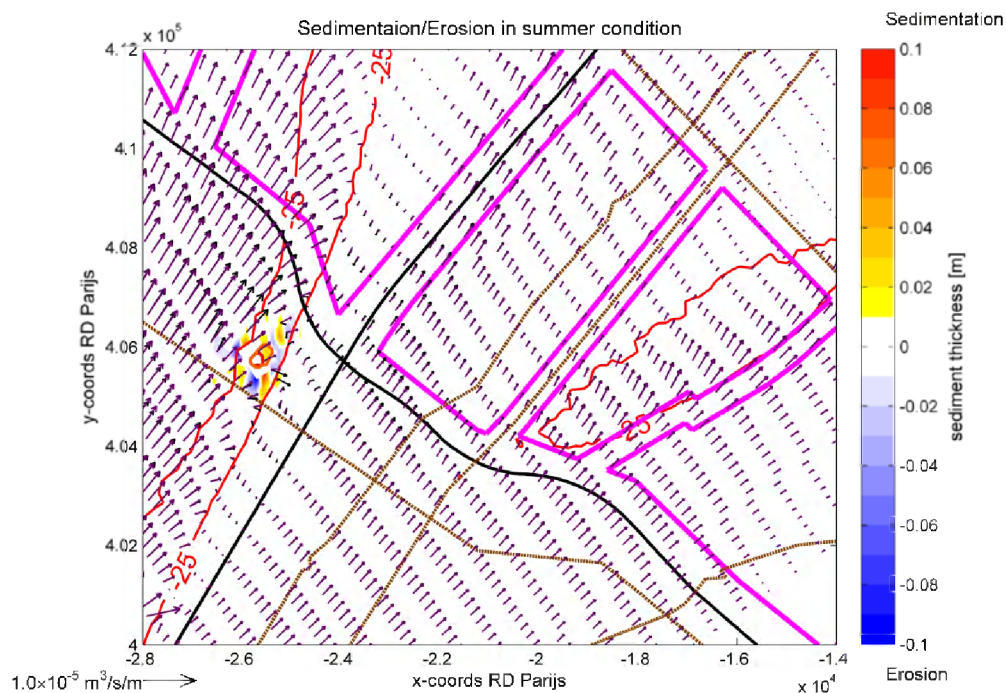


Figure 3-21: Map of residual sediment transport for DIPP II (black) and NC (purple) in summer condition with difference of sedimentation/erosion as background and isobath lines of -25 m NAP.

3.2.2 Winter condition (1-year-returned storm, Morfac=1, +/- 2 weeks)

Compared to the action of only tidal current in the summer condition, the winter condition computes the sediment transport under the combined action of tidal current and wave. In the meanwhile effects of wave on the tidal current are also taken into account for the winter condition.

3.2.2.1 Hydrodynamics

Figure 3-22 ~ Figure 3-27 shows comparison of averaged current ellipse between each schematisation and natural condition, and Figure 3-28 ~ Figure 3-33 shows comparison of residual current between them. The comparison is exactly the same as what is found in the summer condition. The impacts of these schematisations on the residual current are mainly limited to the area near to the artificial island and distributed along the main flow direction from SW to NE. The size of artificial island and orientation of artificial island to the main flow direction are shown to play important roles on the area affected by the artificial island.

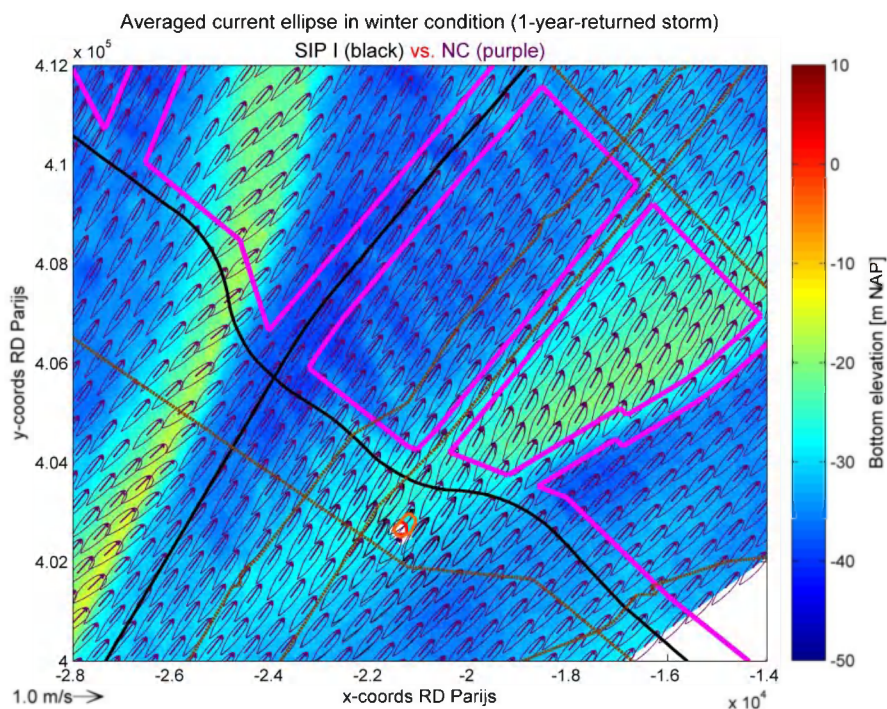


Figure 3-22: Map of averaged current ellipse for SIP I (black) and NC (purple) in winter condition with bathymetry as background.

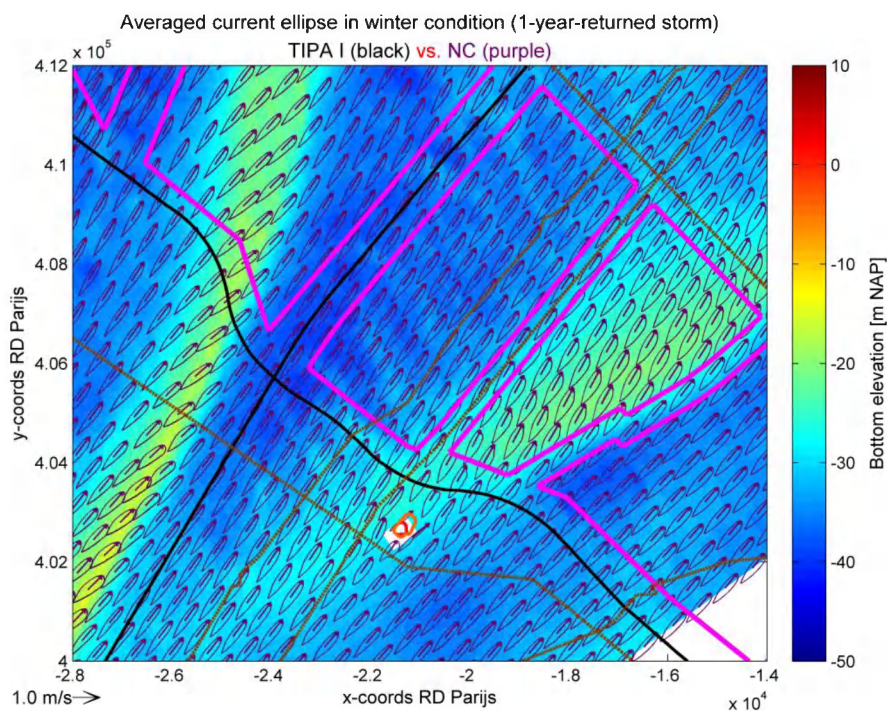


Figure 3-23: Map of averaged current ellipse for TIPA I (black) and NC (purple) in winter condition with bathymetry as background.

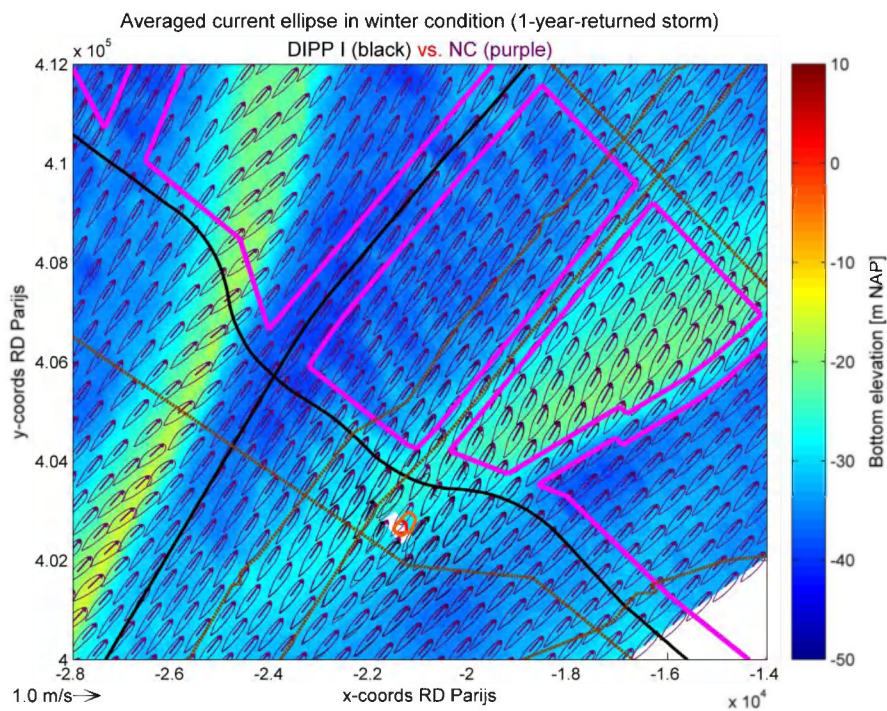


Figure 3-24: Map of averaged current ellipse for DIPP I (black) and NC (purple) in winter condition with bathymetry as background.

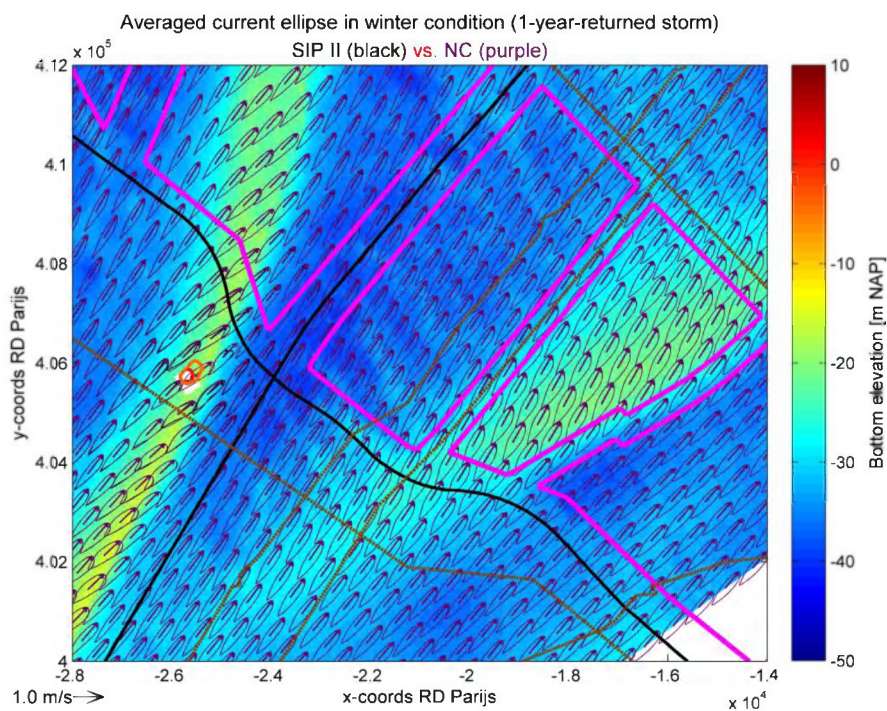


Figure 3-25: Map of averaged current ellipse for SIP II (black) and NC (purple) in winter condition with bathymetry as background.

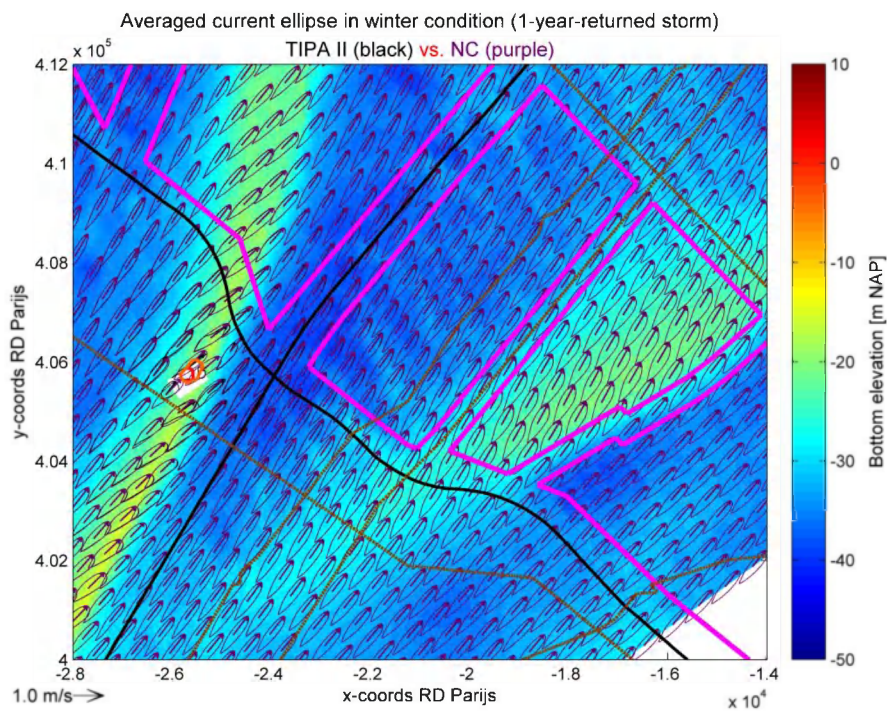


Figure 3-26: Map of averaged current ellipse for TIPA II (black) and NC (purple) in winter condition with bathymetry as background.

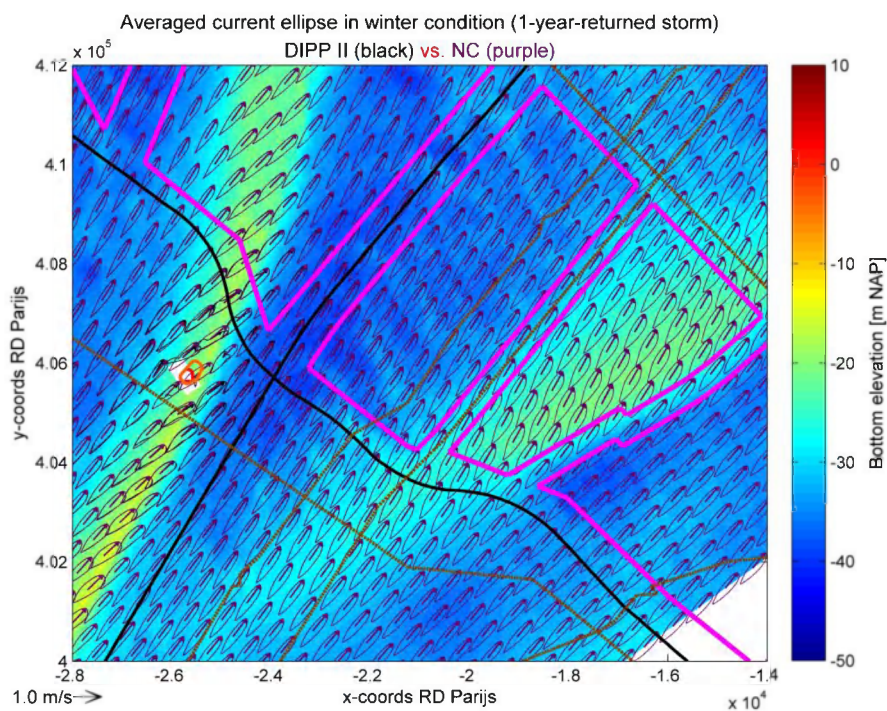


Figure 3-27: Map of averaged current ellipse for DIPP II (black) and NC (purple) in winter condition with bathymetry as background.

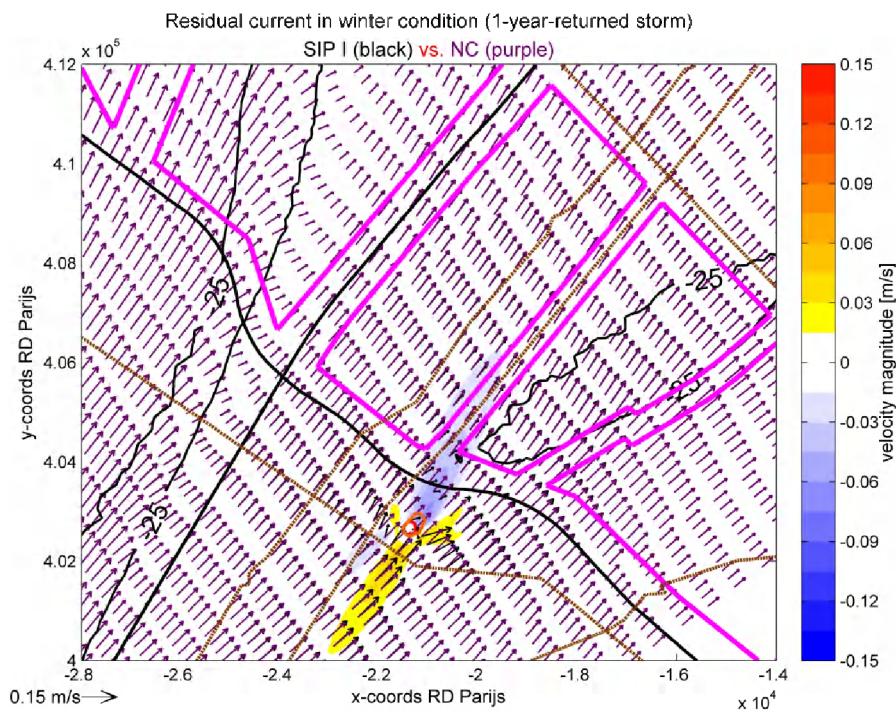


Figure 3-28: Map of residual current for SIP I (black) and NC (purple) in summer condition with difference of residual velocity magnitude as background and isobath lines of -25 m NAP.

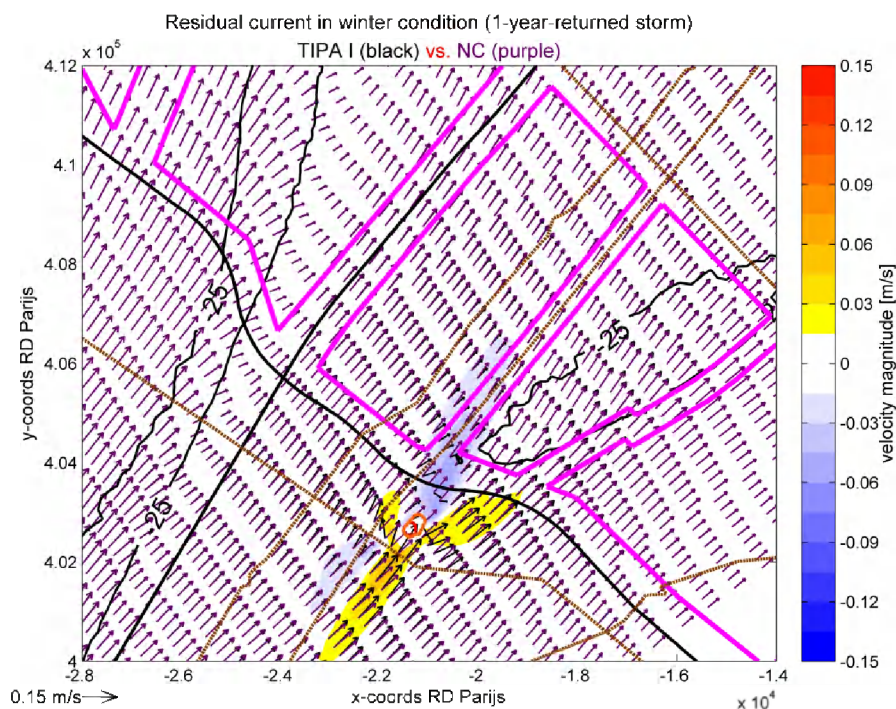


Figure 3-29: Map of residual current for TIPA I (black) and NC (purple) in summer condition with difference of residual velocity magnitude as background and isobath lines of -25 m NAP.

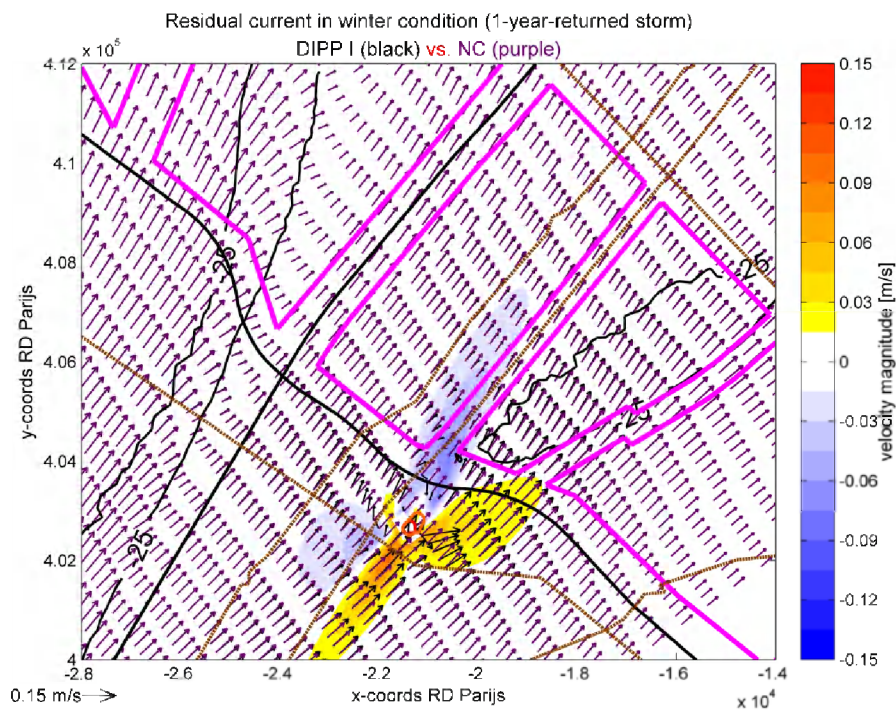


Figure 3-30: Map of residual current for DIPP I (black) and NC (purple) in summer condition with difference of residual velocity magnitude as background and isobath lines of -25 m NAP.

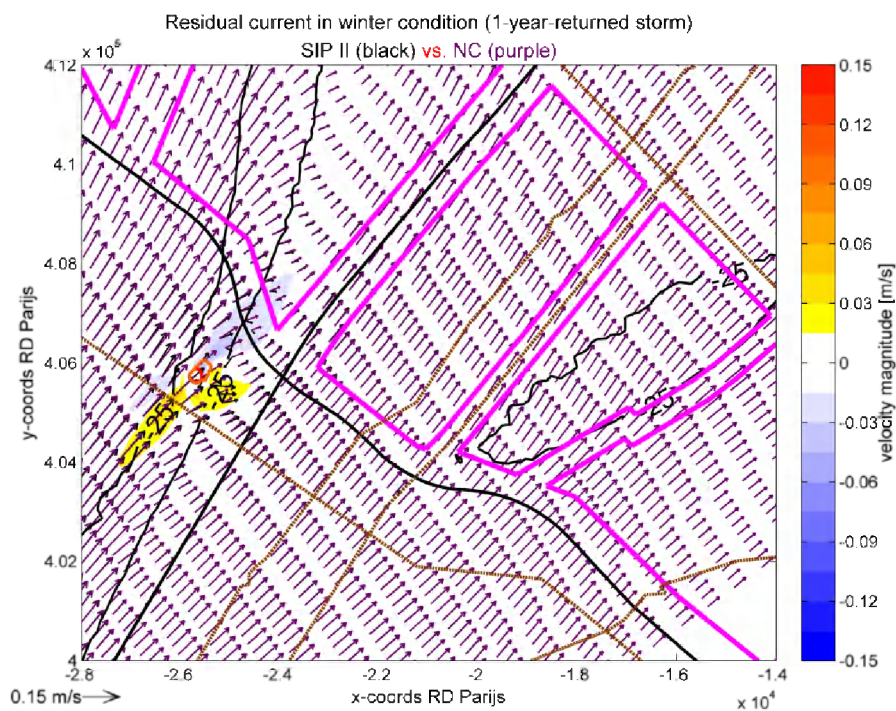


Figure 3-31: Map of residual current for SIP II (black) and NC (purple) in summer condition with difference of residual velocity magnitude as background and isobath lines of -25 m NAP.

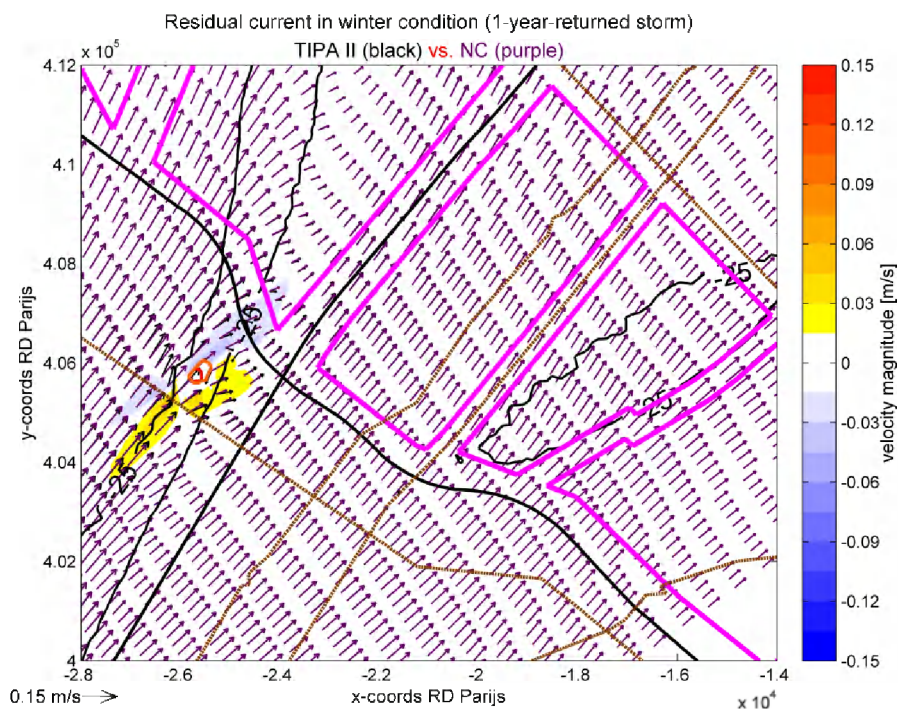


Figure 3-32: Map of residual current for TIPA II (black) and NC (purple) in summer condition with difference of residual velocity magnitude as background and isobath lines of -25 m NAP.

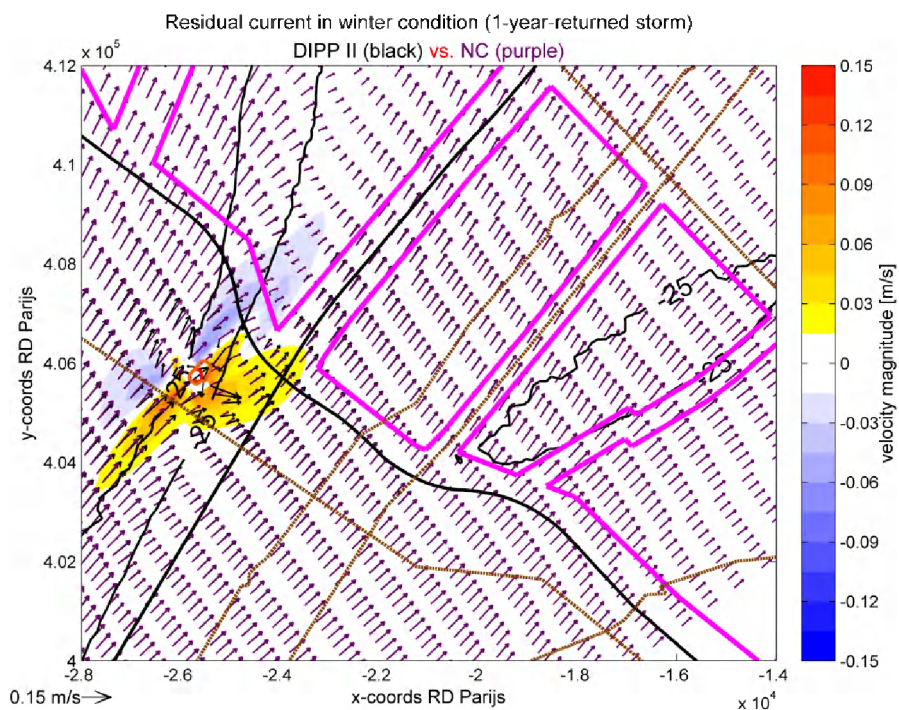


Figure 3-33: Map of residual current for DIPP II (black) and NC (purple) in summer condition with difference of residual velocity magnitude as background and isobath lines of -25 m NAP.

3.2.2.2 Sedimentation/Erosion

The findings of sedimentation/erosion in the winter condition are exactly the same as what is found in the summer condition. It should be equally noticed that compared to the natural condition some small erosion takes place at the submarine cable in the case of TIPA I, TIPA II and DIPP II (Figure 3-35, Figure 3-38 and Figure 3-39).

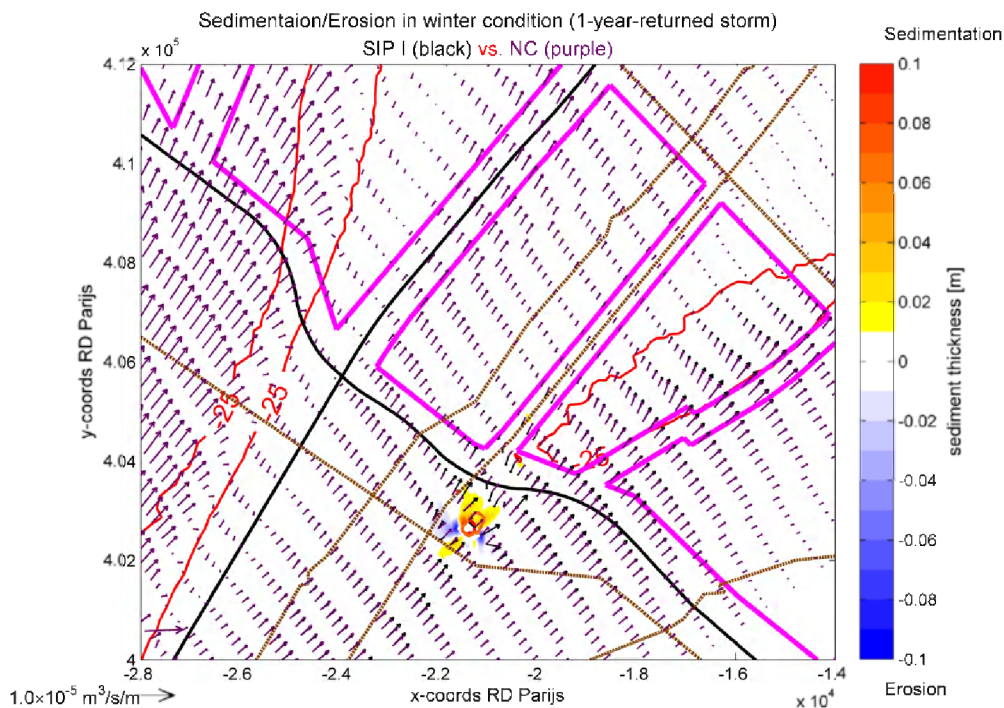


Figure 3-34: Map of residual sediment transport for SIP I (black) and NC (purple) in summer condition with difference of sedimentation/erosion as background and isobath lines of -25 m NAP.

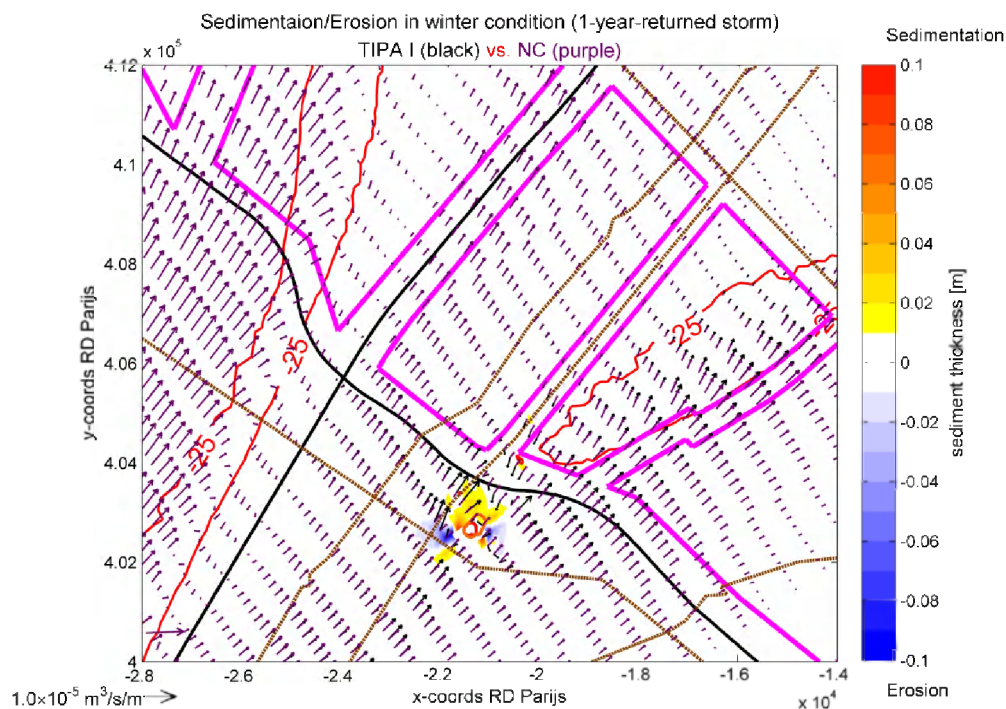


Figure 3-35: Map of residual sediment transport for TIPA I (black) and NC (purple) in summer condition with difference of sedimentation/erosion as background and isobath lines of -25 m NAP.

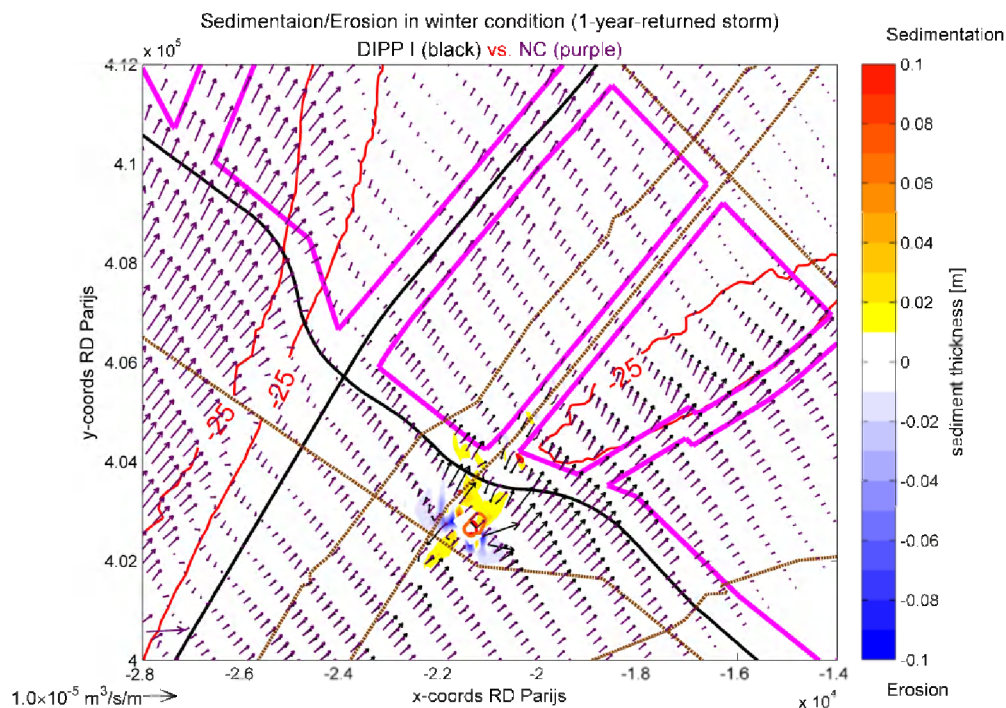


Figure 3-36: Map of residual sediment transport for DIPP I (black) and NC (purple) in summer condition with difference of sedimentation/erosion as background and isobath lines of -25 m NAP.

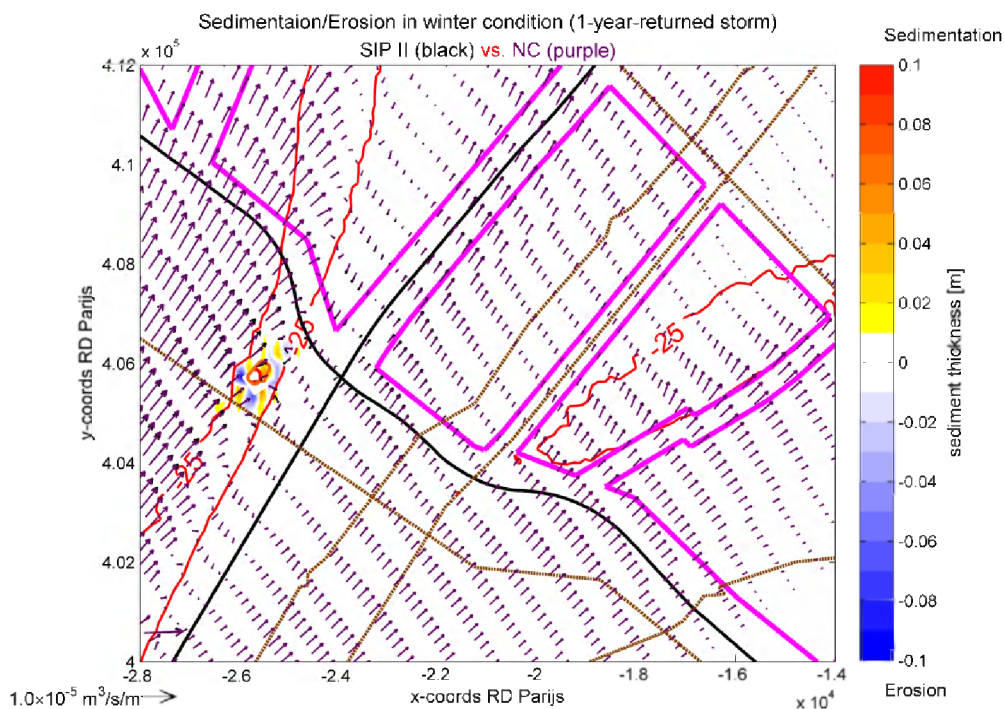


Figure 3-37: Map of residual sediment transport for SIP II (black) and NC (purple) in summer condition with difference of sedimentation/erosion as background and isobath lines of -25 m NAP.

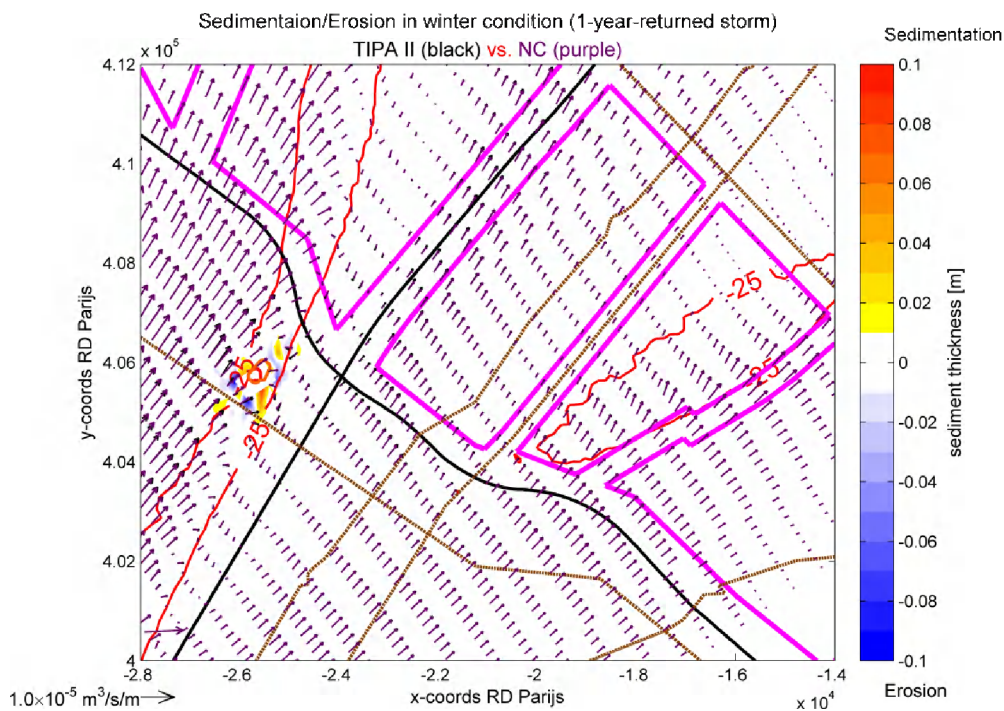


Figure 3-38: Map of residual sediment transport for TIPA II (black) and NC (purple) in summer condition with difference of sedimentation/erosion as background and isobath lines of -25 m NAP.

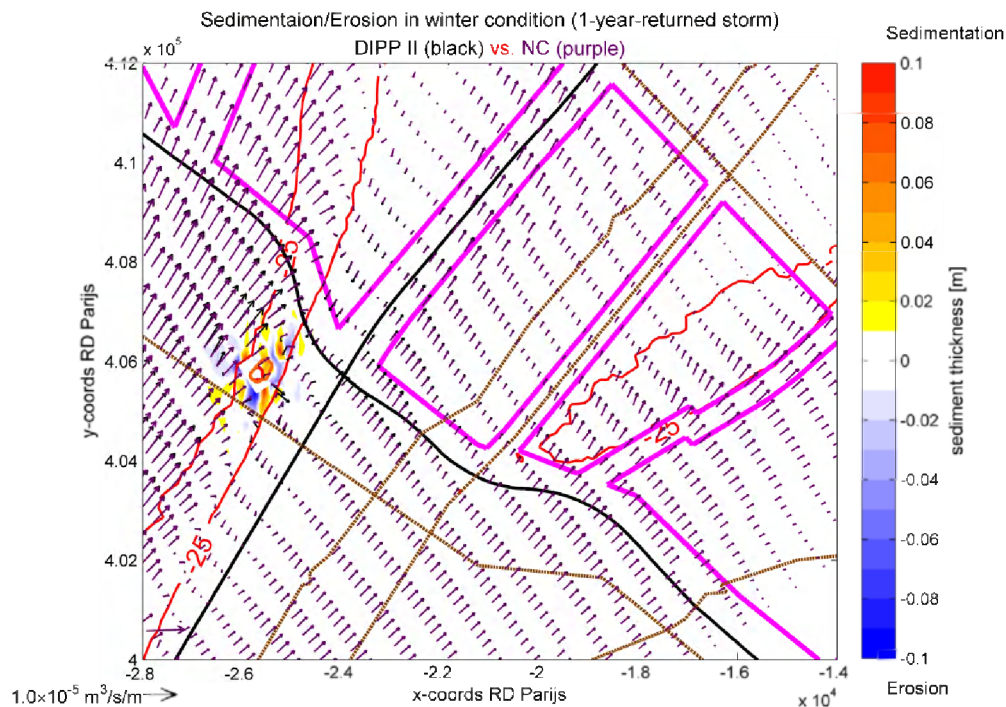


Figure 3-39: Map of residual sediment transport for DIPP II (black) and NC (purple) in summer condition with difference of sedimentation/erosion as background and isobath lines of -25 m NAP.

3.3 STORM IMPACTS

The storm impacts are investigated by comparison with the summer condition. In the summer condition, only tidal forcing is considered for the representative spring-neap tidal period (+/- 2 weeks). While in the winter condition, the tidal and wave forcings are coupled together in the model. For the winter condition, the formerly selected 1- and 5-year-returned storms are simulated respectively by the wave model, which is coupled with the flow model to simulate the sediment transport during the representative spring-neap tidal cycle.

Figure 3-40 shows that the alternative two locations of artificial island are situated between the submarine cables and pipelines. Location II seems to be just on the top of Blighbank; while Location I is situated at the inclined slope of Lodewijkbank. The red cross indicates the location of a point for inspection of time series modelling results.

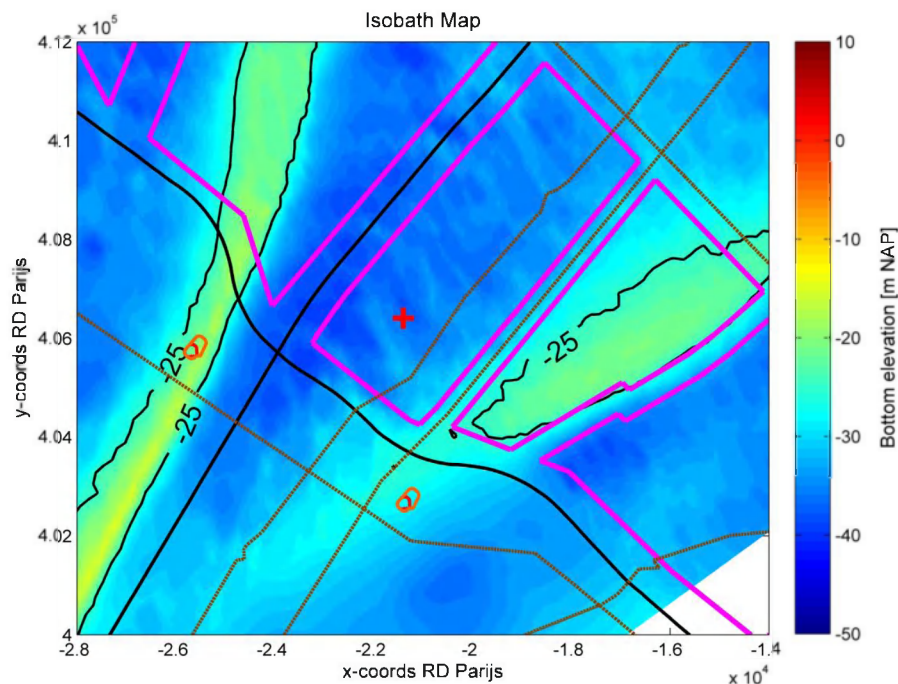


Figure 3-40: Bathymetry map with isobath contour lines of -25 m NAP; red cross point for inspection of time series variables.

3.3.1 1-year-returned storm (Morfac=1, +/- 2 weeks)

3.3.1.1 Wave climate

In order to consider the worst case scenario, the wave peak of the 1-year-returned storm is shifted to the lowest water at spring tide (cf. red arrow in Figure 3-41).

Figure 3-42 present the maximal significant wave height calculated by the wave model. In the BOG domain, the resolution of the computational grids in the wave model is around 235 m × 340 m to 110 m × 180 m, in which the two large banks Blighbank and Lodewijkbank are explicitly described. It can be clearly seen from the figure that the wave from the southwest is remarkably impeded and drastically dissipated when it travels over Blighbank. The maximal significant wave height reaches around 4,3 m at Location I and around 3,9 m at Location II during the 1-year-returned storm period.

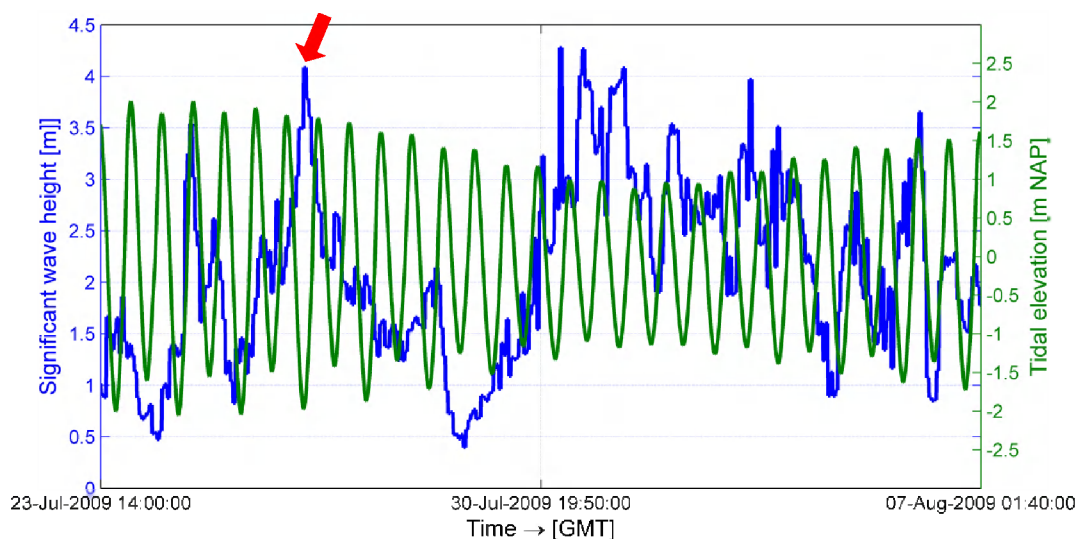


Figure 3-41: Time series of modelled significant wave height and tidal elevation during the representative spring-neap tidal cycle in winter condition (1-year-returned storm) at the red cross point.

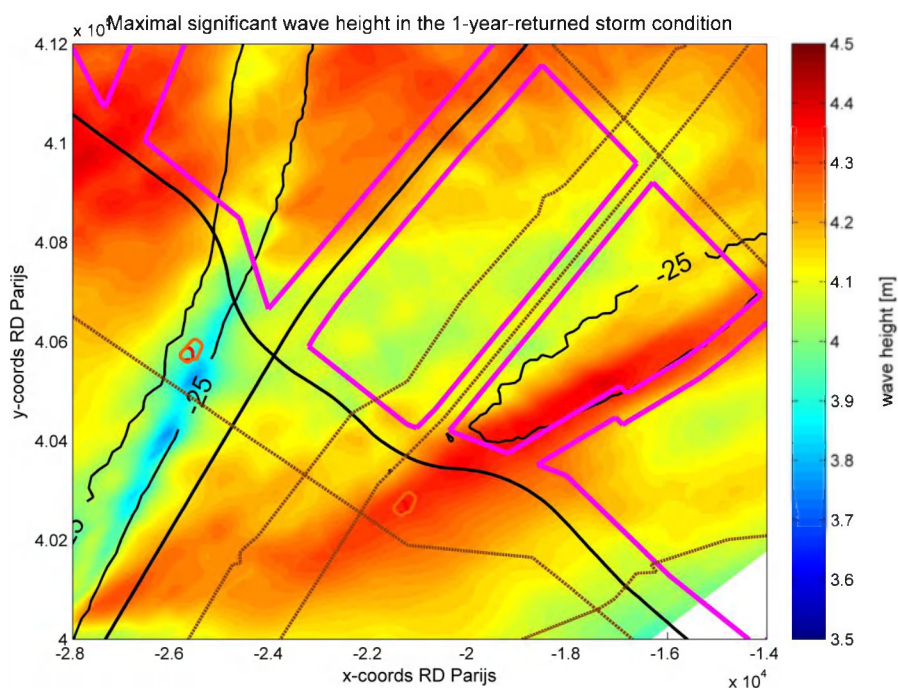


Figure 3-42: Map of maximal significant wave height over the representative spring-neap tidal cycle in winter condition (1-year-returned storm) with isobath lines of -25 m NAP.

3.3.1.2 Hydrodynamics

Figure 3-43 and Figure 3-44 show comparison of averaged current ellipse between the winter and summer conditions for the natural condition and TIPA I, and Figure 3-45 and Figure 3-46 show comparison of residual current between the winter and summer conditions for them. The comparisons for SIP I, DIPP I, SIP II, TIPA II and DIPP II could be found in section 6.1.1 and 6.1.2 of Appendix. Compared to the summer condition, averaged current ellipse and residual current do not exhibit any pronounced difference. The averaged current ellipses and residual currents in the winter condition are almost completely overlapped by those in the summer condition, and the magnitude of residual currents in the winter condition seems to be slightly smaller than that in the summer condition.

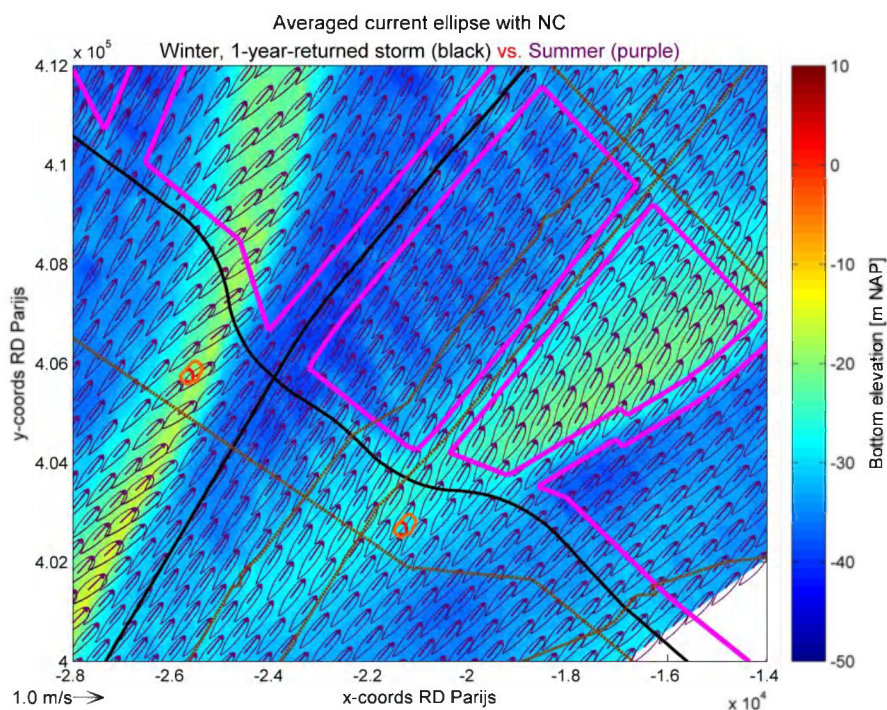


Figure 3-43: Map of averaged current ellipse with natural condition for winter (black) and summer (purple) conditions with bathymetry as background.

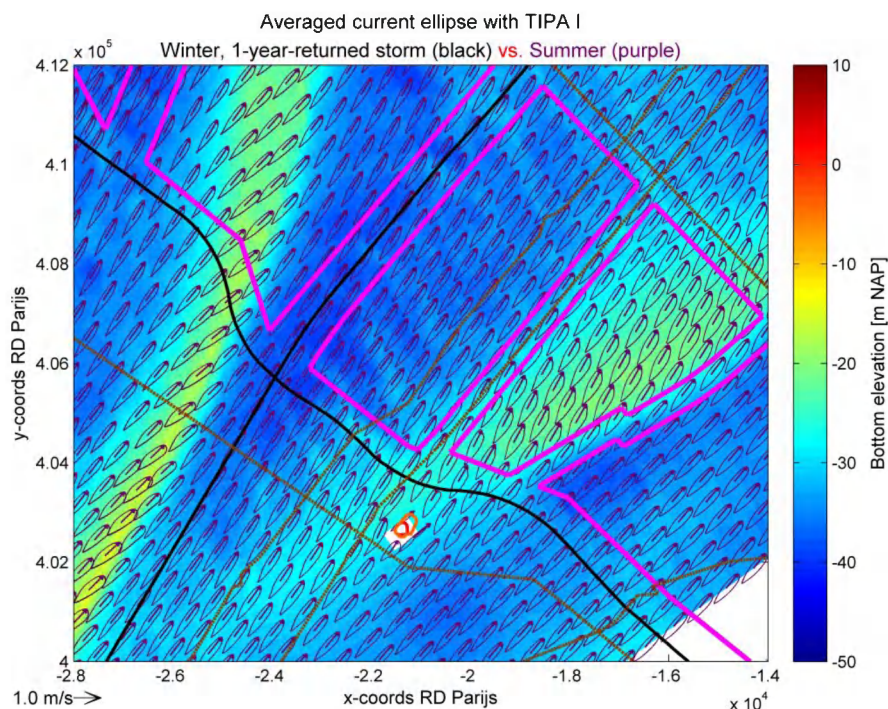


Figure 3-44: Map of averaged current ellipse with TIPA I for winter (black) and summer (purple) conditions with bathymetry as background.

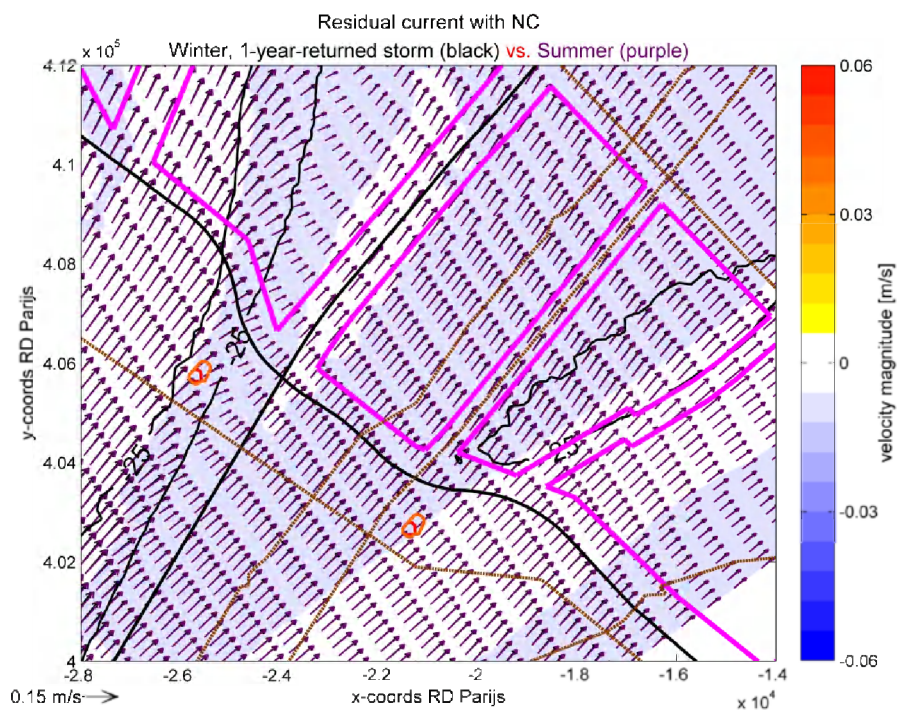


Figure 3-45: Map of residual current with natural condition for winter (black) and summer (purple) conditions with difference of residual velocity magnitude as background and isobath lines of -25 m NAP.

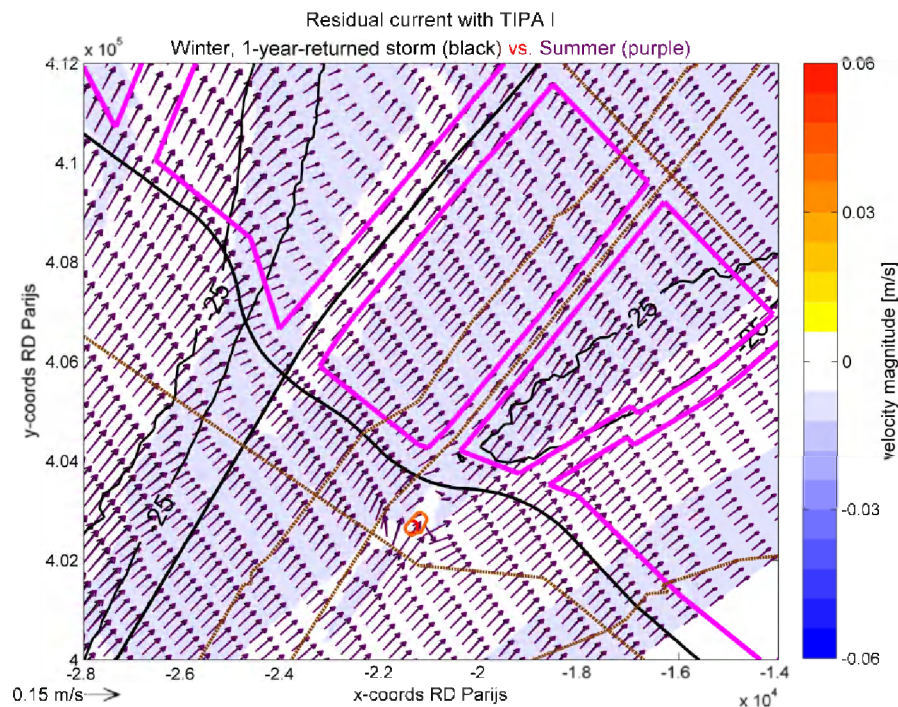


Figure 3-46: Map of residual current with TIPA I for winter (black) and summer (purple) conditions with difference of residual velocity magnitude as background and isobath lines of -25 m NAP.

3.3.1.3 Sedimentation/Erosion

The pattern of residual sediment transport has not changed in the winter condition compared to that in summer condition (Figure 3-42 and Figure 3-43). The residual transport rate in the area west to Blighbank seems to be enhanced more visibly than in other areas. Larger difference of sedimentation/erosion could be found at the top of Blighbank. The comparisons of residual sediment transport and sedimentation/erosion for SIP I, DIPP I, SIP II, TIPA II and DIPP II could be found in section 6.1.3 of Appendix.

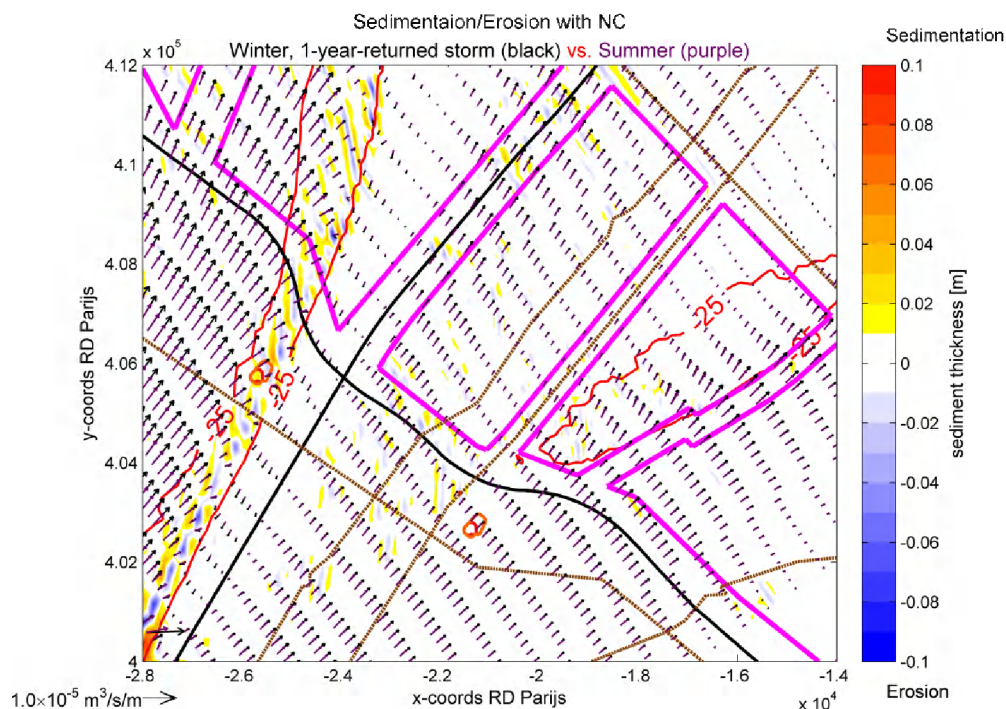


Figure 3-47: Map of residual sediment transport with natural condition for winter (black) and summer (purple) conditions with difference of sedimentation/erosion as background and isobath lines of -25 m NAP.

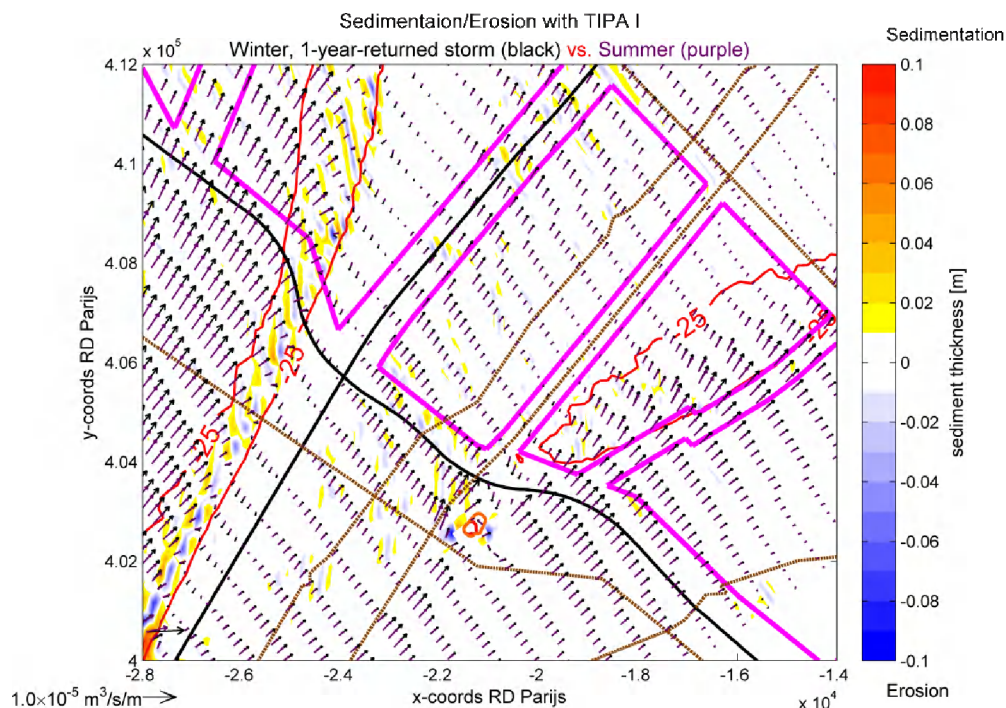


Figure 3-48: Map of residual sediment transport with TIPA I for winter (black) and summer (purple) conditions with difference of sedimentation/erosion as background and isobath lines of -25 m NAP.

3.3.2 5-year-returned storm (Morfac=1, +/- 2 weeks)

3.3.2.1 Wave climate

The wave peak of the 5-year-returned storm is also shifted to the lowest water at spring tide (cf. red arrow in Figure 3-49). In Figure 3-50 the wave from the northwest is significantly enhanced at the top of Blighbank, where the significant wave height at Location II of the artificial island reaches around 6 m. At Location I of the artificial island the significant wave height drops to about 5,5 m.

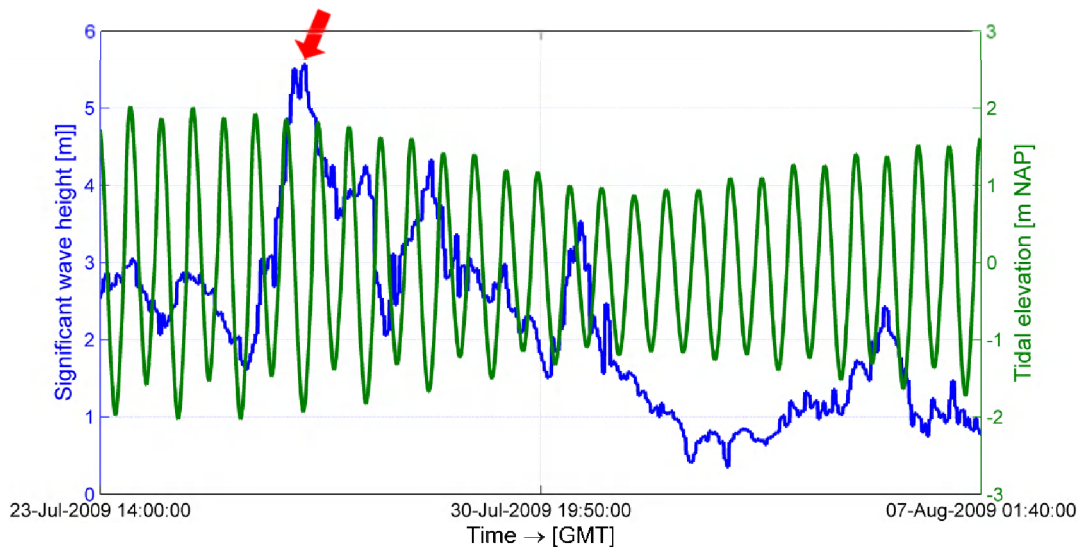


Figure 3-49: Time series of modelled significant wave height and tidal elevation during the representative spring-neap tidal cycle in winter condition at the red cross point.

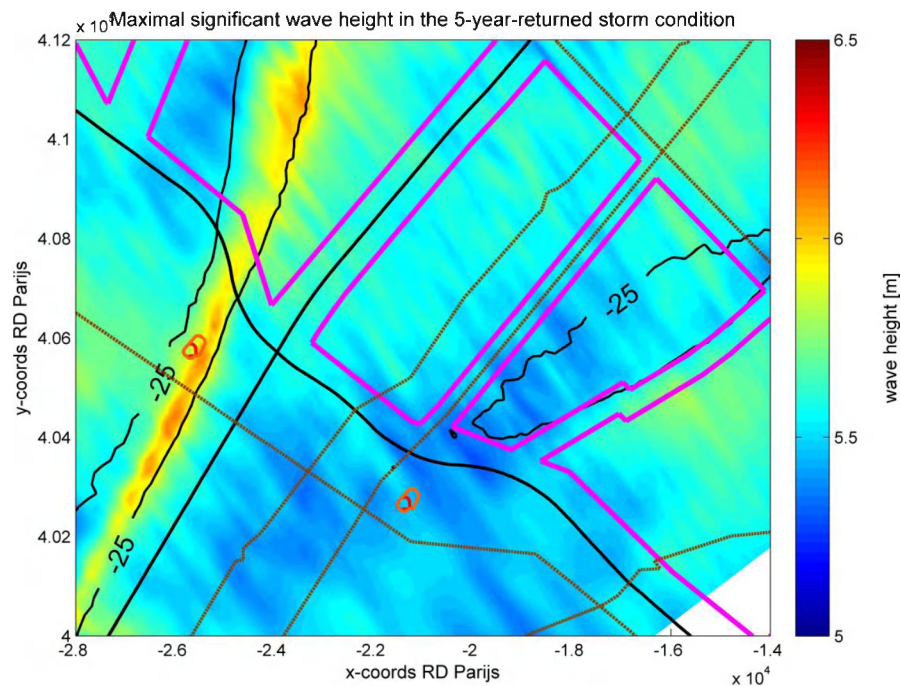


Figure 3-50: Map of maximal significant wave height over the representative spring-neap tidal cycle in winter condition with isobath lines of -25 m NAP.

3.3.2.2 Hydrodynamics

Figure 3-51 and Figure 3-52 show comparison of averaged current ellipse between the winter and summer conditions for natural condition and TIPA I, and Figure 3-53 and Figure 3-54 show comparison of residual current between the winter and summer conditions for them. The comparisons for SIP I, DIPP I, SIP II, TIPA II and DIPP II could be found in section 6.2.1 and 6.2.2 of Appendix. Compared to the summer condition, averaged current ellipse and residual current do not show any obvious difference. The averaged current ellipse and residual current in the winter condition are almost completely overlapped by those in the summer condition, and only at location of the Blighbank the magnitude of residual currents in the winter condition seems to be slightly smaller than that in the summer condition.

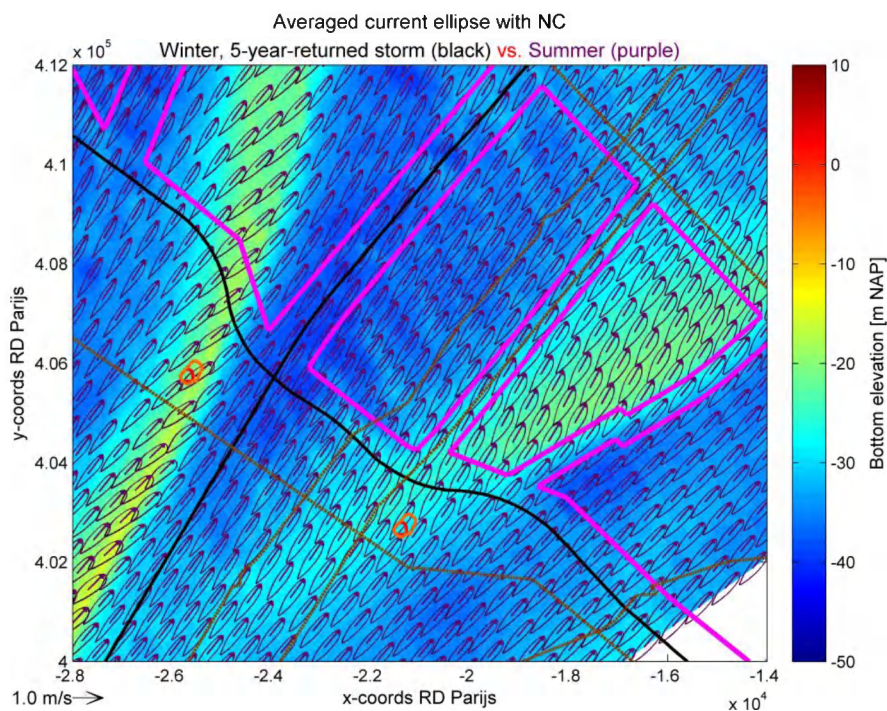


Figure 3-51: Map of averaged current ellipse with natural condition for winter (black) and summer (purple) conditions with bathymetry as background.

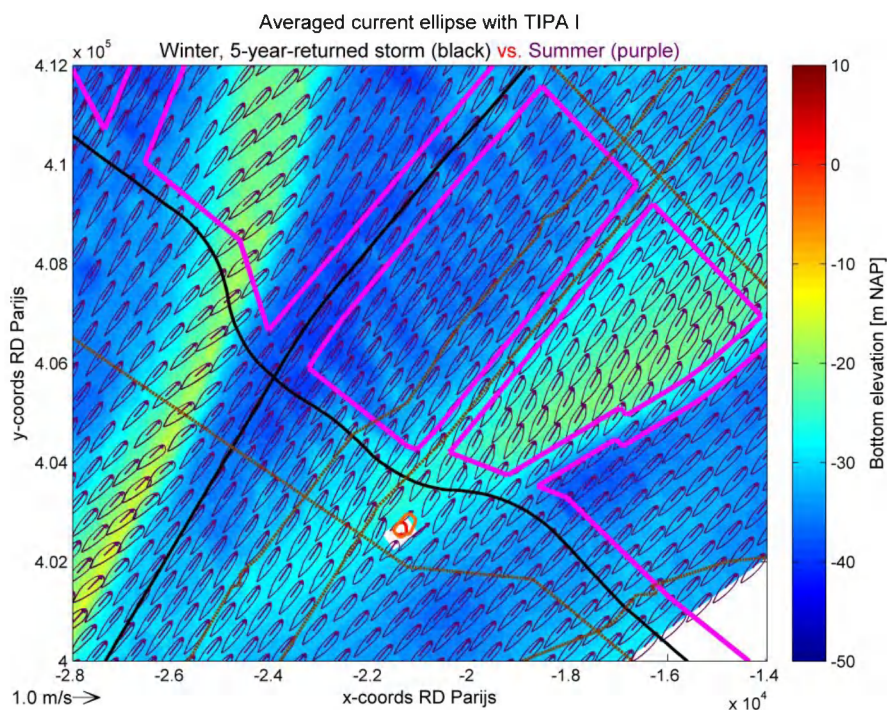


Figure 3-52: Map of averaged current ellipse with TIPA I for winter (black) and summer (purple) conditions with bathymetry as background.

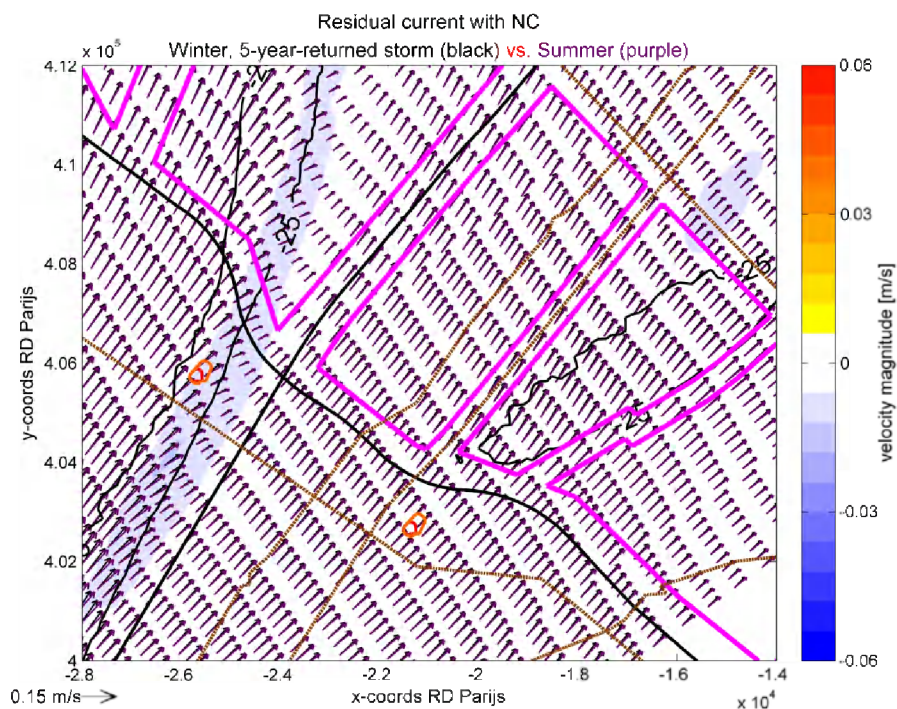


Figure 3-53: Map of residual current with natural condition in winter (black) and summer (purple) conditions with difference of residual velocity magnitude as background and isobath lines of -25 m NAP.

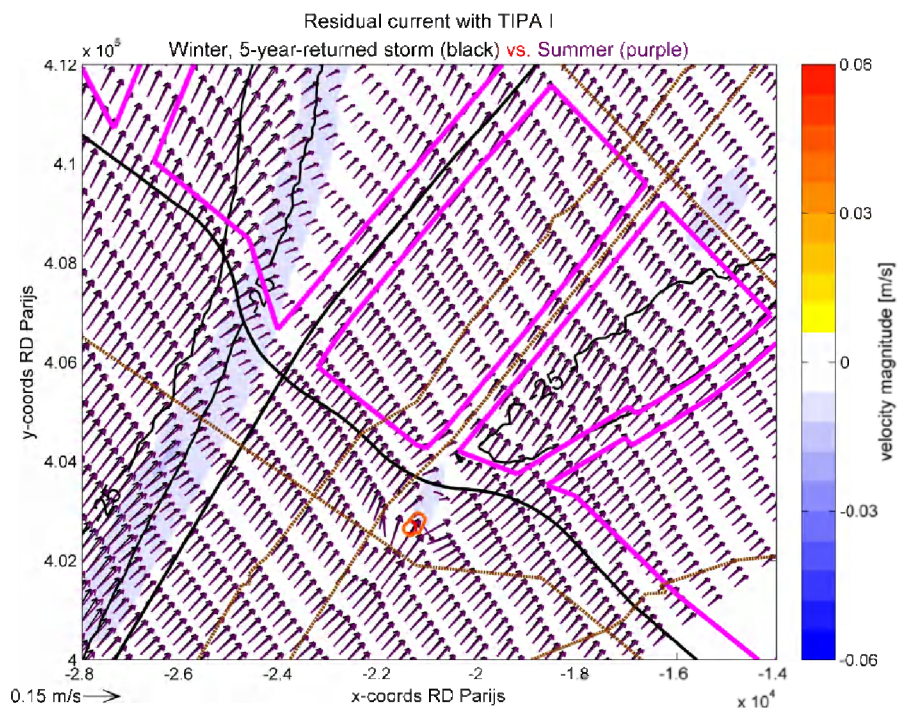


Figure 3-54: Map of residual current with TIPA I in winter (black) and summer (purple) conditions with difference of residual velocity magnitude as background and isobath lines of -25 m NAP.

3.3.2.3 Sedimentation/Erosion

The sediment transport appears to be increased considerably in the winter condition compared to the summer condition (Figure 3-53 and Figure 3-54). At the top of Blighbank and Lodewijkbank, the transport direction is even deviated to the north and the difference of sedimentation/erosion seems to be more visible than other locations (Figure 3-55 and Figure 3-56). The comparisons of residual sediment transport and sedimentation/erosion for SIP I, DIPP I, SIP II, TIPA II and DIPP II could be found in section 6.2.3 of Appendix.

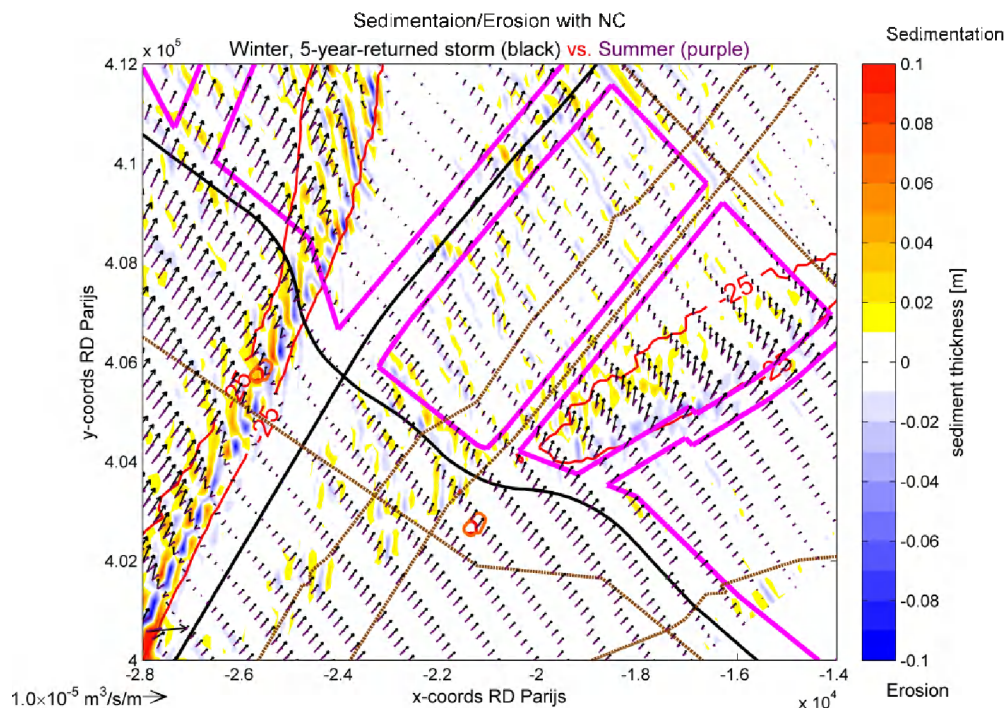


Figure 3-55: Map of residual sediment transport with natural condition in winter (black) and summer (purple) conditions with difference of sedimentation/erosion as background and isobath lines of -25 m NAP.

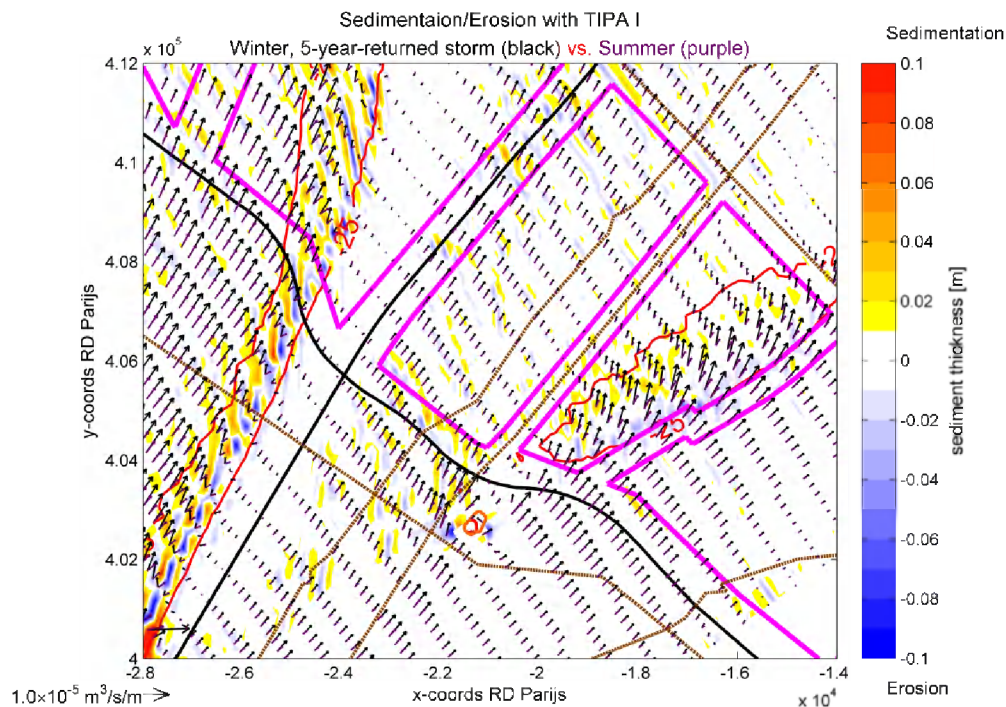


Figure 3-56: Map of residual sediment transport with TIPA I in winter (black) and summer (purple) conditions with difference of sedimentation/erosion as background and isobath lines of -25 m NAP.

3.4 LONG-TERM MORPHOLOGY ANALYSIS

The long-term morphological simulation is run with only tidal forcing (summer condition) and Morfac=125 is used for morphological acceleration. To confirm reliability of this large Morfac number, the simulation with Morfac=125 and 14X24h50min were compared against that with Morfac=25 and 5X14X24h50min. Quite comparable results were found between them (results are not shown), which confirms the reliability that the morphological simulation for 25 years is run with Morfac=125.

3.4.1 Comparison with natural condition (Morfac=125, +/- 25 years)

To investigate impacts of the artificial island from the viewpoint of long-term morphological change, SIP, TIPA and DIPP are compared to the natural condition respectively for the two alternative locations of the artificial island after every 5 years. In this section only the comparison of TIPA I with the natural condition is displayed, the other comparisons of SIP I, DIPP I, SIP II, TIPA II and DIPP II could be found from 6.3.1 to 6.3.5 of Appendix.

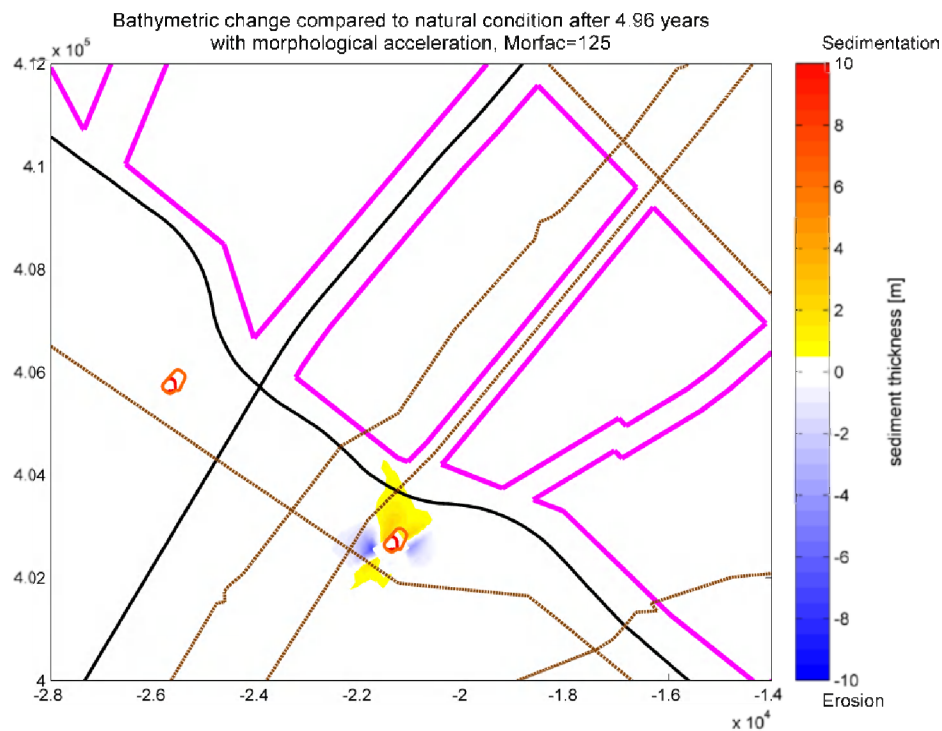


Figure 3-57: Bathymetric change of TIPA I compared to natural condition after +/- 5 years with morphological acceleration (Morfac=125).

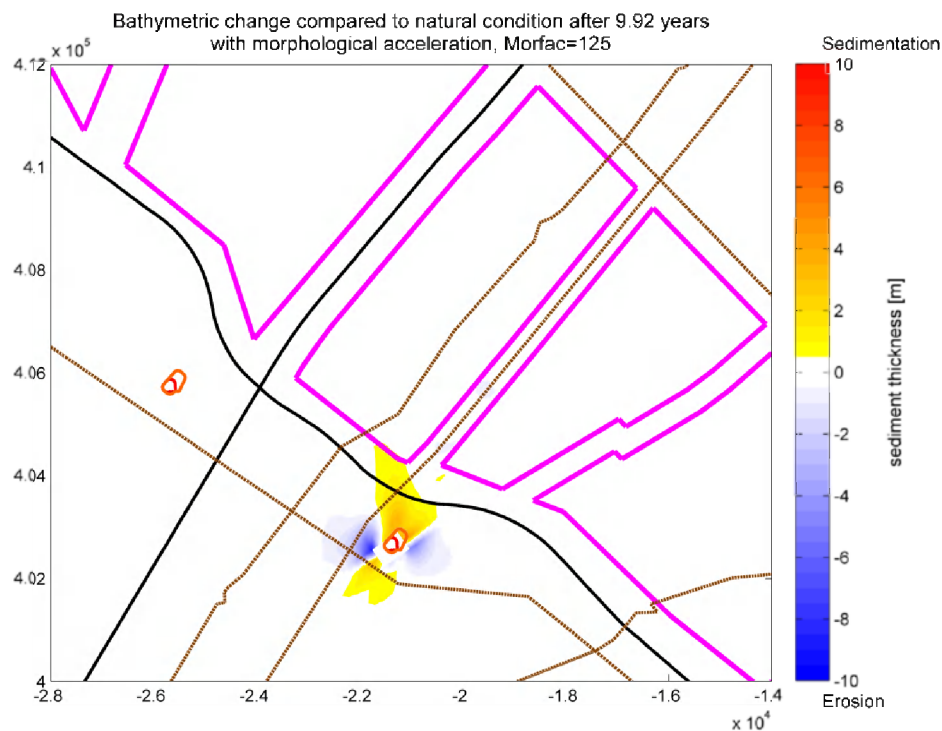


Figure 3-58 : Bathymetric change of TIPA I compared to natural condition after +/- 10 years with morphological acceleration (Morfac=125).

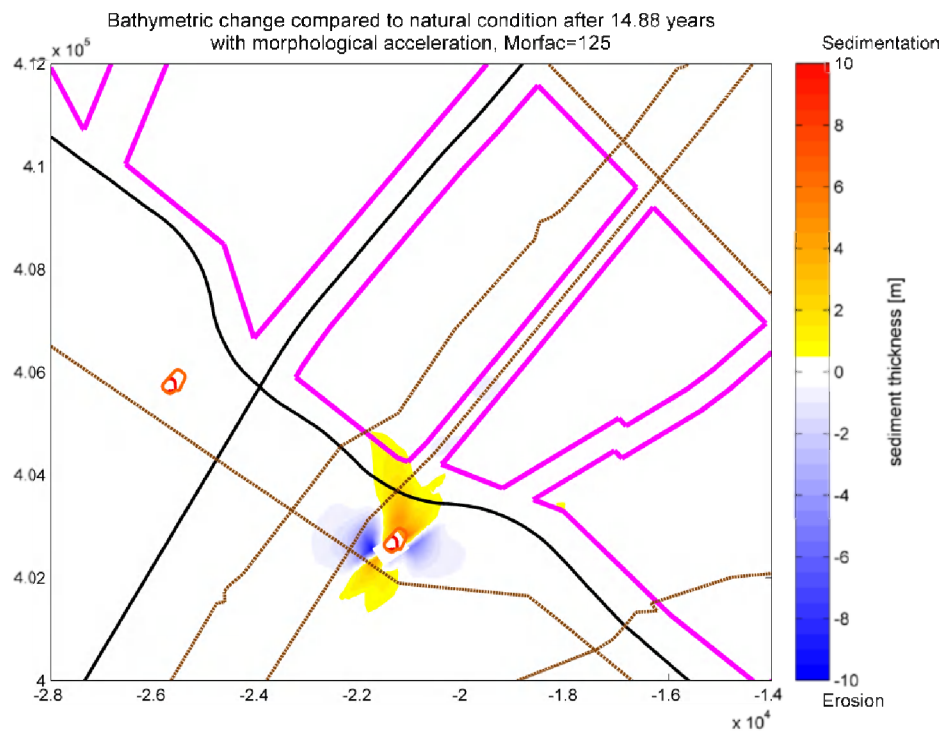


Figure 3-59: Bathymetric change of TIPA I compared to natural condition after +/- 15 years with morphological acceleration (Morfac=125).

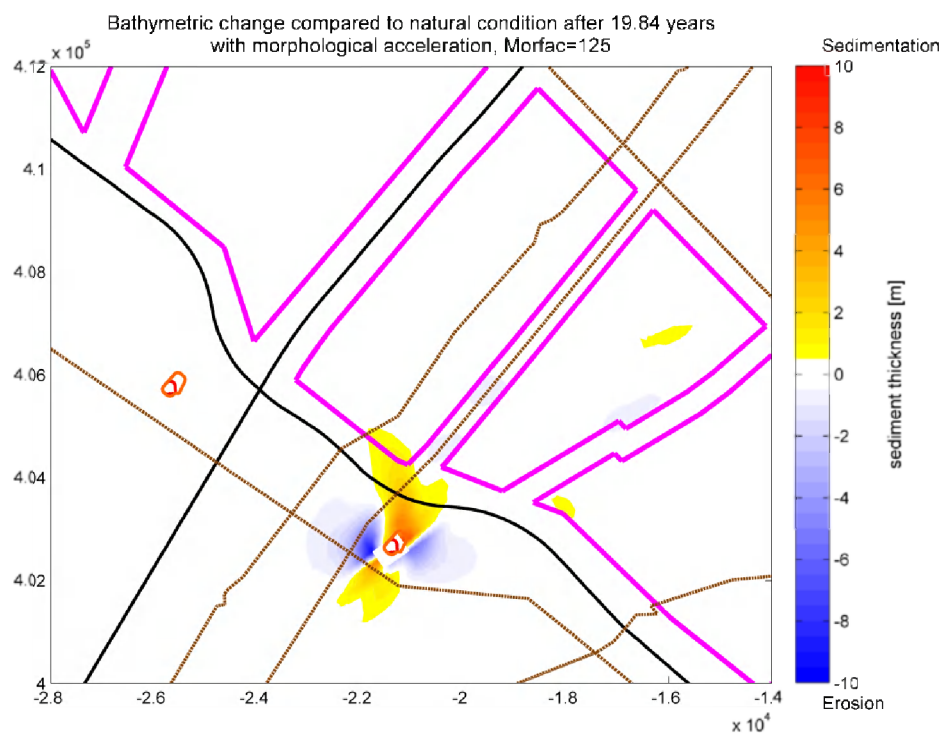


Figure 3-60: Bathymetric change of TIPA I compared to natural condition after +/- 20 years with morphological acceleration (Morfac=125).

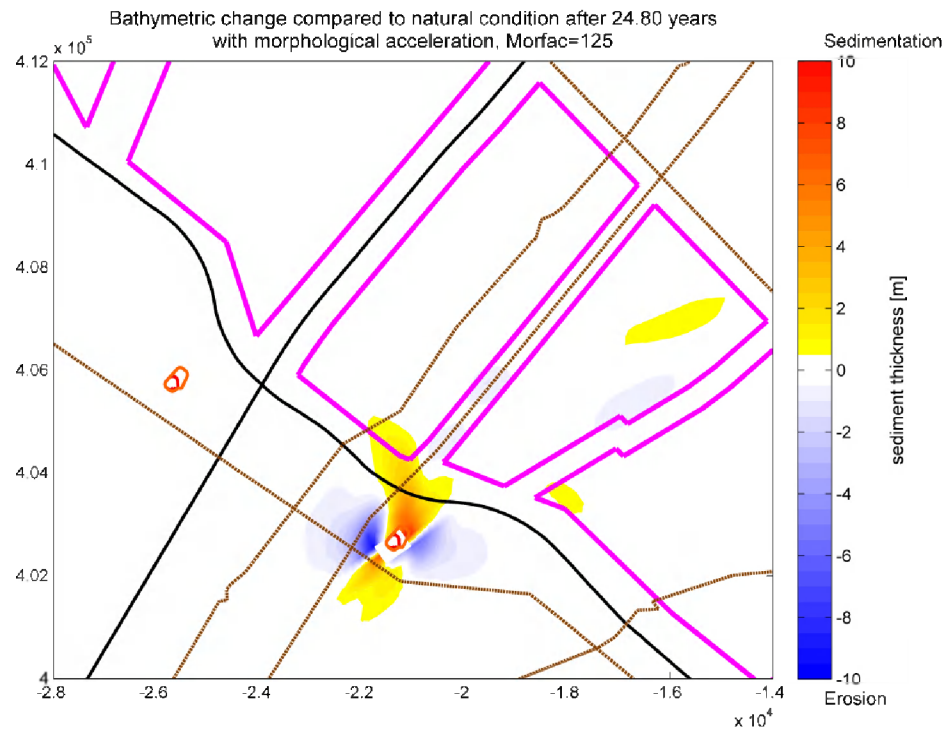


Figure 3-61: Bathymetric change of TIPA I compared to natural condition after +/- 25 years with morphological acceleration (Morfac=125).

From Figure 3-57 to Figure 3-61 it could be seen that the sedimentation/erosion compared to the natural condition is consistent with the orientation of the current ellipse. The sedimentation takes place at the main axis of the current ellipse whereas the erosion takes places at the minor axis of the current ellipse. At lee side of the artificial island the sedimentation seems to be stronger and larger than that at stoss side due to the role of residual currents, and even extend to the Seastar concession zone. In addition, some erosions could be found at the submarine cables, the one to west of the artificial island is around 5 m and the other between the Seastar and Northwind concession zones is less than 1 m after 25 years. Apart from these sedimentations/erosions, some other sedimentation around 1 m could be found in the Northwind and Rentel concession zones and some other erosion around 1 m could be found in the Northwind concession zone after 20 years.

3.4.2 Morphological evolution (Morfac=125, +/- 25 years)

To investigate morphological evolution, the sedimentation/erosion is examined for every 5 years in totally 25 years. In this section, only results of the natural condition (Figure 3-62 ~ Figure 3-66) and TIPA I (Figure 3-67 ~ Figure 3-71) are presented. Results of SIP I, DIPP I, SIP II, TIPA II and DIPP II have been attached from 6.3.1 to 6.3.5 of Appendix.

From both the natural condition and TIPA I it could be seen that the morphological evolution gradually slows down as time goes on, and sedimentation always takes place at east of Blighbank. In the natural condition, the morphology at the two alternative locations of the artificial island seems to be relatively stable without any evident change, only during the first 5 years some sedimentation/erosion could be found at Location II. For TIPA I the erosion occurring to west of the artificial island appears to affect the submarine cables constantly.

As can be seen, the limited erosion that was found in the Northwind concession area in the previous paragraph, also seems to occur without the presence of the island. The presence of the island seems to increase the natural process slightly.

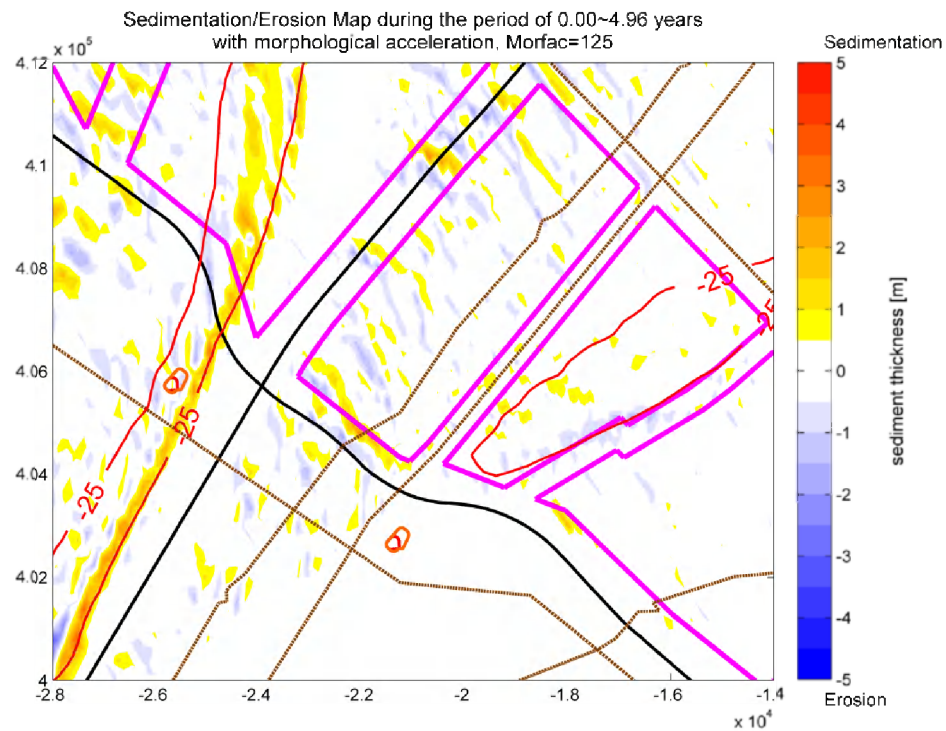


Figure 3-62: Map of sedimentation/erosion with natural condition during the first 5 years with morphological acceleration (Morfac=125).

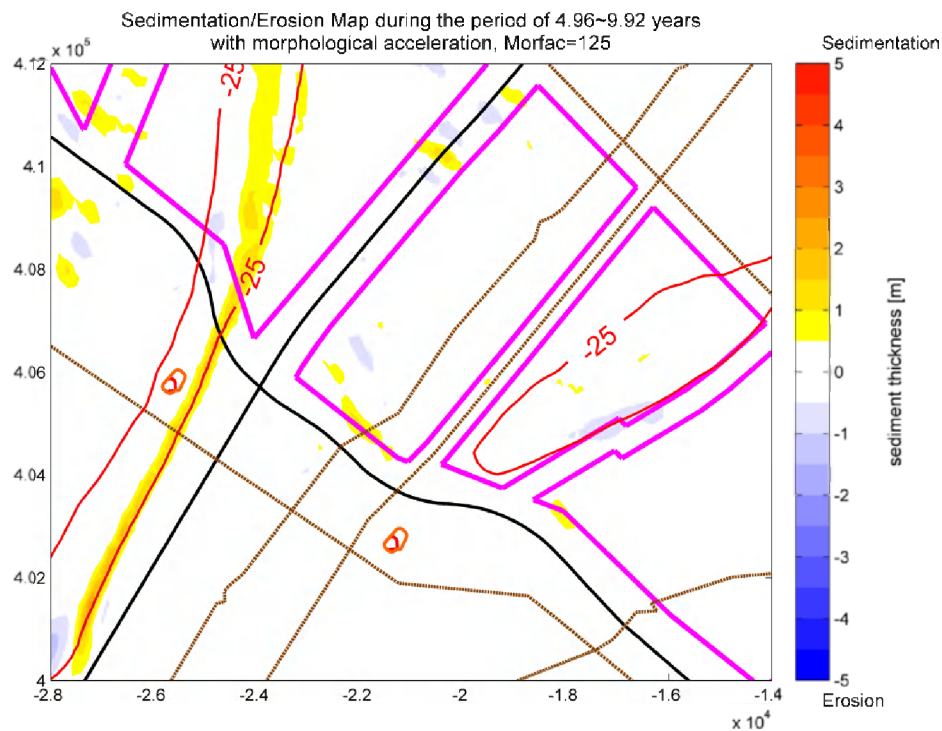


Figure 3-63: Map of sedimentation/erosion with natural condition during the second 5 years with morphological acceleration (Morfac=125).

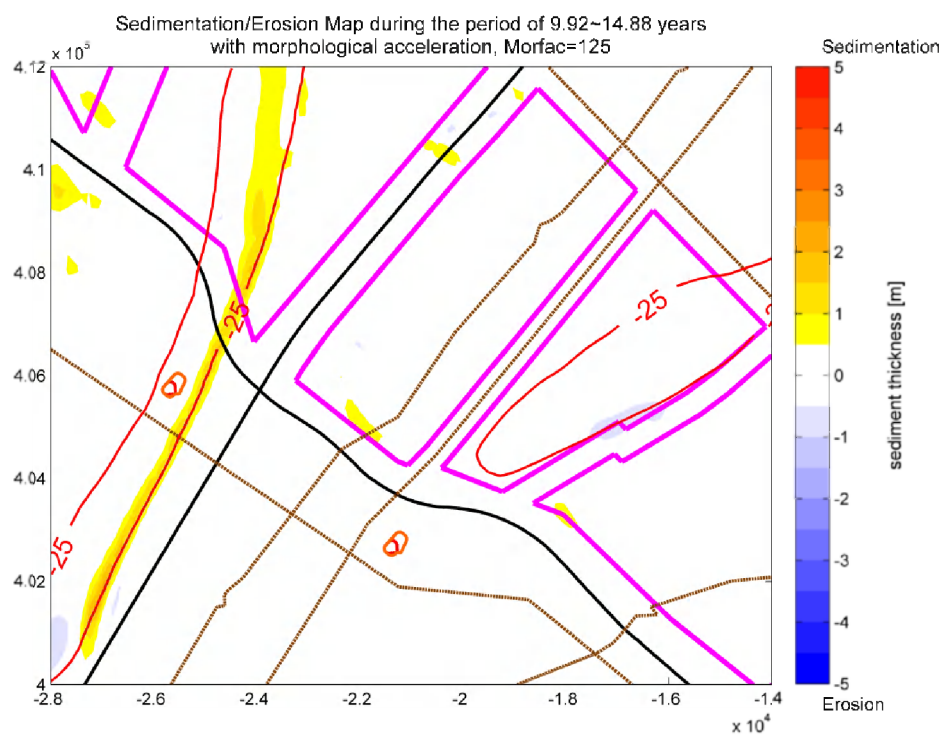


Figure 3-64: Map of sedimentation/erosion with natural condition during the third 5 years with morphological acceleration (Morfac=125).

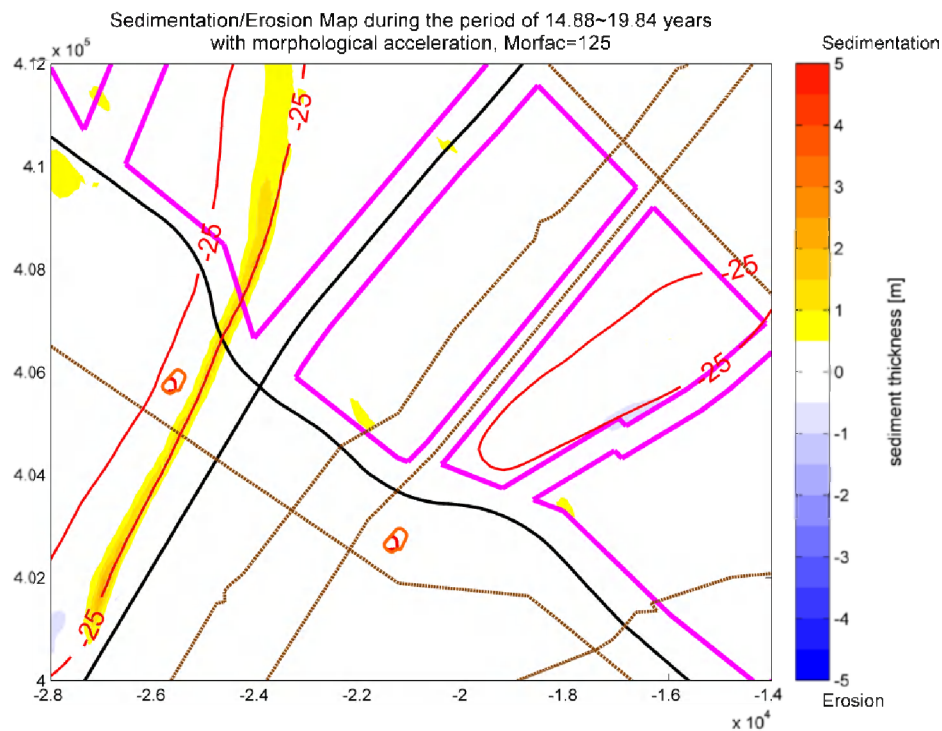


Figure 3-65: Map of sedimentation/erosion with natural condition during the fourth 5 years with morphological acceleration (Morfac=125).

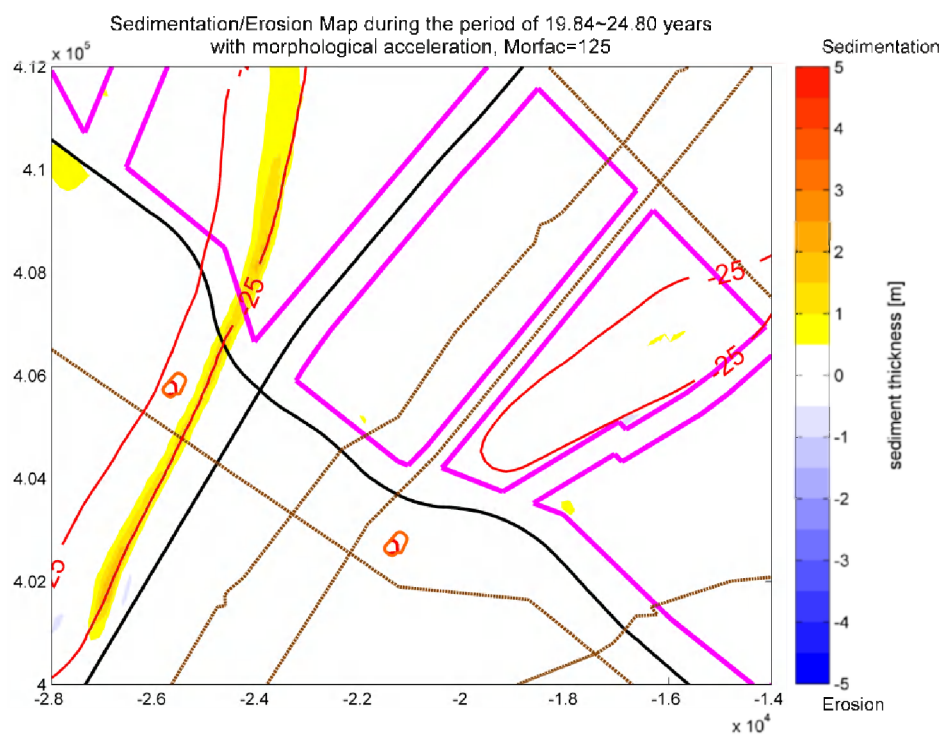


Figure 3-66: Map of sedimentation/erosion with natural condition during the fifth 5 years with morphological acceleration (Morfac=125).

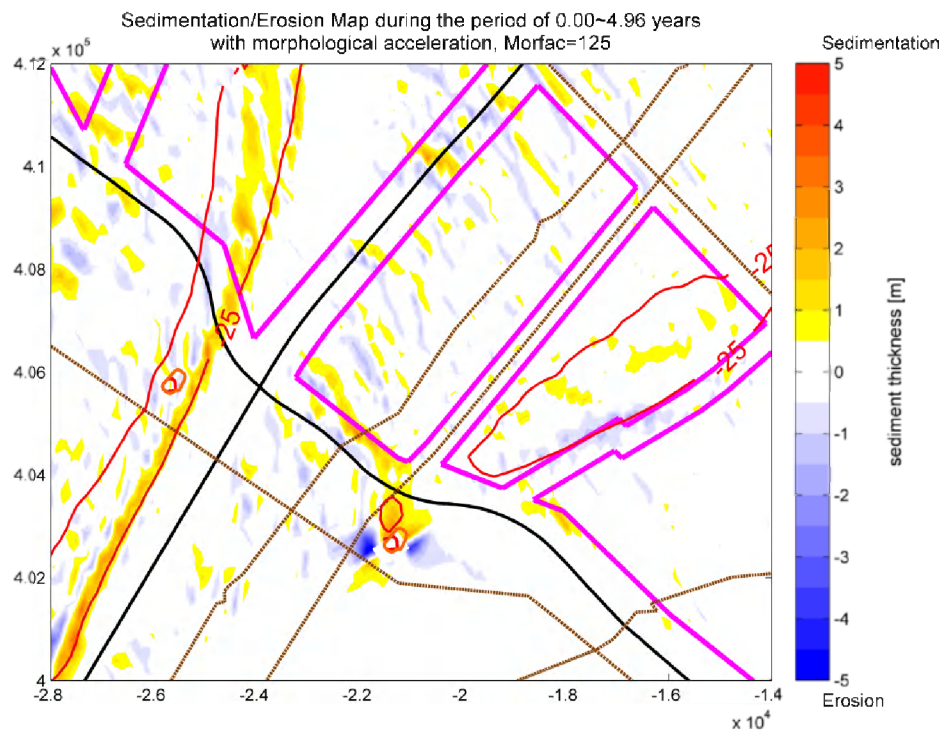


Figure 3-67: Map of sedimentation/erosion with TIPA I during the first 5 years with morphological acceleration (Morfac=125).

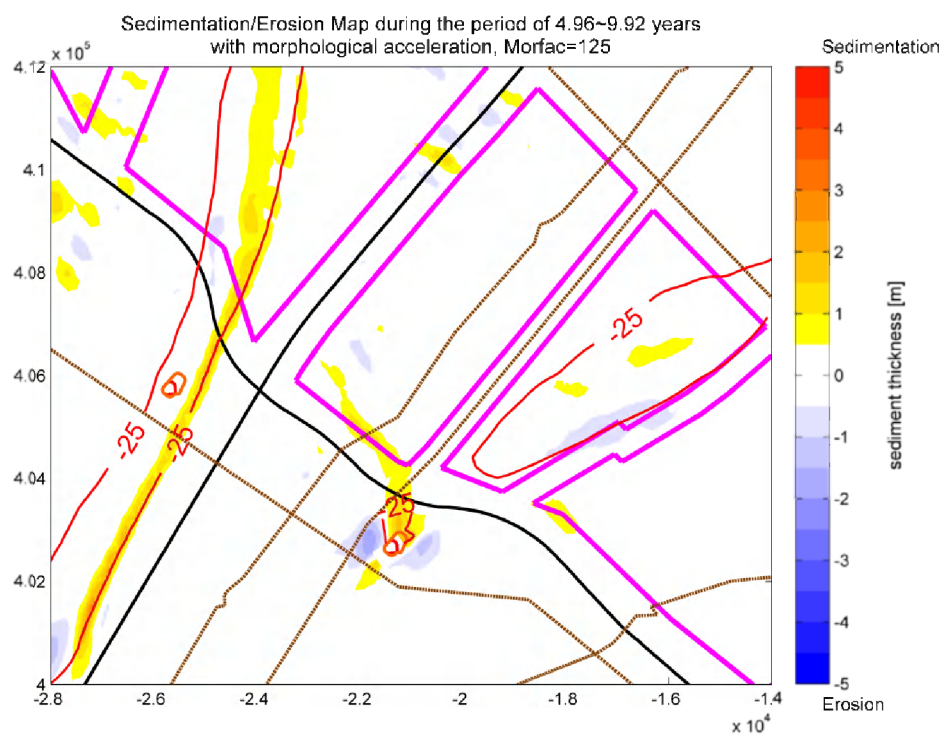


Figure 3-68: Map of sedimentation/erosion with TIPA I during the second 5 years with morphological acceleration (Morfac=125).

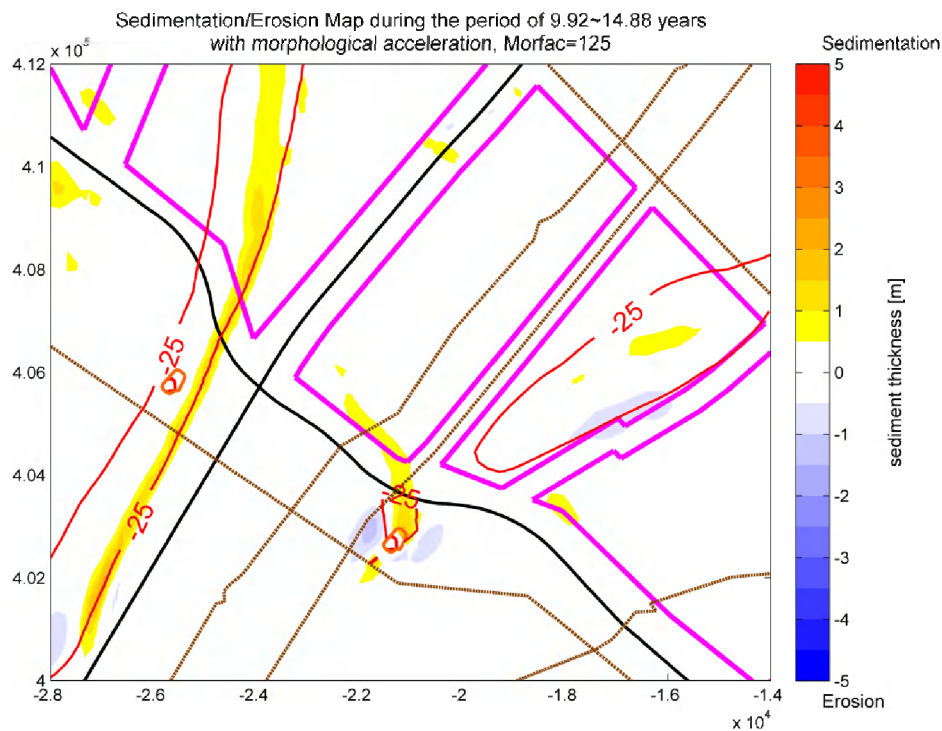


Figure 3-69: Map of sedimentation/erosion with TIPA I during the third 5 years with morphological acceleration (Morfac=125).

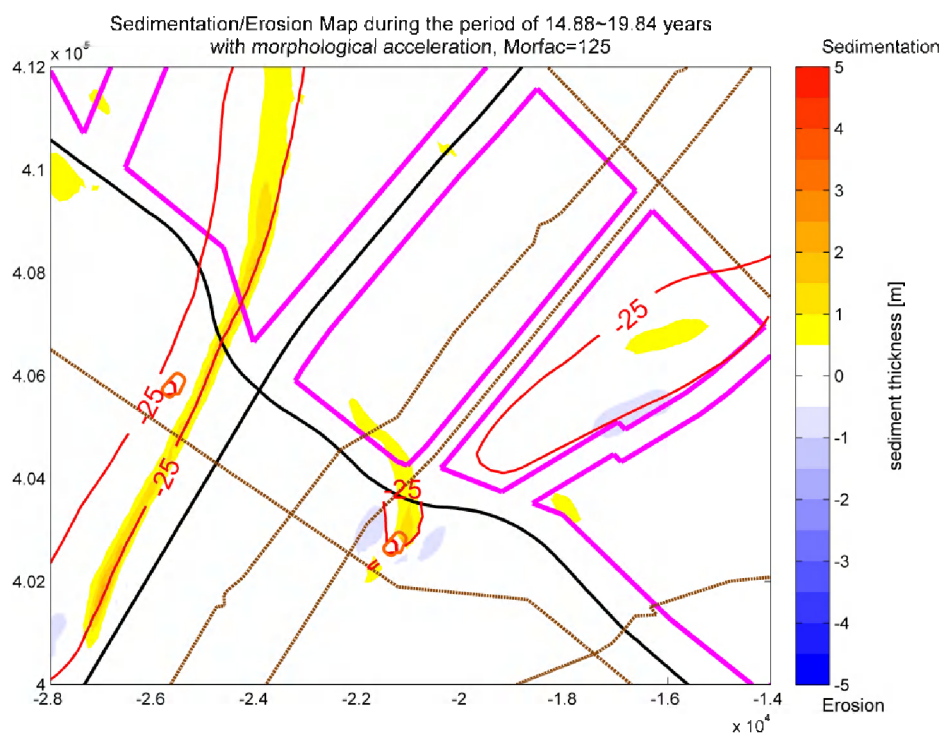


Figure 3-70: Map of sedimentation/erosion with TIPA I during the fourth 5 years with morphological acceleration (Morfac=125).

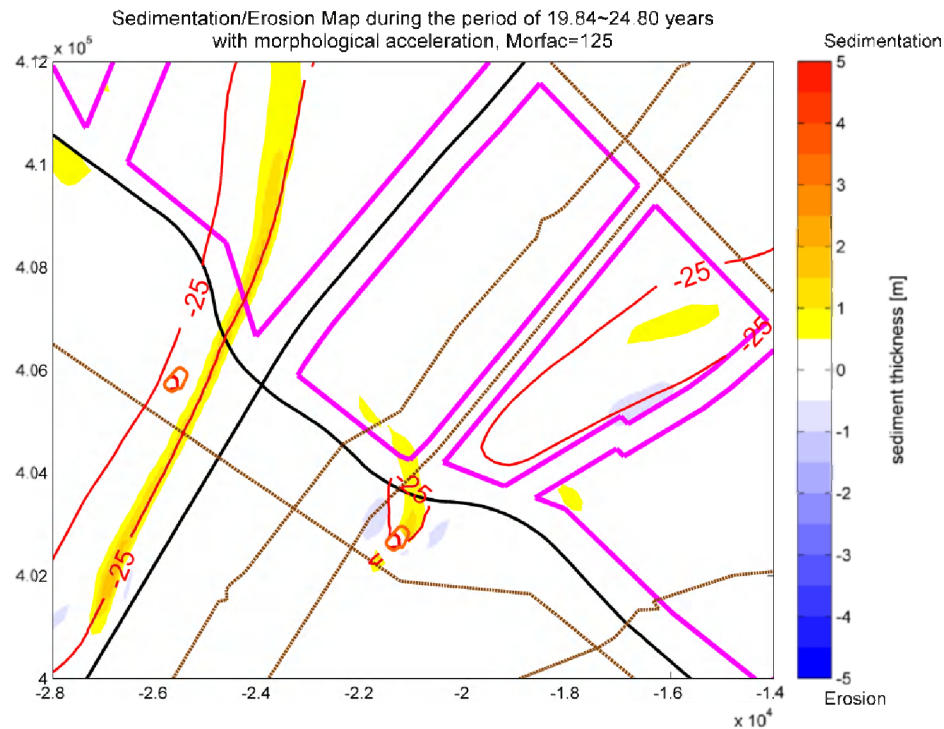


Figure 3-71: Map of sedimentation/erosion with TIPA I during the fifth 5 years with morphological acceleration (Morfac=125).

3.5 NEUTRALISED EFFECTS OF TIDAL FORCING

As mentioned in the last section (section 3.4), only tidal forcing is considered in the long-term morphological simulation. But in reality the wave can also play an important role on the morphodynamics. In this section, the neutralised effects of tidal forcing on the impacts of 1- and 5-years-returned storms are respectively investigated to approve the presumption that the long-term morphodynamics in the study area is mainly driven by tidal forcing, in other words to see if the impacts of 1- and 5-year-returned storms can be neutralised by 1- and 5-year-long tidal forcings. The natural condition and TIPA I (triple inactive points aligned to main flow direction at Location I) are selected to examine neutralisation effects of the tidal forcing.

3.5.1 1-year-returned storm

There are two scenarios which are performed to investigate the neutralised effects of the tidal forcing. One is firstly carried out with the 1-year-returned storm in 2 weeks and immediately followed by only tidal forcing of 1 year; the other is carried out only with the tidal forcing of 1 year. Figure 3-72 shows the difference of final sedimentation/erosion between these two scenarios for the natural condition. It could be observed that the impacts of the 1-year-returned storm can be almost completely neutralised by the 1-year tidal forcing, only at south of Blighbank there is some minor difference less than 0,1 m.

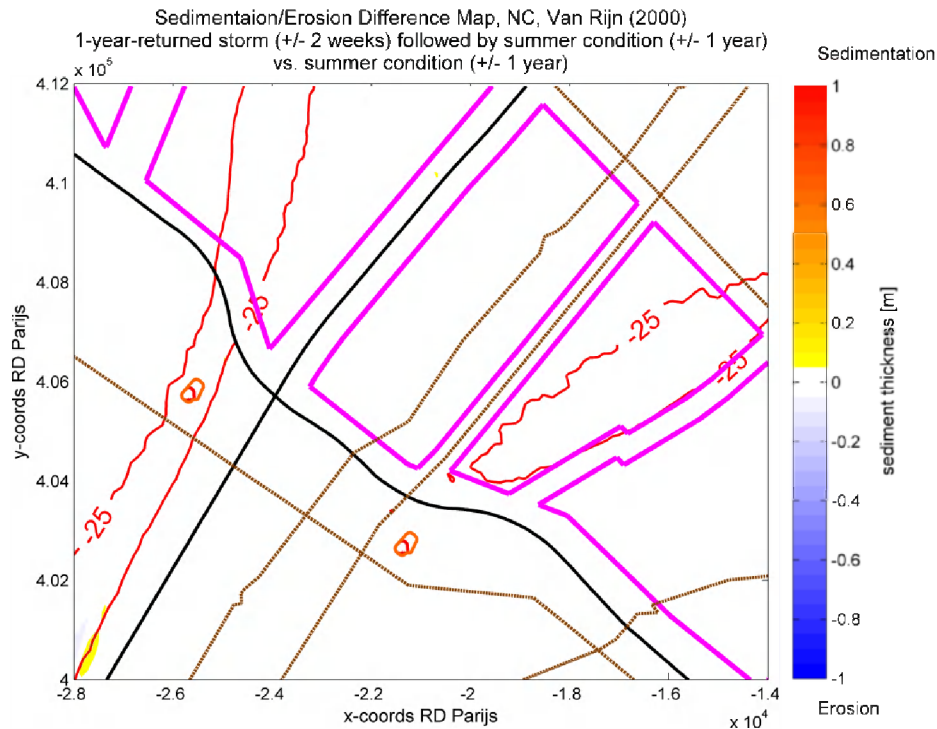


Figure 3-72: Map of sedimentation/erosion difference between the scenario with 1-year-returned storm followed by 1-year tidal forcing and the scenario only with 1-year tidal forcing for natural condition .

In addition to the natural condition, the two scenarios are equally carried out for TIPA I. One is firstly run with the 1-year-returned storm in 2 weeks followed by only tidal forcing of 1 year; the other is run only with tidal forcing of 1 year. From Figure 3-73 it could be also observed that the impacts of the 1-year-returned storm can be almost completely neutralised by the 1-year tidal forcing within the case of TIPA I. Some minor difference can be only found at south of Blighbank as well as next to the artificial island.

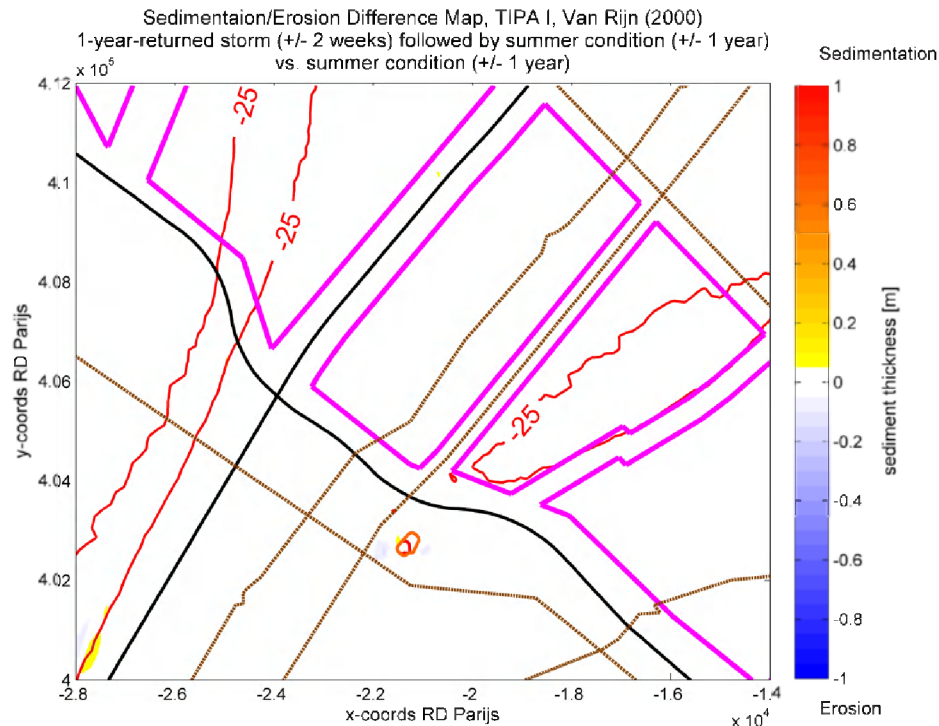


Figure 3-73: Map of sedimentation/erosion difference between the scenario with 1-year-returned storm followed by 1-year tidal forcing and the scenario only with 1-year tidal forcing for TIPA I.

3.5.2 5-year-returned storm

Apart from the 1-year-returned storm, the neutralised effects of tidal forcing on impacts of the 5-years-returned storm are also examined within the natural condition and TIPA I. Figure 3-74 shows the difference of final sedimentation/erosion between the scenario with combination of storm and tidal forcing and the scenario only with tidal forcing for the natural condition. It could be observed that impacts of the 5-year-returned storm can even be more completely neutralised by the 5-year tidal forcing, only at south of Blighbank there is some slight difference less than 0,1 m.

The difference of the two scenarios for the case of TIPA I is demonstrated in Figure 3-75. A slight difference is only found at south of Blighbank. The one found next to the artificial island for the 1-year-returned storm becomes invisible for the 5-year-returned storm followed by the 5-year tidal forcing.

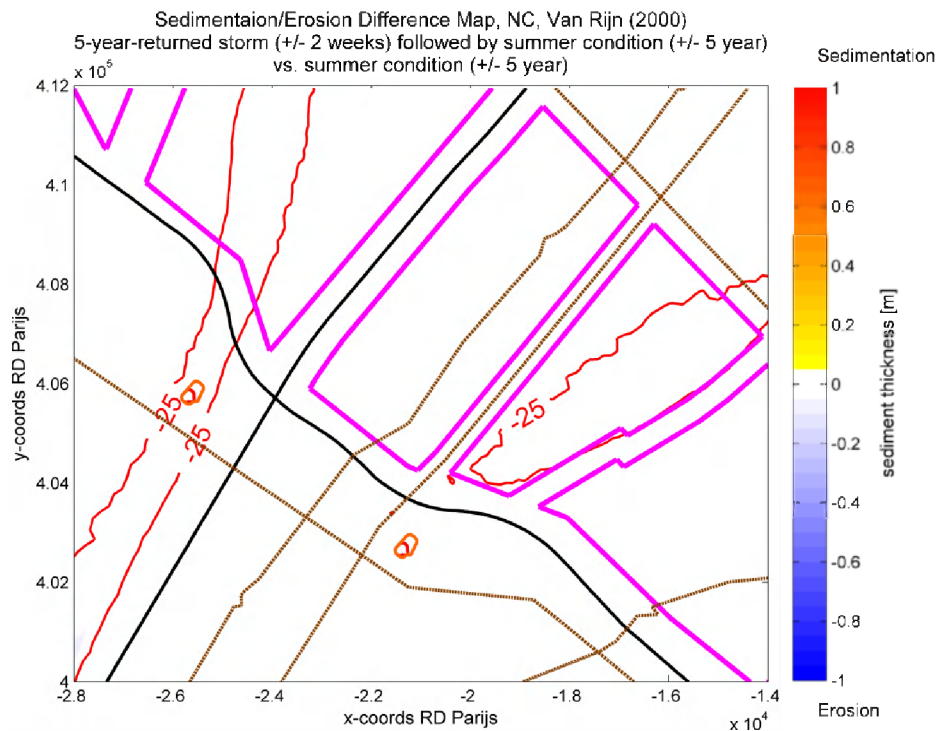


Figure 3-74: Map of sedimentation/erosion difference between the scenario with 5-year-returned storm followed by 5-year tidal forcing and the scenario only with 5-year tidal forcing for natural condition.

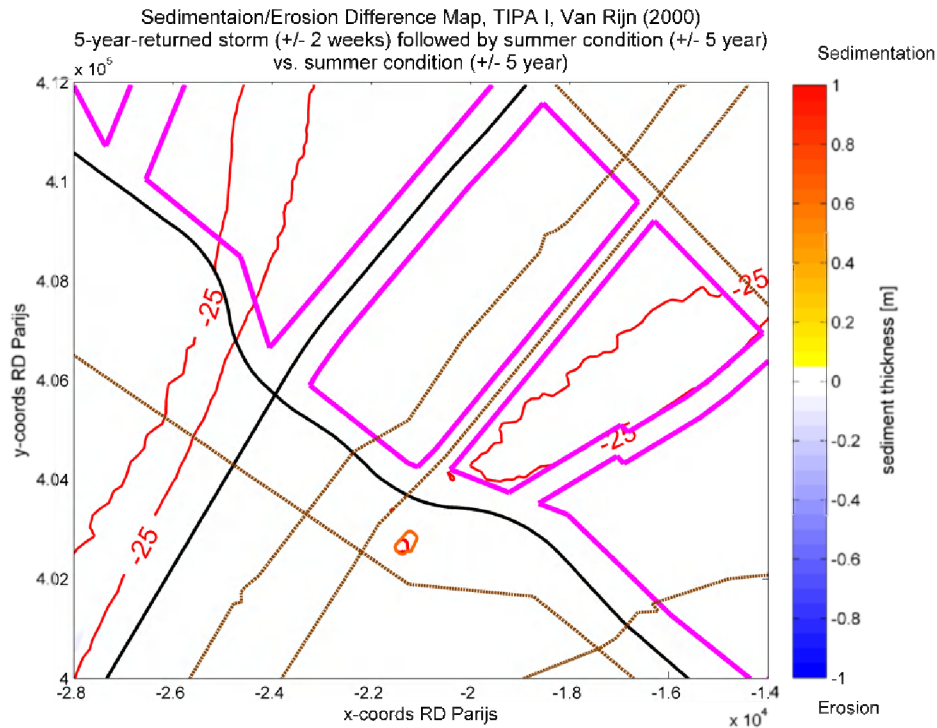


Figure 3-75: Map of sedimentation/erosion difference between the scenario with 5-year-returned storm followed by 5-year tidal forcing and the scenario only with 5-year tidal forcing for TIPA I.

3.6 OTHER SEDIMENT TRANSPORT FORMULAE

The results related to sediment transport presented previously in this study are all calculated based on the default sediment transport formula (STF) Van Rijn (2000). In order to better approve validity and reliability of these results, other two STF Soulsby/Van Rijn and Bijker (1971) are employed and the results calculated by them are compared with those calculated by Van Rijn (2000) respectively in the following study.

3.6.1 Soulsby / Van Rijn

The STF Soulsby/Van Rijn (Soulsby, 1997) is compared to the default STF Van Rijn (2000) within three conditions. The first one is the summer condition only with the 1-year tidal forcing, the second one is the winter condition with the 1-year-returned storm in 2 weeks and the third one is to test neutralisation with the 1-year-returned storm in 2 weeks followed by only tidal forcing of 1 year. Each condition is simulated with the natural condition and TIPA I respectively.

3.6.1.1 Summer condition (Morfac=25, +/- 1 year)

The summer condition is run only with 1-year tidal forcing for the natural condition and TIPA I. From upper left and right panels of Figure 3-76 and Figure 3-77 it could be seen that the patterns of sedimentation/erosion are quite similar between Soulsby/Van Rijn and Van Rijn (2000) and Soulsby/Van Rijn is shown to produce higher sedimentation/erosion than Van Rijn (2000). The lower right panels demonstrate a fairly good linear correlation between them. The sedimentation/erosion calculated by Soulsby/Van Rijn is 60% larger than that calculated by Van Rijn (2000) for both scenarios the natural condition and TIPA I.

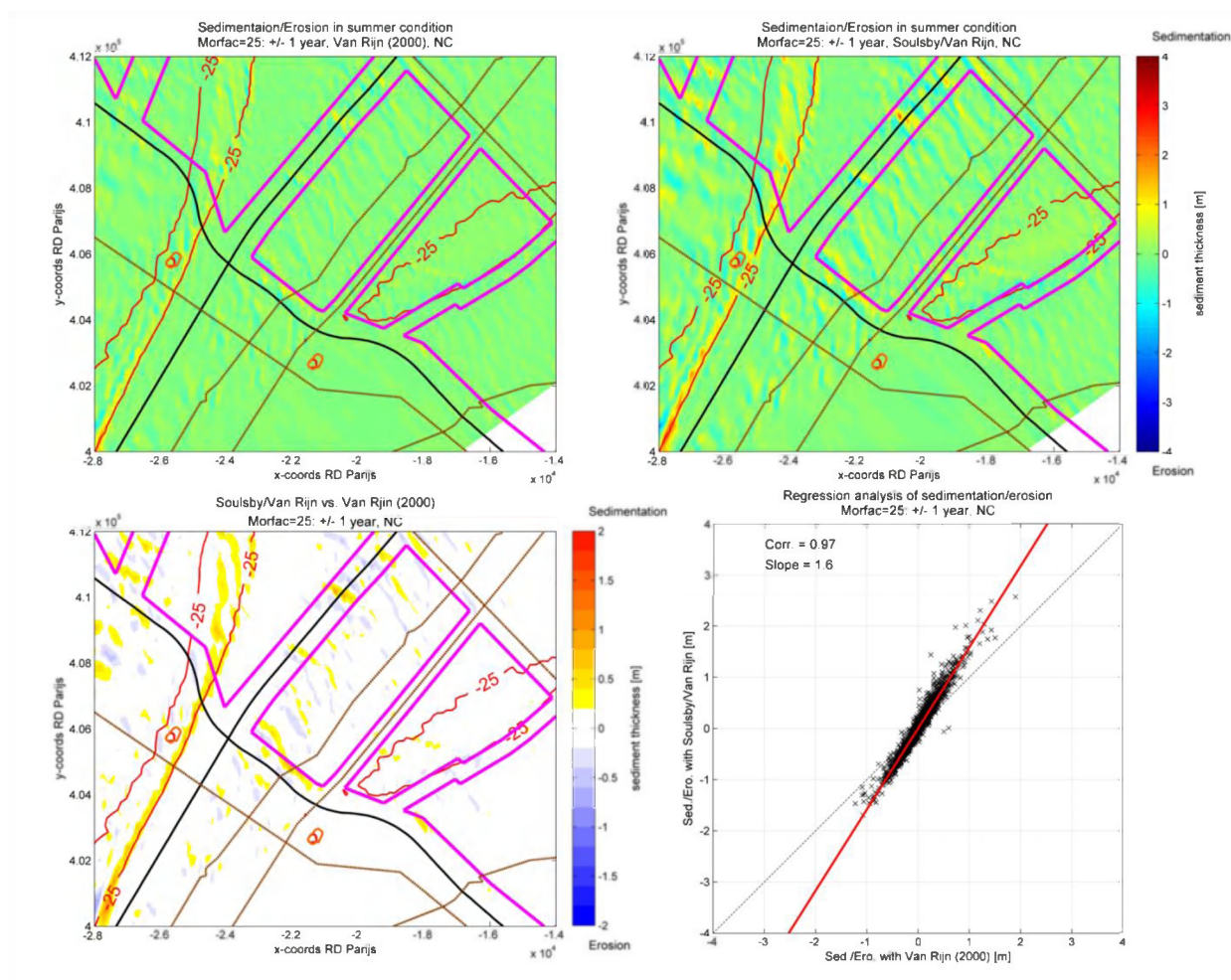


Figure 3-76: left upper panel: sedimentation/erosion calculated by Van Rijn (2000) for natural condition over 1 year only with tidal forcing; right upper panel: sedimentation/erosion calculated by Soulsby/Van Rijn for natural condition over 1 year only with tidal forcing; left lower panel: difference between sedimentations/erosions calculated by Van Rijn (2000) and by Soulsby/Van Rijn; right lower panel: regression analysis of sedimentations/erosions calculated by Van Rijn (2000) and by Soulsby/Van Rijn.

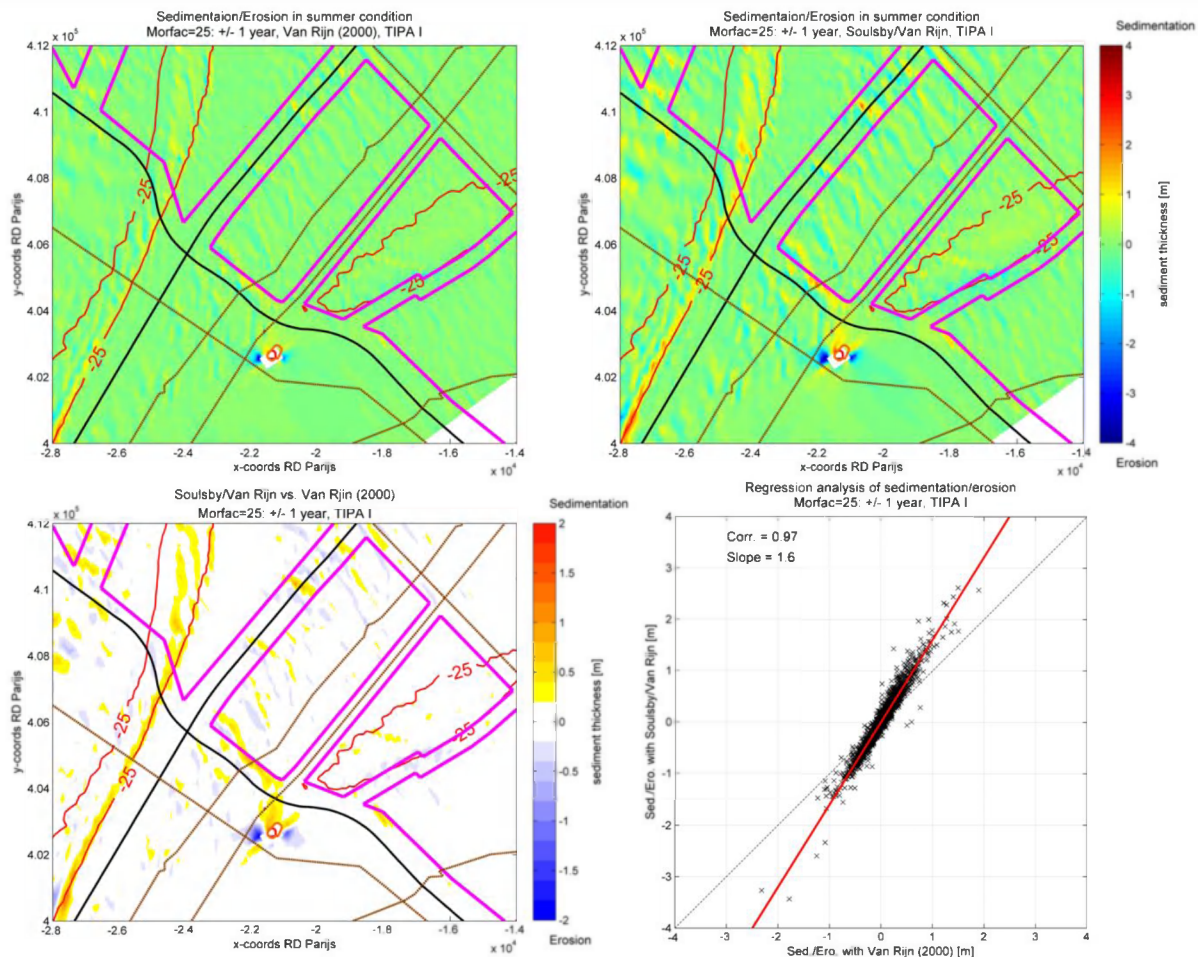


Figure 3-77: left upper panel: sedimentation/erosion calculated by Van Rijn (2000) for TIPA I over 1 year only with tidal forcing; right upper panel: sedimentation/erosion calculated by Soulsby/Van Rijn for TIPA I over 1 year only with tidal forcing; left lower panel: difference between sedimentations/erosions calculated by Van Rijn (2000) and by Soulsby/Van Rijn; right lower panel: regression analysis of sedimentations/erosions calculated by Van Rijn (2000) and by Soulsby/Van Rijn.

3.6.1.2 Winter condition (1-year-returned storm)

The winter condition is run with the 1-year-returned storm for the natural condition and TIPA I. The same results as the summer condition could be found in Figure 3-78 and Figure 3-79. The patterns of sedimentation/erosion are quite similar between Soulsby/Van Rijn and Van Rijn (2000) and a even higher linear correlation (0.99) between them could be found in the lower right panels. The sedimentation/erosion calculated by Soulsby/Van Rijn is still 60% larger than that calculated by Van Rijn (2000).

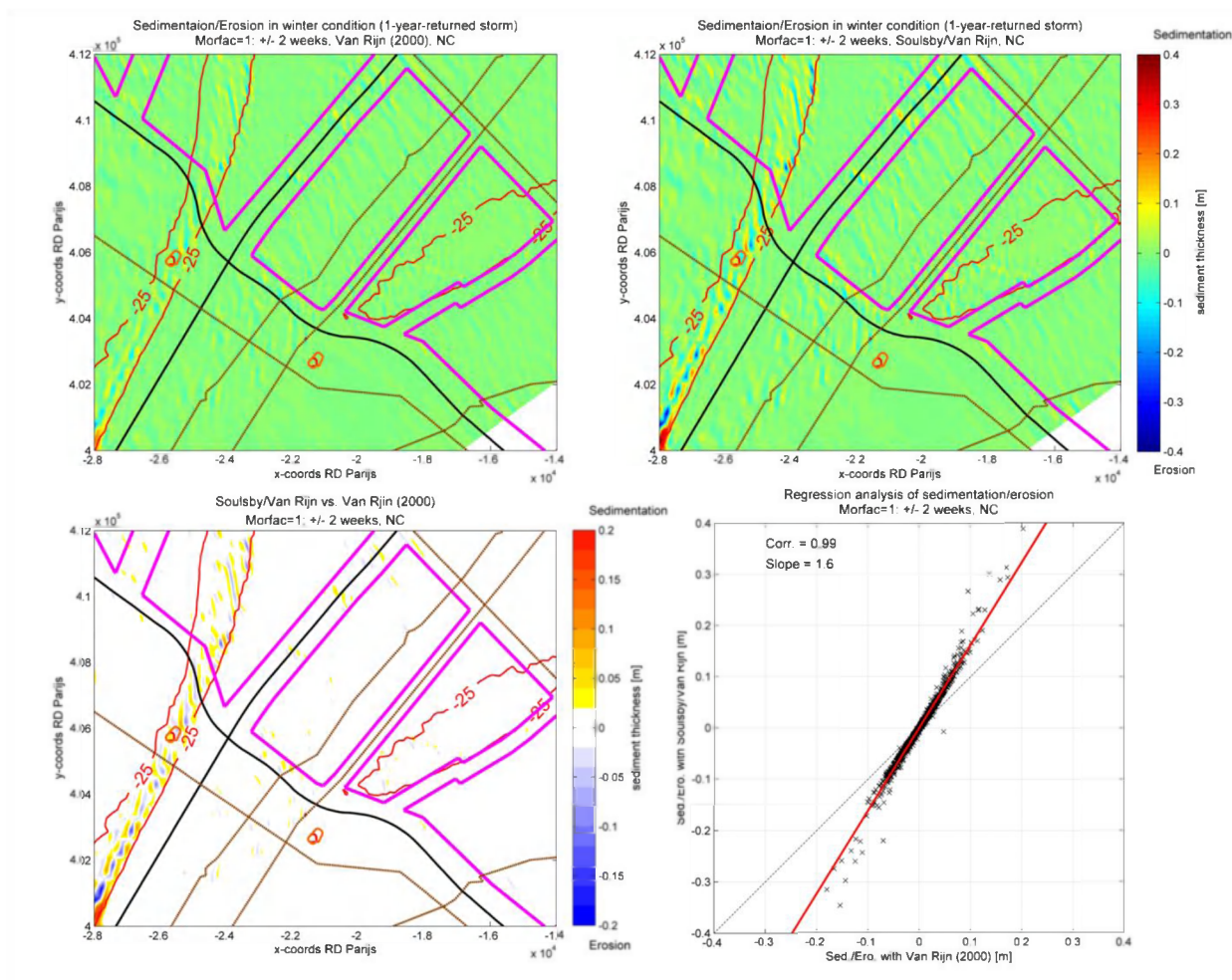


Figure 3-78: left upper panel: sedimentation/erosion calculated by Van Rijn (2000) for natural condition over 2 weeks with 1-year-return storm and tidal forcing; right upper panel: sedimentation/erosion calculated by Soulsby/Van Rijn for natural condition over 2 weeks with 1-year-return storm and tidal forcing; left lower panel: difference between sedimentations/erosions calculated by Van Rijn (2000) and by Soulsby/Van Rijn; right lower panel: regression analysis of sedimentations/erosions calculated by Van Rijn (2000) and by Soulsby/Van Rijn.

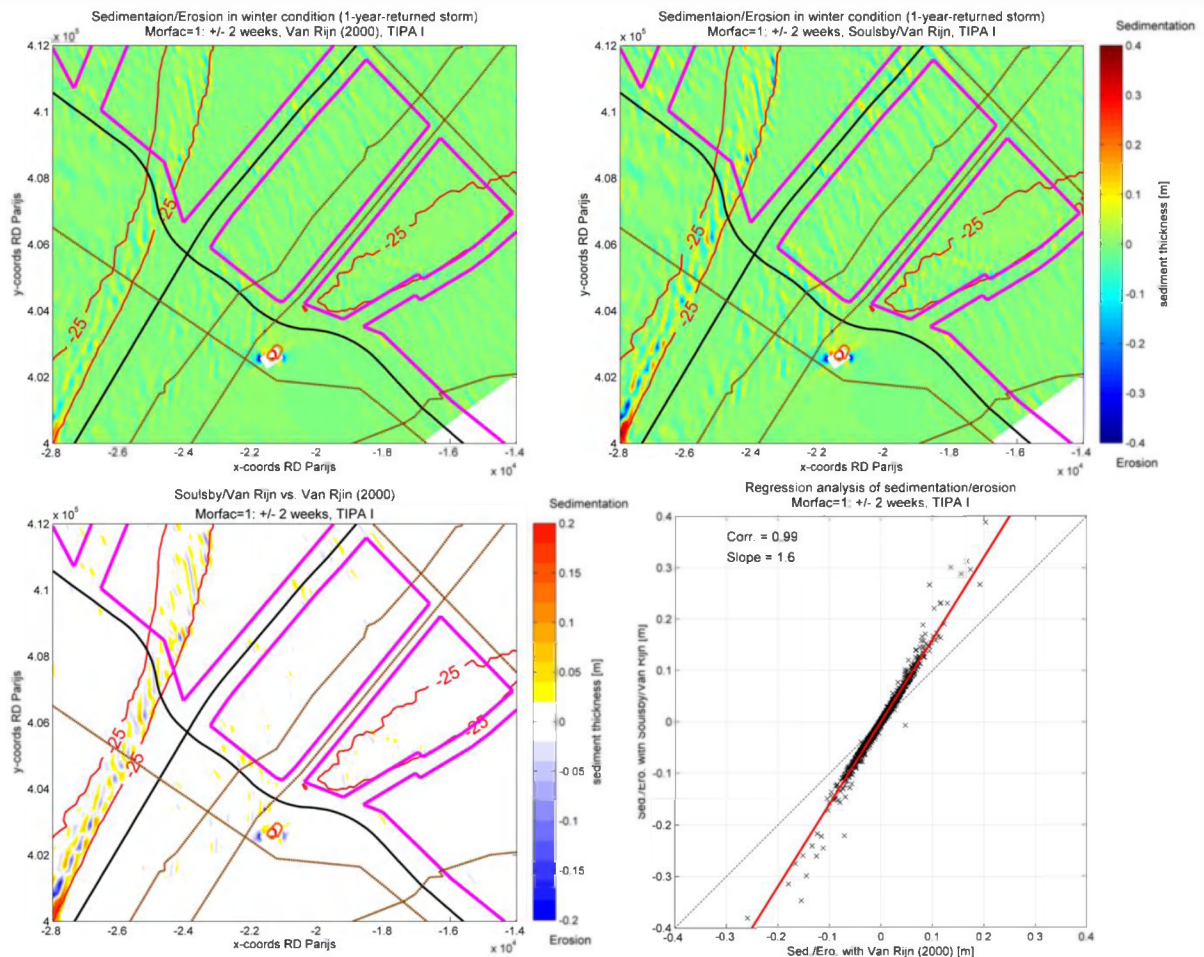


Figure 3-79: left upper panel: sedimentation/erosion calculated by Van Rijn (2000) for TIPA I over 2 weeks with 1-year-returned storm and tidal forcing; right upper panel: sedimentation/erosion calculated by Soulsby/Van Rijn for TIPA I over 2 weeks with 1-year-returned storm and tidal forcing; left lower panel: difference between sedimentations/erosions calculated by Van Rijn (2000) and by Soulsby/Van Rijn; right lower panel: regression analysis of sedimentations/erosions calculated by Van Rijn (2000) and by Soulsby/Van Rijn.

3.6.1.3 Tidal neutralisation for 1-year-returned storm

To further confirm the presumption that the long-term morphodynamics in the study area is mainly driven by tidal forcing, the tidal neutralisation for the 1-year-returned storm is also investigated by the STF Soulsby/Van Rijn for the natural condition and TIPA I. The neutralisation is firstly run with the 1-year-returned storm in 2 weeks and immediately followed by only tidal forcing of 1 year.

Figure 3-72 and Figure 3-73 show the difference of sedimentation/erosion between the scenario with combination of storm and tidal forcing and the scenario only with tidal forcing for the natural condition and TIPA I. Only minor difference around 0.1 m is visible at south of Blighbank and next to the artificial island (in case of TIPA I), which indicates that most impacts of the 1-year-returned storm could be neutralised by the 1-year tidal forcing.

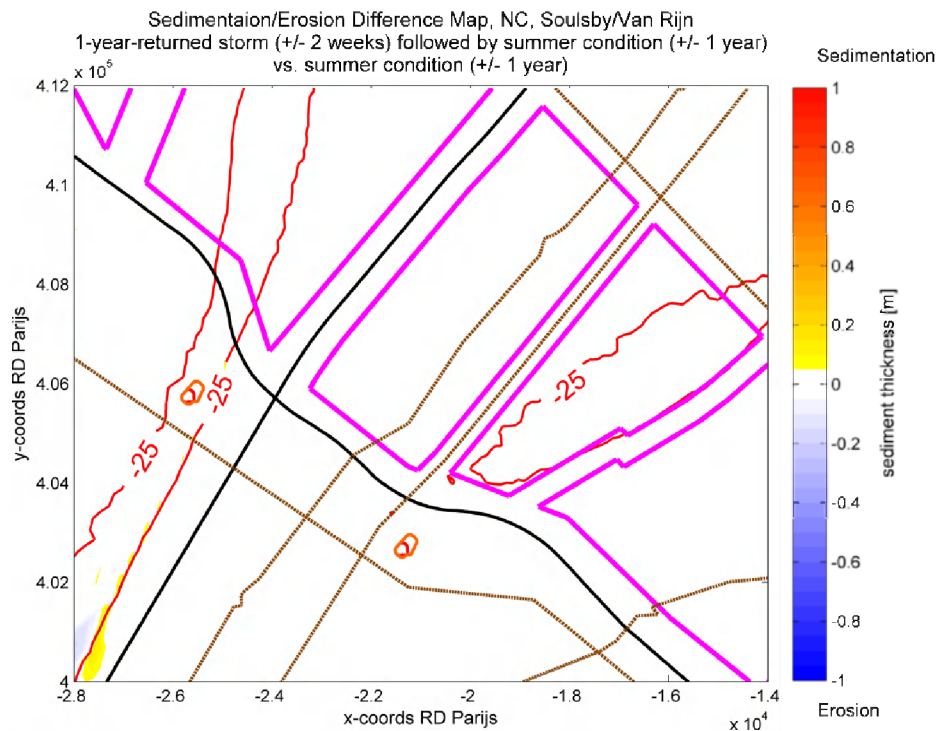


Figure 3-80: Map of sedimentation/erosion difference between the scenario with 1-year-returned storm followed by 1-year tidal forcing and the scenario only with 1-year tidal forcing for natural condition based on the sediment transport formula Soulsby/Van Rijn.

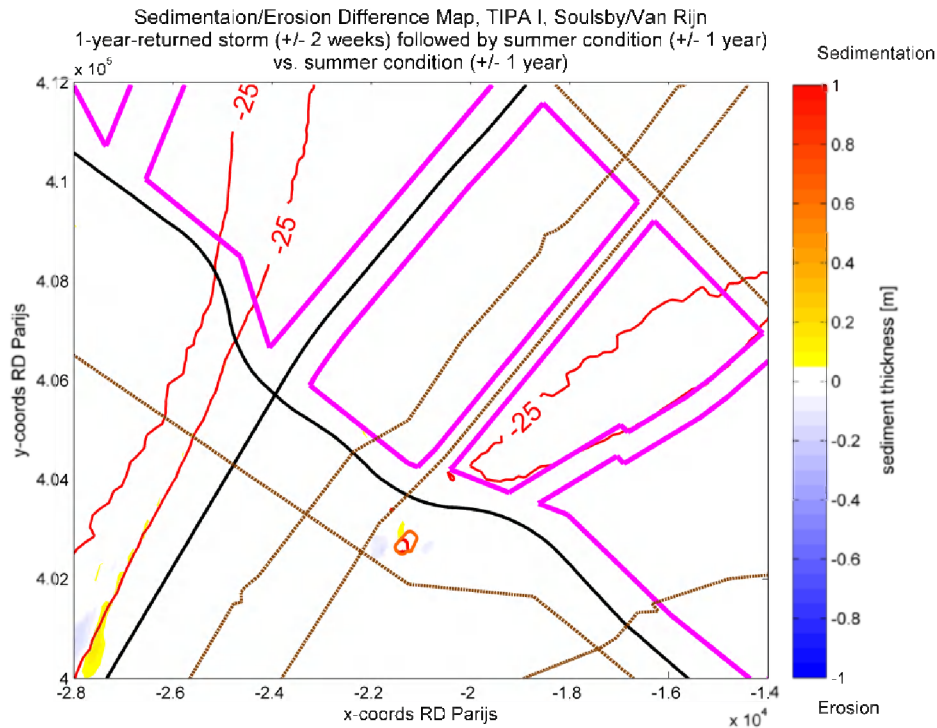


Figure 3-81: Map of sedimentation/erosion difference between the scenario with 1-year-returned storm followed by 1-year tidal forcing and the scenario only with 1-year tidal forcing for TIPA I based on the sediment transport formula Soulsby/Van Rijn.

3.6.2 Bijker (1971)

The STF Bijker (1971) is also compared to the default STF Van Rijn (2000) within the summer, winter and neutralisation conditions. Each condition is simulated with the natural condition and TIPA I respectively.

3.6.2.1 Summer condition (Morfac=25, +/- 1 year)

From upper right panels of Figure 3-82 and Figure 3-83 it could be observed that the sedimentation/erosion calculated by Bijker (1971) is almost invisible using the same scale as Van Rijn (2000). But the lower right panels still demonstrate a good linear correlation between Bijker (1971) and Van Rijn (2000). The sedimentation/erosion calculated by Bijker (1971) is only around a quarter of that calculated by Van Rijn (2000) for both scenarios the natural condition and TIPA I.

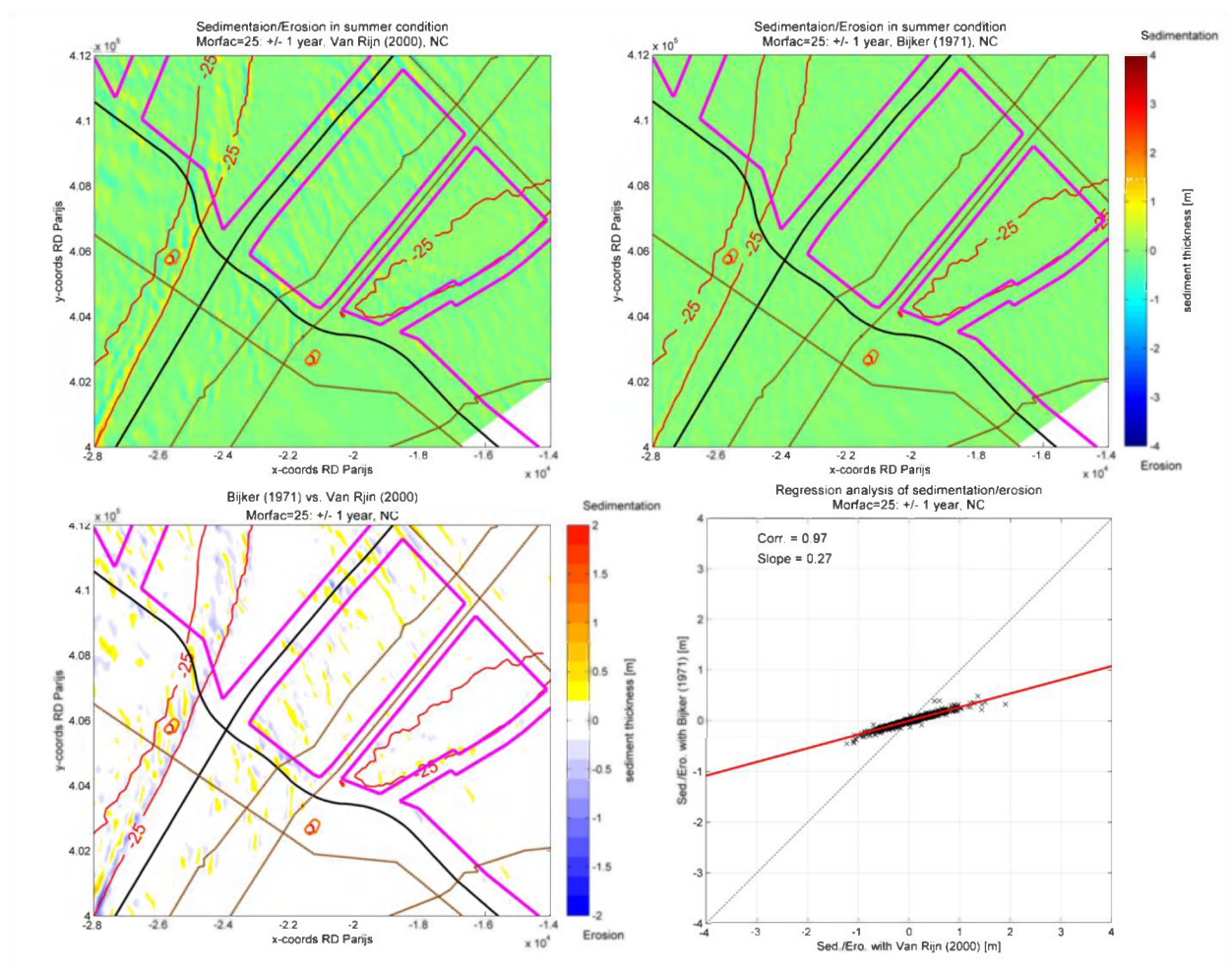


Figure 3-82: left upper panel: sedimentation/erosion calculated by Van Rijn (2000) for natural condition over 1 year only with tidal forcing; right upper panel: sedimentation/erosion calculated by Bijker (1971) for natural condition over 1 year only with tidal forcing; left lower panel: difference between sedimentations/erosions calculated by Van Rijn (2000) and by Bijker (1971); right lower panel: regression analysis of sedimentations/erosions calculated by Van Rijn (2000) and by Bijker (1971).

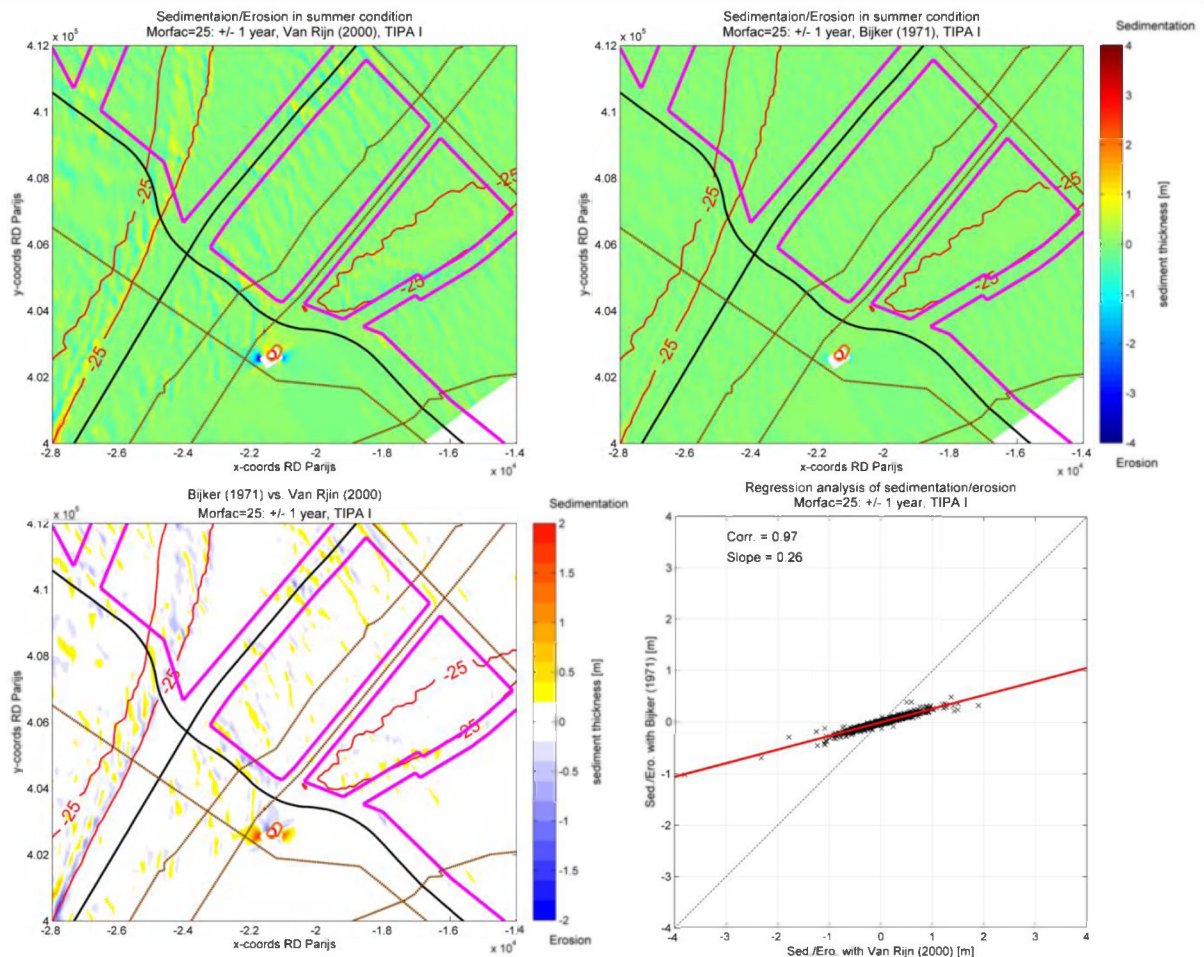


Figure 3-83: left upper panel: sedimentation/erosion calculated by Van Rijn (2000) for TIPA I over 1 year only with tidal forcing; right upper panel: sedimentation/erosion calculated by Bijker (1971) for TIPA I over 1 year only with tidal forcing; left lower panel: difference between sedimentations/erosions calculated by Van Rijn (2000) and by Bijker (1971); right lower panel: regression analysis of sedimentations/erosions calculated by Van Rijn (2000) and by Bijker (1971).

3.6.2.2 Winter condition (1-year-returned storm)

The sedimentation/erosion calculated by Bijker (1971) still looks quite small in the winter condition (Figure 3-84 and Figure 3-85). Only at south of Blighbank some sedimentation/erosion can be easily detected. The linear regression analysis shows that the correlation with Van Rijn (2000) is a little lower than the summer condition, but still reaches over 0.85 for the natural condition and TIPA I. Compared to the summer condition, the ratio of sedimentation/erosion calculated by Bijker (1971) to that calculated by Van Rijn (2000) is increased slightly, and reaches around 0.3.

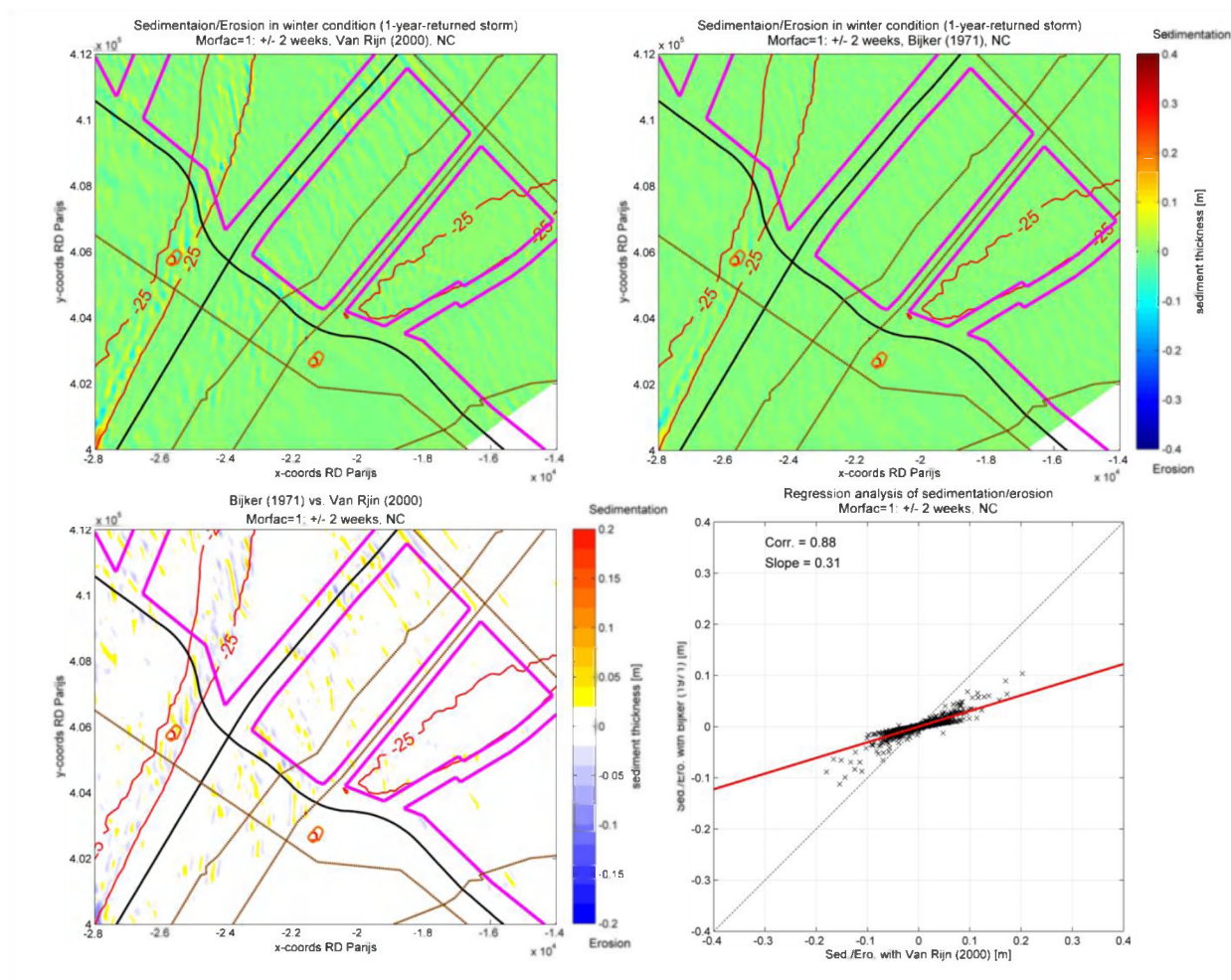


Figure 3-84: left upper panel: sedimentation/erosion calculated by Van Rijn (2000) for natural condition over 2 weeks with 1-year-return storm and tidal forcing; right upper panel: sedimentation/erosion calculated by Bijker (1971) for natural condition over 2 weeks with 1-year-return storm and tidal forcing; left lower panel: difference between sedimentations/erosions calculated by Van Rijn (2000) and by Bijker (1971); right lower panel: regression analysis of sedimentations/erosions calculated by Van Rijn (2000) and by Bijker (1971).

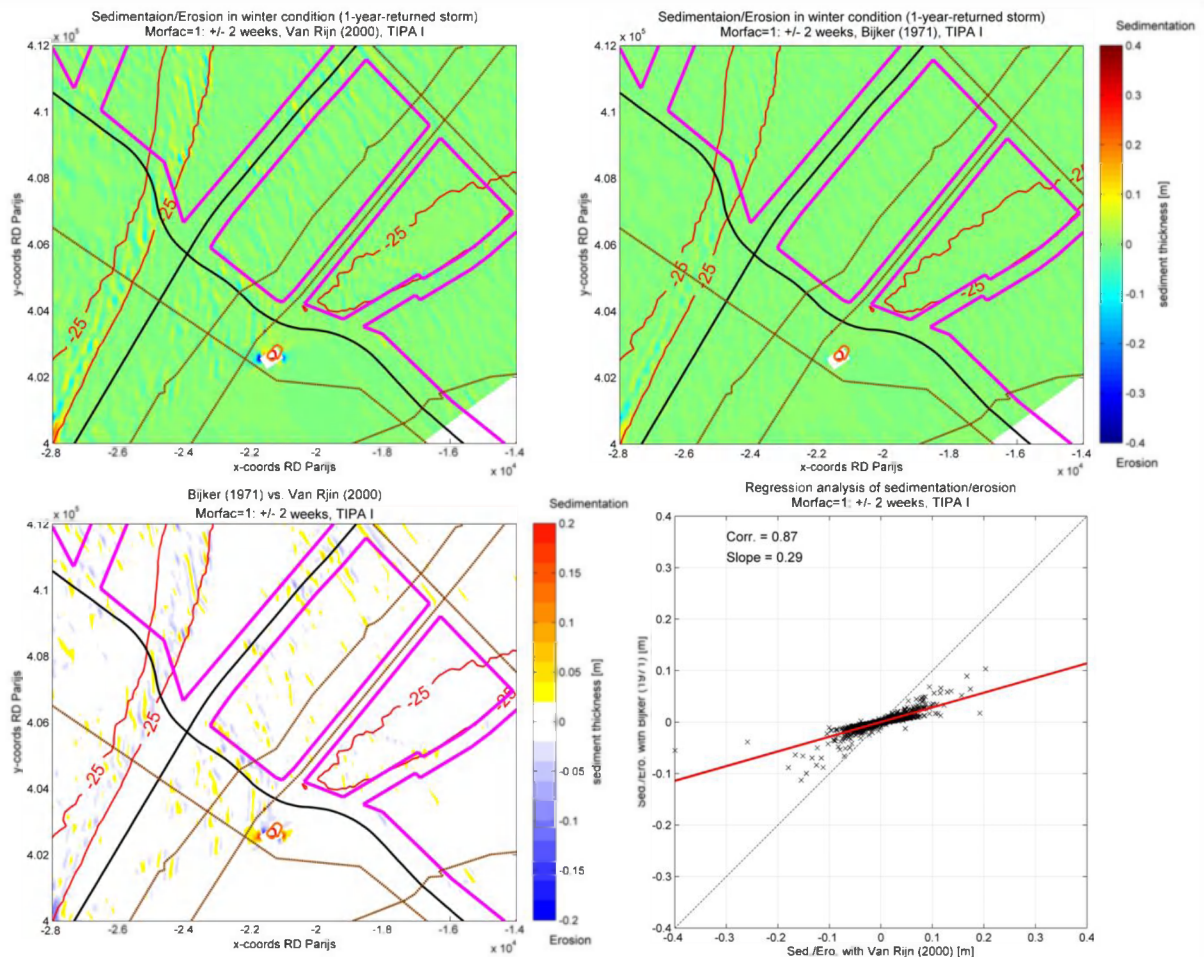


Figure 3-85: left upper panel: sedimentation/erosion calculated by Van Rijn (2000) for TIPA I over 2 weeks with 1-year-returned storm and tidal forcing; right upper panel: sedimentation/erosion calculated by Bijker (1971) for TIPA I over 2 weeks with 1-year-returned storm and tidal forcing; left lower panel: difference between sedimentations/erosions calculated by Van Rijn (2000) and by Bijker (1971); right lower panel: regression analysis of sedimentations/erosions calculated by Van Rijn (2000) and by Bijker (1971).

3.6.2.3 Tidal neutralisation for 1-year-returned storm

The tidal neutralisation for the 1-year-returned storm is also investigated by the STF Bijker (1971) for the natural condition and TIPA I. The difference of sedimentation/erosion between the scenario with combination of storm and tidal forcing and the scenario only with tidal forcing is quite limited and only visible at south of Blighbank for the natural condition and TIPA I (Figure 3-86 and Figure 3-87), which implies that the impacts of the 1-year-returned storm could be also mostly neutralised by the 1-year tidal forcing provided that Bijker (1971) is used to calculate the sediment transport.

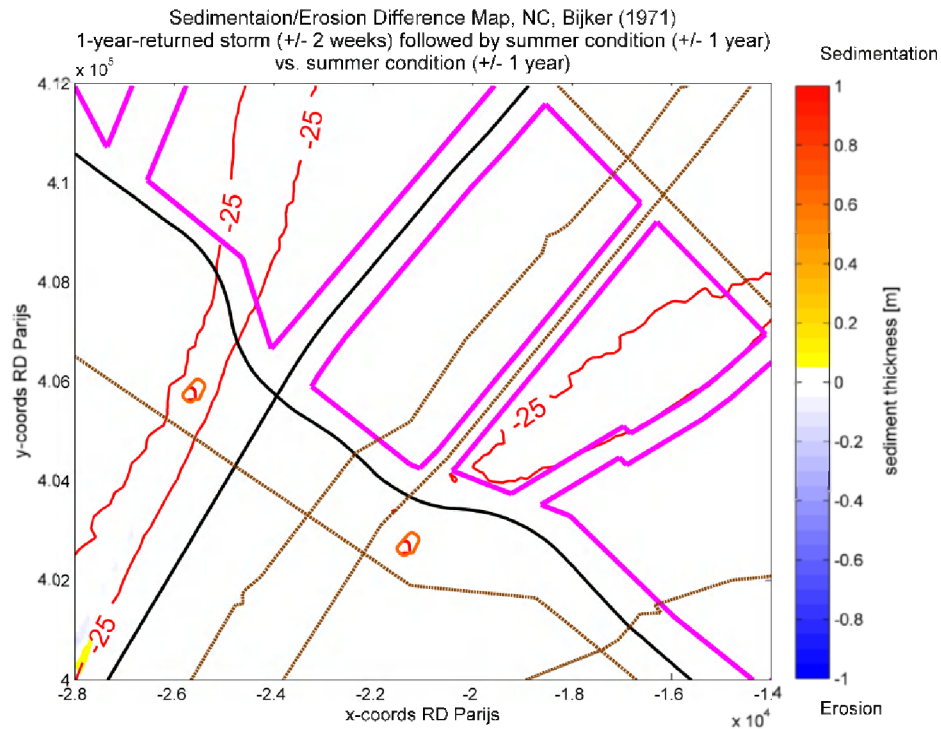


Figure 3-86: Map of sedimentation/erosion difference between the scenario with 1-year-returned storm followed by 1-year tidal forcing and the scenario only with 1-year tidal forcing for TIPA I based on the sediment transport formula Bijker (1971).

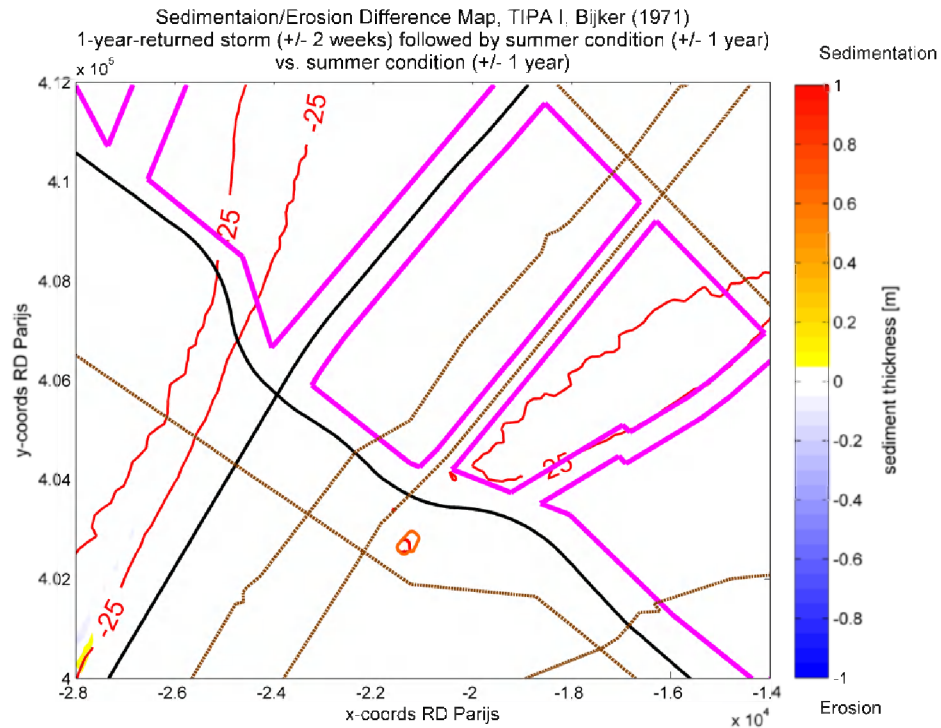


Figure 3-87: Map of sedimentation/erosion difference between the scenario with 1-year-returned storm followed by 1-year tidal forcing and the scenario only with 1-year tidal forcing for TIPA I based on the sediment transport formula Bijker (1971).

4. CONCLUSIONS

In this study, the hydrodynamic model Delft3D-FLOW and standalone wave model Delft3D-WAVE were firstly validated against the measured data in the neighbourhood of the study area. The tidal current at Lodewijkbank seems to be overestimated approximately 25% by the model. This could be attributed to the overestimation of the tidal range due to the boundary conditions generated by the mother model, and to the insufficient resolution of the computational grids to resolve the highly complex topography at the sandbanks. However, variation characteristics of tidal current and elevation were reproduced quite well by the model, and the agreement between the modelling results and measured data is satisfactory. The wave characteristics under storm conditions (with one- and five-year-returned period) were also successfully reproduced by the wave model in view of the comparison of significant wave height, wave period and wave direction between the modelling results and measured data.

The artificial island is schematised by three ways (single inactive point, double inactive points aligned to main flow direction and triple inactive points perpendicular to main flow direction) to consider the impacts of its size and orientation to the main flow direction on the ambient environment by the comparison with the natural condition, and the two alternative locations of the artificial island (at the top of Blighbank and at the western slope of Lodewijkbank) are examined with the three ways of schematisation in the summer and winter conditions of 2 weeks respectively. The results of comparison in the summer and winter conditions are exactly same. The schematisation analysis suggests that the impacts of the three schematisations on the averaged current ellipse are quite minor and only limited to the area adjacent to the artificial island. The impacts on the residual current are also mainly limited to the area near to the artificial island and distributed along the main flow direction from SW to NE. The impacts on the sedimentation/erosion are still very small for the both alternative locations of the artificial island. However compared to the natural condition it should be noticed that some erosion takes place at the submarine cable within the schematisations of TIPA I (triple inactive points perpendicular to main flow direction at Location I), TIPA II (triple inactive points perpendicular to main flow direction at Location II) and DIPP II (double inactive points aligned to main flow direction at Location II).

The storm impacts are investigated by the comparison with the summer condition. The comparison is carried out respectively for 1- and 5-year-returned storms. In the 1-year-returned storm from SW the maximal significant wave height reaches around 4.3 m at Location I and around 3.9 m at Location II whereas in the 5-year-returned storm from NW the maximal one reaches around 6 m at Location I and around 5.5 m at Location II. In the both storm conditions the hydrodynamics including averaged current ellipse and residual current does not exhibit any pronounced difference from the summer condition. Only the magnitude of the residual current in the storm conditions is slightly smaller than that in the summer condition. In the 1-year-returned storm condition, compared to the summer condition the residual sediment transport rate in the area west to Blighbank seems to be enhanced more visibly than that in other locations. Larger difference of sedimentation/erosion from the summer condition is found at the top of Blighbank. While in the 5-year-returned storm condition, compared to the summer condition the residual sediment transport rate seems to be enlarged considerably, and at the top of Blighbank and Lodewijkbank the residual transport direction is

even deviated to the north and the difference of sedimentation/erosion from the summer condition is more visible than at other locations.

Morfac=125 has been successfully approved to be a reliable number for the long-term morphological simulation. TIPA I (triple inactive points perpendicular to main flow direction at Location I) is selected as a typical case to investigate impacts of the artificial island on the long-term morphodynamics by the comparison with the natural condition. In this typical case the sedimentation compared to the natural condition at lee (eastern) side of the artificial island seems to be stronger and larger than that at stoss (western) side and even extend to the Seastar concession zone (+/- 2.400 m vs. +/- 1.300 m). Meanwhile some erosions compared to the natural condition are found at the submarine cables (SEA-ME-WE3 SEG 10.4 and CONCERTO 1S), the one at the joint between SEA-ME-WE3 SEG 10.4 and CONCERTO 1S reaches around 5 m and the other at SEA-ME-WE3 SEG 10.4 between the Seastar and Northwind concession zones is less than 1 m after 25 years. In addition to these sedimentations/erosions, some other sedimentation around 1 m takes place in the Northwind and Rentel concession zones and some other erosion around 1 m takes place in the Northwind concession zone. This limited erosion also seems to occur without the presence of the island. The presence of the island seems to increase the natural process slightly. The bathymetric change in every 5 years shows that the morphological evolution gradually slows down as time goes on, and sedimentation always takes place at east of Blighbank. In the natural condition, the morphology at the two alternative locations of the artificial island seems to be relatively stable without any evident change. Only during the first 5 years some sedimentation/erosion could be found at Location II. For the case of TIPA I the erosion occurring to west of the artificial island is shown to affect the submarine cables continuously.

The presumption that the long-term morphodynamics in the study area is mainly driven by tidal forcing is approved by the fact that impacts of the 1- and 5-year-returned storms can be almost completely neutralised by the 1- and 5-year tidal forcings within the natural condition and TIPA I.

Other two sediment transport formulae Soulsby/Van Rijn and Bijker (1971) are respectively compared with the default transport formula Van Rijn (2000) used in this study. The comparisons of sedimentation/erosion in the 1-year tidal forcing (summer) and 1-year-returned storm (winter) conditions both show good linear correlation between them. The highest one achieves 0.99 and the lowest one reaches 0.87. Soulsby/Van Rijn shows 60% higher sedimentation/erosion than Van Rijn (2000), whereas Bijker (1971) shows only around 25% of sedimentation/erosion calculated by Van Rijn (2000) in the summer condition and around 30% of that in the winter condition. The neutralisation of tidal forcing for the impacts of the 1-year-returned storm is also successfully confirmed by these two sediment transport formulae.

5. REFERENCES

Ashley, G.M. (1990). Classification of large-scale subaqueous bedforms: a new look at an old problem. *Journal of Sedimentary Petrology*, 60(1): 160-172.

IMDC (2009). Afstemming Vlaamse en Nederlandse voorspelling golfklimaat op ondiep water. Deel 4: Technisch wetenschappelijke bijstand: Traject Onderzoek. I/RA/11273/09.007/SDO. In opdracht van het Waterbouwkundig Laboratorium.

Soulsby, R. (1997). *Dynamics of marine sands, a manual for practical applications*. Thomas Telford.

Van Rijn, L.C. (2003). Sand transport by currents and waves; general approximation formulae. Unpublished paper describing TRANSPOR2000 model.

Verfaillie, E., Van Lancker, V. and Van Meirvenne, M. (2006). Multivariate geostatistics for the predictive modelling of the surficial sand distribution in shelf seas. *Continental Shelf Research* 26, 2454-2468.

IMDC (2013a). Belgian Offshore Grid – Environmental Impact Assessment. I/RA/11413/12.266/CPA. → ook hier CPA ipv MSM

IMDC (2013b). Belgian Offshore Grid – Numeric Modelling of Sediment Transport. I/RA/11413/13.006/LWA.

IMDC (2013c). Belgian Offshore Grid – Numeric Modelling of Dredging Plume Dispersion: I/RA/11413/13.167/LWA.

6. APPENDIX

6.1 1-YEAR-RETURNED STORM (MORFAC=1, +/- 2 WEEKS)

6.1.1 Current ellipse

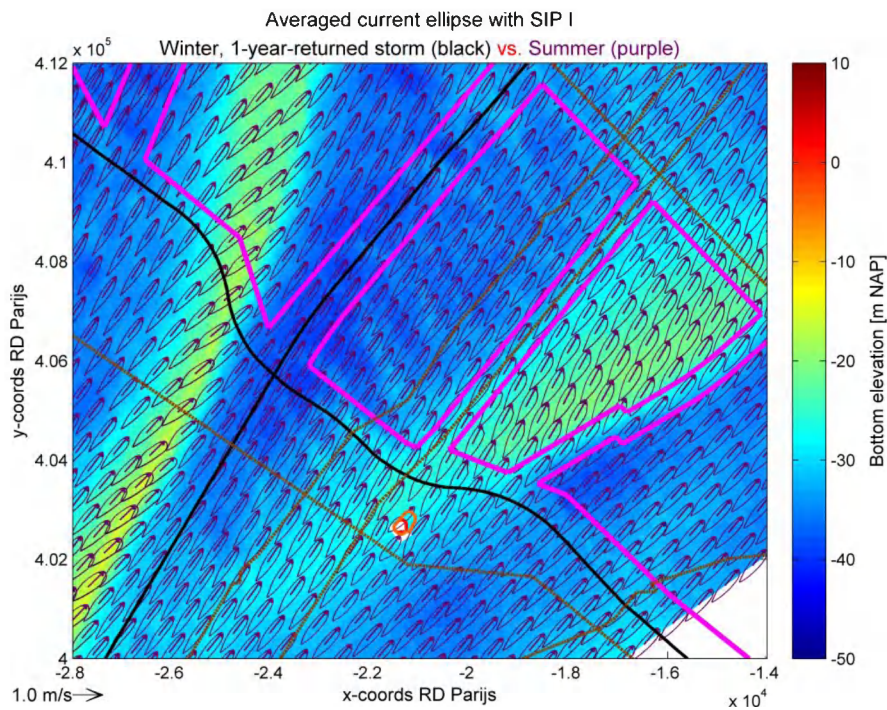


Figure 6-1: Map of averaged current ellipse with SIP I for winter (black) and summer (purple) conditions with bathymetry as background.

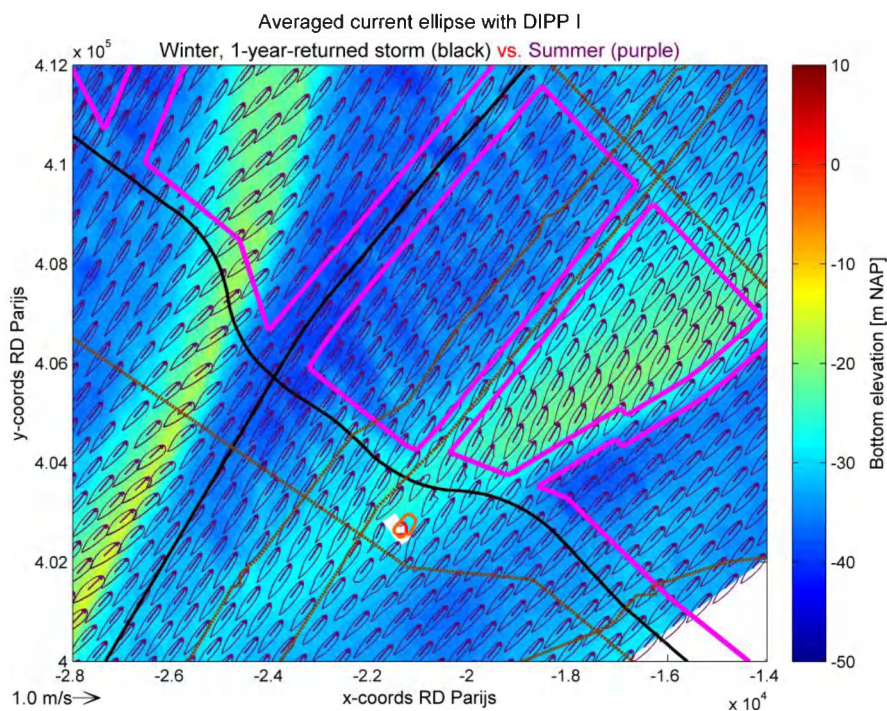


Figure 6-2: Map of averaged current ellipse with TIPA I for winter (black) and summer (purple) conditions with bathymetry as background.

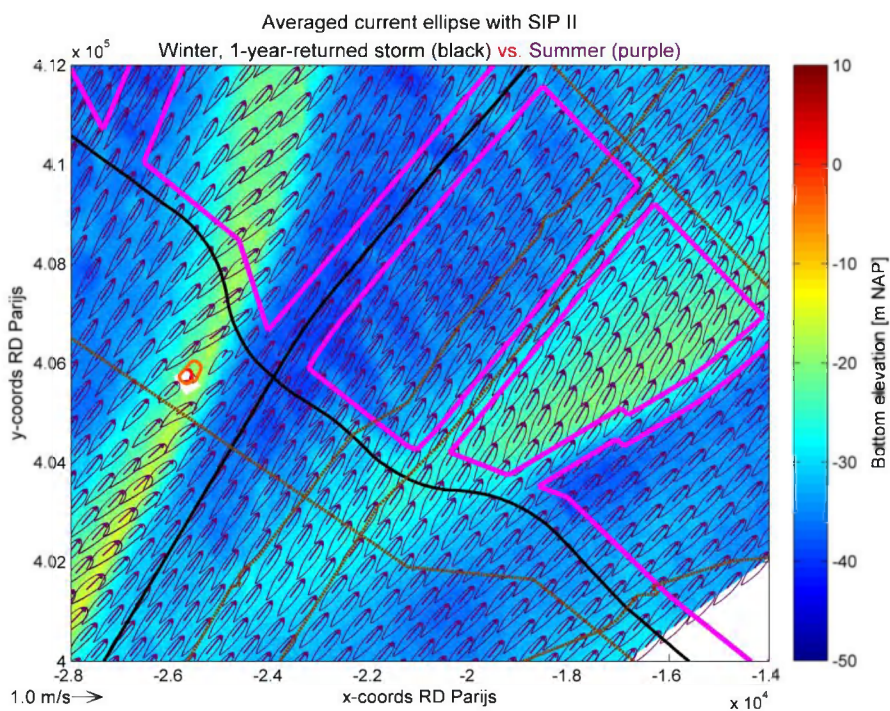


Figure 6-3: Map of averaged current ellipse with SIP II for winter (black) and summer (purple) conditions with bathymetry as background.

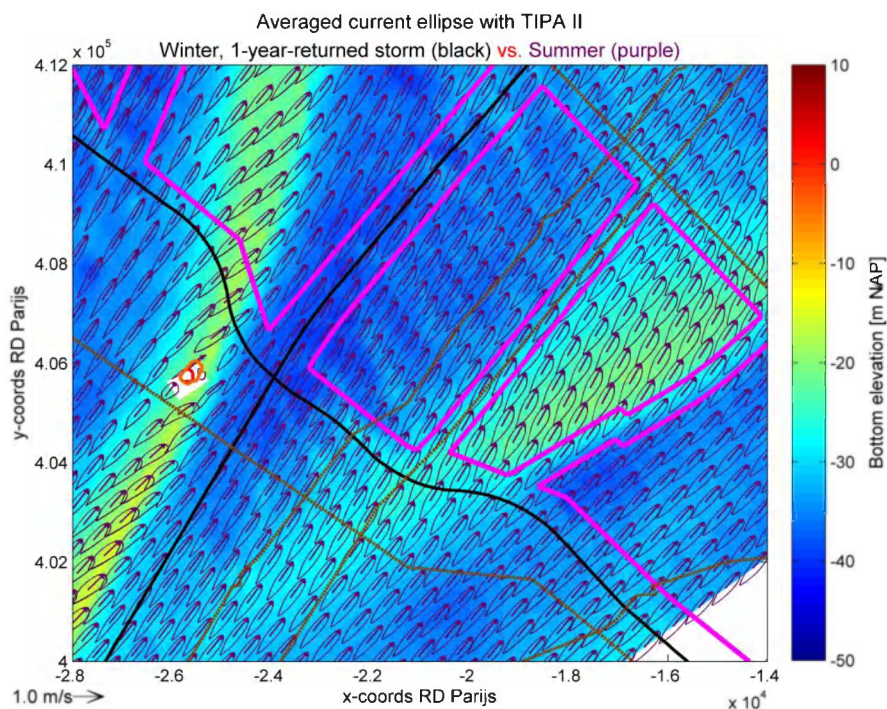


Figure 6-4: Map of averaged current ellipse with TIPA II for winter (black) and summer (purple) conditions with bathymetry as background.

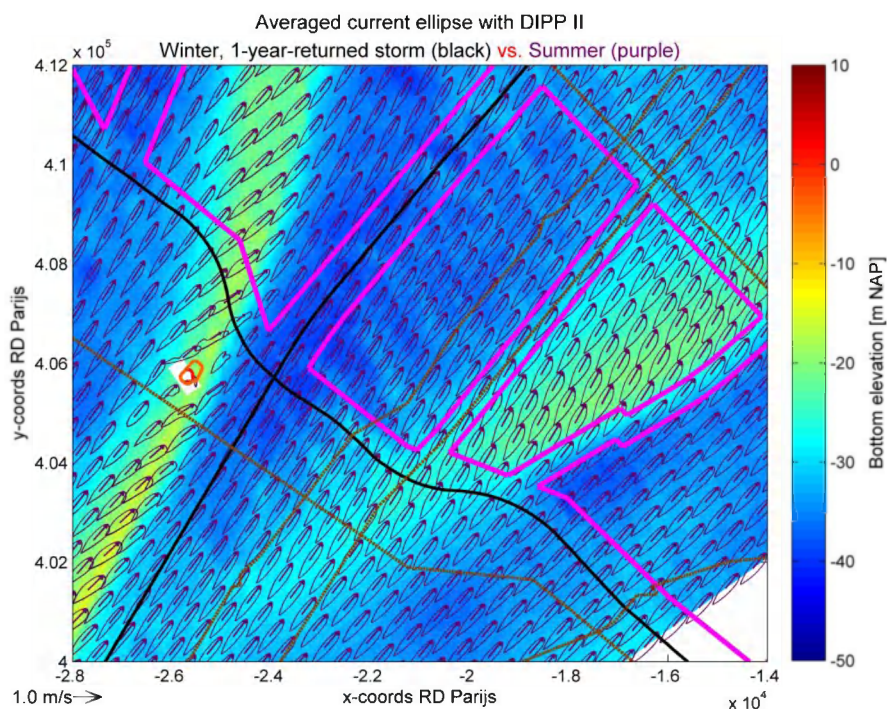


Figure 6-5: Map of averaged current ellipse with DIPP II for winter (black) and summer (purple) conditions with bathymetry as background.

6.1.2 Residual current

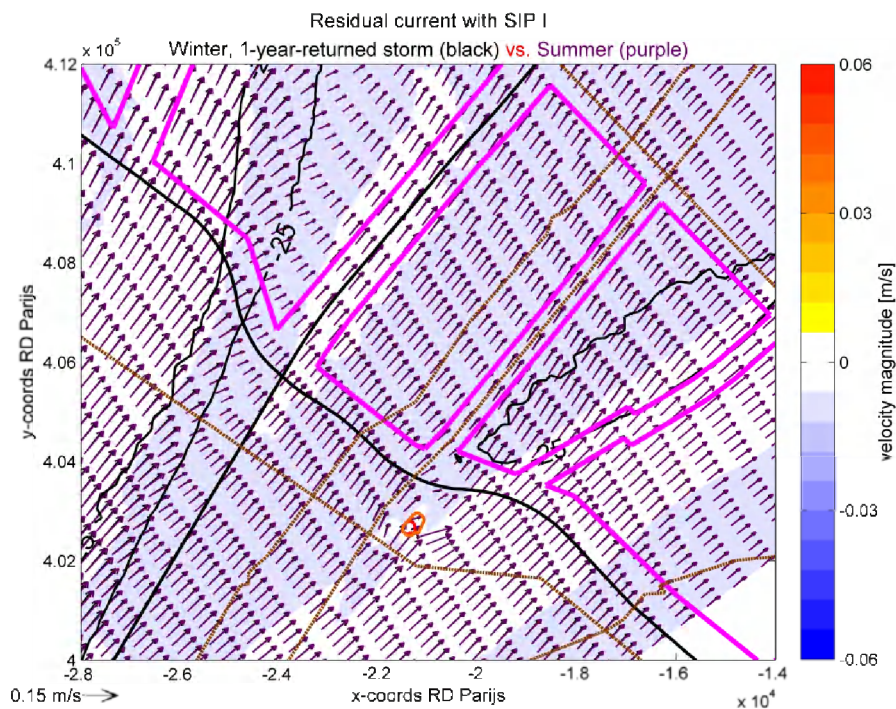


Figure 6-6 of residual current with SIP I for winter (black) and summer (purple) conditions with difference of residual velocity magnitude as background and isobath lines of -25 m NAP.

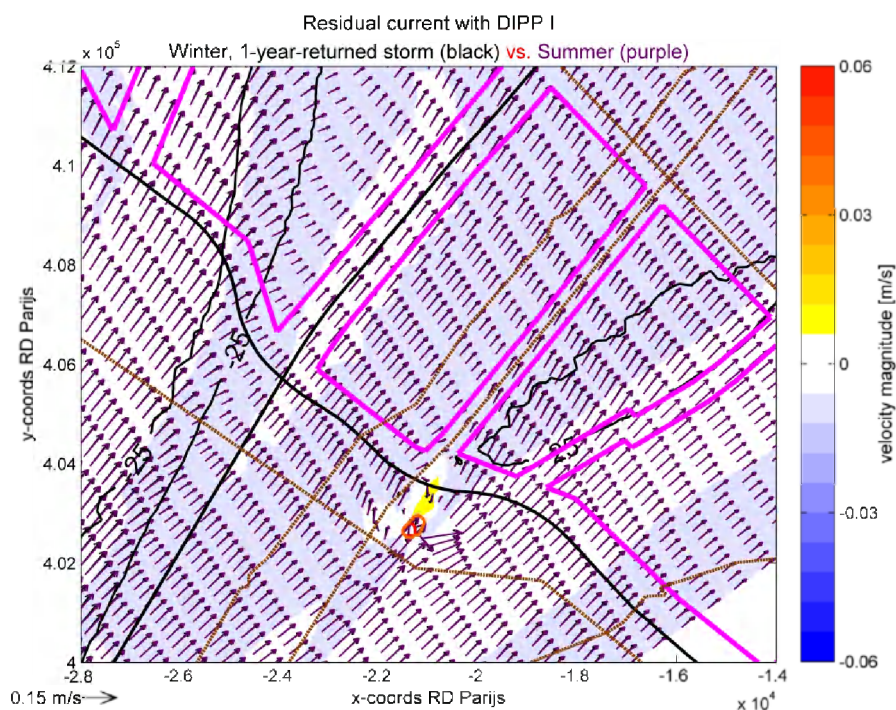


Figure 6-7 of residual current with DIPP I for winter (black) and summer (purple) conditions with difference of residual velocity magnitude as background and isobath lines of -25 m NAP.

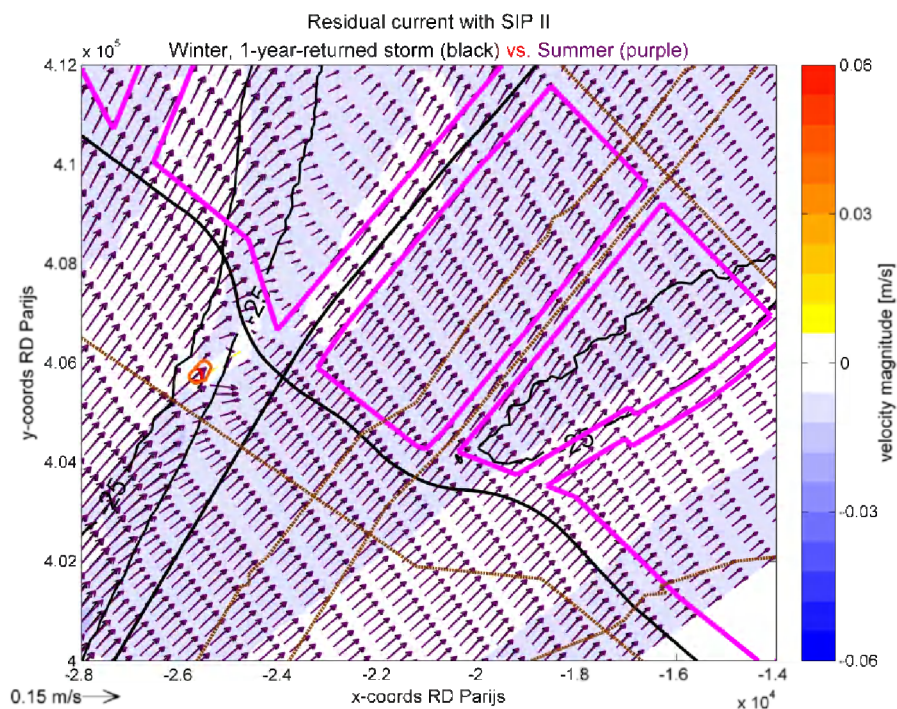


Figure 6-8 of residual current with SIP II for winter (black) and summer (purple) conditions with difference of residual velocity magnitude as background and isobath lines of -25 m NAP.

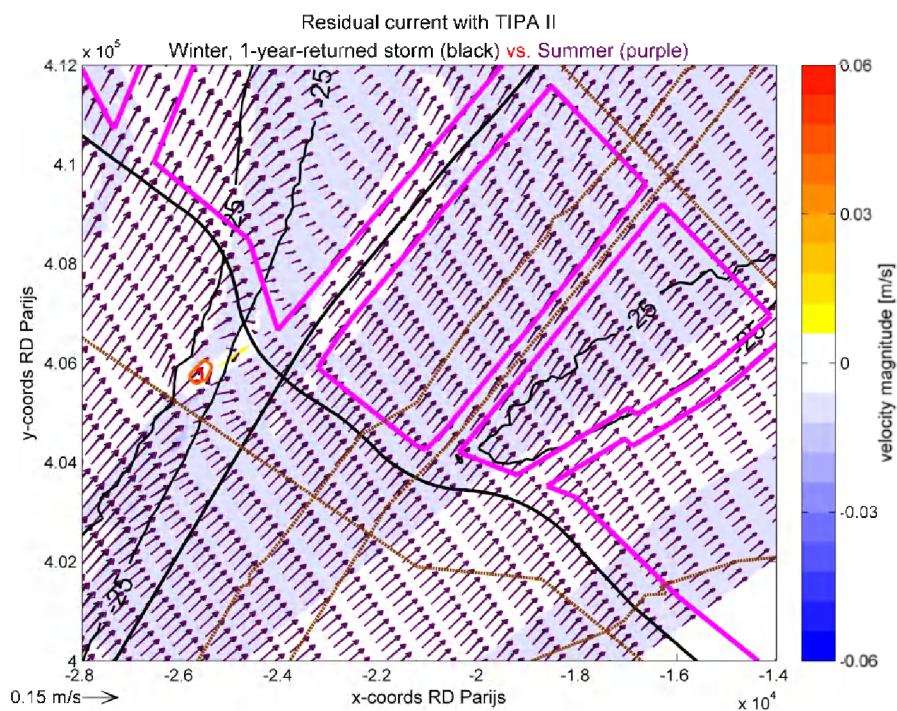


Figure 6-9 of residual current with TIPA II for winter (black) and summer (purple) conditions with difference of residual velocity magnitude as background and isobath lines of -25 m NAP.

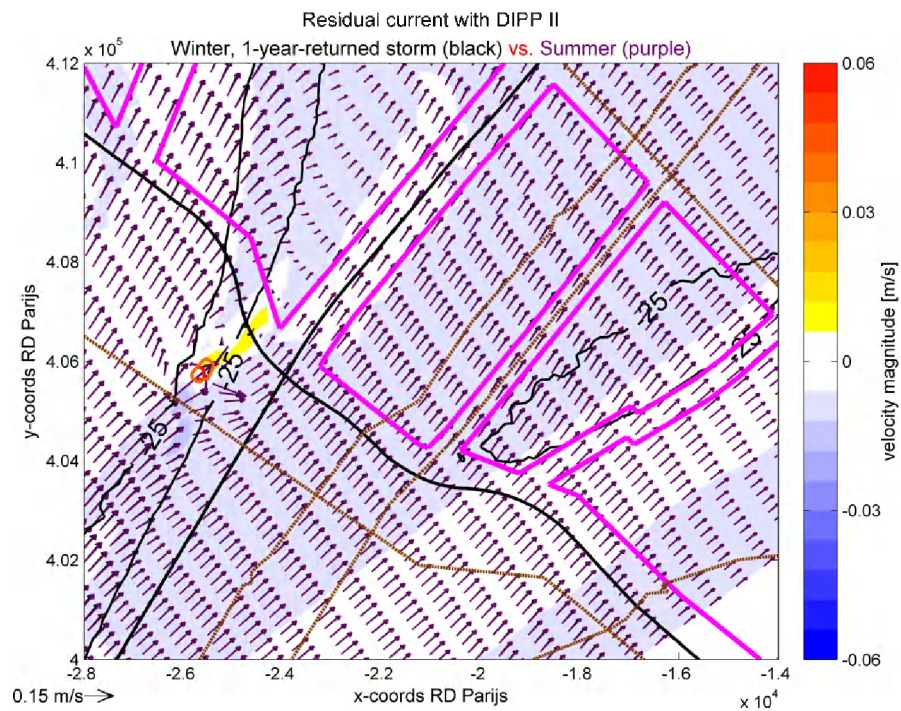


Figure 6-10 of residual current with DIPP II for winter (black) and summer (purple) conditions with difference of residual velocity magnitude as background and isobath lines of -25 m NAP.

6.1.3 Sedimentation/Erosion

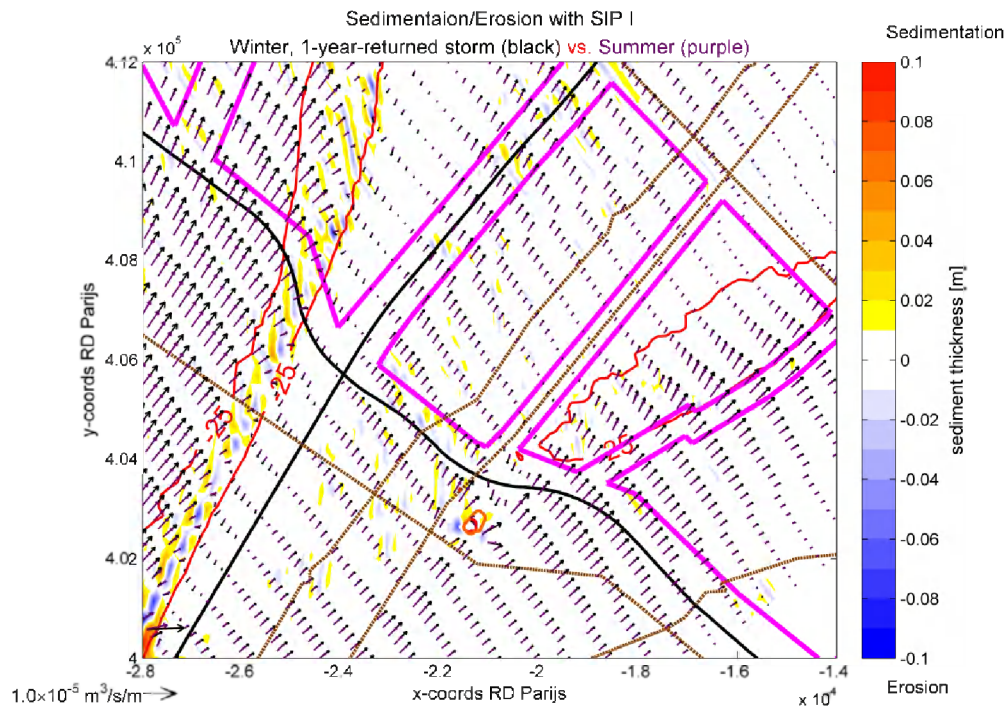


Figure 6-11: Map of residual sediment transport with SIP I for winter (black) and summer (purple) conditions with difference of sedimentation/erosion as background and isobath lines of -25 m NAP.

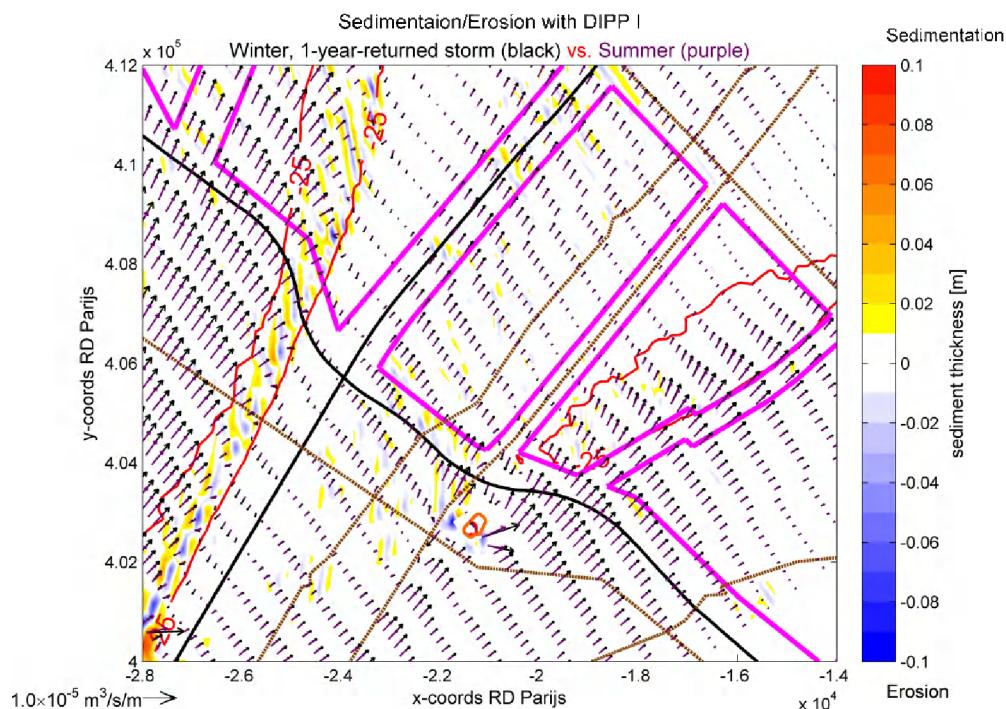


Figure 6-12: Map of residual sediment transport with DIPP I for winter (black) and summer (purple) conditions with difference of sedimentation/erosion as background and isobath lines of -25 m NAP.

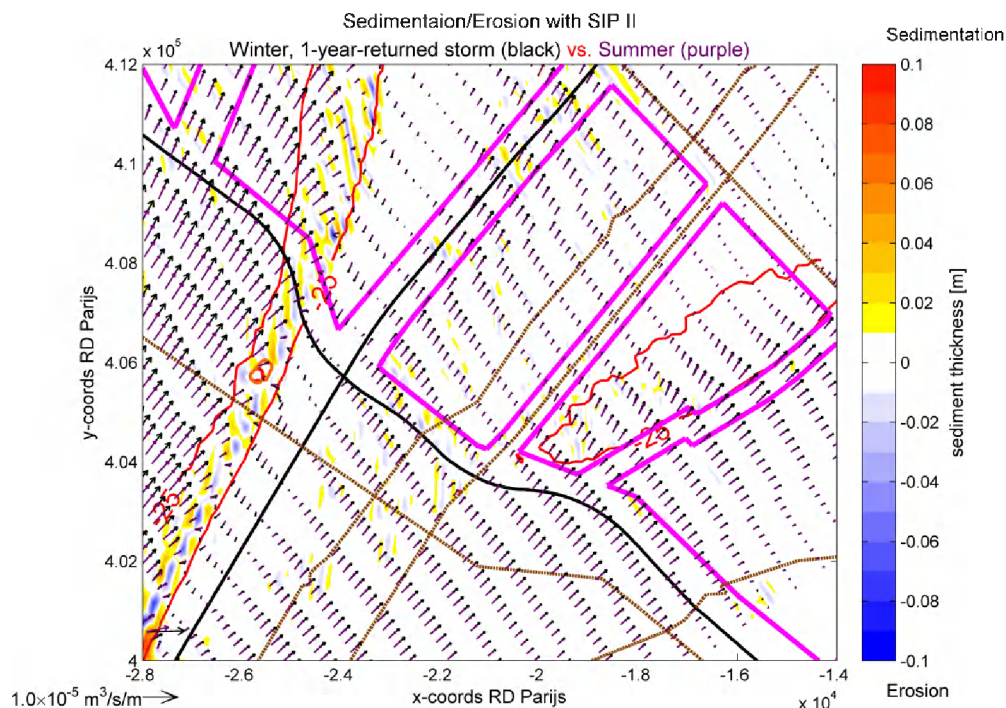


Figure 6-13: Map of residual sediment transport with SIP II for winter (black) and summer (purple) conditions with difference of sedimentation/erosion as background and isobath lines of -25 m NAP.

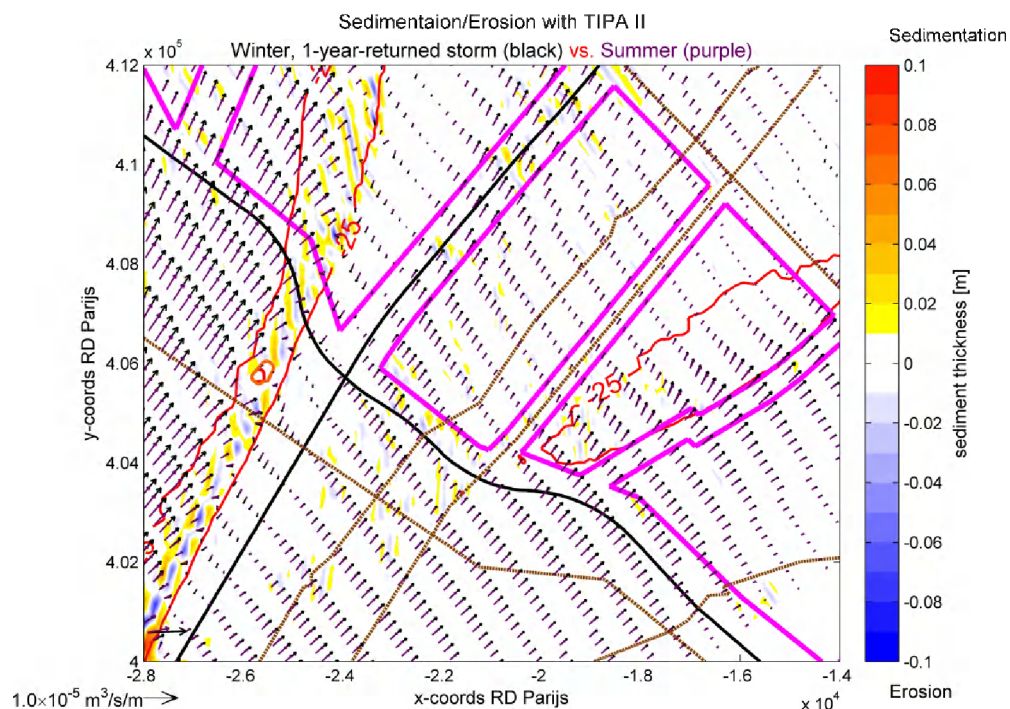


Figure 6-14: Map of residual sediment transport with TIPA II for winter (black) and summer (purple) conditions with difference of sedimentation/erosion as background and isobath lines of -25 m NAP.

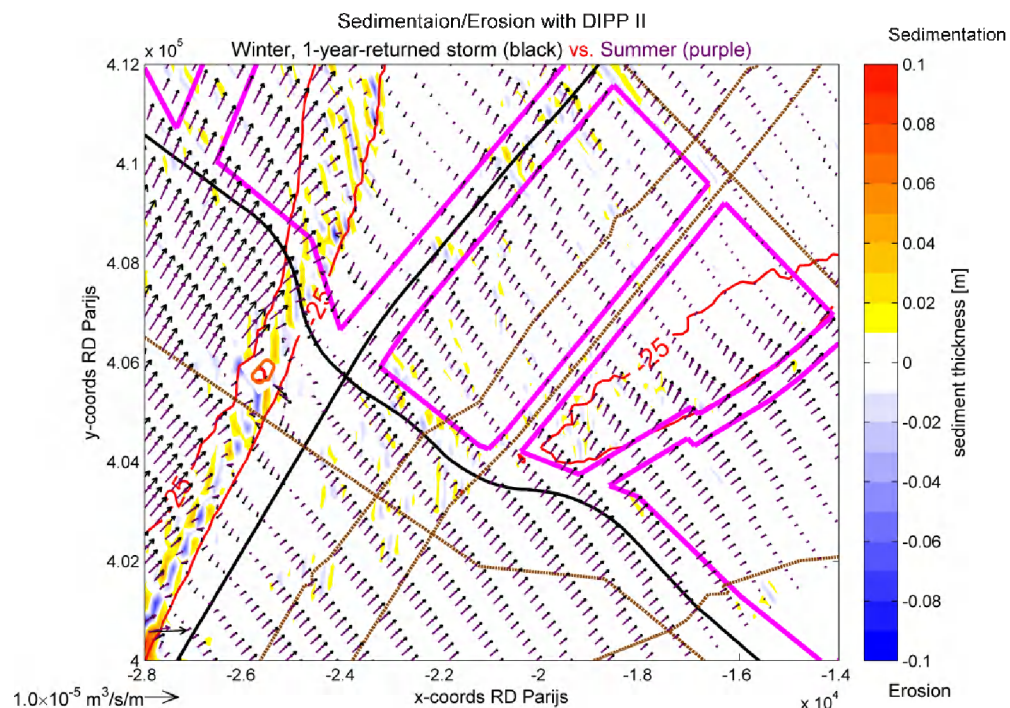


Figure 6-15: Map of residual sediment transport with DIPP II for winter (black) and summer (purple) conditions with difference of sedimentation/erosion as background and isobath lines of -25 m NAP.

6.2 5-YEAR-RETURNED STORM (MORFAC=1, +/- 2 WEEKS)

6.2.1 Current ellipse

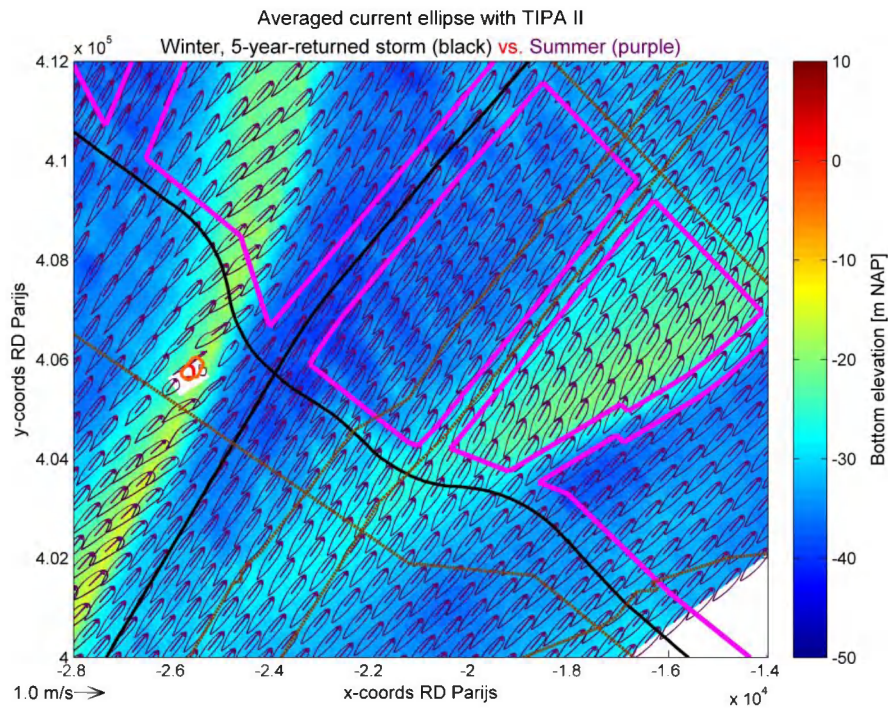


Figure 6-16: Map of averaged current ellipse with TIPA II for winter (black) and summer (purple) conditions with bathymetry as background.

6.2.2 Residual current

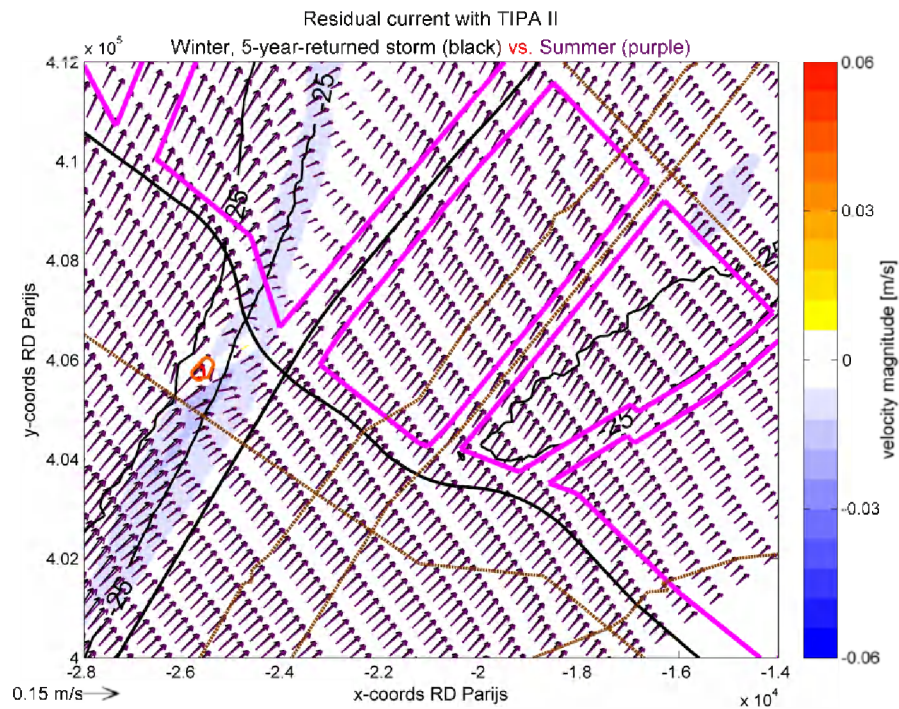


Figure 6-17: Map of residual current with TIPA II in winter (black) and summer (purple) conditions with difference of residual velocity magnitude as background and isobath lines of - 25 m NAP.

6.2.3 Sedimentation/Erosion

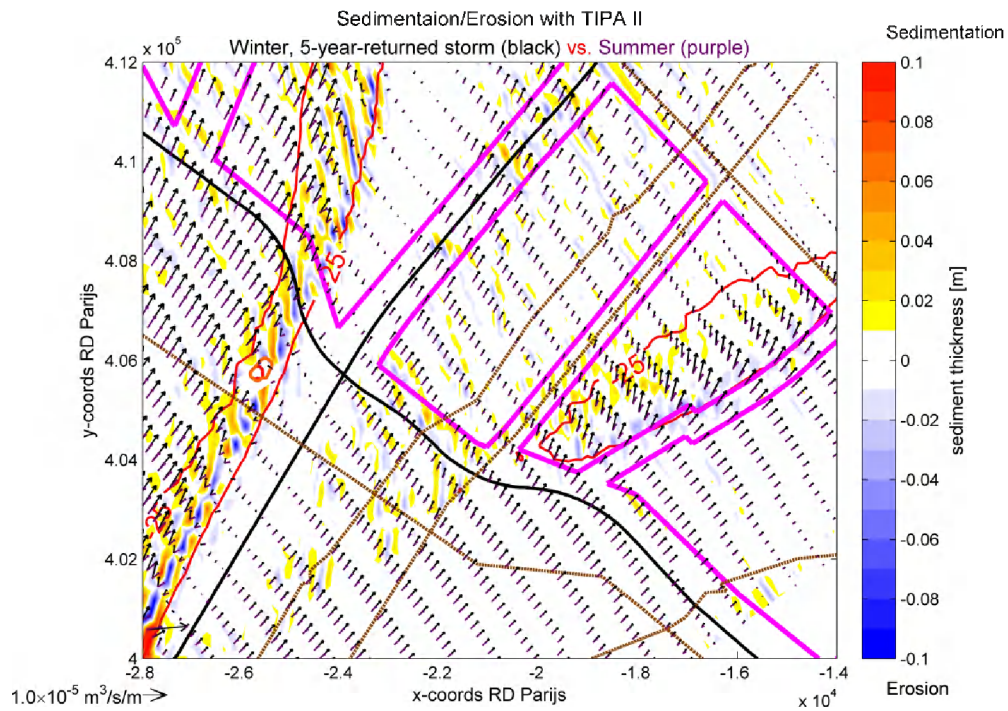


Figure 6-18: Map of residual sediment transport with TIPA II in winter (black) and summer (purple) conditions with difference of sedimentation/erosion as background and isobath lines of -25 m NAP.

6.3 COMPARISON WITH NATURAL CONDITION (MORFAC=125, +/- 25 YEARS)

6.3.1 SIP I (single inactive point at Location I)

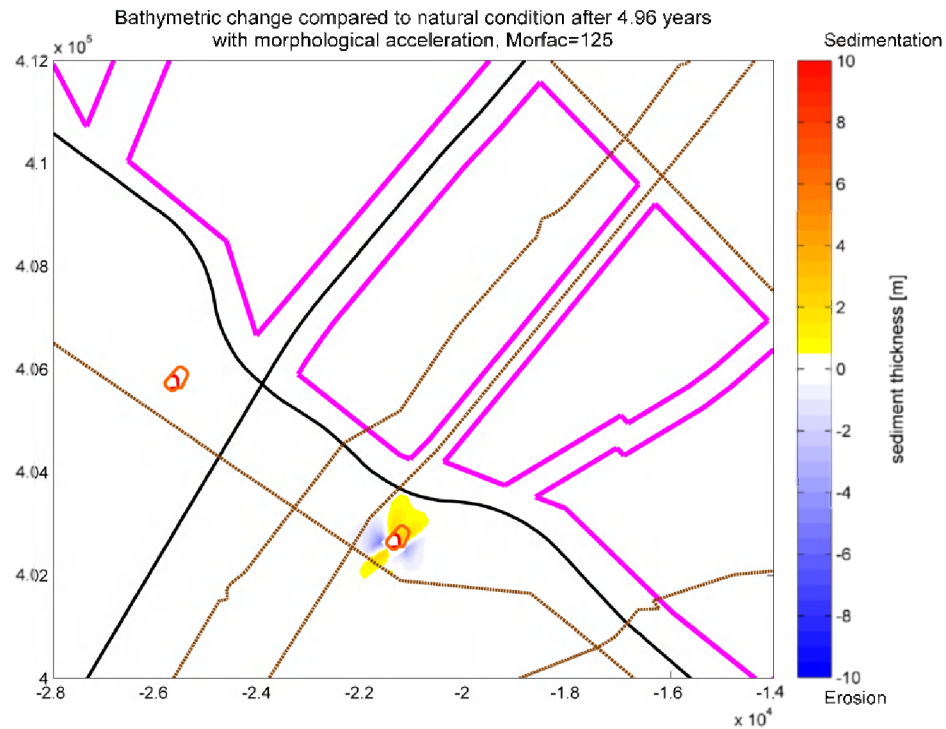


Figure 6-19: Bathymetric change of SIP I compared to natural condition after +/- 5 years with morphological acceleration (Morfac=125).

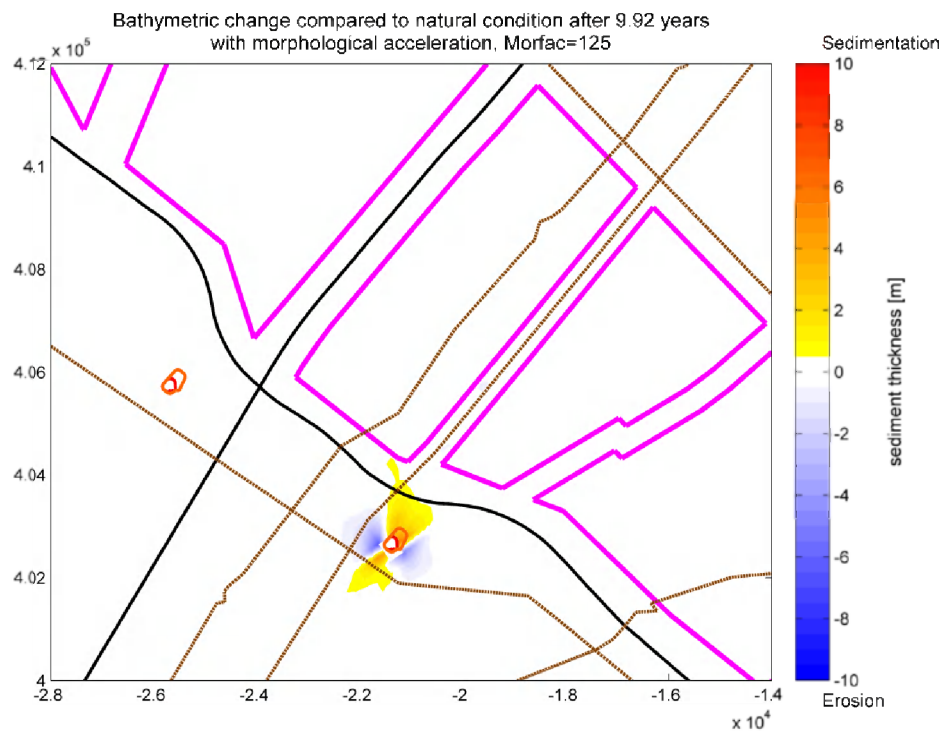


Figure 6-20: Bathymetric change of SIP I compared to natural condition after +/- 10 years with morphological acceleration (Morfac=125).

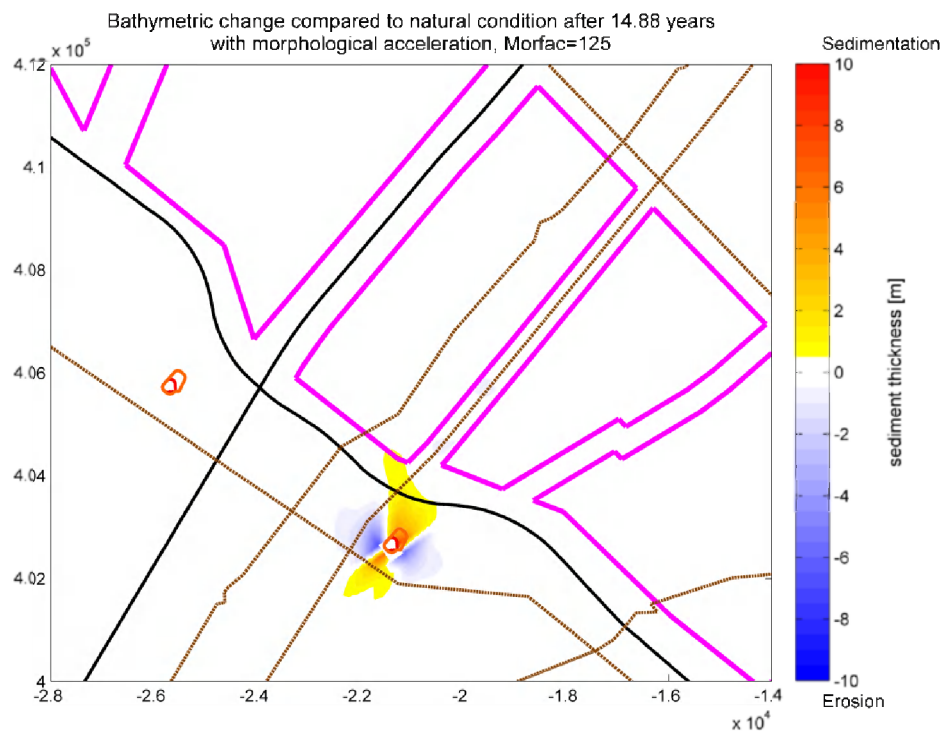


Figure 6-21: Bathymetric change of SIP I compared to natural condition after +/- 15 years with morphological acceleration (Morfac=125).

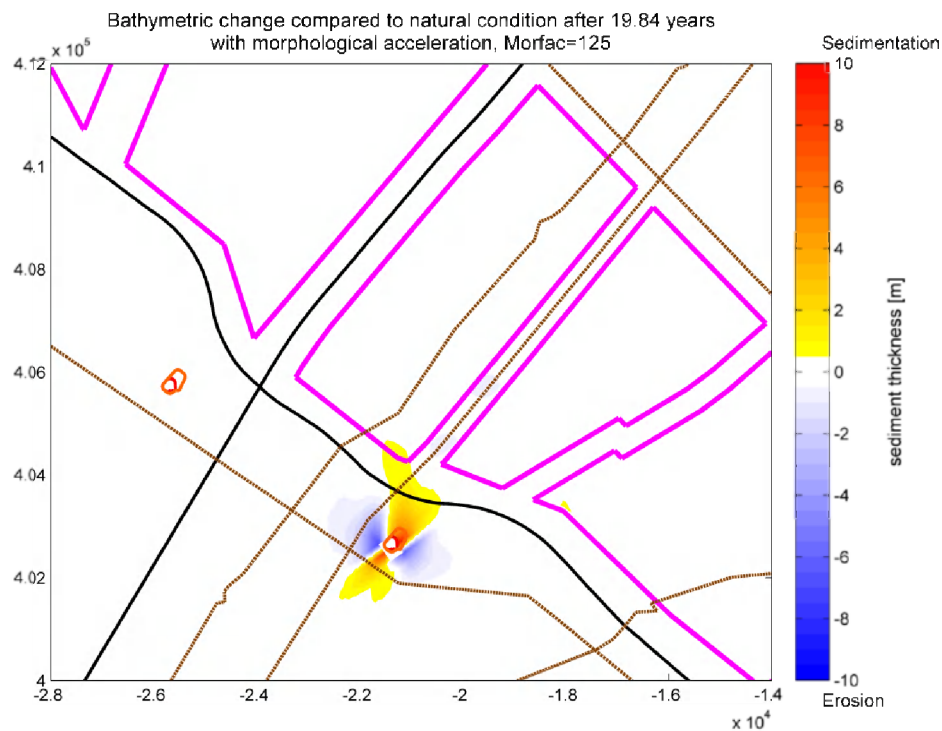


Figure 6-22: Bathymetric change of SIP I compared to natural condition after +/- 20 years with morphological acceleration (Morfac=125).

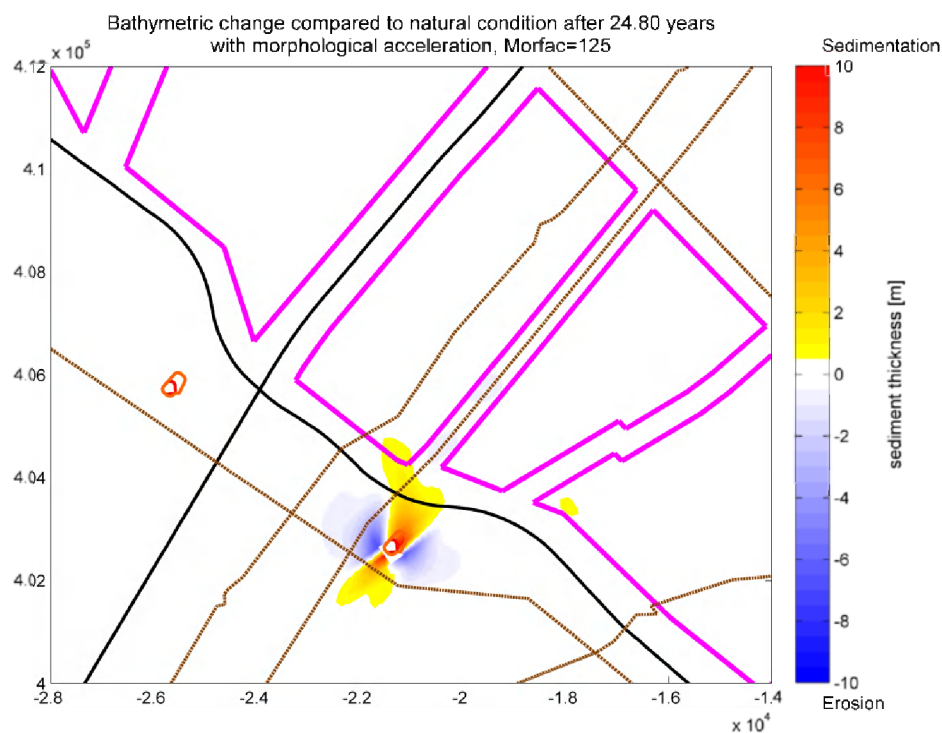


Figure 6-23: Bathymetric change of SIP I compared to natural condition after +/- 25 years with morphological acceleration (Morfac=125).

6.3.2 DIPP I (double inactive points perpendicular to main flow direction at Location I)

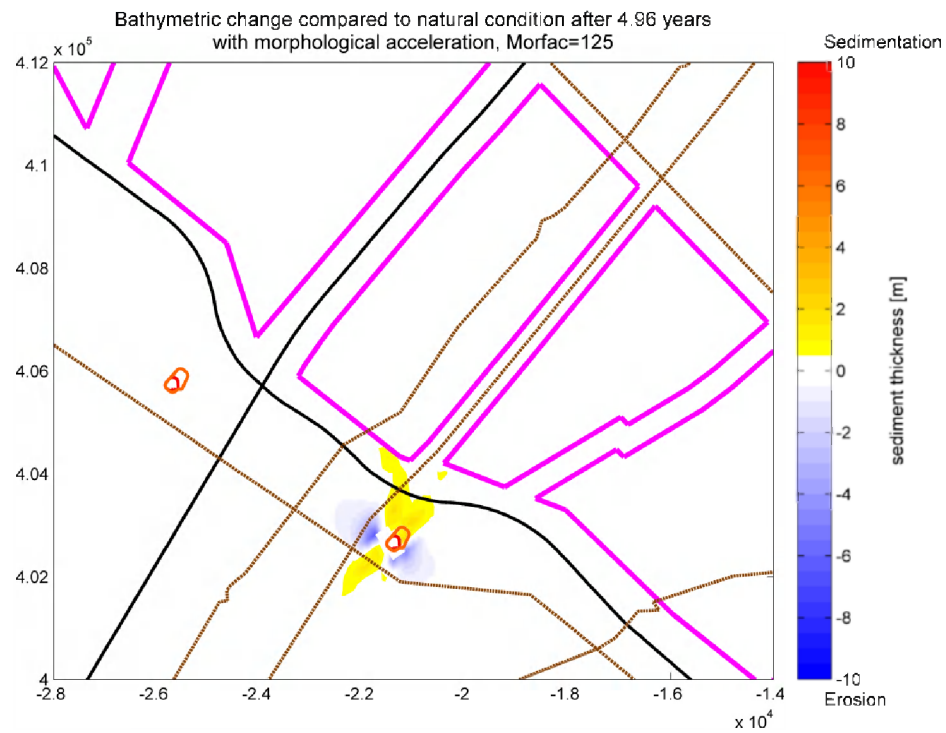


Figure 6-24: Bathymetric change of DIPP I compared to natural condition after +/- 5 years with morphological acceleration (Morfac=125).

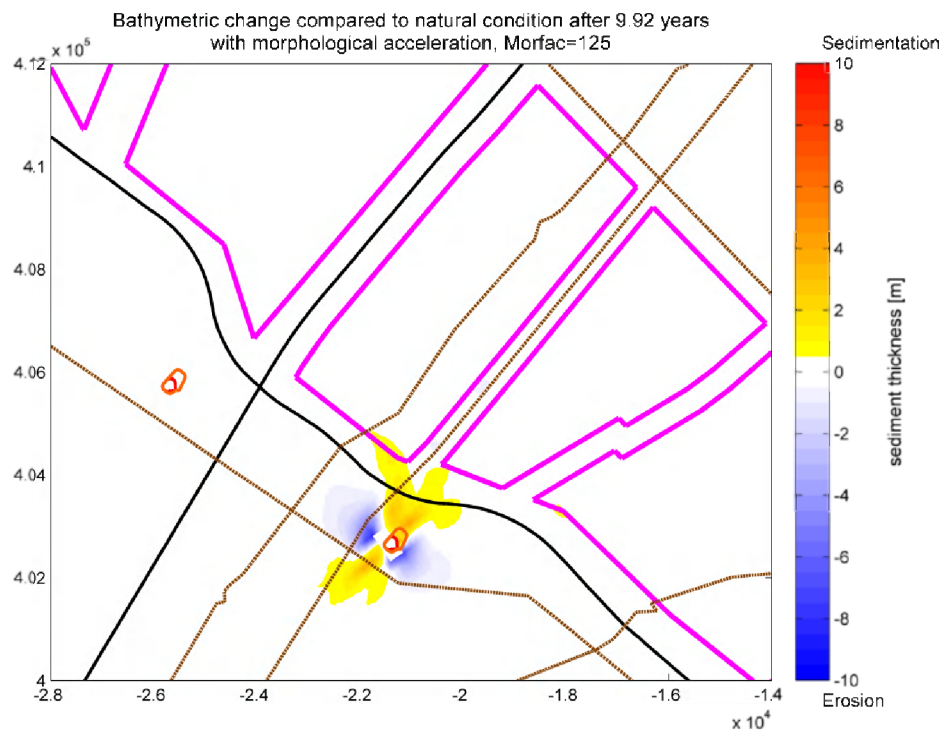


Figure 6-25: Bathymetric change of DIPP I compared to natural condition after +/- 10 years with morphological acceleration (Morfac=125).

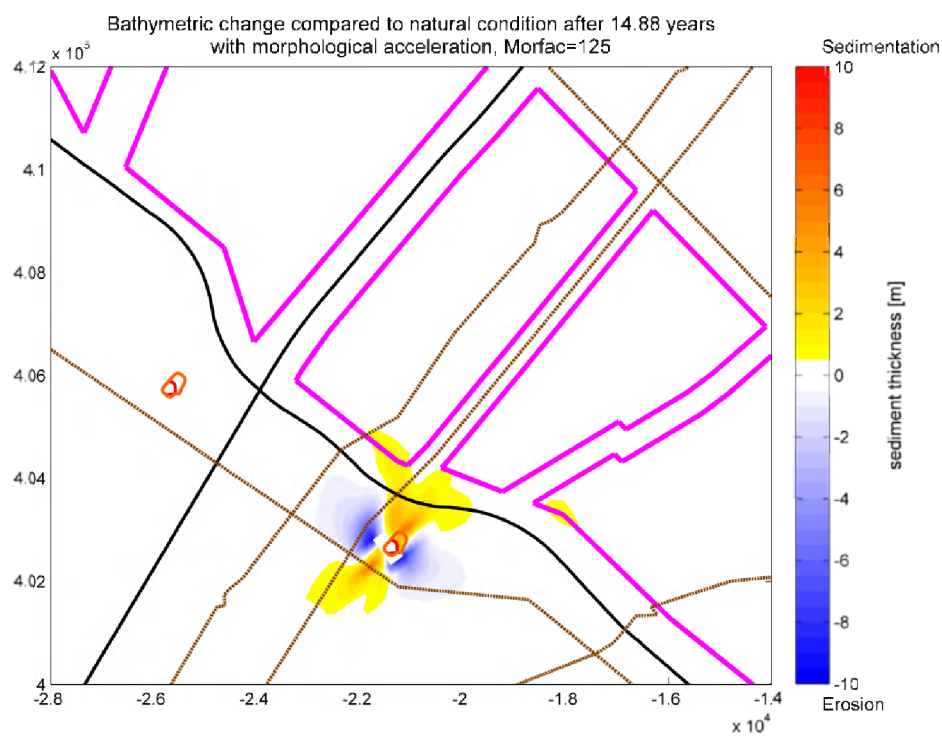


Figure 6-26: Bathymetric change of DIPP I compared to natural condition after +/- 15 years with morphological acceleration (Morfac=125).

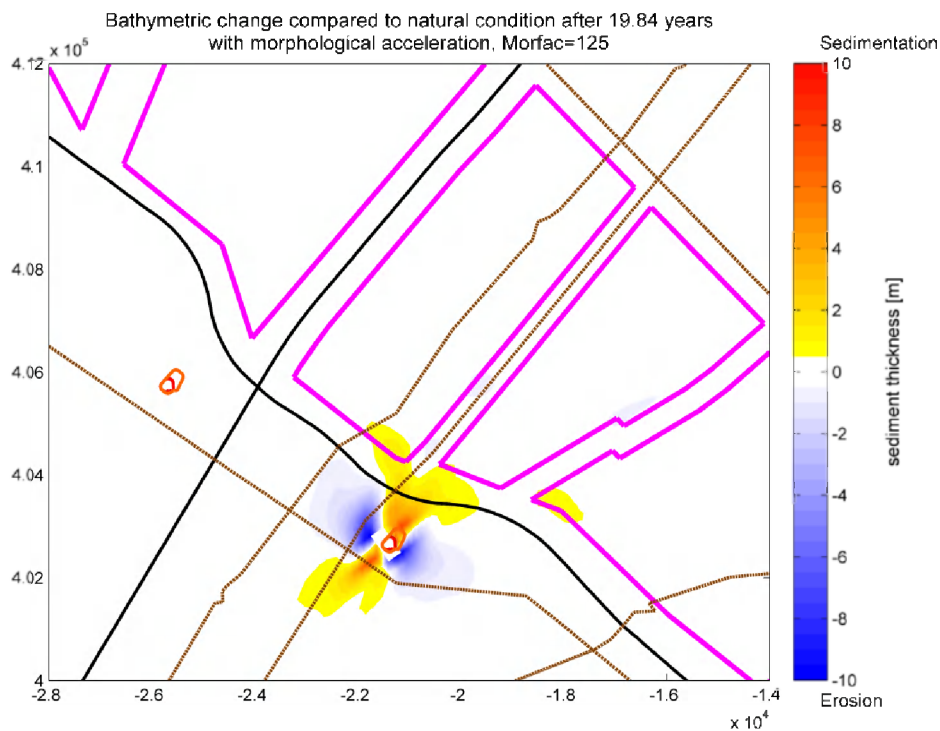


Figure 6-27: Bathymetric change of DIPP I compared to natural condition after +/- 20 years with morphological acceleration (Morfac=125).

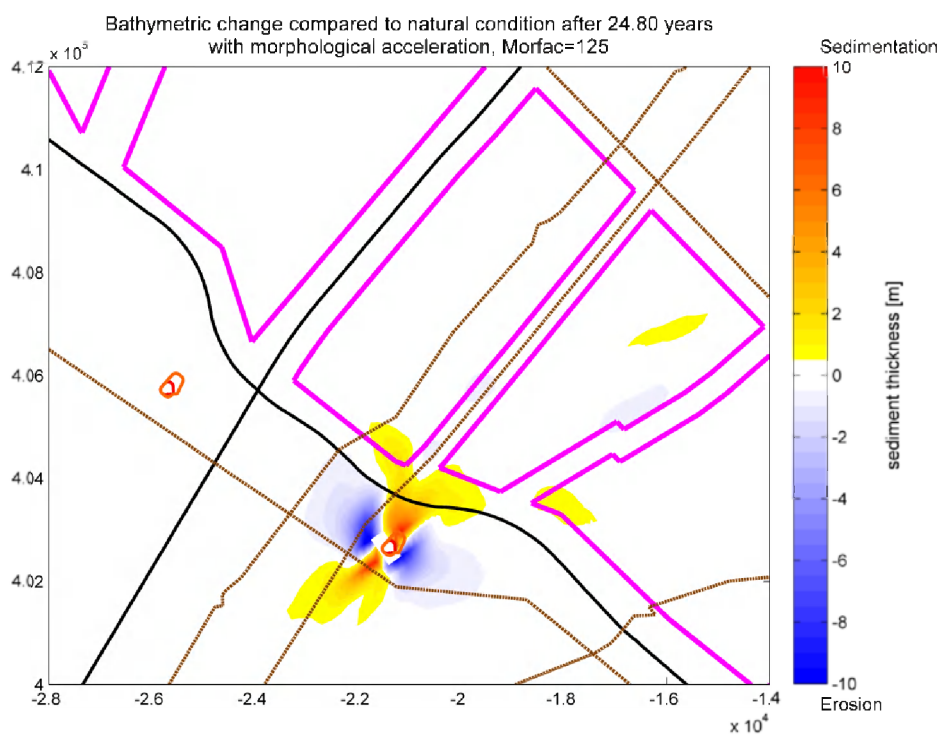


Figure 6-28: Bathymetric change of DIPP I compared to natural condition after +/- 25 years with morphological acceleration (Morfac=125).

6.3.3 SIP II (single inactive point at Location II)

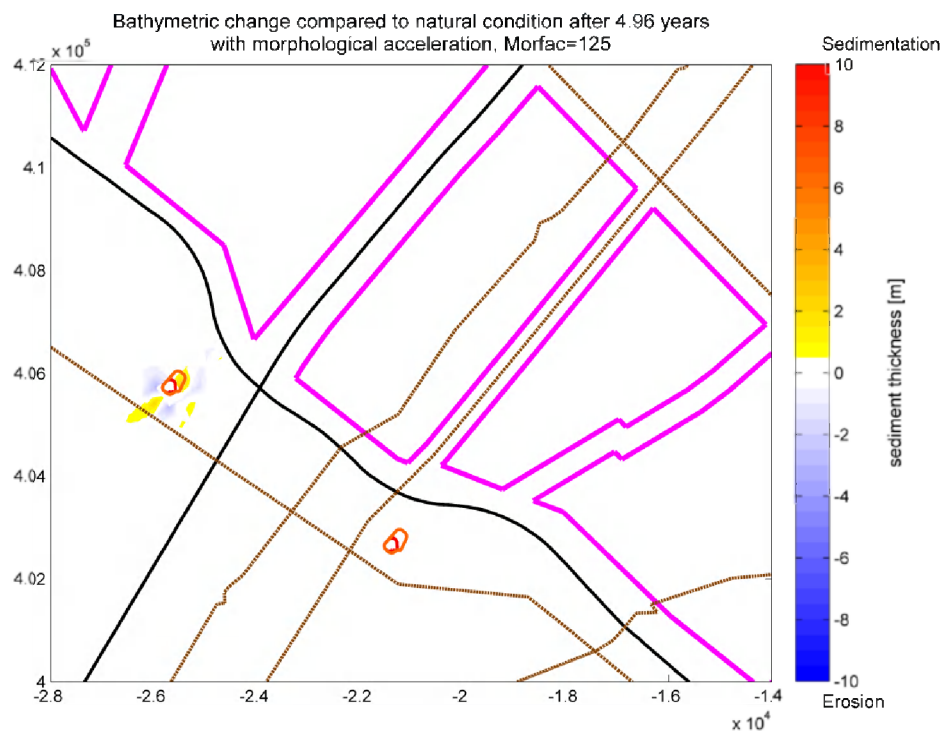


Figure 6-29: Bathymetric change of SIP II compared to natural condition after +/- 5 years with morphological acceleration (Morfac=125).

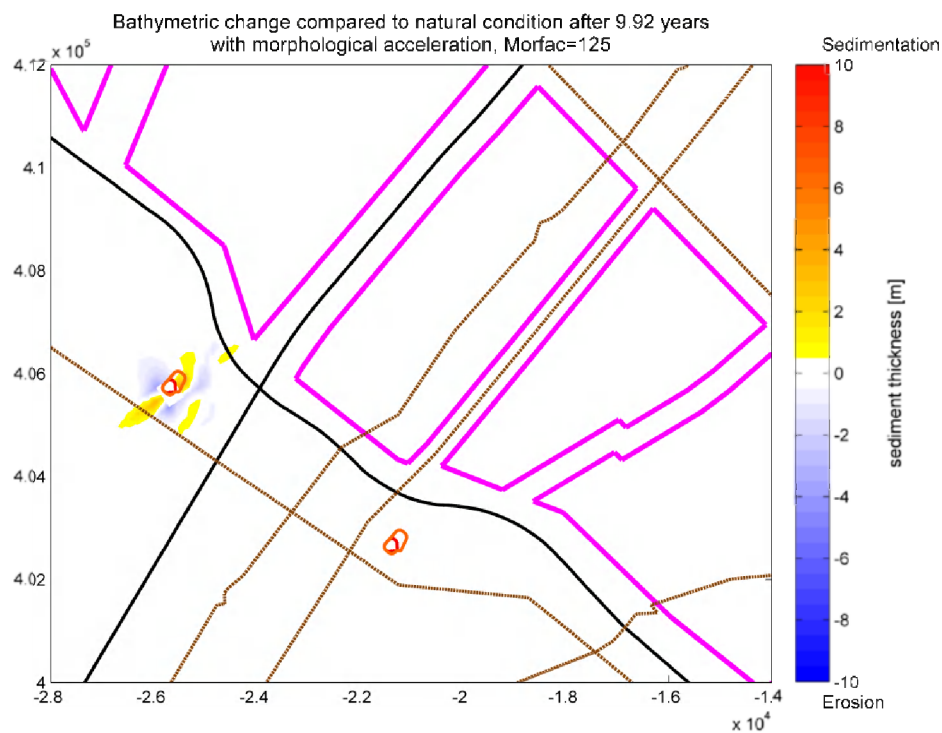


Figure 6-30: Bathymetric change of SIP II compared to natural condition after +/- 10 years with morphological acceleration (Morfac=125).

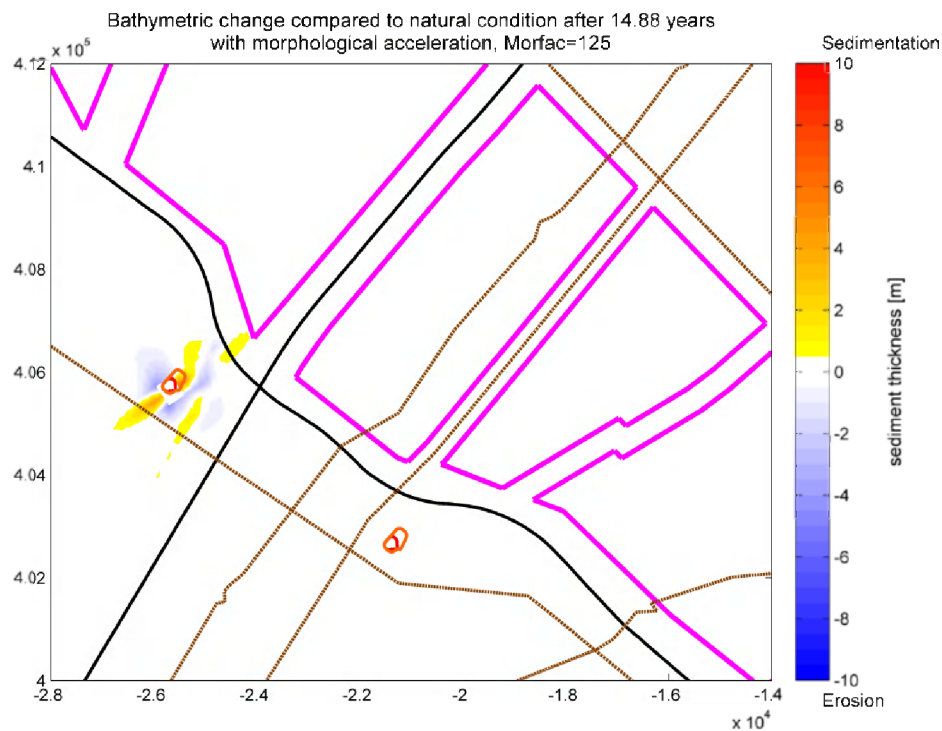


Figure 6-31: Bathymetric change of SIP II compared to natural condition after +/- 15 years with morphological acceleration (Morfac=125).

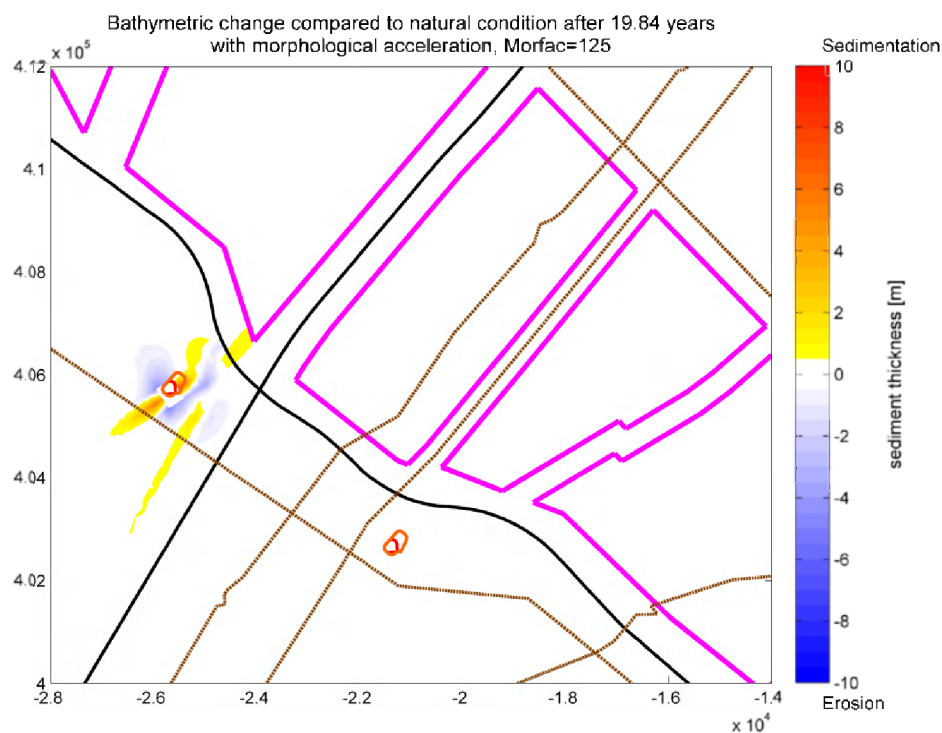


Figure 6-32: Bathymetric change of SIP II compared to natural condition after +/- 20 years with morphological acceleration (Morfac=125).

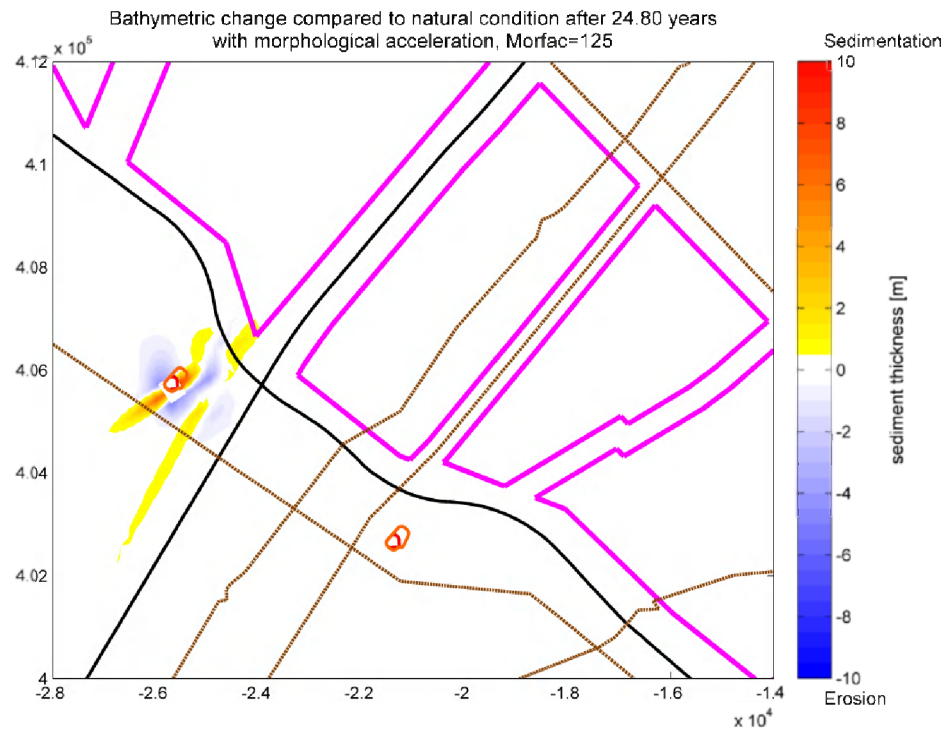


Figure 6-33: Bathymetric change of SIP II compared to natural condition after +/- 25 years with morphological acceleration (Morfac=125).

6.3.4 TIPA II (triple inactive points aligned to main flow direction at Location II)

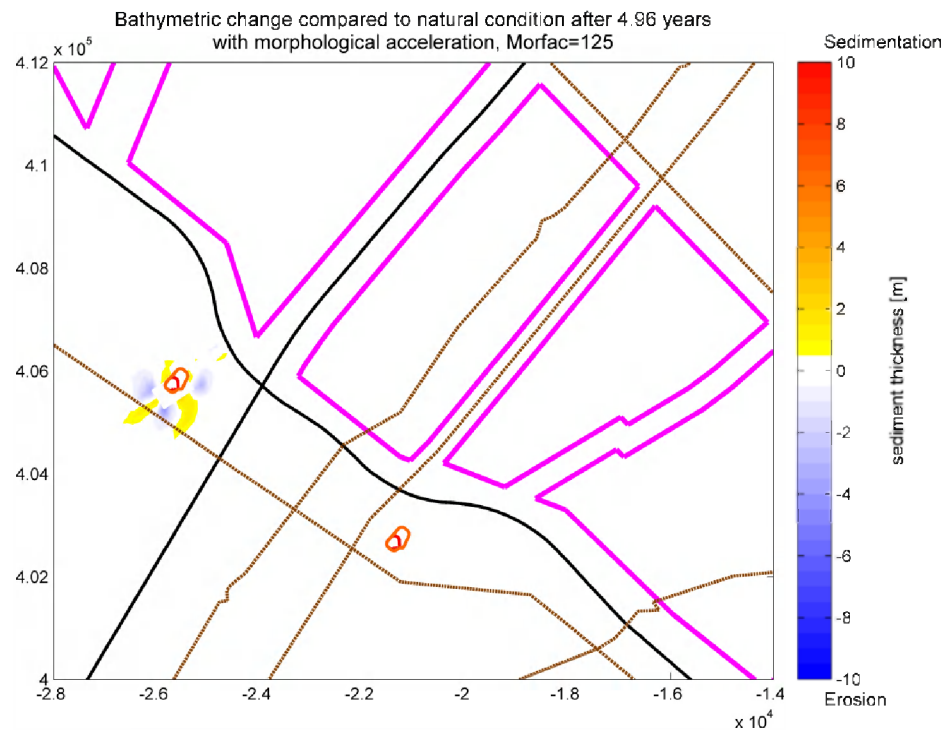


Figure 6-34: Bathymetric change of TIPA II compared to natural condition after +/- 5 years with morphological acceleration (Morfac=125).

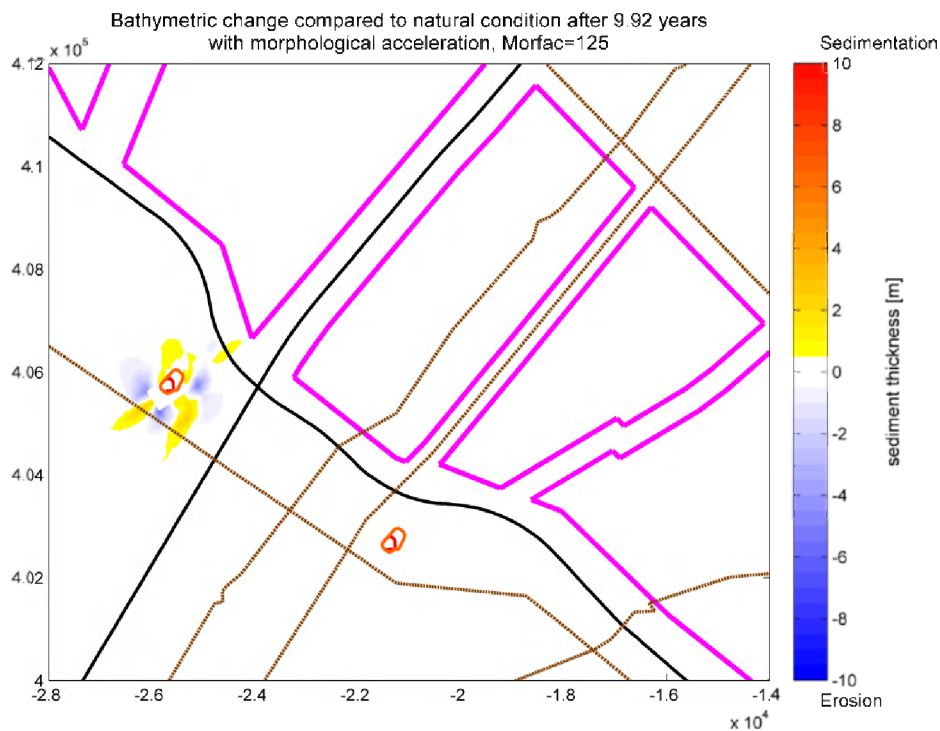


Figure 6-35: Bathymetric change of TIPA II compared to natural condition after +/- 10 years with morphological acceleration (Morfac=125).

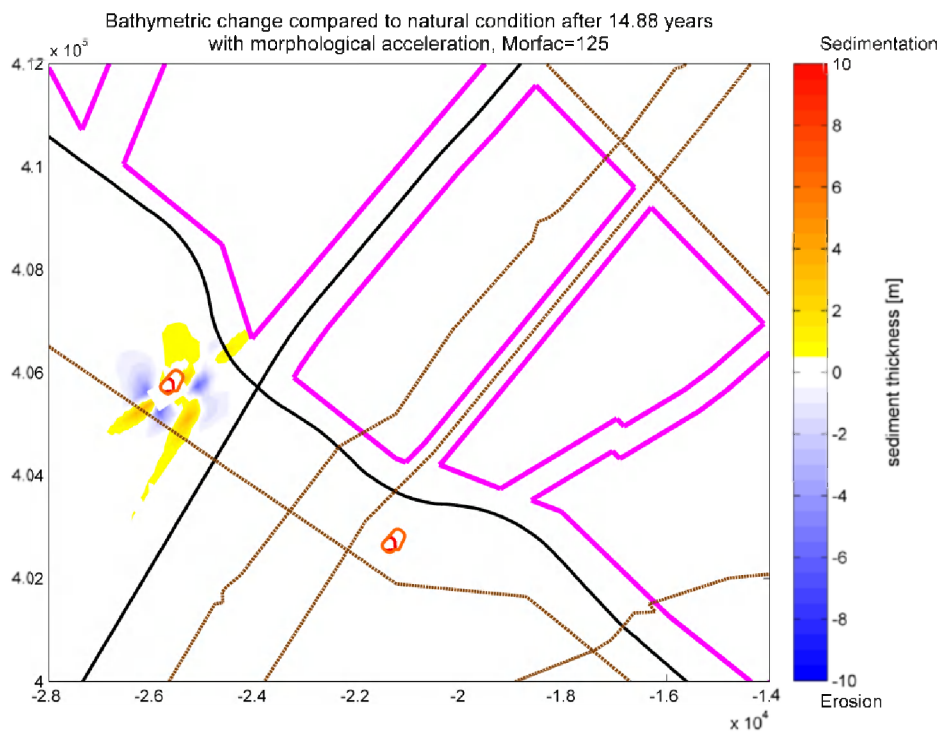


Figure 6-36: Bathymetric change of TIPA II compared to natural condition after +/- 15 years with morphological acceleration (Morfac=125).

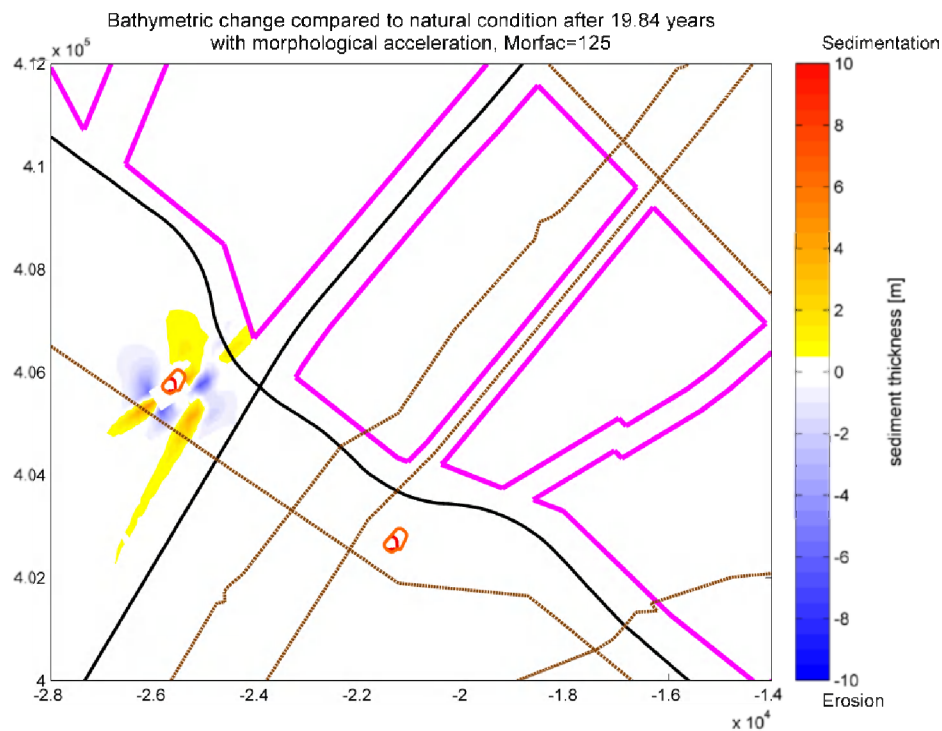


Figure 6-37: Bathymetric change of TIPA II compared to natural condition after +/- 20 years with morphological acceleration (Morfac=125).

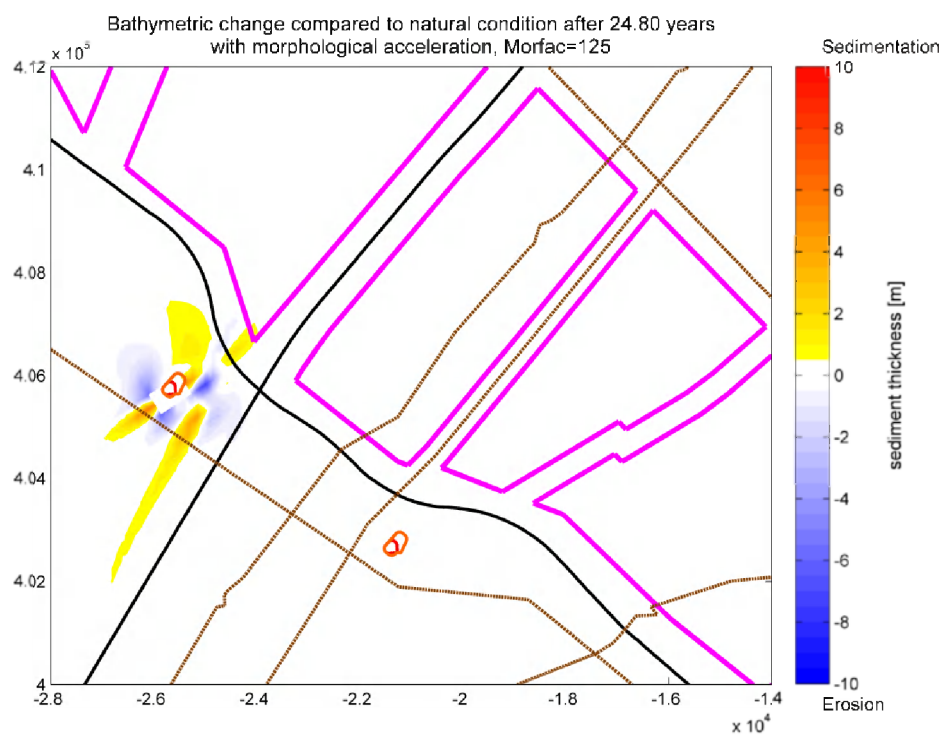


Figure 6-38: Bathymetric change of TIPA II compared to natural condition after +/- 25 years with morphological acceleration (Morfac=125).

6.3.5 DIPP II (double inactive points perpendicular to main flow direction at Location II)

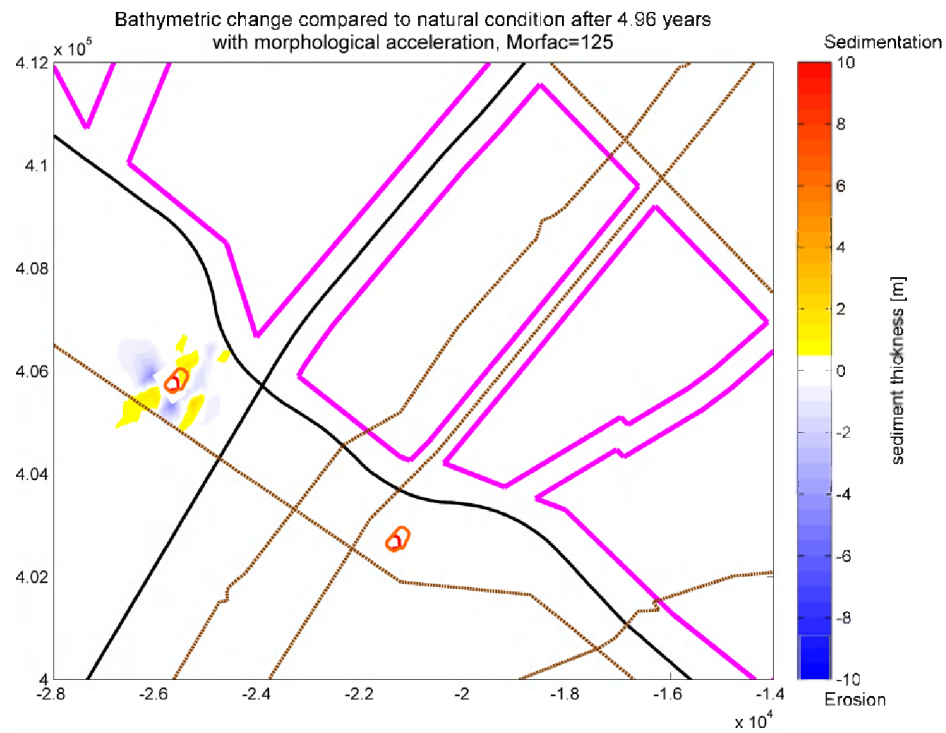


Figure 6-39: Bathymetric change of DIPP II compared to natural condition after +/- 5 years with morphological acceleration (Morfac=125).

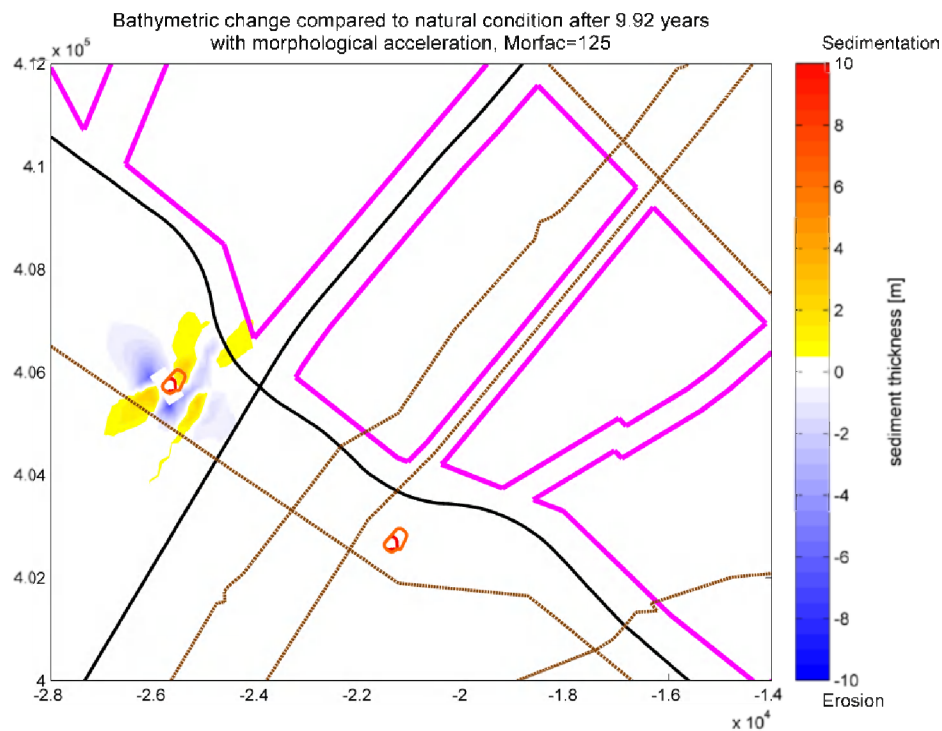


Figure 6-40: Bathymetric change of DIPP II compared to natural condition after +/- 10 years with morphological acceleration (Morfac=125).

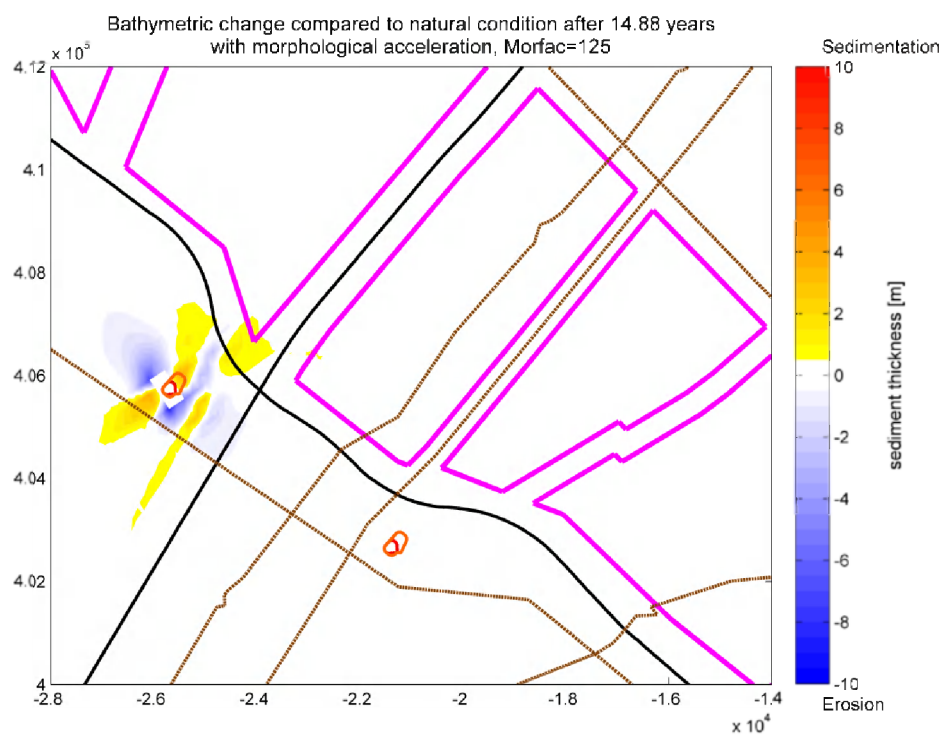


Figure 6-41: Bathymetric change of DIPP II compared to natural condition after +/- 15 years with morphological acceleration (Morfac=125).

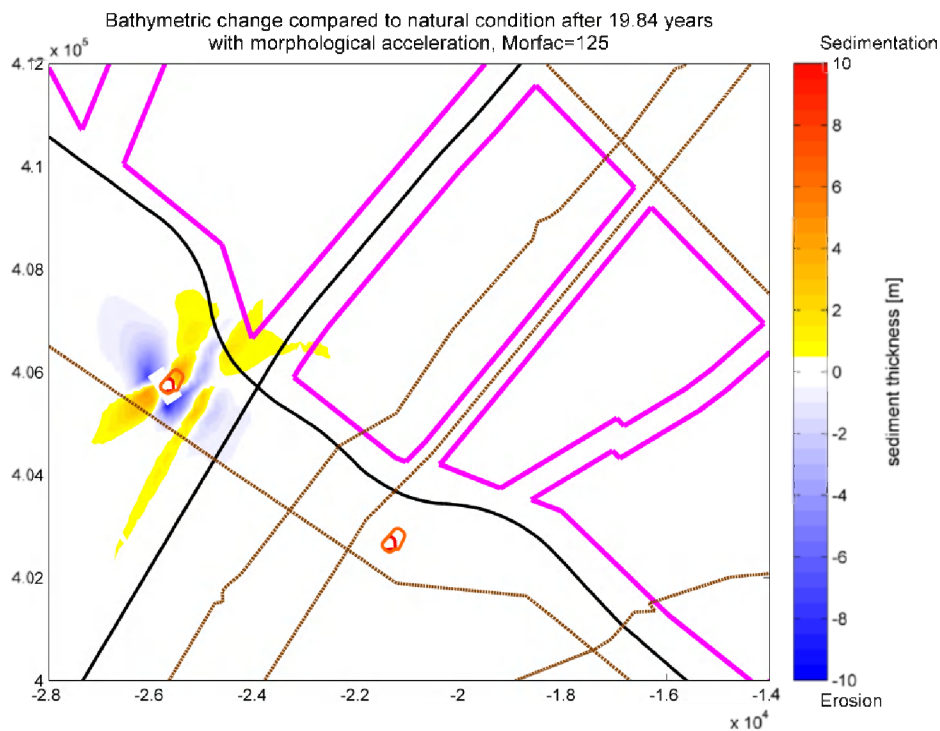


Figure 6-42: Bathymetric change of DIPP II compared to natural condition after +/- 20 years with morphological acceleration (Morfac=125).

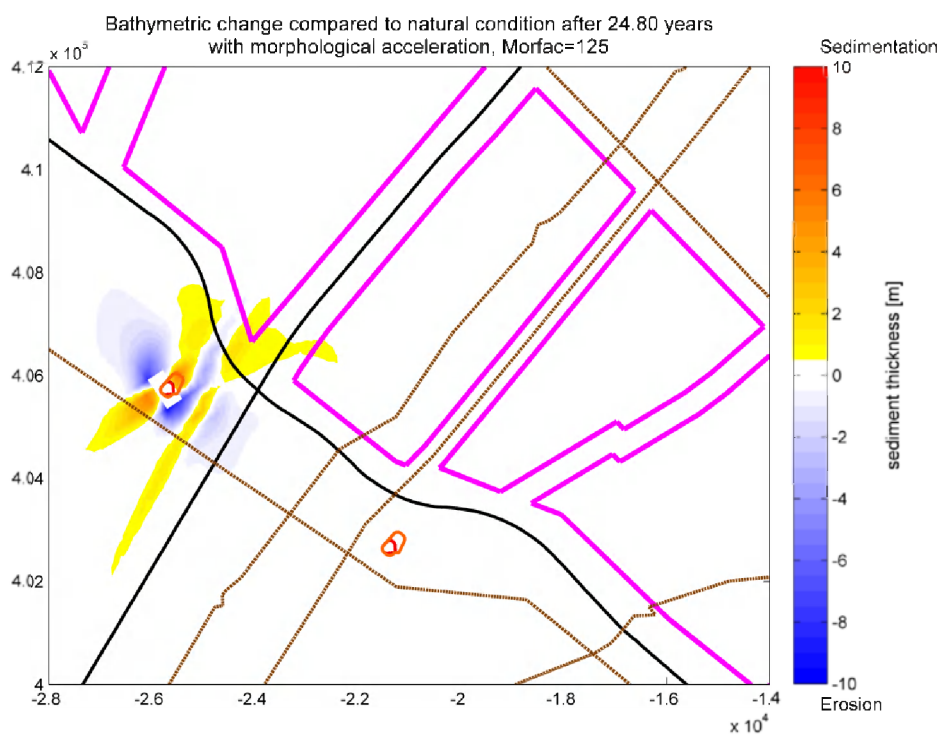


Figure 6-43: Bathymetric change of DIPP II compared to natural condition after +/- 25 years with morphological acceleration (Morfac=125).

6.4 MORPHOLOGICAL EVOLUTION (MORFAC=125, +/- 25 YEARS)

6.4.1 SIP I (single inactive point at Location I)

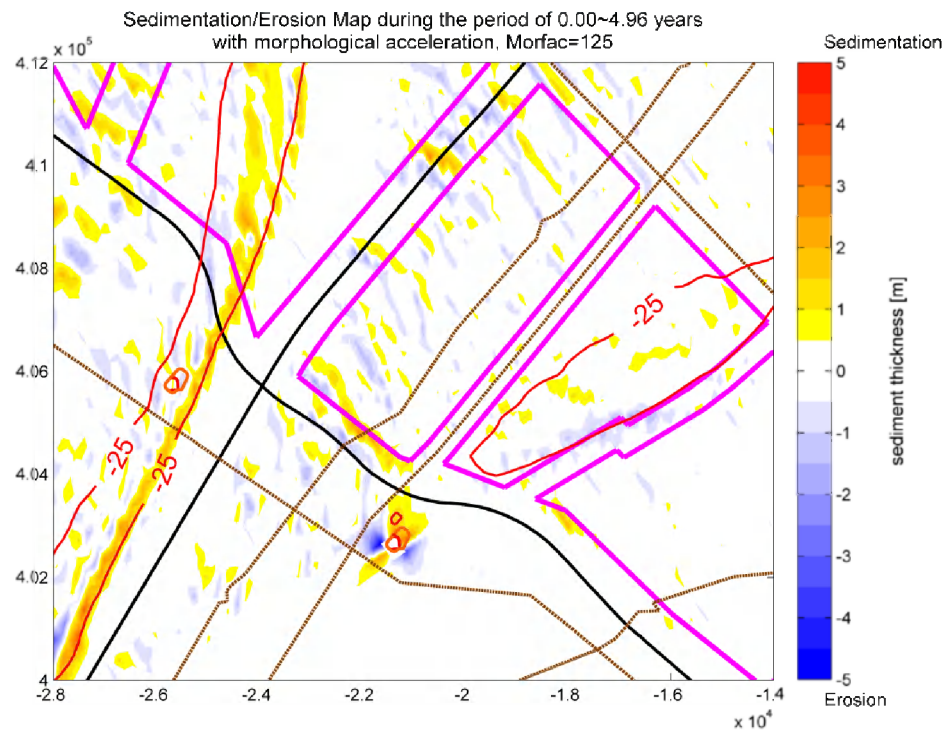


Figure 6-44: Map of sedimentation/erosion with SIP I during the first 5 years with morphological acceleration (Morfac=125).

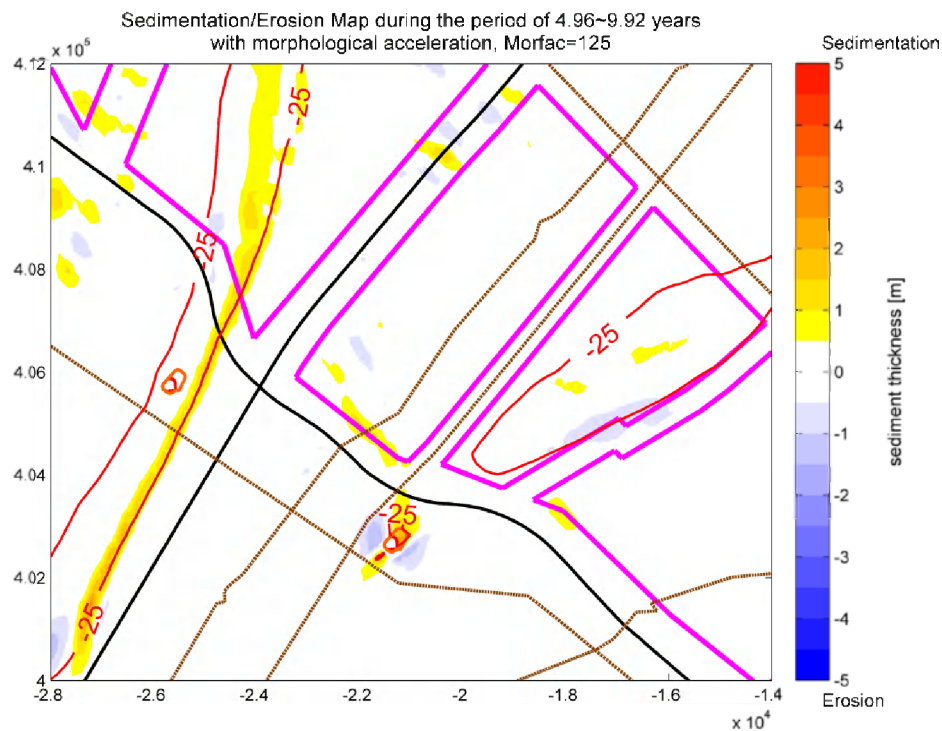


Figure 6-45: Map of sedimentation/erosion with SIP I during the second 5 years with morphological acceleration (Morfac=125).

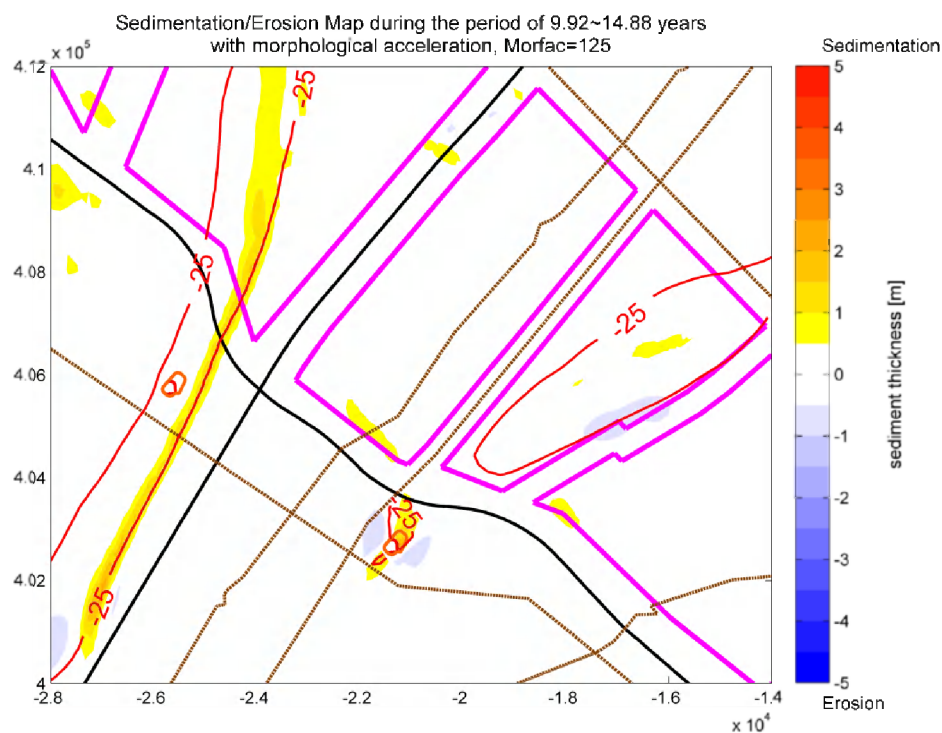


Figure 6-46: Map of sedimentation/erosion with SIP I during the third 5 years with morphological acceleration (Morfac=125).

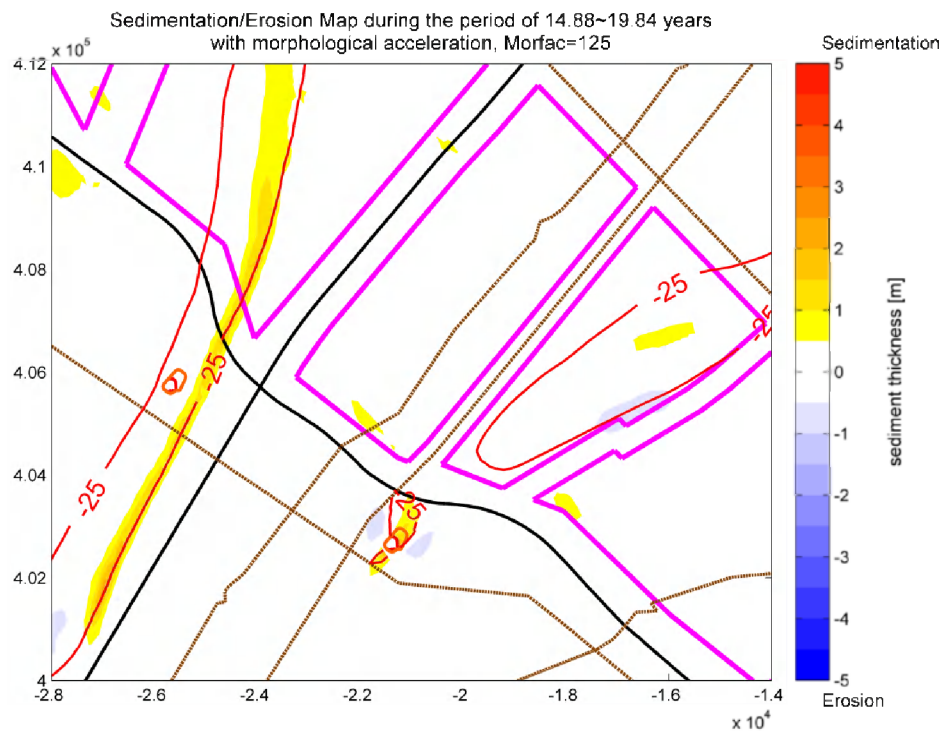


Figure 6-47: Map of sedimentation/erosion with SIP I during the fourth 5 years with morphological acceleration (Morfac=125).

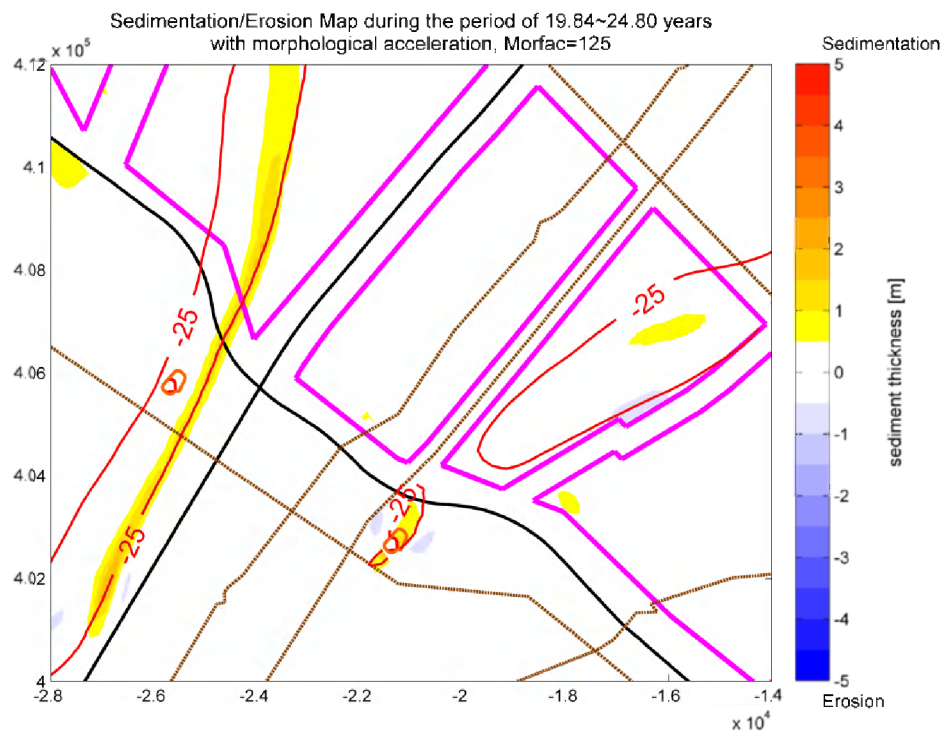


Figure 6-48: Map of sedimentation/erosion with SIP I during the fifth 5 years with morphological acceleration (Morfac=125).

6.4.2 DIPP I (double inactive points perpendicular to main flow direction at Location I)

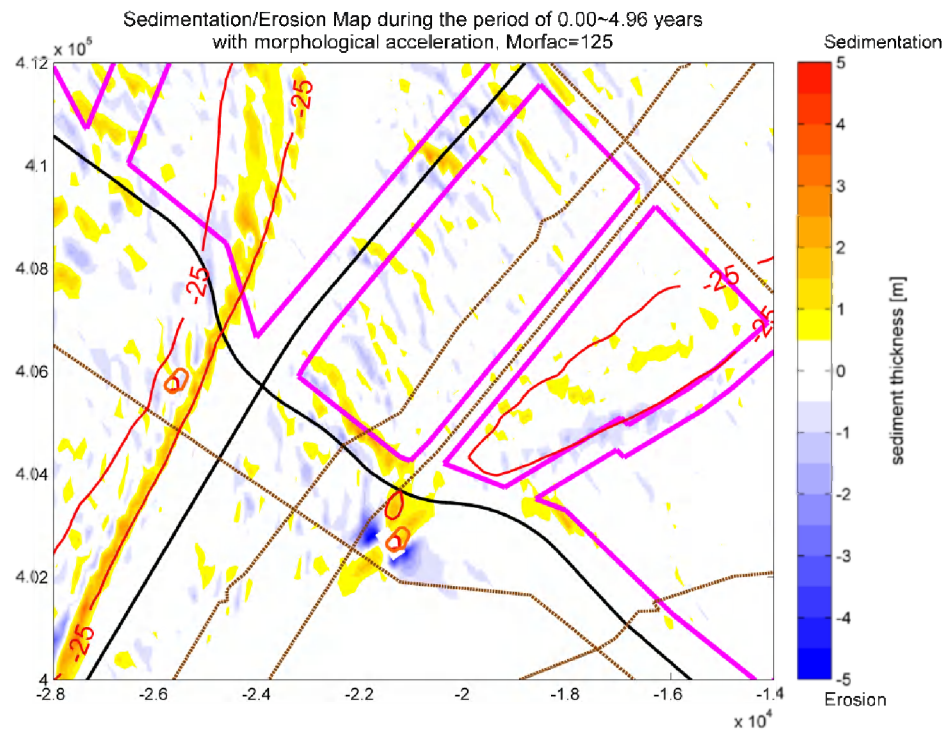


Figure 6-49: Map of sedimentation/erosion with DIPP I during the first 5 years with morphological acceleration (Morfac=125).

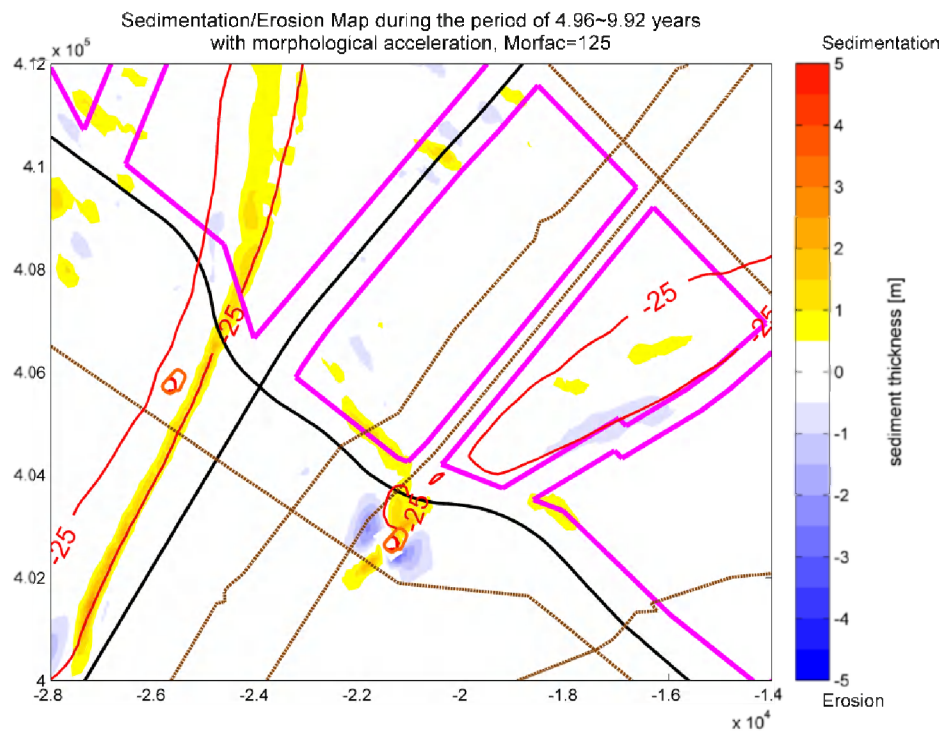


Figure 6-50: Map of sedimentation/erosion with DIPP I during the second 5 years with morphological acceleration (Morfac=125).

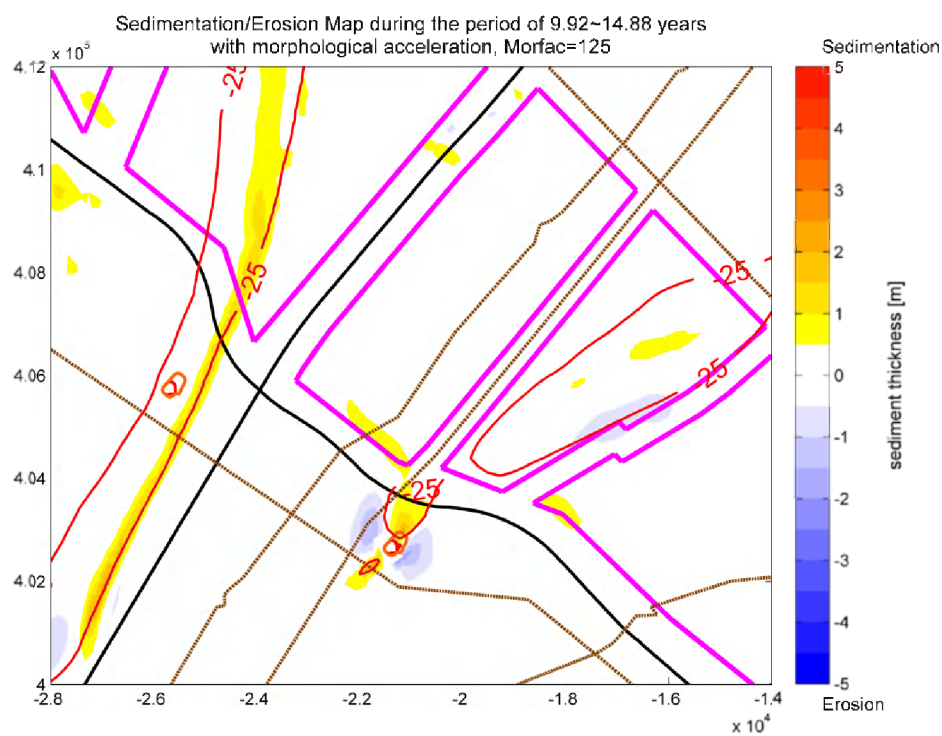


Figure 6-51: Map of sedimentation/erosion with DIPP I during the third 5 years with morphological acceleration (Morfac=125).

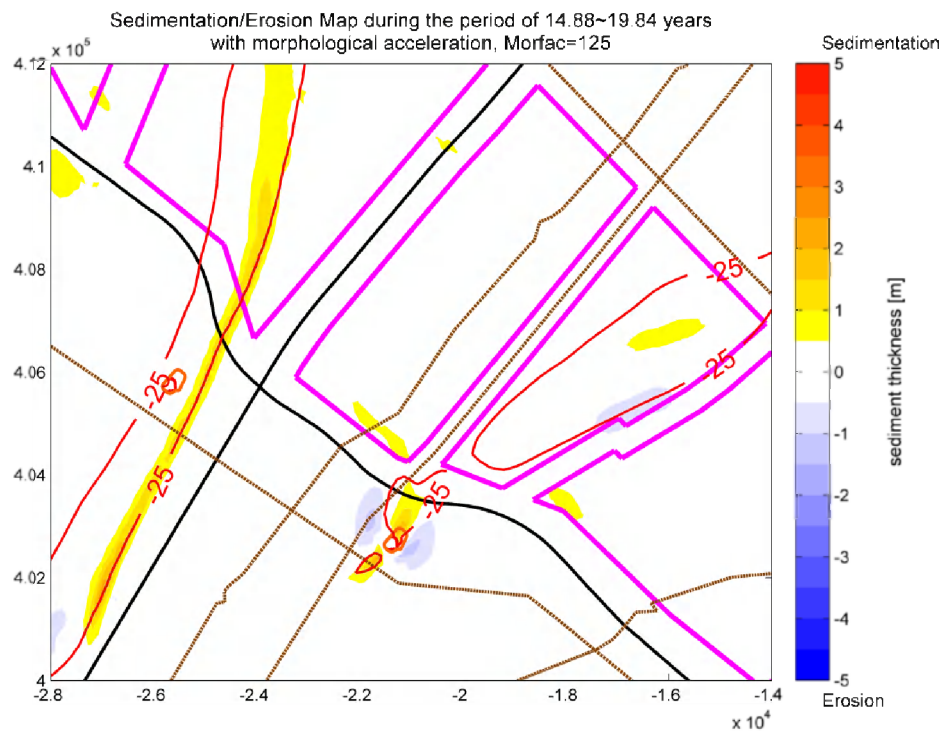


Figure 6-52: Map of sedimentation/erosion with DIPP I during the fourth 5 years with morphological acceleration (Morfac=125).

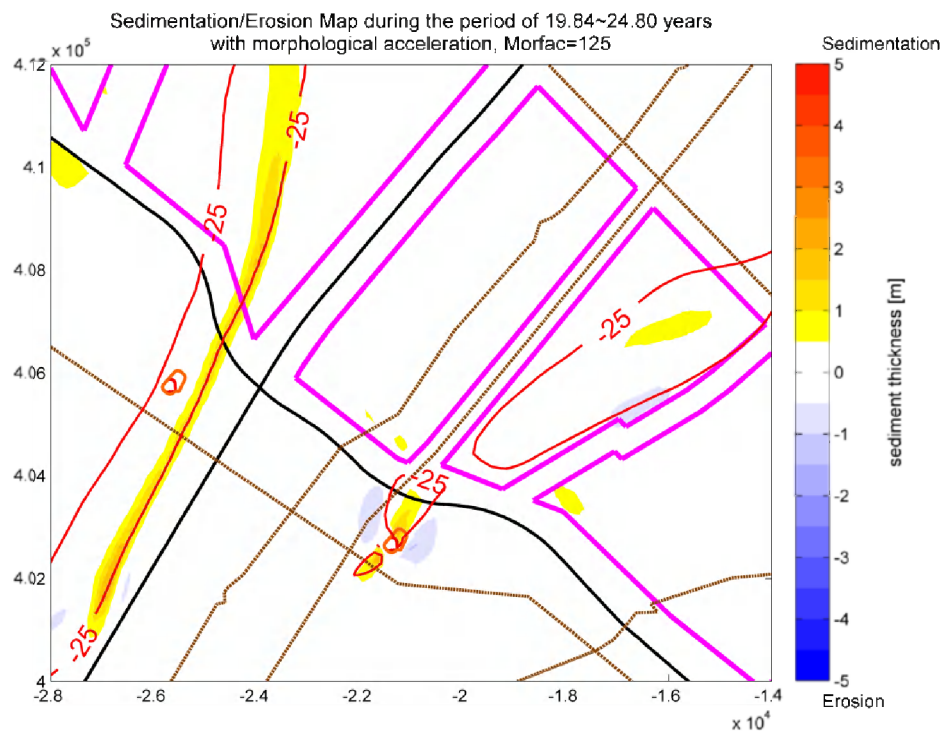


Figure 6-53: Map of sedimentation/erosion with DIPP I during the fifth 5 years with morphological acceleration (Morfac=125).

6.4.3 SIP II (single inactive point at Location II)

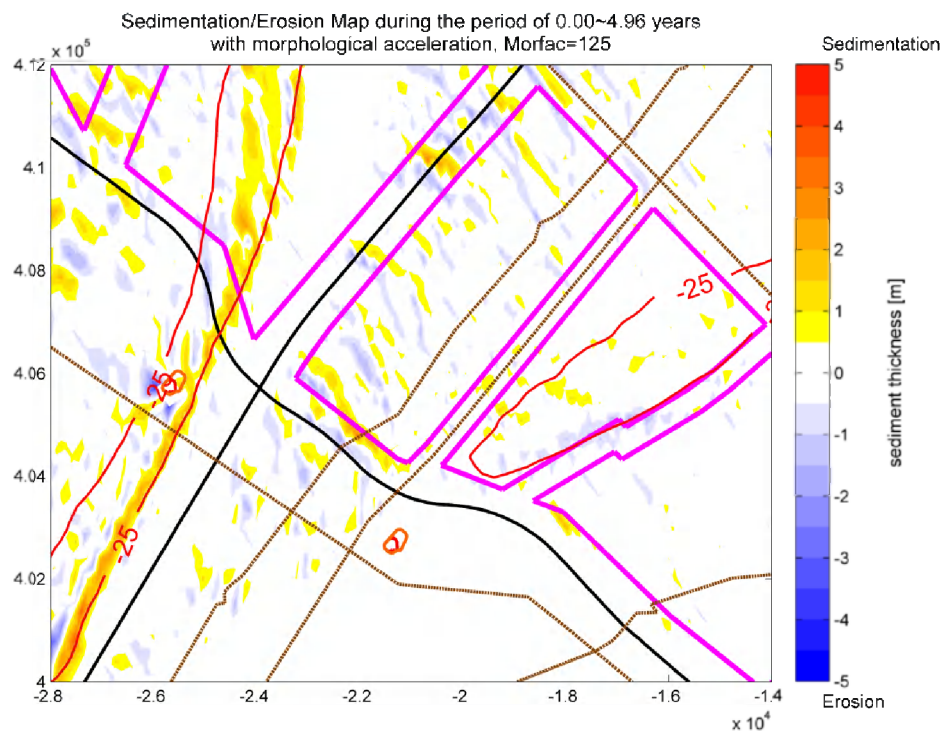


Figure 6-54: Map of sedimentation/erosion with SIP II during the first 5 years with morphological acceleration (Morfac=125).

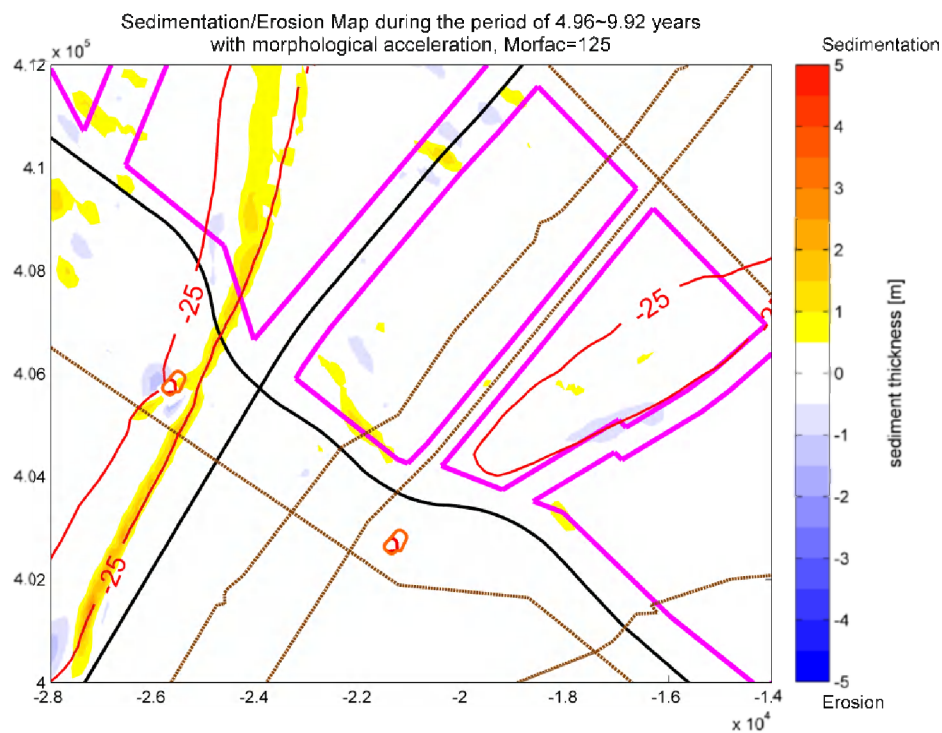


Figure 6-55: Map of sedimentation/erosion with SIP II during the second 5 years with morphological acceleration (Morfac=125).

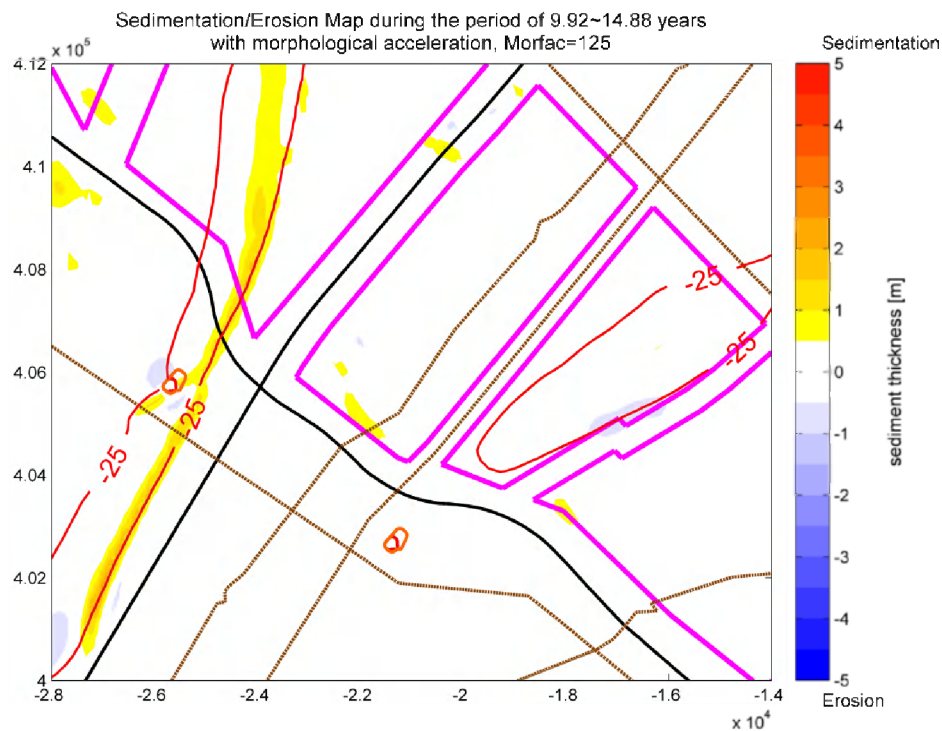


Figure 6-56: Map of sedimentation/erosion with SIP II during the third 5 years with morphological acceleration (Morfac=125).

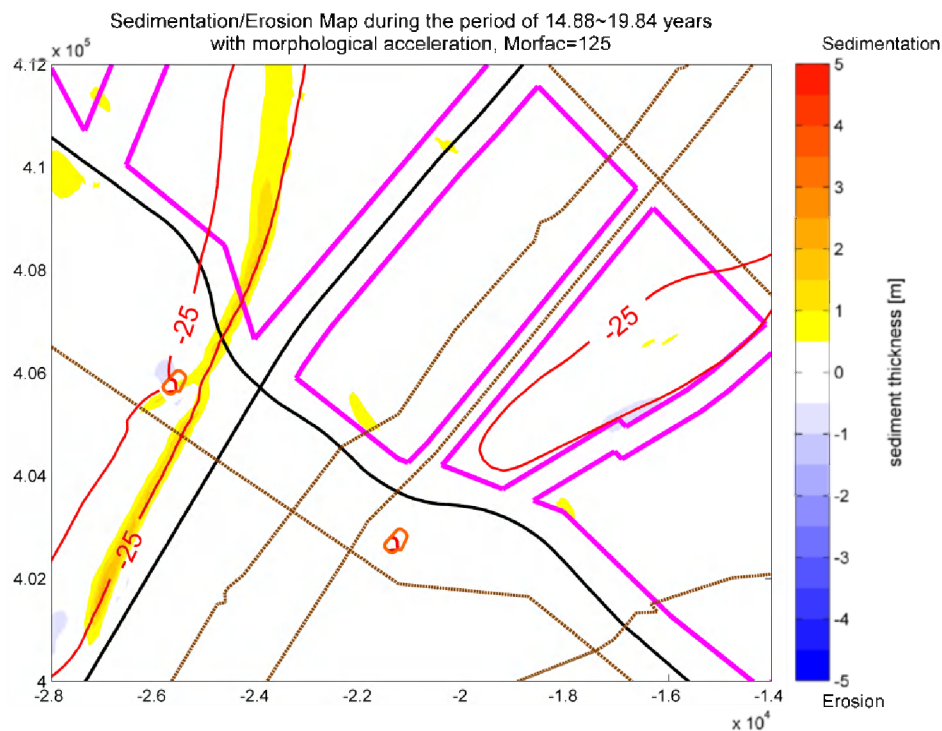


Figure 6-57: Map of sedimentation/erosion with SIP II during the fourth 5 years with morphological acceleration (Morfac=125).

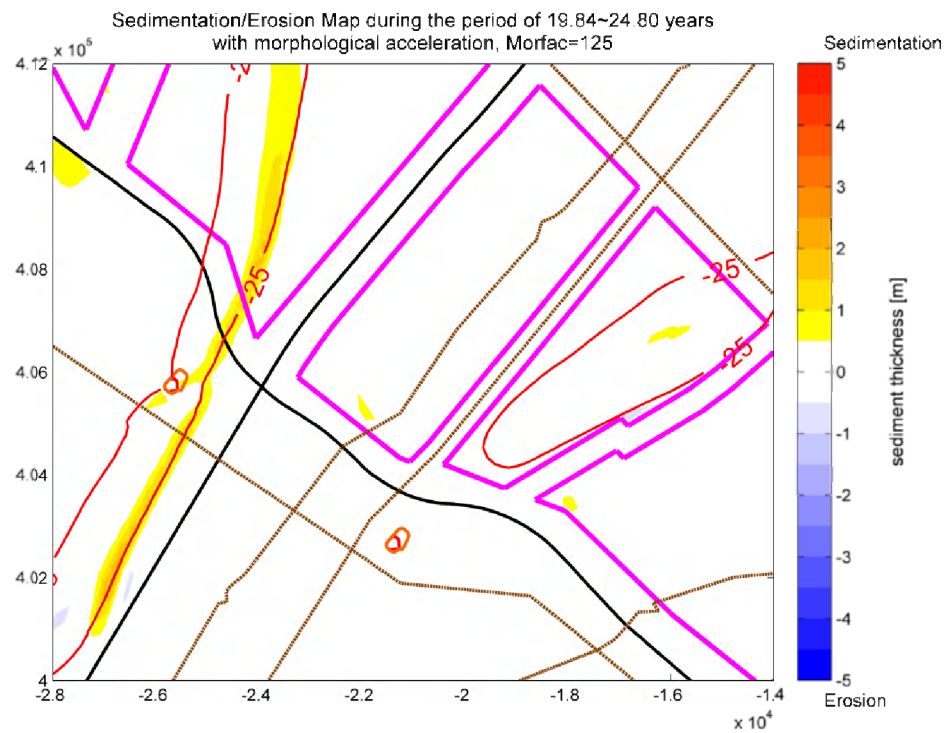


Figure 6-58: Map of sedimentation/erosion with SIP II during the fifth 5 years with morphological acceleration (Morfac=125).

6.4.4 TIPA II (triple inactive points aligned to main flow direction at Location II)

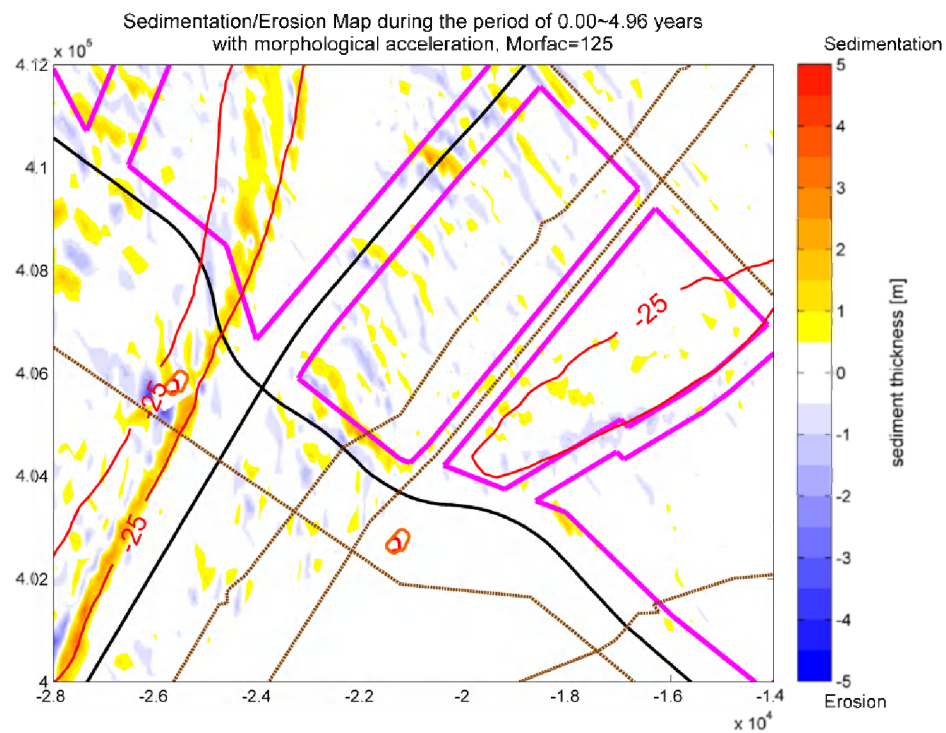


Figure 6-59: Map of sedimentation/erosion with TIPA II during the first 5 years with morphological acceleration (Morfac=125).

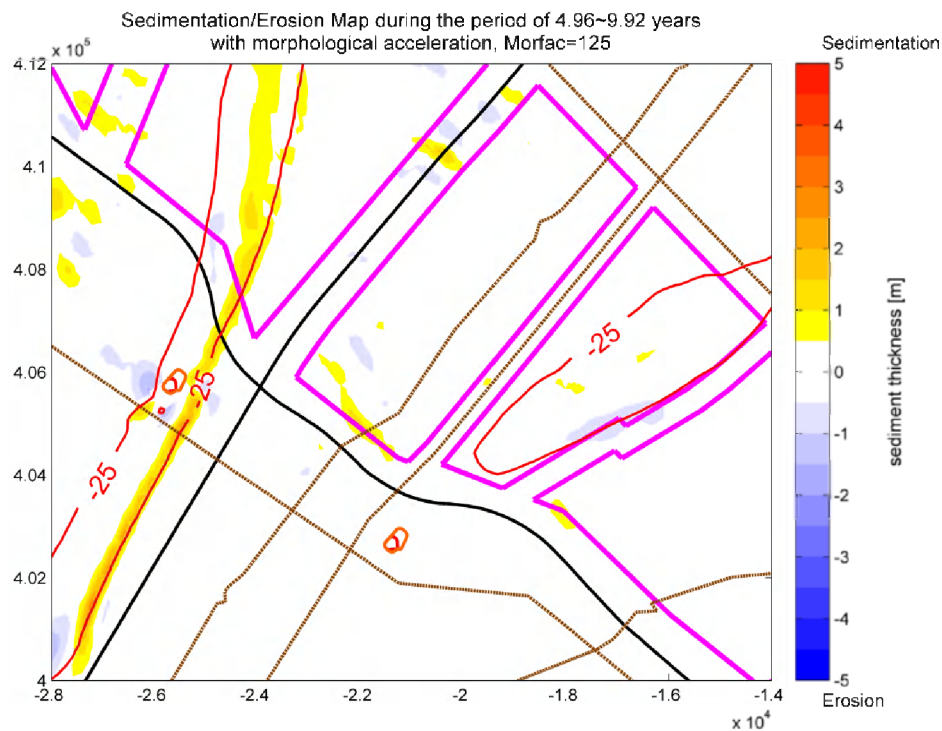


Figure 6-60: Map of sedimentation/erosion with TIPA II during the second 5 years with morphological acceleration (Morfac=125).

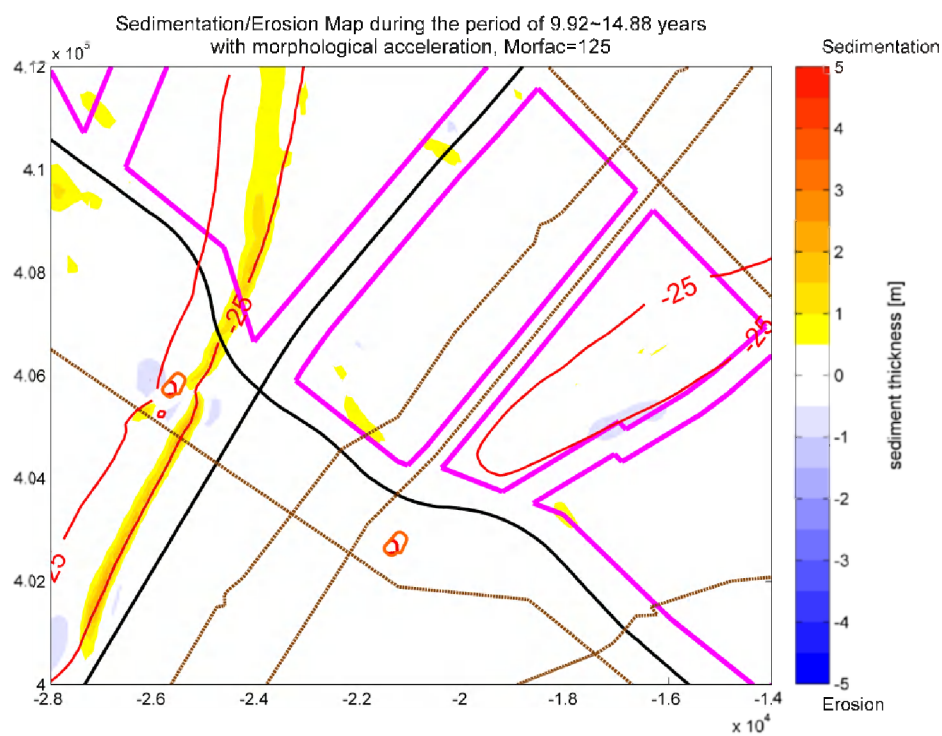


Figure 6-61: Map of sedimentation/erosion with TIPA II during the third 5 years with morphological acceleration (Morfac=125).

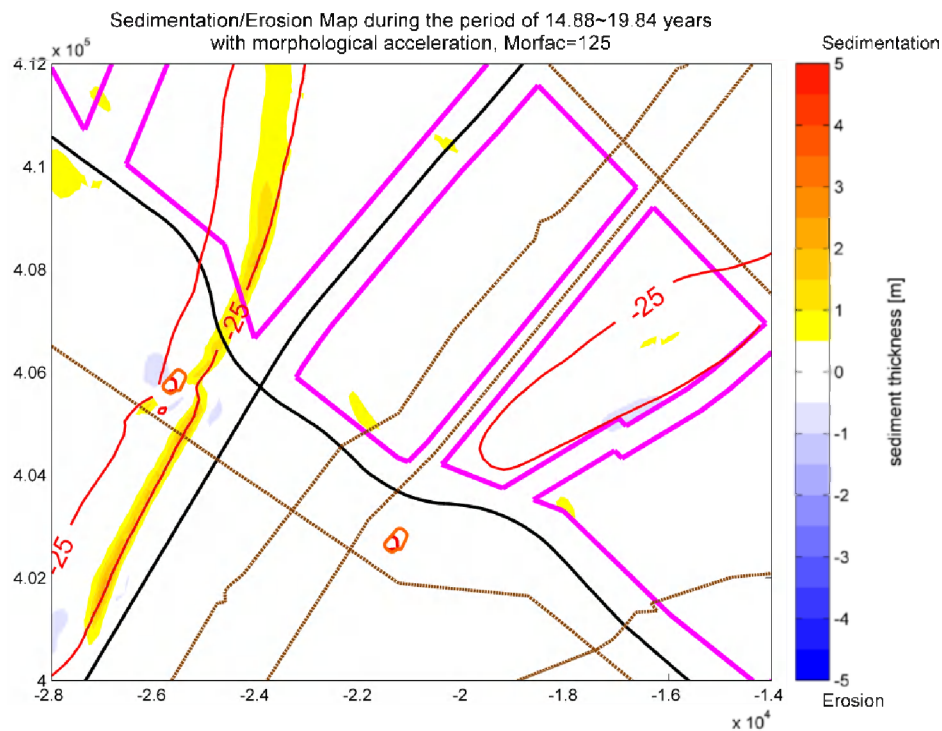


Figure 6-62: Map of sedimentation/erosion with TIPA II during the fourth 5 years with morphological acceleration (Morfac=125).

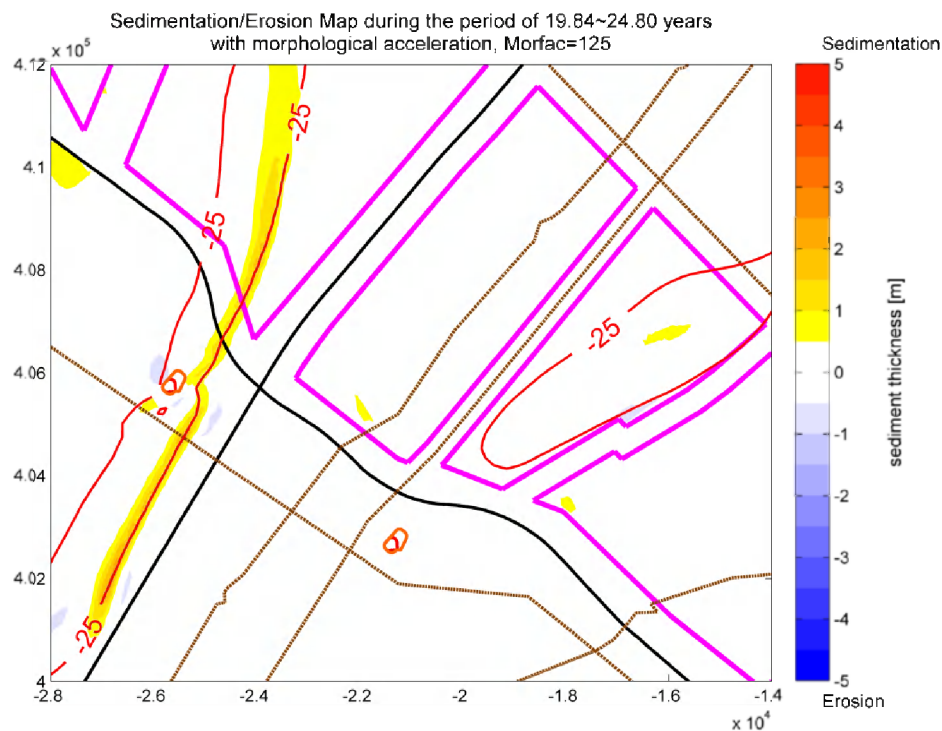


Figure 6-63: Map of sedimentation/erosion with TIPA II during the fifth 5 years with morphological acceleration (Morfac=125).

6.4.5 DIPP II (double inactive points perpendicular to main flow direction at Location II)

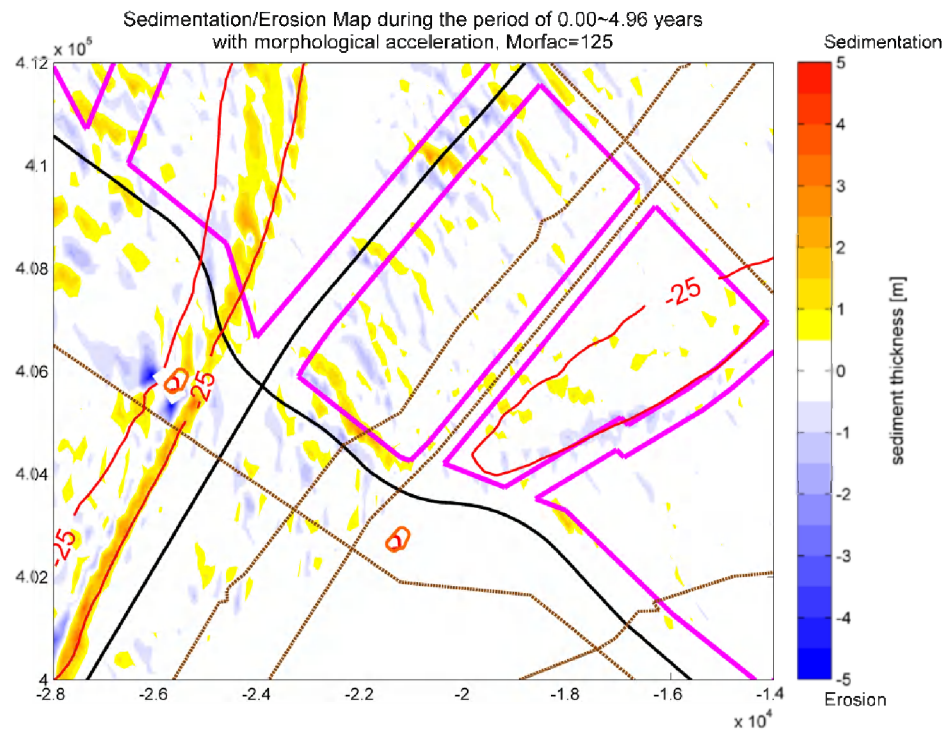


Figure 6-64: Map of sedimentation/erosion with DIPP II during the first 5 years with morphological acceleration (Morfac=125).

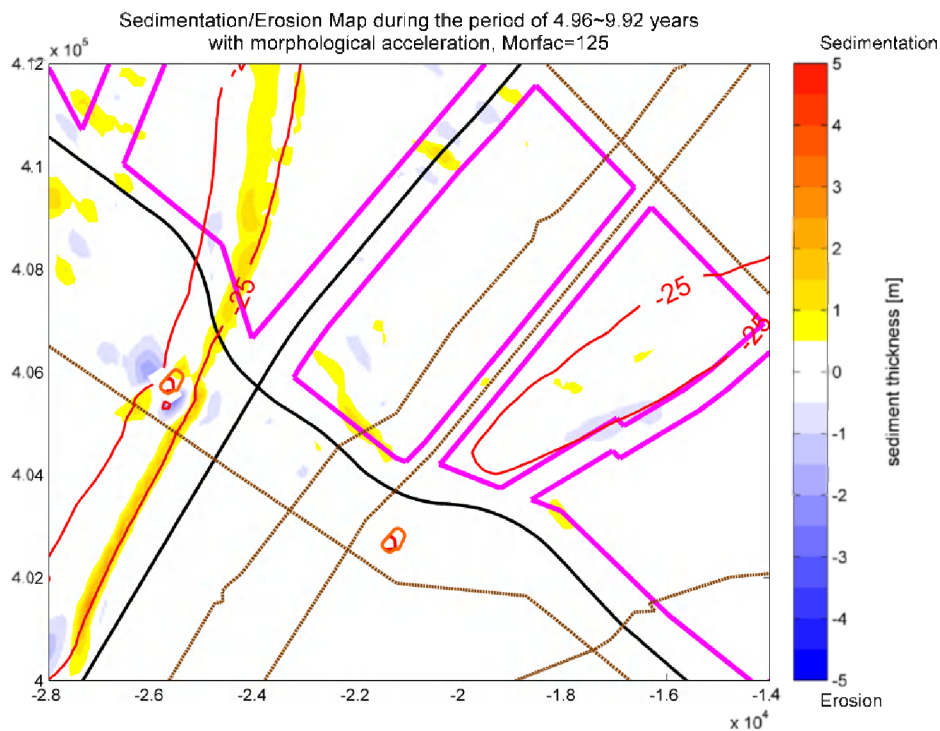


Figure 6-65: Map of sedimentation/erosion with DIPP II during the second 5 years with morphological acceleration (Morfac=125).

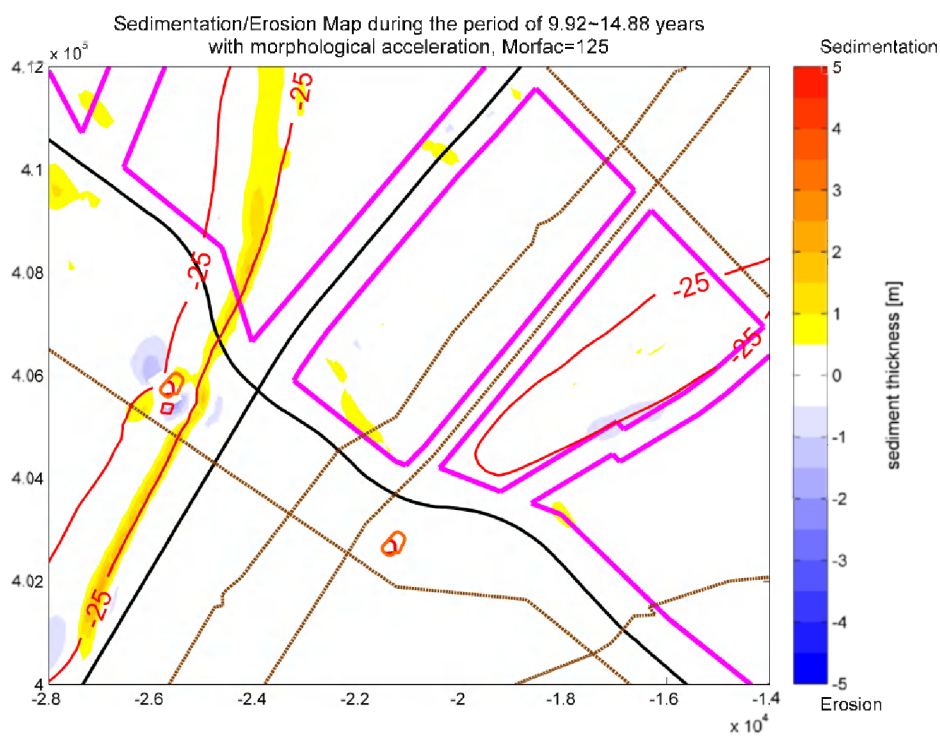


Figure 6-66: Map of sedimentation/erosion with DIPP II during the third 5 years with morphological acceleration (Morfac=125).

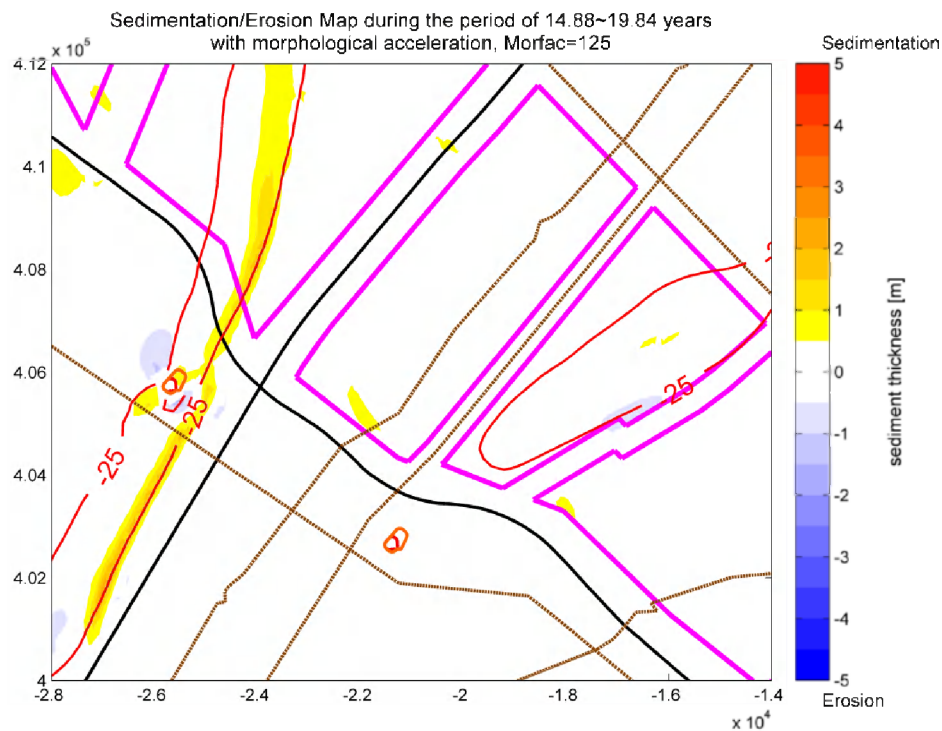


Figure 6-67: Map of sedimentation/erosion with DIPP II during the fourth 5 years with morphological acceleration (Morfac=125).

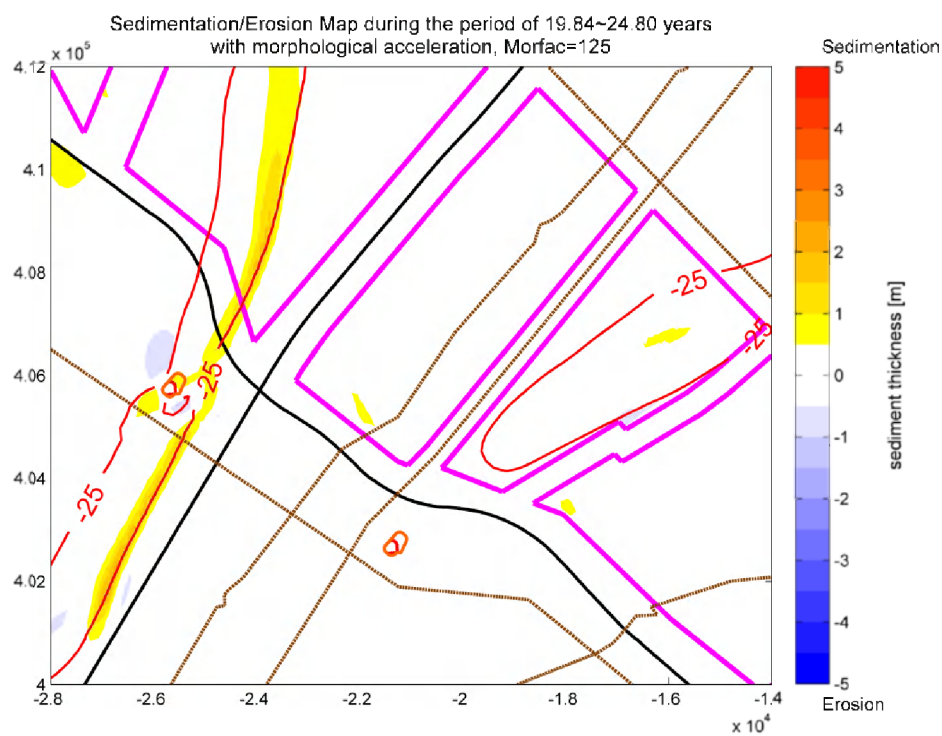


Figure 6-68: Map of sedimentation/erosion with DIPP II during the fifth 5 years with morphological acceleration (Morfac=125).